

Greenhouse Gas Release from Reservoirs in Scotland and North Wales

Roseanne Kimberley McDonald^{1,2}

Thesis submitted for the degree of

Doctor of Philosophy

Biological & Environmental Sciences

Faculty of Natural Sciences

The University of Stirling

March 2019

¹**Biological and Environmental Sciences, School of Natural Sciences, University of Stirling, Stirling, Scotland, UK.**

²**Centre for Ecology and Hydrology, Bush Estate, Edinburgh, Scotland, UK.**

Declaration

I declare that this thesis has been composed by myself and that it embodies the results of my own research. Where appropriate, I have acknowledged the nature and extent of the work carried out in collaboration with others.

Signed.....

Date.....

Abstract

Inland waters play an important role in the transport, transformation, loss and storage of carbon (C) and nitrogen (N) in the pathway between terrestrial and marine systems. Inland waters can act as both sources to the atmosphere through evasion of GHGs such as CO₂, CH₄ and N₂O, but also as sinks through C burial in sediments. To date, there are no major studies on GHG release from reservoirs in the UK, despite drinking water provision being heavily reliant on peatland-fed reservoirs. The overall aim of this thesis was therefore to quantify, compare and understand C and N dynamics, both spatially and temporally, within 30 temperate reservoirs in North Wales (n = 15) and Scotland (n = 15). Chapter 3 presents a broad overview of these 30 reservoirs, where the role of catchment characteristics in determining spatial variation of reservoir biogeochemistry is investigated. Three of the Scottish reservoirs included in Chapter 3 were also selected for greater in-depth sampling at weekly to fortnightly intervals to provide greater temporal understanding of C and N, and become the two remaining data chapters of this thesis. Chapter 4 quantifies GHG export from the catchments of Baddinsgill (moorland) and Black Esk (forested) reservoirs, whilst Chapter 5 determines the importance of water level drawdown on GHG emissions from Waltersmuir reservoir.

In Chapter 3, results show that the 30 sampled reservoirs were overall, oversaturated in CO₂, CH₄ but to a lesser extent in N₂O, largely reflecting differences in catchment land cover and soil types. Large temporal and spatial differences in C and N concentrations were also observed, with seasonal differences occurring between reservoirs in Scotland and North Wales. Influx of CO₂ was occasionally seen, with one reservoir showing overall negative evasion which was linked to the presence of cyanobacteria.

Chapter 4 revealed that GHG evasion from inlets was higher than the reservoirs at both Baddinsgill and Black Esk, emphasising the need for integrated, catchment wide monitoring across stream and reservoir systems. Annual and areal Fluvial C and N fluxes were calculated for both catchments, and the input-output balance also calculated to determine whether the reservoirs were net C and N sources or sinks. Results revealed both reservoirs as overall net sinks for C and N, apart from at Baddinsgill, which was a net CH₄ source. Dissolved inorganic carbon (DIC) was the largest C input to both reservoirs, whilst nitrate (NO₃⁻) was the largest N input.

All aquatic systems experience natural fluctuations in water level, this is often more extreme in reservoir environments due to seasonal demands or operational maintenance. Chapter 5 determines the impact of a controlled water level drawdown on GHG emissions from both

sediments and the surface water area at Waltersmuir reservoir. As the water level drops and sediments become exposed to the air and begin to dry out, biogeochemical processes are temporarily altered. Results showed pulses of GHG fluxes from the reservoir during the drawdown period. Such episodic events were indicative of physical displacement of accumulated sediment gases, which can contribute significantly to total reservoir emissions. The three month drawdown period at Waltersmuir reservoir contributed disproportionately to total annual emissions (66% of CO₂ equivalent-weighted emissions). This study adds to a growing body of evidence that suggests reservoir drawdown zones are active areas of biogeochemical cycling and can stimulate CO₂, CH₄ and N₂O release.

Conclusively, this thesis shows that GHG concentrations and fluxes from UK reservoirs are highly temporally and spatially variable, with magnitudes comparable to other studies in temperate and boreal regions. Fluctuating water levels can regulate emissions and should be considered in budget studies, with the relative importance expected to increase under climate scenarios. Future studies which aim to quantify GHG dynamics from UK reservoirs should focus on integrated catchment wide monitoring (i.e. including any inflows, the reservoir itself, and outflows) to gain fuller understanding of the reservoir impact on C and N, and also potential impacts of catchment management on fluxes. Such monitoring is resource intensive so it is recommended that future efforts focus on reservoirs across different trophic states (i.e. oligotrophic to eutrophic) covering both lowland and upland catchments.

Acknowledgments

First and foremost, I would like to thank my supervisors, Ute Skiba, Chris Evans, Susan Waldron, Mike Billett, Kerry Dinsmore, Zoe Frogbrook, Fraser Leith and Jens-Arne Subke for their support, guidance and encouragement throughout my PhD. I would also like to thank everyone at the Centre for Ecology and Hydrology (CEH), Edinburgh for their ongoing support and advice, and for their open and friendly attitudes that made my time here so enjoyable and memorable. A big thank you to Julia Drewer, Nick Cowan, Amy Pickard and Margaret Anderson for providing support in the labs and many conversations during my never-ending period of manual injections. Thanks also goes to Pete Levy, Nick Cowan and Luc Bussiere for advice on data analysis. I would also like to thank the Freshwater Group who welcomed me into their group, provided lots of helpful advice and another support network within CEH. I would also like to thank those who braved the Scottish and/or Welsh weather and midges to help collect field data: Angus Lepper, Lewis Shillinglaw, Andrea Gadnert, Song Ling, Juliette Maire, Fraser Leith, Ute Skiba, Amy Pickard, Donna Evans and Jess Parslow.

I also wish to extend a big thank you to Dwr Cymru (Welsh Water) and Scottish Water for granting sampling access to the reservoirs and providing background information.

Finally, a special thank you to my mum, friends and especially my partner, Angus for the encouragement and help along the way. Angus, not only did you give up your holidays to be dragged around reservoirs during the spatial campaigns, but you also put up with me, and kept me sane, throughout this PhD.

This research would not have been possible without the funding provided by the Natural Environment Research Council (NERC) through the IAPETUS Doctoral Training Partnership (DTP), grant number NE/L002590/1 and Scottish Water as CASE partner. The DTP provided many memorable events and a fantastic support network throughout the past four years – best of luck to my fellow 2014 cohort with the next steps in their careers.

Table of contents

Declaration	i
Abstract	ii
Acknowledgments	iv
Table of contents	v
List of tables	viii
List of figures	x
1 Introduction	1
1.1 Climate change and greenhouse gases	3
1.2 Inland waters and the carbon cycle	5
1.2.1 Greenhouse gas emission pathways	9
1.2.2 Mineralisation, Sedimentation and GHG emissions	11
1.2.3 Additional factors driving C dynamics and GHG emission processes	13
1.3 Emission estimates from previous research	14
1.4 Conclusions and future research needs	24
1.5 Research aims, objectives and overview of thesis structure	24
2 Materials and methods	28
2.1 Field site selection and characteristics	29
2.1.1 In-depth study sites: Black Esk, Baddingsgill and Waltersmuir reservoirs.....	37
2.2 Field and laboratory methods.....	47
2.2.1 Dissolved CO ₂ , CH ₄ and N ₂ O concentrations – headspace method	47
2.2.2 CO ₂ , CH ₄ and N ₂ O emissions – static chambers	49
2.2.3 Water quality sampling procedure	51
2.2.4 Stage height, river discharge measurements and export	53
2.3 Data analysis	56
2.3.1 Reservoir and stream evasion flux calculations	56
2.3.2 Statistical analysis	57
3 The role of catchment characteristics in determining spatial variation of reservoir biogeochemistry	59
3.1 Introduction	59
3.2 Methods	62
3.2.1 Reservoir characteristics and field sampling.....	63
3.2.2 Measurement of water physico-chemistry, nutrient and GHG concentrations .	63
3.2.3 GIS and statistical analysis	66
Statistical analysis	66

3.3	Results.....	67
3.3.1	General reservoir water quality and catchment characteristics.....	67
3.3.2	Seasonal variability in C and N concentrations.....	73
3.3.3	Spatial variability in evasion and excess partial pressure by reservoir.....	76
3.3.4	Relationships of CO ₂ , CH ₄ and N ₂ O with catchment characteristics.....	79
3.4	Discussion.....	84
3.4.1	Variables controlling spatial variability in GHG concentrations.....	85
3.4.2	Seasonal variability.....	90
3.4.3	Comparison with other lakes and reservoirs.....	92
3.5	Conclusions.....	95
4	Spatio-temporal patterns in carbon dioxide, methane and nitrous oxide emissions from moorland and forested reservoir catchments in Scotland, UK.....	97
4.1	Introduction.....	97
4.2	Materials and methods.....	99
4.2.1	Study sites.....	99
4.2.2	Measurement of C, N and water chemistry parameters.....	101
4.2.3	Calculation of reservoir and stream GHG evasion rates.....	103
4.2.4	Estimating catchment areas.....	104
4.2.5	Aquatic C and N export.....	105
4.3	Results.....	105
4.3.1	Spatial and temporal variability in C and N concentrations.....	105
4.3.2	Greenhouse gas evasion from reservoirs and catchment streams.....	119
4.3.3	Annual, catchment-scale and retained fluvial C and N fluxes.....	122
4.4	Discussion.....	127
4.4.1	Spatial and temporal variability in C and N concentrations and fluxes.....	127
4.4.2	Reservoir balance and comparison to other studies.....	130
4.4.3	Limits to calculations of the evasion and export estimates.....	132
4.5	Conclusions.....	132
5	The importance of water level drawdown on greenhouse gas emissions from a temperate UK reservoir.....	134
5.1	Introduction.....	134
5.2	Materials and Methods.....	137
5.2.1	Site description.....	137
5.2.2	Measurement of dissolved GHG concentrations and aquatic chemistry parameters.....	139
5.2.3	Measurements of sediment GHG fluxes and chemical and physical properties	140

5.2.4	Instantaneous flux calculation	142
5.2.5	Integration and upscaling of GHG fluxes.....	143
5.2.6	Statistical analysis	144
5.3	Results	145
5.3.1	Precipitation effects on reservoir water level and surface area.....	145
5.3.2	The impact of drawdown on aquatic GHGs and water chemistry	146
5.3.3	Drawdown area GHG fluxes and sediment properties	155
5.4	Discussion.....	161
5.4.1	GHG concentrations and evasion rates in the aquatic system	161
5.4.2	GHG fluxes from exposed sediments	166
5.4.3	Upscaling of sediment and aquatic evasion.....	169
5.5	Conclusions	170
6	Overall discussion, synthesis and conclusions.....	173
6.1	Catchment comparisons: In-depth vs. seasonal sampling.....	173
6.2	Recommended further research.....	175
6.3	Implications for catchment and reservoir management and recommendations.....	182
6.4	Research contributions to the wider-knowledge base	186
	References.....	190
	Appendix I – Flow rating curves.....	220

List of tables

Table 1.1 CO ₂ , CH ₄ and N ₂ O fluxes from the surface of temperate and boreal reservoirs. Values stated are either mean and/or (range) of flux.....	19
Table 2.1 Variables measured and methods used in each chapter.	28
Table 2.2 Overview of reservoir and catchment characteristics of all thirty field sites in Scotland and North Wales. Asterisks* indicate reservoirs also included in-depth sampling. Intensive agriculture is the combined area percentage of improved grassland and arable. HOST – Total peat refers to the Hydrology of Soil Types which is further explained in Chapter 3.	33
Table 2.3 Concentrations of certified standards used during GC analysis.....	49
Table 2.4 Overall percentage differences between collected duplicate headspace samples for each sampling campaign and chapter across all three GHGs.	49
Table 3.1 Reservoir and catchment characteristics for the study sites (n = 30), including water quality, geomorphic and biophysical properties. The median, 1 st and 3 rd quartiles (25 th and 75 th percentiles) representing the interquartile range (IQR) are shown.	70
Table 3.2 Open water evasion flux and excess partial pressure across the study reservoirs. Results shown are median with min and max values given for Scotland Wales overall. Note smaller units for N ₂ O evasion.....	78
Table 3.3 Eigenvectors, eigenvalues and variance explained by principle component (PC) analysis of water quality, geomorphic and biophysical variables for the study lake catchments (n = 30).	81
Table 4.1 Variability in concentrations and excess partial pressure of different C and N species at Baddingsgill inlet, reservoir and outlet surface waters. Values are reported to two significant figures as mean ± standard error (minimum-maximum).	116
Table 4.2 Variability in concentrations and excess partial pressure of different C and N species at Black Esk inlet, reservoir and outlet surface waters. Values are reported to two significant figures as mean ± standard error (minimum-maximum).	117

Table 4.3 Variability in water chemistry (pH, conductivity, dissolved oxygen and temperature) at Baddingsgill and Black Esk inlet, reservoir and outlet surface waters. Values are reported to two significant figures as mean \pm standard error (minimum-maximum).....	118
Table 4.4 Mean \pm standard error (range) for stream and open water evasion in the Baddingsgill and Black Esk catchments. Note different units (g) for CO ₂ evasion. Mean, minimum and maximum slope and elevation are also shown.....	121
Table 4.5 GHG, DOC and DIC exports during a 1 year sampling period for Baddingsgill (2015-2016) and a 2 year period for Black Esk (2015-2017), expressed as annual loads (based on measured discharge from flow rating curves at each location) and areal mean fluxes assuming spatially uniform run-off. Note different units. *Balance +/- = OUT – IN; **Out/In = output divided by the sum of the inputs. Net sinks = Out/In <0.9; approximately balanced = 0.9< Out/In <1.1; net sources = Out/In >1.1.....	125
Table 5.1 Water chemistry parameters and concentrations of different C and N species for Waltersmuir inlet (a), reservoir (b) and outlet (c). Results show mean, standard error and range, with a comparison provided for the full sampling period (Jan 2016-Jan2017) and drawdown period (April-July 2016).	150
Table 5.2 Mean, standard error, minimum and maximum values of estimated open water CH ₄ , CO ₂ , and N ₂ O evasion flux at Waltersmuir and global warming potentials, estimated using the IPCC AR5 reported approach (IPCC, 2014).....	154
Table 5.3 Summary of sediment properties at 5-10 cm depth taken during flux measurements from April – July 2016. The mean values and range (in brackets) of measurements from each variable are included in the table. *For Total C and N, n = 3 from each chamber.	158
Table 6.1 Illustrates the differences in seasonal vs. in-depth sampling at Baddingsgill, Black Esk and Waltersmuir reservoirs as mean excess partial pressures.....	174

List of figures

Figure 1.1 Diagram of the global carbon cycle, with numbers representing ‘carbon stocks’ in Pg C and the annual carbon exchange fluxes in Pg C yr ⁻¹ . Red arrows and numbers represent annual anthropogenic fluxes averaged over 2000-2009, whilst black numbers and arrows indicate reservoir mass and exchange fluxes estimates prior to c. 1750 (Ciais, P. et al., 2013). . 5	
Figure 1.2 Possible biogenic CO ₂ and CH ₄ emission pathways from reservoirs (Hertwich, 2013; Kumar, A. et al., 2011)..... 6	
Figure 1.3 Overview of thesis chapters and subsections, including interlinks between the separate chapters. 27	
Figure 2.1 Location map of the thirty reservoir catchments in Scotland and North Wales that were used in this research. The highlighted Scottish catchments (dashed lines), Waltersmuir, Baddinsgill and Black Esk, were sampled more in-depth (1 year, 1.5 years and 2 years 2 months, respectively) and presented in Chapters 4 and 5. 32	
Figure 2.2 Selection of field photographs showing diversity in reservoir characteristics in North Wales (a) and Scotland (b). 37	
Figure 2.3 Monthly rainfall and temperature data from Eskdalemuir weather station near Black Esk reservoir during the sampling period. 39	
Figure 2.4 Felling locations in Black Esk catchment during sampling period, courtesy of Forestry Commission Scotland. Field photograph of broad leaf tree planting in Spring 2017. 40	
Figure 2.5 Photographs of sampling locations of inlets (blue), outlet (orange) and reservoir (purple) at Black Esk. BE1 _{res} and BE2 _{res} show the decomposing felled trees within the reservoir. 41	
Figure 2.6 Examples of a working farm and managed catchment at Baddinsgill reservoir..... 43	
Figure 2.7 Field photographs and locations of inlet (blue), outlet (orange) and reservoir (purple) sampling locations at Baddinsgill reservoir..... 43	
Figure 2.8 Inlet, reservoir and outlet sampling sites and location of Baddinsgill and Black Esk reservoirs in Scotland..... 44	

Figure 2.9 Sub-catchment characteristics at Baddingsgill and Black Esk reservoirs of land cover (a), geology (b) and soil (c).....	45
Figure 2.10 Field photographs at Waltersmuir reservoir during a high flow event at the a) inlet and b) outlet. Photograph c) shows the exposed reservoir sediment during drawdown and d) the typical reservoir water level outside the drawdown period.	47
Figure 2.11 Static chamber transect installation at Waltersmuir reservoir during first week of water-level drawdown.	51
Figure 2.12 LabTOC analyser with autosampler.	52
Figure 2.13 Water samples being run on the SEAL AQ2 discrete analyser for determination of nitrogen species.	53
Figure 2.14 Example of a discharge-stage relationship curve for Black Esk inlet (BE5 _{in}), alongside goodness of fit and the equation used to describe the relationship between stage height and discharge. Rating curves for other inlets and outlets are displayed in Appendix I. .	55
Figure 3.1 Catchment locations of sampled reservoirs in Scotland and North Wales.....	63
Figure 3.2 Bar plot showing the proportion of land cover classes associated with each catchment.	71
Figure 3.3 Bar plot showing the proportion of geology classes associated with each catchment.	72
Figure 3.4 Bar plot showing the proportion of HOST categories within the catchments, with total peat split into categories representing peaty gleys, peaty rankers and blanket peat.	73
Figure 3.5 Seasonal variability in concentrations of CO ₂ , CH ₄ and N ₂ O, across the 30 Scottish and Welsh reservoirs.	74
Figure 3.6 Seasonal variability in concentrations of DOC and DIC across the 30 Scottish and Welsh reservoirs.	75
Figure 3.7 Seasonal variability in concentrations of NH ₄ ⁺ , NO ₂ ⁻ , NO ₃ ⁻ across the 30 Scottish and Welsh reservoirs.	76

Figure 3.8 Correlation biplot displaying the orientation of the environmental variables from Table 3.3 on the first two principle components.....	80
Figure 3.9 Hierarchical clustering by catchment characteristics for land use, geology and soil HOST categories. The number of each cluster (1-5) is shown representing each individual cluster below the dotted line.....	83
Figure 3.10 Boxplot showing concentration of CO ₂ , CH ₄ and N ₂ O by the five catchment clusters (1-5) as shown in Figure 3.9.	83
Figure 4.1 Location map of (a) Baddinsgill and (b) Black Esk reservoir catchments in Scotland, UK. The locations of the inlet, reservoir and outlet sampling points are highlighted.	101
Figure 4.2 Temporal variability in inlet (gray), reservoir (orange) and outlet (blue) GHG concentrations at Baddinsgill (BA) reservoir catchments from July 2015 to January 2017.	109
Figure 4.3 Temporal variability in inlet (gray), reservoir (orange) and outlet (blue) GHG concentrations at Black Esk (BE) catchments from June 2015 to July 2017.	110
Figure 4.4 Temporal variability in inlet (gray), reservoir (orange) and outlet (blue) DIC and DOC concentrations at the sampling locations of Baddinsgill (BA) reservoir from July 2015 to January 2017.	111
Figure 4.5 Temporal variability in inlet (gray), reservoir (orange) and outlet (blue) DIC and DOC concentrations at the sampling locations of Black Esk (BE) reservoir from June 2015 to July 2017.	112
Figure 4.6 Spatial variability in discharge at Baddinsgill and Black Esk catchment inflows and outflows.	113
Figure 4.8 Spatial variability in inlet (gray), reservoir (orange) and outlet (blue) DOC and DIC concentrations at Baddinsgill and Black Esk catchments during the full sampling period.....	115
Figure 4.9 Boxplots show GHG evasion across all sampled inlets (gray), the reservoir (orange) and outlet (blue) sampling sites at Baddinsgill (a) and Black Esk (b) reservoirs.	120
Figure 5.1 a) Location of the Waltersmuir catchment and sampling locations on the digital Elevation Model (DEM) derived from UAV survey. b) Photograph taken in April 2016 during maximum drawdown, illustrating transect location, with chambers 1 and 9 highlighted. c)	

Photographs of chambers one (highest elevation) to nine (lowest elevation) illustrating desiccated surface cracks in the sediment and visibly higher moisture levels in chambers seven to nine.	138
Figure 5.2 Daily precipitation during the sampling period.	146
Figure 5.3 Temporal variability of GHG, DOC and DIC concentrations within the Waltersmuir inlet, reservoir and outlet. The shaded area represents the 11 week drawdown period from April-July 2016.....	153
Figure 5.4 Reservoir evasion at Waltersmuir with spikes occurring during the drawdown period (shaded area).	155
Figure 5.5 Sediment fluxes along the chamber transect (1-9 represent Chamber ID) from the drier reservoir edge (chamber 1) to the wetter centre (chamber 9) during the period of drawdown.	159
Figure 5.6 Boxplots summarising the main sediment properties measured at 5-10 cm depth simultaneously to sediment flux measurements from April to July 2016 during the period of water level drawdown at chambers 1 (reservoir littoral edge) to 9 (centre of reservoir). Further information on the sediment properties are presented in.....	160
Figure 5.7 Cumulative evasion from upscaled sediment and aquatic evasion from UAV derived DEM (shown in Figure 5.1).	161
Figure 6.1 Summary of mean reservoir GHG fluxes in CO ₂ -equivalents from Scotland, Wales and the in-depth sampled reservoirs. N ₂ O and CH ₄ were multiplied by their 100-year GWP, (IPCC, 2014). All values are in mg CO ₂ -equivalents m ⁻² d ⁻¹ and expressed as mean ± standard error. Values are only for aquatic evasion within the reservoirs i.e. excluding stream and sediment evasion.	175

1 Introduction

Scientific debate has been ongoing surrounding the role freshwater reservoirs play in the global carbon cycle, and they are now considered significant contributors to atmospheric greenhouse gas (GHG) emissions (Barros et al., 2011; Bastviken et al., 2011; Deemer et al., 2016; DelSontro et al., 2018; Prairie et al., 2017; Rudd et al., 1993; St. Louis et al., 2000; Tremblay et al., 2005). Reservoirs are anthropogenic aquatic systems that vary from natural lakes in terms of morphometry, biological zones, external loadings and management objectives (Zhen-Gang, 2008). Water storage and regulation are the primary functions of reservoirs, where they are used for drinking water supply, aquaculture, hydroelectricity generation, flood control, irrigation, navigation and recreation (Barros et al., 2011; St. Louis et al., 2000; Tremblay et al., 2005; Zhen-Gang, 2008). Reservoirs are widely distributed globally and numbers are steadily increasing due to growing economies and related water needs, primarily linked to growth in agriculture, domestic use and power generation. Impoundments are likely to increase in area at a rate of ~1-2% per annum, from ~400,000 km² to ~1 million km² by 2050 (Downing et al., 2006). The hydrological cycle has been impacted by reservoir creation (Barros et al., 2011; Bastien and Demarty, 2013; Mendonça et al., 2012), for example, a total of ~10,800 km³ of water has been impounded, reducing the magnitude of global sea level rise by ~30 mm, at an average rate of ~0.55 mm per year during the past half century (Chao et al., 2008).

Inland waters are important to the global carbon cycle, both as carbon sinks due to organic carbon (OC) burial in sediments, and as carbon sources from carbon dioxide (CO₂) and methane (CH₄) emissions to the atmosphere (Cole et al., 2007; DelSontro et al., 2018; Sobek et al., 2012; Tranvik et al., 2009). Rivers naturally emit CO₂ due to terrestrial organic matter decomposition (Cole et al., 2007; Tranvik et al., 2009) but turbulent flow retains high oxygen conditions, meaning CH₄ emissions are less likely (Abril et al., 2005) apart from in organic-rich systems (Lima, 2005). The terrestrial vegetation surrounding rivers typically functions as a CO₂ sink as photosynthesis often exceeds respiration (Mendonça et al., 2012). Reservoir creation from river damming results in the flooding of this terrestrial vegetation which can no longer perform photosynthesis. The organic matter stored in vegetation and flooded soils becomes available for bacterial decomposition, resulting in release of CO₂ and CH₄ – the flooded area shifts from being a net sink to a net source of carbon to the atmosphere (Kelly et al., 1997; Mendonça et al., 2012; St. Louis et al., 2000). Reservoir creations leads to increased water

volume, which in turn can increase water residence time from less than a day to several years in some larger impoundments (Mendonça et al., 2012). With extended residence time, internal processes such as stratification and nutrient fluxes can influence reservoir water quality but if residence time is short, inflow from tributaries can have greater water quality impacts (Zhen-Gang, 2008). Water velocity is also reduced in reservoir headwaters resulting in reduced sediment carrying capacity and the retention of particulate matter transported by rivers (Mendonça et al., 2012). Terrestrial derived organic matter is continuously flushed into reservoir systems as they are typically constructed at the lower end of large drainage basins to ensure optimal inflow (Kahn et al., 2014; Mendonça et al., 2012). Due to this excessive availability of decomposable organic matter, reservoirs typically produce and emit greater emissions than natural systems, particularly in the first twenty years after flooding (Barros et al., 2011).

A key study in the quantification of GHG release from reservoirs was by St. Louis et al. (2000) where they examined an existing GHG flux dataset from the surface of 21 temperate and tropical reservoir sites worldwide and concluded that the reservoirs were in general, sources of CO₂ (average 220 – 4460 mg m² d) and CH₄ (average 3 – 1140 mg m² d) to the atmosphere. The potential for GHG production was shown by St. Louis et al. (2000) to differ from site to site, especially when comparing temperate with tropical reservoirs. Such high variability in GHG emissions is dependent on a variety of factors: i) between reservoirs e.g. reservoir morphology, catchment characteristics, latitude, and climate; ii) within reservoirs e.g. along longitudinal gradients from tributaries to the dam, and downstream of the dam; and iii) over time e.g. reservoir age, diurnal and seasonal variability, changes in anthropogenic related catchment activities, and with dam operation depending in precipitation and supply (Zhe Li et al., 2014; Mendonça et al., 2012; Tranvik et al., 2009). This has led to an irregular database of a large range of fluxes, primarily CH₄, with both potentially important areas and entire continents receiving limited study (Deemer et al., 2016; Diem et al., 2012; St. Louis et al., 2000; Sturm et al., 2014). For example, the temperate climate zone accounts for ~40% of total reservoirs (Barros et al., 2011) but quantification of reservoir emissions by number is limited (e.g. Deemer et al., 2016; DelSontro et al., 2010) and studies are focused on specific regions (e.g. USA, Canada, China, Brazil). The first global analysis of all three GHGs emitted from both lakes and impoundments found lake size and productivity to be important emission drivers (DelSontro et al., 2018). They also showed upscaled GHG emissions (1.25–2.30 Pg of CO₂-equivalents annually) were equivalent to ~20% of global fossil fuel CO₂ emissions (9.3 Pg C-CO₂ yr⁻¹). There also is still loose understanding and more research is needed on emissions

from the drawdown area, degassing from reservoir structural features (turbines and spillways), and the stream reach below the dam (Li and Zhang, 2014; Prairie et al., 2018). Consequently, due to significant knowledge gaps, emissions from reservoirs have been excluded from national GHG inventories (Bastien and Demarty, 2013; Forster et al., 2008; Sturm et al., 2014). Another large knowledge gap is the issue of carbon burial and how to determine the fraction that could be potentially considered an offset to GHG emissions from reservoirs (Prairie et al., 2018). Over the next century, aquatic productivity is expected to increase due to climate change and population growth, which in turn is expected to cause an increase in aquatic CH₄ emissions. In a recent paper by Beaulieu et al. (2019) eutrophication of lentic waters under different nutrient loading scenarios was stimulated and results showed that enhanced eutrophication will substantially increase CH₄ emissions (+30–90%) over the next century. Research presented in this thesis aims to quantify, compare and understand carbon and nitrogen concentrations and dynamics within temperate freshwater reservoirs across Scotland and North Wales. The overall aim is to improve understanding of temperate reservoir systems and determine how significant CO₂, CH₄ and N₂O concentrations and emissions are from reservoirs in Scotland and North Wales, particularly from peatland draining systems where C exports can be high.

1.1 Climate change and greenhouse gases

The climate system is warming, with many changes in physical and biological systems being seen, for example: ocean and atmospheric warming, global mean sea level rise, diminished ice and snow extents, and increasing concentrations of GHGs (Stocker et al., 2013). The atmosphere's radiative properties are strongly influenced by the abundance of well-mixed GHGs, mainly CO₂, CH₄ and N₂O. Altogether, CO₂, CH₄ and N₂O amount to 80% of the total radiative forcing from GHGs, and these gases also have different radiative properties which alter the degree of warming. The Global Warming Potential (GWP) is a metric used to quantify the different absorption capacities, scaling the warming potential of each gas relative to that of CO₂ (Forster et al., 2008; Stocker et al., 2013). For example, over a 100-year time horizon, CH₄ and N₂O have a GWP 34 and 298 times that of CO₂, respectively. Atmospheric concentrations of CO₂, CH₄ and N₂O in 2011 exceeded the range recorded in ice cores during the past 800 kyr (Stocker et al., 2013). The observed concentrations from these gases result from the dynamic balance between anthropogenic emissions, and the perturbation of natural processes that leads to their partial removal from the atmosphere (Ciais, P. et al., 2013). Biogeochemical cycles of CO₂, CH₄ and N₂O and the physical climate system are coupled, with emissions occurring from natural aquatic systems (e.g. rivers, lakes, wetlands, estuaries),

terrestrial systems (e.g. soils, forests) (Figure 1.1), and from anthropogenic sources (Cole et al., 1994; Tremblay et al., 2005).

Global CH₄ emissions can be biogenic, thermogenic or pyrogenic in origin, with sources from both natural processes and human activities (Ciais, P. et al., 2013). Most relevant in this thesis are biogenic sources which are produced in the final stages of organic carbon degradation, and are particularly prevalent in anoxic sediments of reservoirs and lakes (Emilsson et al., 2018; Eugster et al., 2011; Hertwich, 2013). In a recent global synthesis of GHG emissions from reservoir surfaces, estimated total CH₄ fluxes are 13.3 Tg CH₄-C yr⁻¹ (Deemer et al., 2016). Reservoirs are of particular concern as they tend to be of a higher trophic status (St. Louis et al., 2000). In terms of carbon units compared to CO₂ emissions (220 – 4460 mg m² d), inland water CH₄ emissions (3 – 1140 mg m² d) are smaller (data from the surface of 21 temperate and tropical reservoir studies compiled by St. Louis et al. (2000)). However, given the 34 times greater GWP of CH₄, studies quantifying reservoir emissions should include CH₄ (Sobek et al., 2012). Lakes and reservoirs may also act as sources or sinks of N₂O (Tranvik et al., 2009) but globally, only 58 reservoirs (Deemer et al., 2016) have data available on N₂O emissions despite having a much higher GWP than CH₄ (Guérin et al., 2008; Sturm et al., 2014; Tremblay et al., 2005). Studies have also shown that aquatic systems can be important N₂O sources, suggesting more research needs to integrate N₂O emissions (Beaulieu et al., 2015; Rosamond et al., 2012). In a first-order approximation of global N₂O emissions by inland waters using an upscaling approach, it is suggested that lakes and impoundments could be emitting 0.63 Tg of N₂O-N per year (Soued et al., 2015).

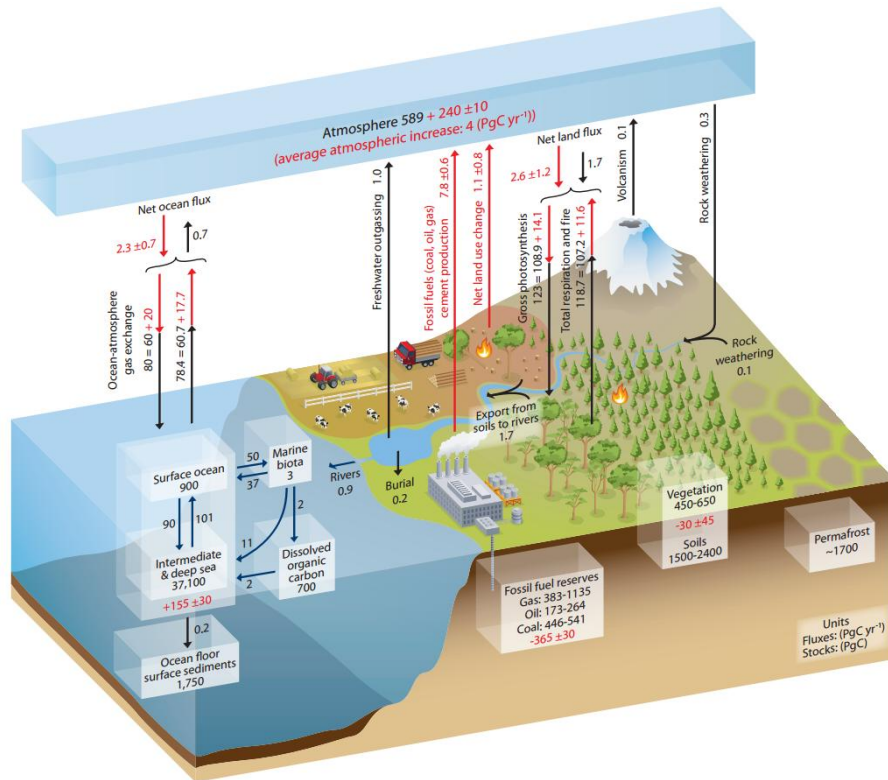


Figure 1.1 Diagram of the global carbon cycle, with numbers representing ‘carbon stocks’ in Pg C and the annual carbon exchange fluxes in Pg C yr⁻¹. Red arrows and numbers represent annual anthropogenic fluxes averaged over 2000-2009, whilst black numbers and arrows indicate reservoir mass and exchange fluxes estimates prior to c. 1750 (Ciais, P. et al., 2013).

1.2 Inland waters and the carbon cycle

At the regional scale, inland waters affect the climate through heat and water exchange with the atmosphere (Krinner, 2003). They also play a major role in the global carbon cycle (Figure 1.1) despite occupying a small surface area of the Earth (Cole et al., 2007; Hertwich, 2013). The Global Water Bodies database contains ~27 million water bodies larger than 0.01 km² which is approximately 3.5% of Earth’s nonglaciated land surface area (Verpoorter et al., 2014). Inland waters have been estimated to receive approximately 1.9 Pg C yr⁻¹ from the terrestrial landscape, where approximately 0.23 Pg is buried in sediments, 0.75 Pg is returned to the atmosphere, and the remaining 0.9 Pg is transported to the oceans (Cole et al., 2007). Uncertainty in such numbers exist with a similar study estimating that freshwaters receive 2.9 Pg C yr⁻¹, where 0.6 Pg goes to sedimentation and 1.4 Pg is emitted to the atmosphere (Tranvik et al., 2009). Reservoirs have been recognised as important carbon cycling ‘hotspots’, with some being important sinks for terrestrial-derived organic carbon, and a source of CO₂ from mineralisation (Abril et al., 2005; Dai et al., 2013). Reservoirs have also been predicted to be responsible for ~20% of total inland water CH₄ emissions (Bastviken et al., 2011). It is

recognised that GHG emissions are highest in early years and decrease as the initially present labile biomass and soil organic carbon degrades (Barros et al., 2011; Hertwich, 2013; Kelly et al., 1997; Rudd et al., 1993). Given the large amounts of carbon being processed, it is important to continue to improve the quantification of these fluxes to understand the global carbon cycle and climate system (Prairie et al., 2018; Tranvik et al., 2009). Carbon sources found in reservoirs are typically from i) submersion of soil and decayed plant materials following impoundment; ii) continual vegetation decay from water level fluctuation; and ii) organic matter input through catchment runoff (Dai et al., 2013; Tranvik et al., 2009).

There are also three major pathways of allochthonous and autochthonous carbon loss in reservoirs and lakes, the relative importance of each determining whether a given aquatic system is a GHG source or sink (Dai et al., 2013; Karlsson et al., 2007; Tranvik et al., 2009): i) dissolved organic carbon (DOC) and particulate organic carbon (POC) are transported from the water column to the sediment via organic carbon flocculation, integration into biological material, and sedimentation of particulate organic matter (POM); ii) photochemical and microbial processes degrade DOC and POC, leading to organic carbon mineralisation to CH_4 and CO_2 ; and iii) carbon compounds flowing downstream to other aquatic systems (Figure 1.2). Exceptions are highly eutrophic reservoirs which are CO_2 sinks regardless of age or latitude (Beaulieu et al., 2019; Roland et al., 2010).

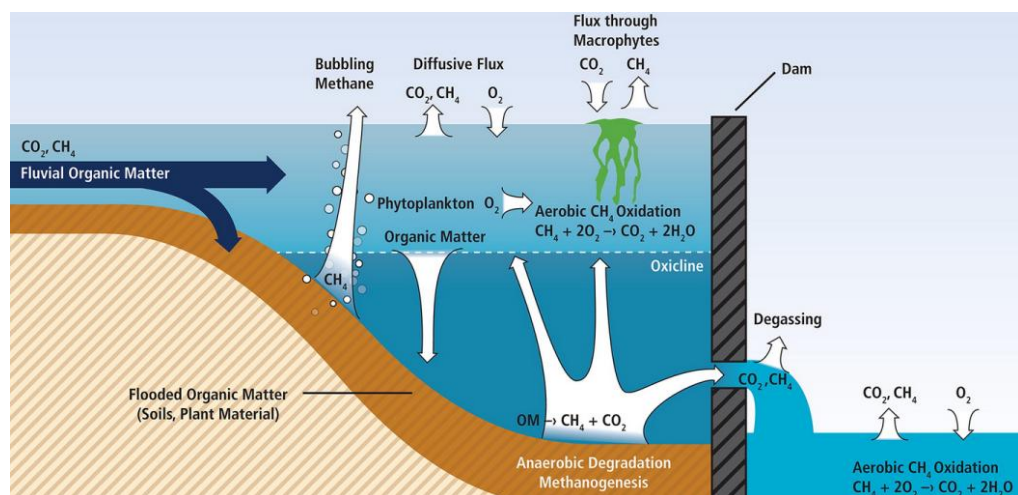


Figure 1.2 Possible biogenic CO_2 and CH_4 emission pathways from reservoirs (Hertwich, 2013; Kumar, A. et al., 2011).

Commonly the world's inland waters are supersaturated with dissolved CO_2 and CH_4 (Cole et al., 1994; Z. Li et al., 2014; Pighini et al., 2018; St. Louis et al., 2000), resulting from the balance of GHGs transported in and out of the aquatic system (Cole et al., 2007). Evasion of these

gases from water surfaces may represent a significant pathway for carbon loss (Hope et al., 2004; Kling et al., 1991) which is controlled by the gas transfer velocity (K) and gas concentration gradient (Cole et al., 1994). Estimates of CO_2 evasion from running waters varies widely, for example in Scottish peatland streams, estimates are between 21-806 $\mu\text{g m}^{-2} \text{s}^{-1}$ (Billett and Harvey, 2013; Dinsmore et al., 2010; Hope et al., 2001; Jovana. Kocic et al., 2015). In terms of total catchment budgets, stream and river CO_2 evasion contributions have been estimated to equal up to 70% of net annual carbon accumulation for peatlands (Hope et al., 2001).

Typically, GHG emissions rapidly increase after flooding, after which emission rates begin to reduce to values typical of natural aquatic systems (Demarty and Bastien, 2011; Kelly, 2001; Teodoru et al., 2011; Tremblay et al., 2005). In a study of flooded boreal reservoirs between 1991 and 2004, Tremblay et al. (2005) found GHG fluxes were typically 3-10 times higher than those in natural lakes at their maximum, usually 2-5 years after impoundment. They also showed emissions declined about 10 years post-impoundment. Galy-Lacaux et al. (1999) estimated that emissions would reach a steady state after ~ 20 years. In addition, a significant relationship between GHG emissions and age has been shown for temperate reservoirs (St. Louis et al., 2000) and for reservoirs globally (Barros et al., 2011).

Continual organic matter inputs from inflowing tributaries, phytoplankton production and plant regrowth during drawdown periods may become the main sources of organic carbon and subsequent emissions as reservoirs age (Fearnside, 2005; Hertwich, 2013; Roland et al., 2010). (Mendonça et al. (2012) found GHGs emitted from reservoir surfaces are not always produced within the system, as tributaries can export significant amounts of GHGs to reservoirs. Reservoirs are intrinsically linked to the rivers and streams that feed them (Baxter, 1977) in which water and sediment inputs are functions of catchment land-use (Burford et al., 2007; Kelly, 2001; Jovana Kocic et al., 2015).

In the UK, peatlands comprise a large proportion of the total soil C pool (~ 2302 Mt C), with most extensive areas in cooler and wetter (mainly upland) regions (Billett et al., 2010). Peatlands can also export carbon, mainly DOC, downstream to lakes and reservoirs through runoff (Evans et al., 2013; Jovana Kocic et al., 2015). Reservoirs located downstream of peatlands, especially those affected by erosion, accumulate organic matter in the sediments (Evans et al., 2013). DOC can be transported long distances downstream, whereas most fluvial CO_2 is rapidly lost to the atmosphere by evasion (Billett and Harvey, 2013). There are large uncertainties over the fate of DOC as well as its source within peatland ecosystems (Evans et

al., 2014). Streams and rivers associated with peatland systems have also been found to be supersaturated in CO₂ and CH₄ (Dinsmore and Billett, 2008; Hope et al., 2001; Wallin et al., 2011) which provides an indication of the aquatic system degassing potential (Billett et al., 2015). Although N₂O supersaturation is less common, due to the large GWP, even small evasion losses could contribute significantly to catchment GHG budgets (Dinsmore et al., 2013) gases are lost from the aquatic pathway as surface water gas concentrations gradually equilibrate with lower atmospheric concentrations (Billett et al., 2015). In addition to fluvial inputs from the catchment area, CO₂ can also enter lakes and reservoirs through direct groundwater inputs (Striegl and Michmerhuizen, 1998). The location of soil types within the catchment also influence stream water concentrations, for example, biogenic CO₂ concentrations are generally higher where organic soils, rather than mineral, form alongside stream channels (Wallin et al., 2011).

Streams and lakes have been studied separately due to limited integrated research, and because physical atmospheric gas exchange and oversaturation drivers are usually system specific (Jovana. Kokic et al., 2015). Such lack of connectivity between studies deters understanding of inland water C dynamics at landscape scales. Past research has focussed more on lakes and reservoirs since they cover a larger area of Earth's surface (Algesten et al., 2004) but recently, studies have provided evidence that streams also have a significant influence on C dynamics (Crawford et al., 2013; Lundin et al., 2013; Marescaux et al., 2018). For example, fluvial stream networks have been found to be important for CO₂ evasion in the U.S. (Butman and Raymond, 2011) and for small-order streams (Raymond et al., 2013). Wallin et al. (2013) showed that stream CO₂ evasion in a boreal catchment surpassed fluvial downstream DOC and DIC transport. Even at small spatial scales, Jovana Kokic et al. (2015) showed that CO₂ evasion from headwater systems of a boreal lake catchment can be the dominant C loss pathway in the aquatic continuum. Streams of the Lake Gäddejärven catchment covered ~0.1% of the catchment area but were responsible for an atmospheric C loss greater than the sum of all C losses from the lake, which includes CO₂ evasion and DOC/DIC export via the outlet. Higher stream evasion rates can often be explained by higher turbulence from the flowing water, increasing the gas exchange ability (Teodoru et al., 2011). At the global scale, streams and rivers have been estimated to evade up to six times more CO₂ to the atmosphere than lakes and reservoirs (Raymond et al., 2013). However, small low-order streams are difficult to integrate into global CO₂ evasion estimates as knowledge of their area and K is limited (Cole et al., 2007; Jovana Kokic et al., 2015). It has become increasingly important to

integrate and compare studies, which investigate C dynamics at small spatial scales for reservoirs, lakes and streams.

DOC influences water quality through the transport of metals and nutrients, and also affects pH. Water supply companies have been known to remove DOC to meet drinking quality standards (Clark et al., 2007; Driscoll et al., 1989; A. Stimson et al., 2017). DOC input has also been found to positively correlate with reservoir CO₂ and CH₄ emissions (Barros et al., 2011). POC typically represents a small proportion of the total aquatic flux (Dinsmore et al., 2013), reaching less than 100 g C m⁻² yr⁻¹ in eroding systems (Evans et al., 2006; Pawson et al., 2012). In terms of export rates, typically POC fluxes are episodic and highly variable (Dinsmore et al., 2010) due to linkages with high flow events, creating quantification difficulties (Dinsmore et al., 2013). Dissolved inorganic carbon (DIC) is mainly derived from the bedrock-soil system and controlled by processes such as drawdown, weathering, organic matter decomposition, root respiration, or produced in-stream from either terrestrial or aquatic-derived substrate decomposition (Billett et al., 2007; Hope et al., 2004; Johnson et al., 2007).

1.2.1 Greenhouse gas emission pathways

There are several possible fates of GHGs produced in reservoirs (Figure 1.2) and it is important to quantifying reservoir emissions from all pathways (Hertwich, 2013; Prairie et al., 2018; Tranvik et al., 2009). Emissions can occur through molecular diffusion at the water-air interface of reservoir surfaces (e.g. Mosher et al., 2015; Roland et al., 2010). Diffusive fluxes of CO₂, CH₄ and N₂O are dependent on a concentration gradient and on gas solubility in water, which according to Le Chatalier's principle, is negatively related to temperature and positively related to pressure (Mendonça et al., 2012). Therefore, GHG emissions through diffusion tend to be greater in reservoirs located at lower altitudes and in warmer regions. Diffusion is also dependent on wind speed and rainfall (Hertwich, 2013). Reservoir surfaces are typically dominated by diffusive CO₂ fluxes due to oxidation of diffusive CH₄ by methanotrophic bacteria above the anoxic-oxic layer interface (Barros et al., 2011). CH₄, and any other gases can also be emitted via diffusion through plant stems but this pathway has also received little attention in reservoir studies (Bastviken et al., 2011; Bolpagni et al., 2017; Tranvik et al., 2009). It is also important to consider waterbodies inflowing to the reservoir as they can add considerable amounts of dissolved GHGs to the epilimnion, which influences diffusive surface fluxes (Diem et al., 2012; Kokic et al., 2015).

Bubbles (ebullition), is a second major emission pathway, produced at the anoxic sediment-water interface where they migrate through the water column and into the atmosphere (Beaulieu et al., 2017; DelSontro et al., 2016; Hertwich, 2013). Ebullition is related to

temperature and the hydrostatic pressure in the water column (Harrison et al., 2017; Hertwich, 2013) and is dominated by CH₄ due to its low water solubility (DelSontro et al., 2010; McGinnis et al., 2016). The bubbles can be of varying sizes but typically 2-8 millimetres. In deeper systems (>40 meters), bubbles usually dissolve during the rise through the water column due to oxidation exposure by aquatic methanotrophs (Harrison et al., 2017; McGinnis et al., 2016; Sobek et al., 2012). Methane ebullition is commonly captured when released from shallow sediments (<10 meters) as aquatic CH₄ oxidizers are bypassed, resulting in high atmospheric CH₄ emissions. In addition, studies have also demonstrated that ebullition can occur from deeper regions of reservoirs (DelSontro et al., 2010; Harrison et al., 2017; Rosa et al., 2004). Factors controlling CH₄ ebullition release in aquatic systems are relatively well understood (Bastviken et al., 2011, 2004) but ebullition quantification remains underestimated largely due to its stochastic nature (Beaulieu et al., 2017; DelSontro et al., 2011; Harrison et al., 2017). This is a result of numerous environmental factors influencing its spatial and temporal variability (Eugster et al., 2011), for example, temperature and levels of organic carbon input directly impact methanogenesis rates and therefore, most likely control the probability of ebullition occurring (Bastviken et al., 2004). Lake Wohlen is a small temperate (2.5 km²), shallow (9m mean depth), run of the river Swiss hydropower reservoir (constructed in 1920) that has been extensively studied (e.g. DelSontro et al., 2010; Eugster et al., 2011; Sobek et al., 2012). Lake Wohlen on average emits ~86 mg CH₄ m⁻² d⁻¹ via ebullition alone (DelSontro et al., 2010; Sobek et al., 2009). Lake Wohlen has been found to typically exceed ebullition in boreal, tropical and other temperate reservoirs (St Louis et al., 2000; Abril et al., 2005; DelSontro et al., 2010). Globally, temperate reservoirs are often an overlooked source of CH₄, particularly since larger reservoirs are more commonly located in tropical regions where temperatures support year round methanogenesis (St Louis et al., 2000; Sobek et al., 2009). For example, the global synthesis study Deemer et al. (2016), ebullition measurements were included at only 75 (out of 267) reservoirs worldwide, 11 of which were in Europe and 23 in North America.

The science of reservoir GHGs has considerably matured in recent years, but there are still fluxes that are only loosely constrained and for which active research is required, such as in the following pathways (Prairie et al., 2018). Downstream of the reservoir dam, GHGs can be emitted by turbulent degassing as water passes through turbines, becoming a GHG source, though more common in hydropower reservoirs (Mendonça et al., 2012; Rosa et al., 2004; Tremblay et al., 2005). The water inlet and spillway depths are generally located in lower to medium depths of the reservoir, where large amounts of CH₄ are produced in anoxic environments. As water is drawn from deeper layers, the process of CH₄ oxidation in the water

column is evaded (Rosa et al., 2004; Abril et al., 2005; Tranvik et al., 2009). There is a sudden drop in hydrostatic pressure as CH₄ rich water emerges from the turbines and spillway, with much of the gas dissolved in the water being rapidly released to the atmosphere (Rosa et al., 2004; Tranvik et al., 2009; Mendonça et al., 2012). In addition, diffusive flux and ebullition of CO₂ and CH₄ also occur across the air-water interface in the river outflow or spillway downstream of the dam (Mendonça et al., 2012; Tranvik et al., 2009; Tremblay et al., 2005).

In many systems, water-level fluctuations leave periodically exposed surface areas known as drawdown zones. A growing number of studies are now reporting GHG emissions from these zones (Deshmukh et al., 2018; Harrison et al., 2017; Li et al., 2016a; Yang et al., 2015) but it is important to continue to quantify emissions, especially if flooding and droughts are expected to become more frequent from climate change (Prairie et al., 2018). Enhanced emissions can occur when the hydrostatic pressure is reduced, a result of current-induced bottom shear stress from the lowering of water storage levels (Ostrovsky et al., 2008). The reported measurements have shown large variation in fluxes, for example, CH₄ can range from small to significant sources (Serça et al., 2016; Yang et al., 2012), and even CH₄ sinks (Li et al., 2016). High emissions could potentially be minimised by preventing prolonged exposure of reservoir sediments to the atmosphere during drawdown periods (Evans et al., 2013).

1.2.2 Mineralisation, Sedimentation and GHG emissions

River segmentation and disruption from the creation of dams change bed load, suspended particle and organic matter transport, leading to an accumulation behind the dam wall (St Louis et al., 2000; Maeck et al., 2013). Covering only 3% of continents, inland waters bury ~50% more carbon than the oceans and emit ~1.4 Pg of C yr⁻¹ in gaseous form to the atmosphere (Tranvik et al., 2009). Reservoir sediments were estimated to accumulate 0.16-0.2 Pg of organic carbon annually (Dean and Gorham, 1998) which is more than what is buried in lakes (Cole et al., 2007).

Organic-rich sediments in reservoirs and lakes are 'hotspots' for methanogenesis since conditions are typically anoxic below the surface layer. They show low concentrations of electron acceptors for anaerobic respiration, and receive a continuous supply of particulate organic matter from terrestrial sources and internal primary production (Bastviken et al., 2004). Once organic matter is in reservoir sediments, it can become i) mineralised by aerobic or anaerobic bacteria and released as CO₂ and CH₄ in the water column; ii) re-suspended; or iii) remain buried (Aberg et al., 2004; Mendonça et al., 2012; Sobek et al., 2012; Emilson et al.,

2018). Each of these processes is system-specific and will influence whether the reservoir is an overall net sink or source of atmospheric GHGs (Mendonça et al., 2012).

Aerobic mineralisation is limited to the upper sediment layer (Mendonça et al., 2012), where the layer thickness varies depending on factors such as: hypolimnetic oxygen concentrations, the oxygen diffusion coefficient at the sediment-water interface, and oxygen consumption rates during organic matter mineralisation. Below this top oxygenated layer, anaerobic processes dominate sediment metabolism, which produce both CH₄ and CO₂. These gases accumulate in the sediment pore-water and are typically released to the water column (Abril et al., 2005; Mendonça et al., 2012; Sturm et al., 2014; Emilson et al., 2018). In stratified reservoirs, O₂ consumption from organic matter mineralisation in bottom layers is no longer offset by water exchange from the top oxygenated layers (Mendonça et al., 2012). This gradually causes bottom water layers to become anoxic. Under these conditions methanogenic bacteria metabolise organic compounds, hydrogen and CO₂ into CH₄ (methanogenesis), which leads to high CH₄ concentrations in reservoir bottom layers (Abril et al., 2005; Sturm et al., 2014). Zones within a reservoir may also contain large gradients in dissolved oxygen availability, for example the metalimnion under stratified conditions or the upper layers of shallow sediments, and promote oxidation of dissolved CH₄ via methanotrophic bacteria (Guérin and Abril, 2007) which can significantly reduce diffusive emissions from the reservoir surface (Sturm et al., 2014). The extent of CH₄ oxidation is dependent on oxygen availability so can be higher in deeper reservoirs (Lima, 2005).

In organic-rich sediments, high mineralisation rates combined with the hydrophobic characteristics of CH₄, can result in ebullition and rapid atmospheric emission release (Bastviken et al., 2004). Mendonça et al. (2012) found that GHG production is small overall in reservoir water columns compared to production in sediments. There have been recent advances in understanding organic carbon fate in freshwater sediments but significant knowledge gaps remain (Sobek et al., 2009; Sobek et al., 2012; Emilson et al., 2018). For example, the proportion of sediment organic carbon converted to CH₄ and released to the atmosphere is difficult to predict (Sobek et al., 2012) as CH₄ is emitted by diffusion but also ebullition which is stochastic (Bastviken et al., 2004). Despite the importance of sediment for organic matter mineralisation and GHG production, more research is still required for sediment fluxes (Abe et al., 2005; Åberg et al., 2004; Emilson et al., 2018).

Production and consumption of N₂O is also linked to zones where large dissolved oxygen gradients occur (Sturm et al., 2014). Under oxic conditions, N₂O is mainly produced as a by-

product of nitrification. At the oxic-anoxic boundary, N_2O is produced by denitrification. Denitrification products are N_2O and N_2 , and their emission ratios depending on the redox status of the system, with increasing N_2 production as O_2 concentrations decline (Mengis et al., 1997). This oxic-anoxic boundary can be found in the water column of stratified reservoirs. In well-mixed systems or at shallower sites, dissolved oxygen can reach the sediment surface, resulting in N_2O production in either the water column or the upper sediment layers (Sturm et al., 2014).

1.2.3 Additional factors driving C dynamics and GHG emission processes

There are a variety of additional factors which can also influence GHG emissions from reservoirs. Thermal stratification is triggered by water density differences, which leads to water layer formations, the epilimnion (top), metalimnion (middle) and hypolimnion (bottom) (Mendonça et al., 2012). Once these layers form, there is no mixing between the top and bottom unless stress such as wind, increased inflows or temperature shifts, can break water column stability. Stratification affects oxygen dynamics and thus reservoir GHG emissions. In reservoirs, velocity, suspended matter and available nutrients gradually decrease downstream, whilst light penetration, vertical stratification and internal nutrient cycling increases (Zhen-Gang, 2007). Changes in light penetration to depth are also a direct effect of high water colour. Photosynthesis in reservoirs is typically performed by light-limited phytoplankton due to the deep water column. For example, in eutrophic reservoirs (high nutrient concentrations and phytoplankton production) photosynthesis can greatly reduce CO_2 concentrations causing the reservoir to become an atmospheric CO_2 sink (Mendonça et al., 2012). Barros et al. (2011) observe this in reservoirs across the globe but reservoirs acting as carbon sinks are very few compared to those acting as CO_2 sources.

In addition to vertical stratification, reservoirs can display significant longitudinal gradients in water quality and hydrodynamic variables due to upstream inflows and a downstream outflow (Zhen-Gang, 2007). Generally, reservoirs have three distinct zones: i) the riverine zone is typically narrow but well mixed, with greater advection and where the flow can still transport substantial quantities of suspended particles; ii) the transition zone sees the water surface slope decreasing resulting in reduced velocities and suspended particles settling, and buoyancy forces become more significant due to density differences between inflows and lake waters; and iii) the lacustrine zone has characteristic lake-like conditions, particularly in the fore bay behind the dam, where buoyancy forces dominate flow patterns and suspended particles are generally low due to low flow velocities and deep waters (Zhen-Gang, 2007; Zheng et al., 2011; Mendonça et al., 2012).

Furthermore, precipitation, temperature and wind influence reservoir spatial and temporal variability, which in turn influences the rate of gas exchange from the water-atmosphere interface (Eugster et al., 2011; Mendonça et al., 2012; Bastien and Demarty, 2013; Hertwich, 2013). Wind is an important control on water movement within reservoirs and lakes; it can create turbulence, surface and internal waves, and horizontal and vertical currents (Zhen-Gang, 2007; Mendonça et al., 2012). Such processes are influenced by a variety of factors, including: morphological basin characteristics, surrounding terrain, fetch, wind direction and temperature. Reservoirs can develop complex circulation patterns due to their dendritic geometry, for example, dissolved compounds can be transported by deep water circulation (Mendonça et al., 2012). In summer months, reservoirs are highly temperature stratified and weakly forced by wind, whereas in spring and winter, higher wind velocities can enhance mixing processes.

Precipitation can vary annually in frequency and intensity and can also produce diverse seasonal patterns that alter water residence time and shift the intensity of environmental processes occurring within the water column (Mendonça et al., 2012). Previous studies have also shown that lateral aquatic carbon export is biased towards high flow events (Dinsmore and Billett, 2008; Dyson et al., 2011). Increases in storm frequency or intensity are also likely to impact total CO₂ export from soils to surface waters (Dinsmore et al., 2013). Understanding stormflow GHG dynamics has become increasingly important to accurately quantify and predict catchment carbon losses via the aquatic pathway.

Temperature changes can directly and indirectly affect processes involved in reservoir GHG production, consumption and emission (Mendonça et al., 2012). For example, primary production (Flanagan et al., 2003) and respiration (Sand-Jensen et al., 2007) are considerably influenced by temperature. Damming can also cause increased surface water temperatures, providing an opportunity for biomass growth and nutrient absorption (Hertwich, 2013). Reservoirs in warmer latitudes typically have higher GHG emissions (Barros et al., 2011) linked to greater mineralisation and less carbon burial in sediments (Gudasz et al., 2010). It is likely, especially in colder and temperate regions, that reservoir GHG emissions will increase based on IPCC global temperature change scenarios (Mendonça et al., 2012).

1.3 Emission estimates from previous research

Early GHG emission studies focused on CO₂ and CH₄ surface fluxes from hydroelectric reservoirs (e.g. Rudd et al., 1993; Kelly et al., 2001;) as they were broadly regarded as carbon-free energy sources. Research has focused on reservoirs in Canada (e.g. Rudd et al., 1993),

Brazil (e.g. Fearnside, 2005) and more recently, Finland (Bergström et al., 2007; Huttunen et al., 2002), Switzerland (e.g. Diem et al., 2012) and China which has some of the world's largest reservoirs (Chen et al., 2009; Li and Zhang, 2014; Wang et al., 2006; Zheng et al., 2011). Table 1.1 displays a variety of flux and ebullition results from some reservoir and lake studies.

In an early study by Rudd et al. (1993), it was hypothesised that reservoir GHG production was not zero and could be dependent on the amount of organic carbon flooded during reservoir creation. This initiated the Experimental Lakes Area Reservoir Project (ELARP), which aimed to create a reservoir in a controlled manner and quantify net change in GHG fluxes as a result of flooding (Kelly et al., 1997; St Louis et al., 2000). Results showed that on average, the wetland was a carbon sink of $6.6 \text{ g C m}^{-2} \text{ yr}^{-1}$ before the flooding. After flooding, it became a large carbon source of $120 \text{ g CO}_2 \text{ m}^{-2} \text{ yr}^{-1}$ and $9 \text{ g CH}_4 \text{ m}^{-2} \text{ yr}^{-1}$ (Kelly et al., 1997). Similarly, in Canada, three boreal upland areas with varying amounts of organic carbon stored in vegetation and soils were flooded for five years via the Flooded Upland Dynamics Experiment (FLUDEX) (Matthews et al., 2005). During the first three years, the flooded soils and forests became net sources of both CO_2 and CH_4 to the atmosphere, with a peak in CH_4 ebullition in the third year and net DIC production declined noticeably over the five years.

St Louis et al. (2000) published the first global estimate of GHG emissions from the surface of reservoirs at approximately $321 \text{ Tg C m}^{-2} \text{ yr}^{-1}$ ($273 \text{ Tg CO}_2 \text{ m}^{-2} \text{ yr}^{-1}$ and $48 \text{ Tg CH}_4 \text{ m}^{-2} \text{ yr}^{-1}$). When the GWP of CH_4 is considered, these emissions correspond to $2600 \text{ Tg CO}_2\text{-eq yr}^{-1}$ (Mendonça et al., 2012). Average fluxes of $1400 \text{ mg m}^{-2} \text{ d}^{-1}$ of CO_2 and $20 \text{ mg m}^{-2} \text{ d}^{-1}$ of CH_4 were also estimated from 21 temperate reservoirs across Canada, US and Finland which ranged widely in age (1-73 years) and size ($0.2\text{-}2500 \text{ km}^2$) (St Louis et al., 2000). In another key assessment of GHG emissions compiled from 85 hydroelectric reservoirs (covering ~20% of the global area occupied by hydroelectric reservoirs), it was estimated that globally emissions were 51 Tg C yr^{-1} ($48 \text{ Tg CO}_2 \text{ yr}^{-1}$ and $3 \text{ Tg CH}_4 \text{ yr}^{-1}$ or $288 \text{ Tg CO}_2\text{-equ yr}^{-1}$) (Barros et al., 2011). Compared to the estimate by St Louis et al. (2000), this figure is lower but can be explained by the smaller area occupied by hydroelectric reservoirs ($350,000 \text{ km}^2$ compared to the $1,500,000 \text{ km}^2$ from all reservoir types) and the bias of more limited data. Barros et al. (2011) also showed emissions to correlate with latitude and reservoir age, with highest emission rates in the Amazon.

In a revised assessment of GHG emissions from hydropower reservoirs through consideration of the drawdown zone, surface area and downstream degassing, total CO_2 emissions were estimated at $301.3 \text{ Tg CO}_2 \text{ yr}^{-1}$ (Li and Zhang, 2014). This is 1.7 times higher than Barros et al. (2011) but approximate to Hertwich (2013) at $278.7 \text{ Tg CO}_2 \text{ yr}^{-1}$. Total CH_4 emissions were

estimated at 13.3 Tg CH₄ yr⁻¹ (Li and Zhang, 2014), which is three times higher than the Barros et al. (2011) estimate. The sum of downstream and drawdown emissions were thought to represent 42% of CO₂ and 67% of CH₄ total emissions, both of which are generally overlooked. Such results suggest more data are required on drawdown and downstream emissions for greater accuracy in reservoir GHG emission quantification (Li and Zhang, 2014).

In a recent global synthesis of GHG emissions from reservoir surfaces, estimated total fluxes were 13.3 Tg CH₄-C yr⁻¹, 36.8 Tg CO₂-C yr⁻¹ and 0.03 Tg N₂O-N yr⁻¹ (Deemer et al., 2016). This study estimated that GHG emissions from reservoir water surfaces account for 0.8 (0.5–1.2) Pg CO₂ equivalents per year, with the majority of this forcing due to CH₄. Factors linked to reservoir productivity were also found to better explain emission predictors than e.g. age and latitude as per the study by Barros et al. (2011). As previously mentioned, aquatic systems are also considered a source of N₂O emission, however estimates are mainly from streams and rivers (Venkiteswaran et al., 2014) and knowledge still remains limited on lake and reservoir N₂O emissions (Beaulieu et al., 2015; Guérin et al., 2008). A first-order approximation of global N₂O emissions by inland waters using an upscaling approach suggested that lakes and impoundments could be emitting 0.63 Tg of N₂O-N per year (Soued et al., 2015).

Across temperate European studies, Deemer et al. (2016) also found a total of 31 reservoirs (out of 267 reservoirs worldwide) to have GHG emission estimate data. Despite a growing spatial coverage of GHG flux measurements, they identified that in many regions, few measurements remain and that there are currently threefold and fourfold more reservoirs with CO₂ estimates than for CH₄ (ebullition and diffusion) and N₂O, respectively. For example, no studies were identified for UK reservoirs so their contribution as GHG emitters is not recognised. Emission studies here would shed light on this underappreciated region, which is important for inclusion in global GHG estimates.

Most recently, DelSontro et al. (2018) presented the first global analysis of all three GHGs emitted from both lakes and impoundments, and found lake size and productivity to be important drivers of emissions. They also showed that the upscaled GHG emissions (1.25–2.30 Pg of CO₂-equivalents annually) are equivalent to ~20% of global fossil fuel CO₂ emissions (9.3 Pg C-CO₂ yr⁻¹). With continued eutrophication, emissions are expected to rise further, DelSontro et al. (2018) estimated this could lead to a 5-40% increase in the GHG effects to the atmosphere i.e. adding the equivalent effect of another 13% of fossil fuel combustion. Over the next century, aquatic productivity is expected to increase due to climate change and population growth, which in turn will cause an increase in aquatic CH₄ emissions. In a recent

paper by Beaulieu et al. (2019), eutrophication of lentic waters under different nutrient loading scenarios was stimulated and results showed enhanced eutrophication will substantially increase CH₄ emissions (+30–90%) over the next century. Such an increase in CH₄ emission has an atmospheric impact of 1.7–2.6 Pg C-CO₂-eq y⁻¹, equivalent to 18–33% of annual CO₂ emissions from fossil fuel burning.

Studies also began taking a more holistic approach, incorporating emission pathways from turbines and downstream of the dam (Mendonça et al., 2012). More research is still required to estimate the magnitude of downstream emissions from reservoirs, especially those that are stratified (Prairie et al., 2018). For example, Galy-Lacaux et al. (1997) began a 10-year emission study of the tropical Petit Saut reservoir and showed downstream degassing can represent a major CH₄ pathway. Temperate reservoirs have also been found to have high emissions downstream of the dam but there remains scope for further study on this point (Abril et al., 2005; Roehm and Tremblay, 2006; Soumis et al., 2004). An increasing number of studies have also shown that streams have important landscape scale impact on C budgets (e.g. Crawford et al., 2013) but integrative inland water studies which combine GHG measurements across lentic and lotic systems still remain limited (e.g. Kocic et al., 2015, Marescaux et al., 2018). Aquatic ecosystems have a unique dual role in that they can simultaneously act as a carbon source to the atmosphere while accumulating and storing carbon in sediments. Another large knowledge gap is the issue of carbon burial and how to determine the fraction that could be potentially considered an offset to GHG emissions (Prairie et al., 2018).

A variety of studies also focused on quantifying CH₄ emissions from reservoirs, for example, total CH₄ emissions from an old temperate reservoir, Lake Wholen in Switzerland, were estimated at 43 g C m⁻² yr⁻¹, mostly in the form of ebullition and a strong correlation was also found with temperature (DeSontro et al., 2010). This is approximately an order of magnitude higher than the range of CH₄ emissions reported from temperate reservoirs (4.6–5.5 g C m⁻² yr⁻¹) (Bastviken et al., 2011; St. Louis et al., 2000), lakes (3.2 g C m⁻² yr⁻¹) (Bastviken et al., 2011) and within the range reported from tropical reservoirs (37–82 g C m⁻² yr⁻¹) (Bastviken et al., 2011; Soumis et al., 2004; St. Louis et al., 2000). This suggests that temperate reservoirs can be an important but overlooked source of atmospheric CH₄ (DeSontro et al., 2010). In a later study by Sobek et al. (2012), it was discussed that Lake Wholen acts as a strong organic carbon sink and CH₄ source because of very high sedimentation rates supplying reactive organic matter to deep, anoxic sediment layers, stimulating methanogenesis and CH₄ ebullition from the sediment.

The science of reservoir GHG has considerably matured in recent years, however, there are still fluxes that are only loosely constrained and for which active research is required. In many systems, water-level fluctuations leave periodically exposed surface areas known as drawdown zones. A growing number of studies are now reporting GHG emissions from the drawdown zones (e.g. Yang et al., 2015, Li et al., 2016, Harrison et al., 2017, Deshmukh et al., 2018). The reported measurements have shown large variation in fluxes, with CH₄ ranging from small to significant sources (Yang et al., 2012, Serca et al., 2016), and in some studies, even CH₄ sinks (Li et al., 2016). Studies on the Three Gorges Reservoir in China have also included drawdown zone N₂O emission measurements; for example, mean sediment N₂O flux has been estimated at 3.6 mg m⁻² d⁻² (Li et al., 2016). It is important to continue measuring emissions from drawdown zones, especially if predicted changes in precipitation patterns from global warming, will affect both the frequency and magnitude of extreme events like droughts and flooding, influencing the C and N balance of aquatic systems.

Table 1.1 CO₂, CH₄ and N₂O fluxes from the surface of temperate and boreal reservoirs. Values stated are either mean and/or (range) of flux.

Location	Reservoir/Lake	Year Flooded	Diffusive flux (mg m ⁻² d ⁻¹)		N ₂ O Diffusive flux (µg m ⁻² d ⁻¹)	CH ₄ Ebullition flux (mg CH ₄ m ⁻² d ⁻¹)	References
			CO ₂	CH ₄			
Canada	La Grande-2	1978	2313 (100-11,966)	(0.5-53)			Duchemin et al. (1995)
	3 Québec lakes	-				17.6	DeSontro et al. (2016)
	224 Québec lakes	-		2-49 (0.04-246)			Rasilo et al. (2015)
	Eastmain-1, Québec	2006	2426 (-4-19,676)	0.77 (-0.04-8.18)			Demarty et al. (2009)
	Robert-Bourassa, Québec	1979	661 (45-6509)	0.14 (-0.09-2.56)			Demarty et al. (2009)
	Rivière-des-Prairies, Québec	1929	665 (-234-9380)	0.49 (-0.05-6.38)			Demarty et al. (2009)
	26 Ontario/Québec reservoirs	1927-1998	1508 (-3408-16,720)	8.8 (-25.7-724.9)	100 (-1380-1570)		Tremblay et al. (2005)
	15 British Columbia	1911-	198 (-1786-3666)	42.1 (-6.8-347.7)	50 (-1220-		Tremblay et al. (2005)

Location	Reservoir/Lake	Year Flooded	Diffusive flux (mg m ⁻² d ⁻¹)		N ₂ O Diffusive flux (μg m ⁻² d ⁻¹)	CH ₄ Ebullition flux (mg CH ₄ m ⁻² d ⁻¹)	References
			CO ₂	CH ₄			
	reservoirs	1979			1390)		
Poland	Solina	1968	-914.5-648.26	0			Gruca-Rokosz et al. (2011)
	Rzeszów	1973	2042.5-7152	(737.63-3860)		0.16-2.27	Gruca-Rokosz et al. (2011)
	Wilcza Wola	1988	3894-4162.4	(31.92-452.72)		0-3.84	Gruca-Rokosz et al. (2011)
	Lokka	1967	1972.8 (-672-6120)	33.3 (-6.2-244)	92.6 (-14-507)	46.4 (0-186)	Huttunen et al. (2002)
	Porttipahta	1970	1536 (1512-3456)	3.5 (-2.0-7.6)	115.25(-260-173)	0.8 (0-8.0)	Huttunen et al. (2002)
Switzerland	Lake Wohlen	1920		1.5 (0.1-4)		1000 (0-5758)	DeSontro et al. (2010)
	Lake Klöntal			1.7-2.2			Sollberger et al. (2017)
	Lake Wohlen	1920	962.33 (276-1558)	1.53	72		Diem et al. (2012)
	Lake Gruyère	1947	979	0.15			Diem et al. (2012)

Location	Reservoir/Lake	Year Flooded	Diffusive flux ($\text{mg m}^{-2} \text{d}^{-1}$)		N_2O Diffusive flux ($\mu\text{g m}^{-2} \text{d}^{-1}$)	CH_4 Ebullition flux ($\text{mg CH}_4 \text{m}^{-2} \text{d}^{-1}$)	References
			CO_2	CH_4			
	Lake Lungern	1920	242	0.13	50		Diem et al. (2012)
	Lake Zeuzier	1957		0.065	-27		Diem et al. (2012)
	Lake Santa Maria	1968		0.316			Diem et al. (2012)
U.S.A	Douglas Lake	1943	(236- 18,806)	(0-0.95)			Mosher et al. (2015)
	Fontana	1944	994	6			Bevelhimer et al. (2016)
	Guntersville	1939	1796	21			Bevelhimer et al. (2016)
	Hartwell	1962	1168	23			Bevelhimer et al. (2016)
	Watts Bar	1942	2760	8			Bevelhimer et al. (2016)
	Harsha Lake	1978		48 (9.4-162)		775	Beaulieu et al. (2017)
	6 Pacific NW Reservoirs	-				42 (0-719)	Harrison et al. (2017)
	F.D. Roosevelt	1942	-462 (-852-251)	3.2 (1.6-8.2)			Soumis et al. (2004)
	Dworshak	1973	-1195 (-2278 to -	4.4 (0.6-14.8)			Soumis et al. (2004)

Location	Reservoir/Lake	Year Flooded	Diffusive flux ($\text{mg m}^{-2} \text{d}^{-1}$)		N_2O Diffusive flux ($\mu\text{g m}^{-2} \text{d}^{-1}$)	CH_4 Ebullition flux ($\text{mg CH}_4 \text{m}^{-2} \text{d}^{-1}$)	References
			CO_2	CH_4			
			720)				
	Wallula	1954	-349 (-1629-1060)	9 (3.5-17.0)			Soumis et al. (2004)
	Oroville	1968	1026 (266-2430)	4.2 (1.1-10.5)			Soumis et al. (2004)
	New Melones	1979	-1186 (-3415 to -275)	7.1 (2.7-6.4)			Soumis et al. (2004)
China	Three Gorges Reservoir	2008		6.24 (-2.4-53.5)			Chen et al. (2009)
	Three Gorges Reservoir	2008	4268	7.22	0.529		Zhao et al. (2013)
	Nihe	-	173.6				Li et al. (2015)
	Baihua	1960	1056 (-352.1-3388.7)				Wang et al. (2006)
Germany	Rappbode and Hassel Reservoirs	1959-1960	(-1056.2-4268.92)				Halbedel and Koschorreck (2013)

Location	Reservoir/Lake	Year Flooded	Diffusive flux ($\text{mg m}^{-2} \text{d}^{-1}$)		N_2O Diffusive flux ($\mu\text{g m}^{-2} \text{d}^{-1}$)	CH_4 Ebullition flux ($\text{mg CH}_4 \text{m}^{-2} \text{d}^{-1}$)	References
			CO_2	CH_4			
	5 River Saar reservoirs	1976-2000		4.71		127	Maeck et al. (2013)
France	Eguzon reservoir	1926		16.68	779		Descloux et al. (2017)
UK	Priest Pot (natural lake)	-	1760.38 (172-4488.97)	6.42 (0.963-22.5)		192.5 (0.00-1739)	Casper et al. (2000)

1.4 Conclusions and future research needs

Inland waters play an important role in landscape C budgets by acting as both C sources to the atmosphere through evasion of GHGs such as CO₂, CH₄ (and N₂O), but also as sinks through C burial in reservoir and lake sediments (Bastviken et al., 2011; Kling et al., 1991; Tranvik et al., 2009). In lakes, reservoirs and streams, the terrestrial load of organic matter fuels microbial processes, affects stratification, light penetration and oxygen, and thus further modulates the mineralisation and C outgassing processes (Bastviken et al., 2004; Sobek et al., 2005). Despite evidence of GHG emissions from reservoirs, there is still debate over their real impact and contribution to the global C cycle, with data remaining sparse and fragmentary (Barros et al., 2011; Eugster et al., 2011; Dai et al., 2013; Deemer et al., 2016). The variety of studies and estimates for C sources from freshwaters is attributing to the complexity of the C cycle in different freshwater systems. Studies typically measure diffusive fluxes, but knowledge gaps still remain for terrestrial material transported in and out, carbon accumulation in reservoir sediments, the impact of drawdown, and downstream emissions (Barros et al., 2011; Deemer et al., 2016; Prairie et al., 2018) and should be the focus of future research efforts.

1.5 Research aims, objectives and overview of thesis structure

This research aims to quantify, compare and understand carbon and nitrogen concentrations and dynamics within temperate freshwater reservoirs across Scotland and North Wales. The overall aim of this PhD is to improve understanding on temperate reservoir systems and determine how significant CO₂, CH₄ and N₂O concentrations and emissions are from reservoirs in Scotland and North Wales, particularly in systems draining peatlands as they are known to export carbon, especially DOC, downstream to lakes and reservoirs (Evans et al., 2013; Kocic et al., 2015). Knowledge is particularly limited on the role UK reservoirs play in inland water GHG emissions. In order to achieve this, a number of specific objectives were investigated:

- To quantify and understand spatial and seasonal dissolved CO₂, CH₄ and N₂O concentrations and emissions via evasion from freshwater reservoirs across Scotland and North Wales. To determine what catchment and reservoir characteristics drive differences in GHG concentrations across sampled reservoirs. To determine whether there are regional spatial differences between concentrations in Scotland and North Wales (Chapter 3).
- To quantify and understand spatial and temporal C and N concentrations and fluvial export to and from the Baddinsgill and Black Esk reservoir catchments in South

Scotland. To produce annual CO₂, CH₄ and N₂O balances for the reservoirs and determine factors regulating export. To evaluate the differences in GHG concentrations and export from catchments with different managed land uses, moorland and coniferous forestry, commonly found in upland reservoirs in Scotland (Chapter 4).

- To investigate the production of CO₂, CH₄ and N₂O fluxes from exposed reservoir sediments during a period of water level drawdown. To determine controlling environmental drivers of water and sediment fluxes. To determine the overall impact drawdown has on total annual reservoir emissions (Chapter 5).

Going forward, this thesis is divided into three main results chapters from field based studies that address the objectives listed above (Figure 1.3). They are self-contained studies with their own introduction, methods, results, discussions and conclusions. An overview of key methods and their underlying theory used to generate the data are presented in Chapter 2, with study specific details provided in the respective results chapters.

Chapter 3 – The first part of this research presents baseline results from a synoptic spatial sampling survey that aims to quantify aquatic C and N concentrations from a variety of temperate freshwater reservoirs (n = 30) in Scotland and North Wales. Sampling took place seasonally over a one-year period from September 2015 to October 2016 to determine concentrations of dissolved CO₂, CH₄, N₂O, DOC, DIC, NH₄⁺, NO₃⁻ and NO₂⁻. GIS-based analysis allowed catchment and reservoir characteristics to be determined to assess their impact on reservoir C and N concentrations. Quantifying GHG concentrations and evasion from reservoirs in Scotland and Wales will better constrain GHG budgets, which is particularly important for CH₄ and N₂O due to limited data. Greater understanding of catchment controls on inland water GHG dynamics could also inform potential responses of reservoir systems to future pressures.

Chapter 4 – The second component of this research investigates spatial and temporal patterns of aquatic C and N concentrations and fluxes within two temperate reservoir catchments that have different land uses (coniferous forest and moorland) in Scotland, UK. Both study sites were also included in the spatial sampling survey outlined in Chapter 3, above. This chapter reports on 18-25 months of CO₂, CH₄ and N₂O concentrations measured at fortnightly intervals using the headspace method, fluvial fluxes of DOC and DIC and other characterising measurements taken from inlets, outlets and main body of the reservoirs. Consideration is

also given to the wider implications for climate change, water treatment and catchment management.

Chapter 5 – The final stage of this project reports on a year of weekly-to-fortnightly field measurements from a Scottish reservoir, focussing on a three-month period of water level drawdown. Many reservoirs undergo drawdown seasonally or for operational maintenance and thereby temporarily alter the biogeochemical processes in previously submerged sediments as they dry out. It is proposed that the drawdown zone, currently poorly understood, will contribute disproportionately to GHG emissions from the reservoir system as a whole. Dissolved CO₂, CH₄ and N₂O concentrations and their fluxes from exposed sediments together with DOC, DIC, NH₄⁺, NO₃⁻, NO₂⁻ concentrations and physicochemical parameters were measured over a one year period from Waltersmuir Reservoir, Scotland, UK. Evasion rates from the water surface were calculated before, during and after drawdown. Using an estimate of the areal extent of exposed sediment from a UAV survey during maximum drawdown, the total annual emissions attributed to drawdown were calculated. This reservoir was also included in the analysis and interpretations of the spatial study in Chapter 2.

Chapter 6 – Finally, this chapter brings together the main findings from the above studies to address the overall thesis aim, whilst placing results in context of other temperate lakes and reservoirs. Recommendations for future research directions in the context of continual understanding of UK reservoir emissions are made. Suggestions discuss how to reduce C and N loading to the reservoir from a catchment management perspective. This research may be of particular interest to the water industry, catchment management professions, or those working on land use, land use change GHG inventories.

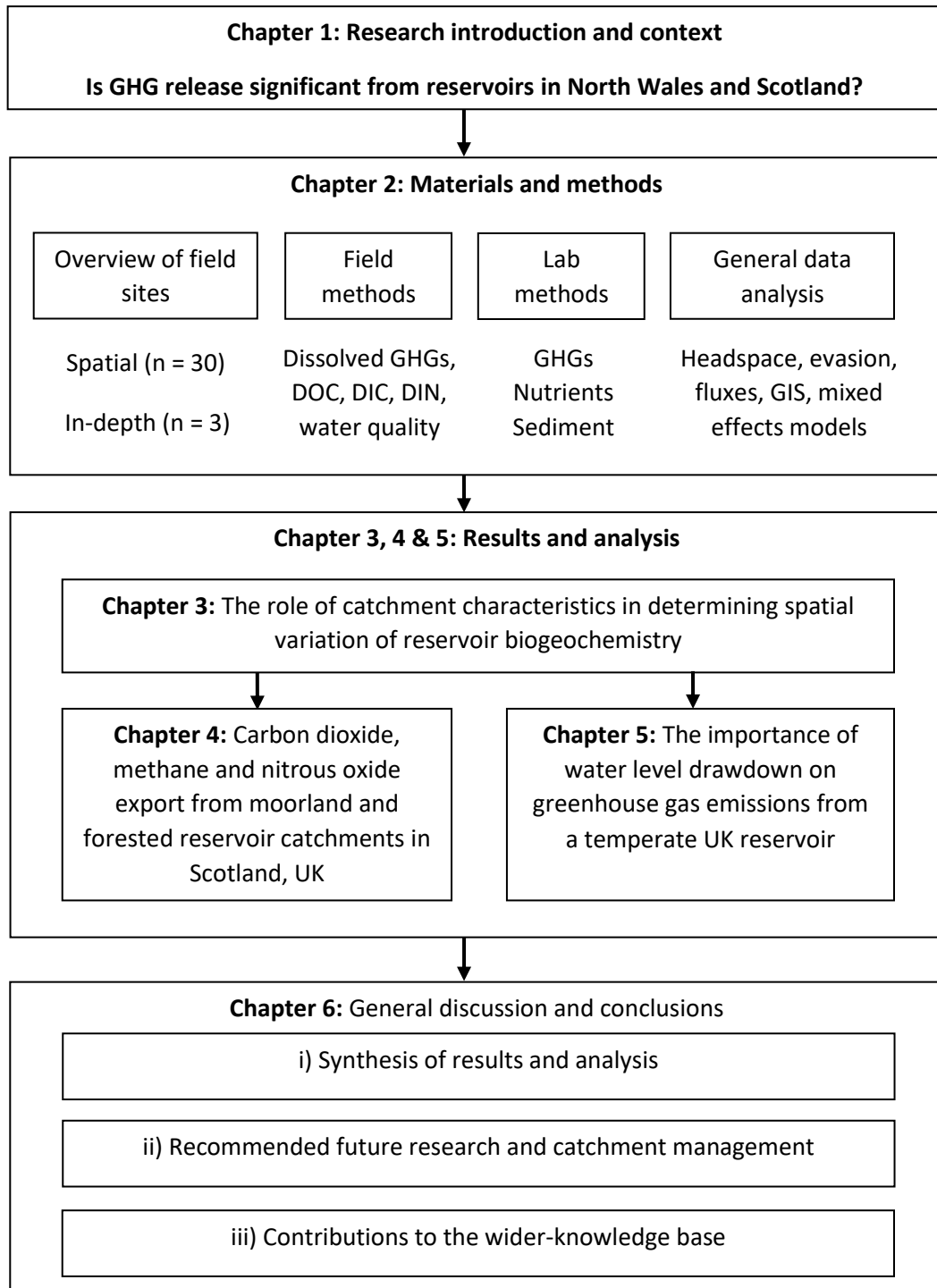


Figure 1.3 Overview of thesis chapters and subsections, including interlinks between the separate chapters.

2 Materials and methods

This chapter provides an overview of the thirty study catchments used in this research and details the underlying theory behind methods of particular importance. Additional study specific field and laboratory methods are presented in individual Chapters 3-5 and an overview is provided in Table 2.1, below.

Table 2.1 Variables measured and methods used in each chapter.

Variable	Field method	Laboratory method	Chapter		
			I	II	III
Reservoir Water					
Dissolved CH ₄ , CO ₂ and N ₂ O	Headspace sampling	Gas chromatography	X	X	X
DOC and DIC	Water sample	LabTOC analyser	X	X	X
NO ₂ ⁻ , NO ₃ ⁻ and NH ₄ ⁺	Water sample	SEAL AQ2	X	X	X
Water Temperature, pH, Dissolved Oxygen and Conductivity	Hanna Probes	----	X	X	X
Discharge/Stage height calibration	Velocity-area method with Electromagnetic flow meter/rating curve	----		X	
Reservoir Sediment					
Sediment CH ₄ , CO ₂ and N ₂ O emissions	Static chambers	Gas chromatography			X
Sediment respiration & temperature	EGM-4 with static chamber	----			X
Sediment temperature	Temperature probe	----			X
Sediment moisture	Theta probe	----			X
Water table depth	Dip well	----			X
Sediment pH	Sediment sampling with soil auger	Solution with deionised water/pH meter			X
Sediment	Sampling with soil auger	Extraction with deionised			

extractable DOC		water/LabTOC analyser	X
Sediment extractable NO ₂ ⁻ , NO ₃ ⁻ and NH ₄ ⁺	Sampling with soil auger	Extraction with KCL/SEAL AQ2 analyser	X
Sediment Dry Weight	Sediment sample	Oven drying	X
Sediment % TC and TN	Sediment sample	Elemental analyser	X

2.1 Field site selection and characteristics

This research incorporates thirty reservoir catchments that vary in location, size and catchment characteristics, across Scotland and North Wales (Figure 2.1, Table 2.2). As identified in Chapter 1, reservoir GHG emissions are highly variable and dependent on a variety of factors, for example: i) between reservoirs e.g. catchment characteristics, morphology, latitude and climate; ii) within reservoirs e.g. along longitudinal gradients from inputting tributaries to the dam; and iii) over time e.g. reservoir age, seasonal variability, changes in catchment activities and dam operation (e.g. Tranvik et al., 2009; Mendonça et al., 2012; Barros et al., 2013). Reservoirs were therefore selected in coordination with associated water companies to exhibit a wide variation in water quality and upland catchment characteristics, including elevation, precipitation gradients, soil (particularly peatland percentage), geology and land use types using GIS derived data (Table 2.2). Information was also provided by Water companies on whether DOC and colour concentrations were low, moderate or high which assisted in selecting reservoirs with varying carbon gradients. Due to the remoteness of many of the reservoirs, consideration also had to be made for access, health and safety, costs and time associated with reaching the sites.

Reservoirs in the UK are primarily used for public water supply, the production of hydroelectric power, and the provision of compensation water. Much of the UK water supply infrastructure was developed at the end of the 19th century when impounding reservoirs were constructed in upland locations to provide a direct supply of water to urban areas (Henderson-Sellers, 1979). Most of these early dams and reservoirs were constructed in the uplands, along the west of the country, in Wales, the Lake District and Scotland. Reservoirs were typically located where the catchment received little or no disturbance. The selected reservoirs in Scotland and Wales therefore represent typical upland UK drinking water catchments. Despite many reservoirs

located in forested and peatland catchments in the UK uplands, there are no in-depth studies considering GHG emissions in and out of lakes or reservoirs, with only a handful of studies focussing on DOC export (e.g. Evans et al., 2017; Stimson et al., 2017) or reservoir sedimentation (e.g. Holliday et al., 2008). Lowland reservoirs in the UK are more commonly associated with pumped storage reservoirs and thus contain water abstracted at a point downstream, where pollution levels may be high. Many UK lowland water bodies are enriched with higher phosphorus and nitrogen concentrations, with eutrophic waters more typical of the lowlands of southern and eastern England. Due to logistical reasons, it was not practical to sample such lowland reservoirs in the South of England, however, a couple of lower lying reservoirs were selected on the Isle of Anglesey (Wales) in catchments with agricultural whilst other sampled reservoirs had problems with cyanobacteria and eutrophication (e.g. Cefni, Plas Uchaf and Dolwen reservoirs). Despite a small geographic area, a range of catchment and water quality characteristics were sampled across the 30 reservoirs.

As funding for this thesis was provided by Scottish Water, focus was placed on Scottish reservoirs in both the spatial and in-depth studies. Other already established carbon research collaboration projects with Welsh Water, permitted access to reservoir sites and background data for this research. The sites in North Wales ($n = 15$) also provided an opportunity to evaluate GHG release from a relatively small but diverse area which represented a range of catchment characteristics e.g. from the lower nutrient rich reservoirs on Anglesey, to the undisturbed high elevation but wet catchments in Snowdonia National Park, to catchments with high peatland percentage such as Llyn Conwy.

A number of the Scotland sites ($n = 10$) are located in the region of the Southern Uplands which has a predominantly mild climate, dominated by a frontal system resulting in a west-east rainfall gradient. In the west of the region, deep peats have formed on extensive areas of gently sloping land at altitudes of 100-300 m. The vegetation is dominated by semi-rough grassland used for low intensity grazing for sheep and cattle and another major land-use is forestry plantations. The other Scottish reservoir sites ($n = 5$) are located in the Central Lowlands region which extends across Scotland between the Highlands and the hills of the Southern Uplands.

The in-depth study sites selected for Chapter 4, Baddinsgill and Black Esk, are drinking water reservoirs owned and operated by Scottish Water. These reservoirs were selected as they provide contrasting catchment land use (coniferous forestry vs. moorland, Figure 2.9) and nutrient status (oligotrophic vs. mesotrophic). The sites were also identified by Scottish Water

for having problems with natural organic matter which can cause issues with the water treatment process as it affects colour, taste and odour and increases usage of treatment chemicals and energy. This led to Scottish Water increasing water quality and catchment monitoring at both sites which also provides greater background data to supplement data collected during this research project.

The third in-depth site, Waltersmuir reservoir (Chapter 5), has been actively used as an aquaculture holding facility for Atlantic salmon (*Salmo salar*) smolt and is owned and operated by Howietoun Fishery, University of Stirling. It was selected as it is a local reservoir that is subject to an annual drawdown event, providing access to exposed sediments for flux measurements in a controlled and safe manner. Aquaculture is commonly found in reservoirs across the UK and other parts of Europe so this is also not an unusual activity for reservoirs. The reservoir also has only one inflow stream, allowing improved quantification of C and N in and out of the system, thus allowing inferences to be made about the effect of the drawdown period on overall GHG emissions.

At each site, sampling was carried out over a minimum of four seasons to a maximum of two years and two months, in order to capture a range of seasons and hydrological conditions. Within each field site, sampling locations were chosen to ensure spatial variability in C and N concentrations were captured. The following sections provide an overview of the characteristics of the reservoirs included in the seasonal sampling campaign (Chapter 3), with greater details provided of the three catchments selected for in-depth monitoring in Chapters 4 and 5.

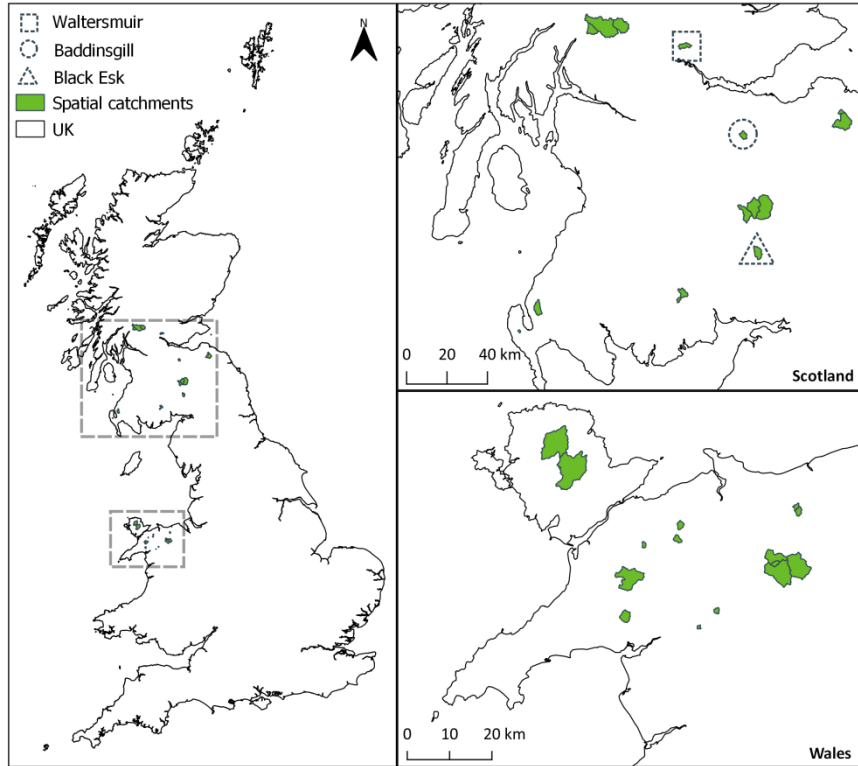


Figure 2.1 Location map of the thirty reservoir catchments in Scotland and North Wales that were used in this research. The highlighted Scottish catchments (dashed lines), Waltersmuir, Baddinsgill and Black Esk, were sampled more in-depth (1 year, 1.5 years and 2 years 2 months, respectively) and presented in Chapters 4 and 5.

Table 2.2 Overview of reservoir and catchment characteristics of all thirty field sites in Scotland and North Wales. Asterisks* indicate reservoirs also included in-depth sampling. Intensive agriculture is the combined area percentage of improved grassland and arable. HOST – Total peat refers to the Hydrology of Soil Types which is further explained in Chapter 3.

Scotland	Location (Latitude/Longitude)	Coniferous Forestry (%)	Moorland (%)	Intensive Agriculture (%)	HOST Total Peat (%)	Dominant Bedrock (%)	Dominant Soil Types
Arklet	N 56° 14', 51", W 04° 36' 18"	1	33.5	0.6	89	Sandstones (99.2)	Podzols, gleys
Baddinsgill*	N 55° 47', 24", W 03° 23' 24"	1	94.1	0	84.7	Sandstones (56.8)	Gley, podzols, peat
Black Esk*	N 55° 15' 36", W 03° 15' 0"	95.9	0.4	0	89	Mudstones and Sandstones (74.3)	Blanket peats, gleys, podzols
Dindinnie	N 54° 54' 0", W 05° 05' 24"	0	0	88.3	6.5	Sandstones (100)	Gleys, brown earths
Finglas	N 56° 15' 0", W 04° 22' 48"	3.1	13	0.6	29.5	Mudstones and Sandstones (81.4)	Podzols, brown earths
Glenkiln	N 55° 04' 48", W 03° 48' 36"	24.5	3.4	7.5	82.4	Sandstones (100)	Brown earth, podzols, peat
Katrine	N 56° 15' 0", W 04° 28' 12"	2.2	23.3	0.5	54.5	Sandstones (46.2)	Podzols, gleys
Lochenkit	N 55° 03' 36", W 03° 52' 12"	4.8	0.2	0	100	Sandstones (100)	Peat, podzols
Megget	N 55° 28' 48", W 03° 18' 0"	0.1	0.8	0	72.5	Mudstones and Sandstones (99.2)	Podzols, blanket peat, gleys
Penwhirn	N 54° 59' 24", W 04° 56' 24"	44.6	8.8	0	95	Sandstones (100)	Blanket peats, podzols, gleys
St Mary's	N 55° 29' 24", W 03° 11' 24"	6.3	1.1	0.9	73.7	Mudstones and Sandstones (96.2)	Brown earths, gleys, podzols, blanket peats
Talla	N 55° 28' 48", W 03° 24' 0"	8.1	0.5	0.2	47.7	Mudstones and Sandstones (99.7)	Podzols, gleys
Thorters	N 55° 55' 51", W 02° 37' 48"	4.4	28.6	12.3	59.2	Sandstones (100)	Brown earths
Waltersmuir*	N 56° 10' 54", W 03° 55' 11"	9.3	2.2	19.7	53.1	Basalts (55.5)	Brown earths, gleys
Whiteadder	N 55° 51' 36", W 02° 33' 0"	0.4	78.7	0	75.5	Sandstones (89.8)	Podzols, brown earths

North Wales	Location (Latitude/ Longitude)	Coniferous Forestry (%)	Moorland (%)	Intensive Agriculture (%)	HOST Total Peat (%)	Dominant Bedrock (%)	Dominant Soil Types
Alaw	N 53° 21' 0", W 04° 25' 12"	0	0.1	88.6	2.9	Mudstones and Sandstones (93.8)	Acid loamy, clayey, blanket peat
Aled Isaf	N 53° 07' 12", W 03° 37' 48"	0	0.2	88.3	0	Mudstones and Silts (100)	Wet acid with peaty surface, blanket bog
Alwen	N 53° 04' 12", W 03° 34' 48"	29.8	9.1	0.6	91.8	Mudstones and Silts (96.1)	Wet acid with peaty surface, blanket bog
Brenig	N 53° 04' 48", W 03° 31' 48"	44.5	22.3	86	82.7	Mudstones and Silts (99.8)	Wet acid with peaty surface, blanket bog
Cefni	N 53° 16' 12", W 04° 19' 48"	7.4	8.9	7.5	73.3	Metamorphic (52.2)	Acid loamy and clayey
Cwellyn	N 53° 04' 12", W 04° 09' 0"	0	30.6	2.2	100	Fine grained acidic igneous (74.3)	Acid loamy, clayey floodplain, peaty soils
Cwm Dulyn	N 53° 01' 12", W 04° 15' 0"	0	10	0	100	Mudstones and Silts (59.4)	Acid loamy, wet peaty surface
Cwmystradllyn	N 52° 58' 12", W 04° 08' 24"	1.7	1.1	9.2	0	Sandstones (68.3)	Blanket peat; acid loamy, wet peaty surface
Dolwen	N 53° 13' 12", W 03° 32' 24"	0	1.5	0.5	100	Mudstones and Silts (99.2)	Acid loamy, clayey
Ffynnon Llugwy	N 53° 09' 0", W 03° 57' 36"	2.6	1.8	0	0	Medium/coarse grained igneous (30.5)	Acid loamy, wet peaty surface; peaty soils
Llyn Aled	N 53° 06' 0", W 03° 37' 12"	7.3	8.9	0	100	Fine grained acidic igneous (58.7)	Blanket bog, wet upland acid with peaty surface
Llyn Conwy	N 53° 00' 0", W 03° 49' 12"	0	0	0	100	Mudstones and Silts (97.3)	Blanket peat
Llyn Morwynion	N 52° 57' 36", W 03° 52' 48"	0	45.6	0.9	100	Sandstones (51.8)	Blanket peat; acid loamy, wet peaty surface;
Marchlyn Bach	N 53° 08' 24", W 04° 04' 48"	0	25.2	2.2	100	Mudstones and Silts (88.9)	Acid peaty soils, acid loamy, wet peaty surface
Plas Uchaf	N 53° 13' 48", W 03° 33' 0"	0	0	0.2	100	Mudstones and Silts (99.2)	Acid loamy

Scotland	Catchment area (ha)	Mean catchment elevation (m)	Mean catchment slope (°)	Annual average rainfall (mm)	Age	Capacity (m ³)	Water Surface Area (ha)
Arklet	1832	320	17	>3000	1914	12,283,000	226
Baddinsgill*	962	420	9	800-1000	1930	2,250,270	25
Black Esk*	1813	331	8	1500-2000	1962	3,147,000	34
Dindinnie	126	133	5	1000-1250	1908	491,400	7
Finglas	3877	412	17	>3000	1965	19,048,075	143
Glenkiln	1314	249	8	1250-1500	1934	1,618,376	28
Katrine	9527	334	17	>3000	1859	64,610,000	1334
Lochenkit	333	252	8	1250-1500	1938	196,000	10
Megget	4042	529	7	1500-2000	1982	63,600,000	247
Penwhirn	1834	208	4	1000-1250	1954	2,591,000	54
St Mary's	10922	466	14	1500-2000	1985	2,990,000	255
Talla	2516	552	18	1500-2000	1905	12,728,800	129
Thorters	398	295	9	600-700	1900	286,363	7
Waltersmuir*	1169	352	9	1000-1250	~1950	113,636	3
Whiteadder	4584	363	8	600-700	1968	7,955,000	79

North Wales	Catchment area (ha)	Mean catchment elevation (m)	Mean catchment slope (°)	Annual average rainfall (mm)	Age	Capacity (m ³)	Water Surface Area (ha)
Alaw	4068	63	2	1000-1250	1966	7,638,000	68
Aled Isaf	3339	63	3	800-1000	1918	14,564,200	314
Alwen	2432	407	5	1000-1250	1915	14,564,200	149
Brenig	2225	419	6	1000-1250	1975	61,500,000	371
Cefni	2081	357	16	1000-1250	1950	1,548,000	91
Cwellyn	1143	408	5	2000-3000	1979	1,687,000	30
Cwm Dulyn	503	341	17	1250-1500	1901	704,016	41
Cwmystradllyn	358	217	9	1500-2000	1961	3,640,000	4
Dolwen	232	794	17	700-800	1905	221,000	14
Ffynnon Llugwy	226	237	7	>3000	1919	1,754,000	7
Llyn Aled	225	736	25	800-1000	1934	1,725,000	17
Llyn Conwy	166	389	3	2000-3000	~1963	3,074,000	46
Llyn Morwynion	137	468	7	2000-3000	1879	621,970	39
Marchlyn Bach	105	668	22	>3000	1969	352,000	5
Plas Uchaf	59	416	12	700-800	1870	225,500	12

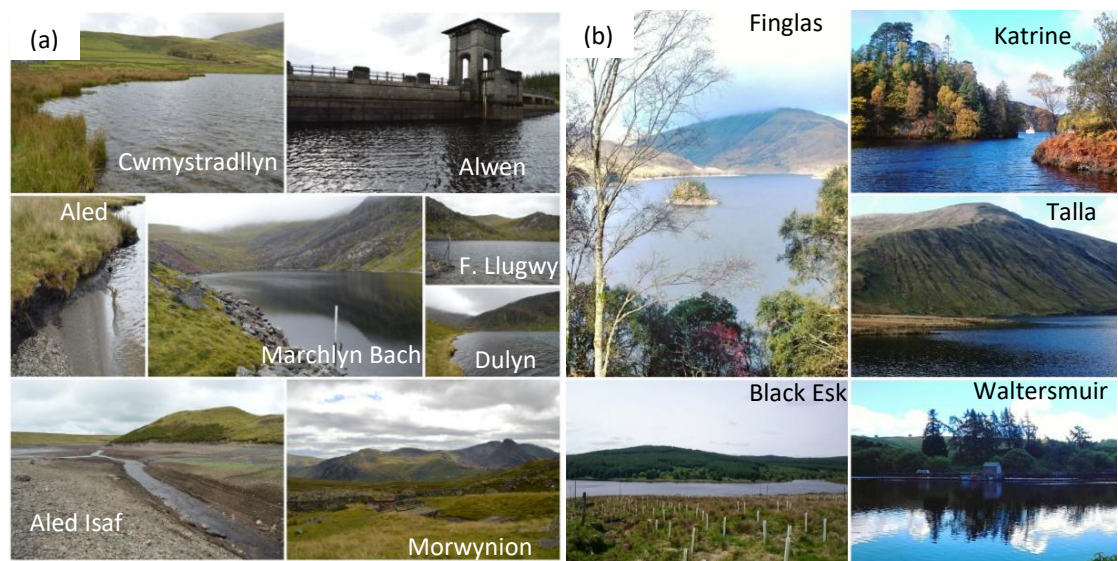


Figure 2.2 Selection of field photographs showing diversity in reservoir characteristics in North Wales (a) and Scotland (b).

2.1.1 In-depth study sites: Black Esk, Baddingsgill and Waltersmuir reservoirs

Of the thirty field sites, three were selected for more in-depth sampling – Black Esk, Baddingsgill (Chapter 4) and Waltersmuir (Chapter 5) reservoirs. Both Baddingsgill and Black Esk are drinking water reservoirs owned and operated by Scottish Water. These reservoirs were selected as they provide contrasting catchment land use (coniferous forestry vs. moorland, Figure 2.9) and nutrient status (oligotrophic vs. mesotrophic). The sites were also identified by Scottish Water for having problems with natural organic matter which can cause issues with the water treatment process as it affects colour, taste and odour and increases usage of treatment chemicals and energy. This led to Scottish Water increasing water quality and catchment monitoring at both sites which also provides greater background data to supplement data collected during this research project. Waltersmuir reservoir has been actively used as an aquaculture holding facility for Atlantic salmon (*Salmo salar*) smolt and is owned and operated by Howietoun Fishery, University of Stirling. It was selected as it is subject to an annual drawdown event, providing access to exposed sediments for flux measurements.

2.1.1.1 Black Esk

Black Esk (BE) reservoir is located ~5km from Eskdalemuir, Dumfries and Galloway, south-west Scotland (N 55° 15' 36", W 03° 15' 0"). The climate is temperate, with mean maximum annual temperature of 11.2 °C, mean minimum annual temperature of 3.9 °C and mean annual rainfall of 1742 mm (1981 – 2010; Eskdalemuir station 7 km north east of the reservoir dam,

Met Office, 2016). Monthly rainfall and temperature data from this station during the sampling period is presented in Figure 2.3. Constructed in 1962 and managed by Scottish Water, Black Esk supplies drinking water to Lockerbie and surrounding areas. During 2014, the height of the dam was raised by 2.5 m to increase the reservoir's storage capacity from 2,280 million litres to 3,147 million litres and improve the security of water supply. This led to the felling of trees and removal of vegetation around the reservoir shoreline to accommodate the rise in water level. The felled tree trunks and roots were left standing and partially submerged in the newly flooded areas of the reservoir, while a handful of trees at the upper end of the reservoir (furthest from the dam) were not removed after felling so were left floating (Figure 2.5).

The spillway sits inside the main reservoir body so water is drawn from the surface. Black Esk reservoir has a surface area of 404,900 m², and maximum depth of 17.3 m. The reservoir catchment is 18.13 km² and has a mean elevation of 331 m (range of 247-536 m). The catchment has overall gentle slopes (mean = 7.6°) with the majority of slopes north-west facing (mean aspect = 145°). Black Esk has seven inlets and one outlet, with the main inlet being the River Black Esk, a 4th Strahler-order stream where its headwaters are located ~6.2 km away from the reservoir. Measurements were made at five of the main inflows (BE1-5_{in}) (due to vegetation obstruction and drying out during summer months, two small inflows were excluded) and the outflow (BE_{out}). The river and streams ranged from 1st to 4th order, the channels were 0.5 to 6 m wide, and bed sediment was a mixture of boulders, pebbles and soft sediment. Fieldwork was carried out between June 2015 and July 2017.

The catchment land cover of Black Esk is dominated by coniferous forestry (96%) (Figure 2.9) plantations (Castle O'er forest). Felling was also active throughout the sampling period (Figure 2.4) and was not directly located near the sampling locations however activity is within the headwaters of the main inflow, the River Black Esk. Sitka spruce (*Picea sitchensis*) and Norway spruce (*Picea abies*) are the dominant tree species. The catchment also has small areas (<2%) of rough grazing (acid grassland) and moorland (heather grassland).

Harvesting activity resulted in extensive areas of brash mats near sampling locations, which are the above-ground parts of the tree composed of branches, tree tops and needles not normally removed from site after thinning and clear felling operations and typically used to protect soils from heavy machinery. If brash is poorly sited, it can affect water quality through leachate from decomposing brash entering water courses, whilst inadequate brash mat coverage can result in soil erosion and a risk of sediment entering water courses (Stevens et

al., 1995). Brash contains a significant proportion of the above-ground content of nutrients in plants, with an estimated 219-300 N kg ha⁻¹ in Sitka spruce (Stevens et al., 1995) and 280 N kg ha⁻¹ in Norway spruce (Hyvönen et al., 2000) Buffer strips were present along the inflows running through these brash mat areas. Restocking of broadleaf trees was also evident during the spring 2017 sampling period in these same areas surrounding the reservoir and inflows (Figure 2.4).

The main catchment soil type is peaty podzols (72%) and peaty gleys (26%). Based on the Hydrology of Soil Type (HOST) classification system (Boorman et al., 1995) which classifies UK soils into 29 groups based on hydrological characteristics, classes 19 (11%), 15 (89%) and 29 (<1%) are dominant in the catchment. This suggests that the majority of the catchment (89%) has wet, peaty topped upland soils over relatively free draining permeable rocks. In terms of catchment geology, the bedrock was comprised of metasandstones and mudstones (74%), wacke (25%) and quartz-microgabbro (<1%), with superficial deposits of diamicton (51%), peat (9%) and silt, sand and gravel (5%) (Figure 2.9).

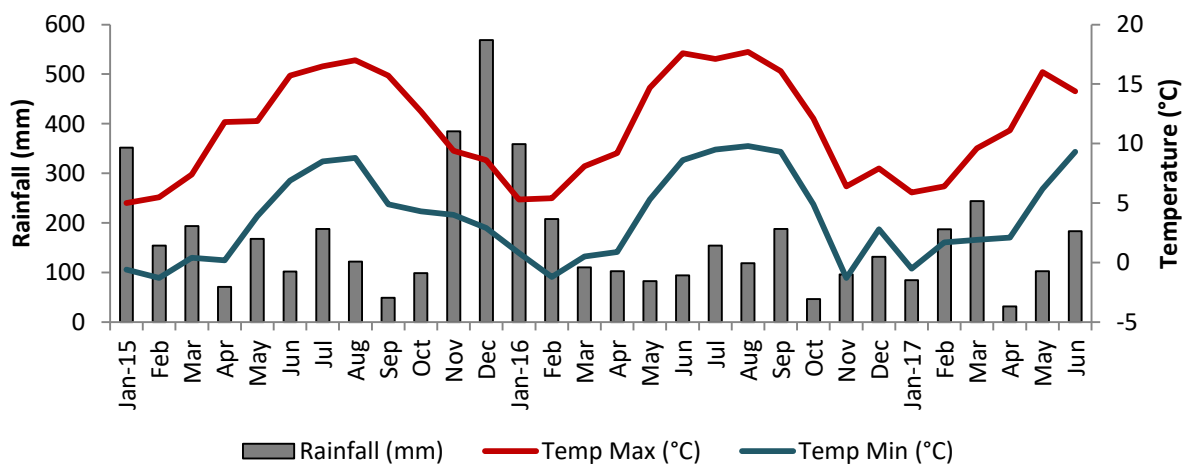
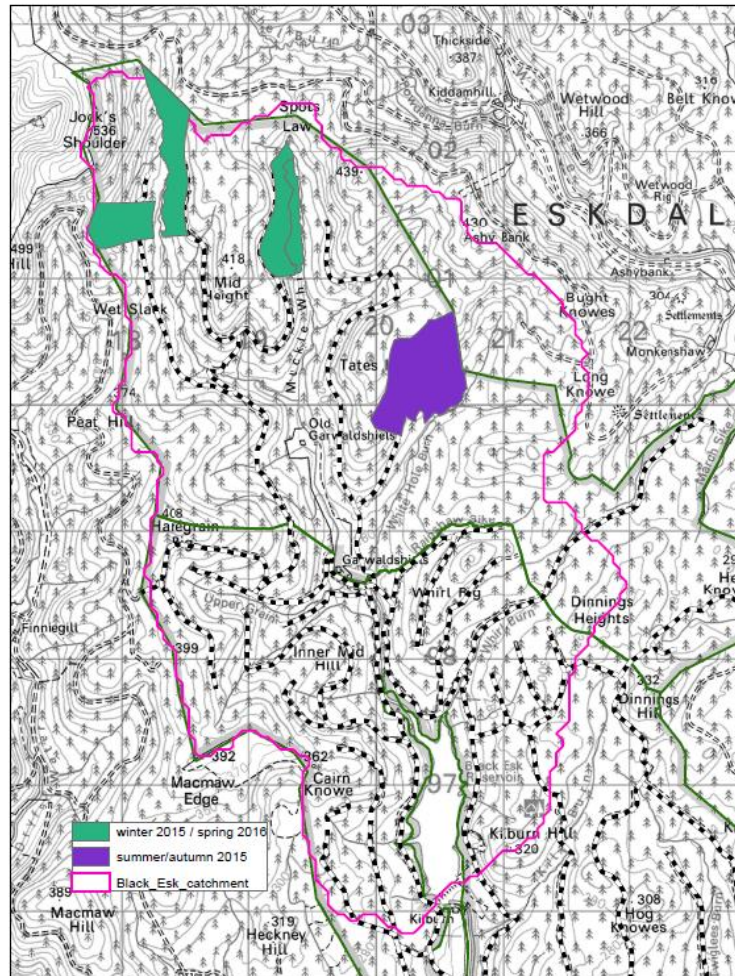

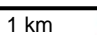


Figure 2.3 Monthly rainfall and temperature data from Eskdalemuir weather station near Black Esk reservoir during the sampling period.




 Felling in Black Esk reservoir catchment between 2015 and 2017
 


 Reproduced by permission of Ordnance Survey on behalf of HMSO. © Crown copyright and database right 2017. All rights Reserved. Ordnance Survey Licence number 100021242



Figure 2.4 Felling locations in Black Esk catchment during sampling period, courtesy of Forestry Commission Scotland. Field photograph of broad leaf tree planting in Spring 2017.



Figure 2.5 Photographs of sampling locations of inlets (blue), outlet (orange) and reservoir (purple) at Black Esk. BE1_{res} and BE2_{res} show the decomposing felled trees within the reservoir.

2.1.1.2 Baddingsgill

Baddingsgill (BA) is an upland mesotrophic reservoir located in the Pentland Hills near West Linton, in the Scottish Borders region of Scotland, UK (N 55° 47' 24", W 03° 23' 24"). It is also managed by Scottish Water and provides water supply to the West Lothian local authority area. This area has a temperate climate, with a mean minimum and maximum annual temperature of 4.2 °C and 11.8 °C, respectively and a mean annual rainfall of 980 mm (1981 – 2010; Penicuik station, 13 km north west of Baddingsgill dam, Met Office, 2016).

Baddingsgill reservoir has a catchment area of 9.6 km², surface area of 0.25 km² and a maximum depth of 22.6 m. The mean catchment elevation is 420 m, ranging from 314 to 565 m. The catchment slopes are of a gentle rolling to hilly topography (mean 9°), with the majority of slopes facing to the south (mean 167°). The catchment land use is predominately moorland (heather and heather grassland, 94%), with small areas of rough grazing (acid grassland 2%), coniferous woodland (1%) and improved grassland (<1%) (Figure 2.9). The main catchment soil type is peaty podzols (59%), peaty gleys (20%) and non-calcareous gleys (18%). Based on the

Hydrology of Soil Type (HOST) classification system (Boorman et al., 1995), classes 24 (15%) and 15 (85%) are the most dominant. This suggests that 85% of the catchment has permanently wet, peaty topped upland soils over relatively free draining permeable rocks, where class 24 areas are slowly permeable, seasonally waterlogged soils over impermeable clay substrates with no storage capacity. The catchment bedrock is composed of sandstones (57%), conglomerates (35%), mudstones and silts (6%) and has small areas (2%) of igneous rocks (quartz-diorite and mafite). Diamicton (25%), peat (22%) and small areas of clay, silt, sand and gravel make up the superficial deposits.

Baddinsgill has five main inflows and one outflow, with the main inflow being the Lyme Water, a 4th order stream where its headwaters are located ~3 km north of the reservoir dam. Measurements were made at all five inflows (BA1-5_{in}) and the outflow (BA_{out}). The streams ranged from 1st to 4th order, the channels were 0.6 – 3.5 m wide, and bed sediment was a mixture of boulders, pebbles, gravel and soft peaty sediment (Figure 2.9). Fieldwork was carried out between July 2015 and January 2017.

The catchment has a long history of hill sheep farming and at time of sampling, was populated by ~1400 sheep and a small fold of Highland cattle. Baddinsgill is also a shooting estate where managed burning (muirburn) of heather is practiced. During the sampling period, muirburn did not occur (it occurred during time of write up in October 2018) but burn scars across the hillside are visible. The catchment also has ~0.9 km² of mixed woodlands which are actively managed by the estate, for example, small-scale areas were harvested for timber products and wood fuel during the sampling period in the east of the catchment. Old drainage ditches in-filled with vegetation were also evident across the moor, particularly between Hareshaw and Lymewater inlets. There are also numerous areas of exposed and eroding peatland, and peat hags also present near three of the main inflows. Exposed peat is likely a result of trampling by sheep and cattle, with tracks seen across the catchment and near peat hags next to water courses and through past muirburn activity where the soil is beginning to erode.



Figure 2.6 Examples of a working farm and managed catchment at Baddingsgill reservoir.

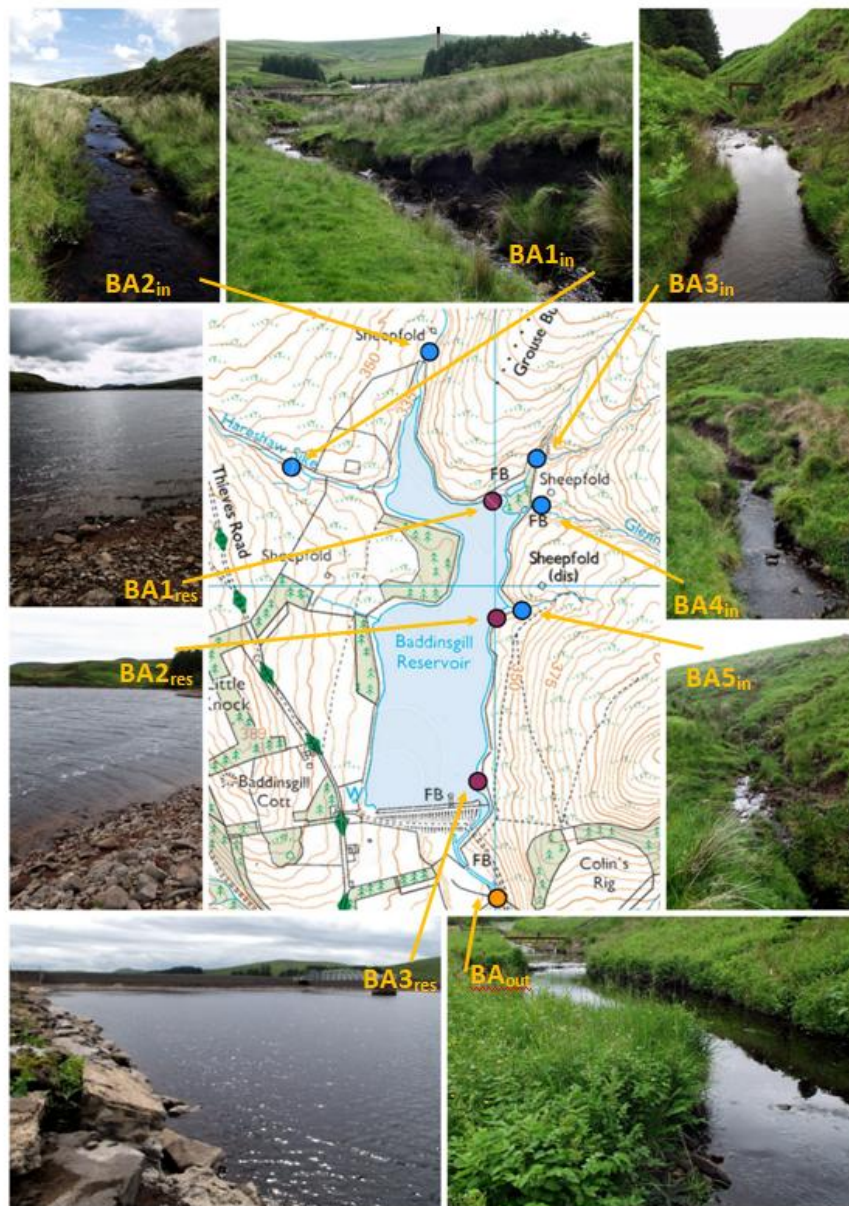


Figure 2.7 Field photographs and locations of inlet (blue), outlet (orange) and reservoir (purple) sampling locations at Baddingsgill reservoir.

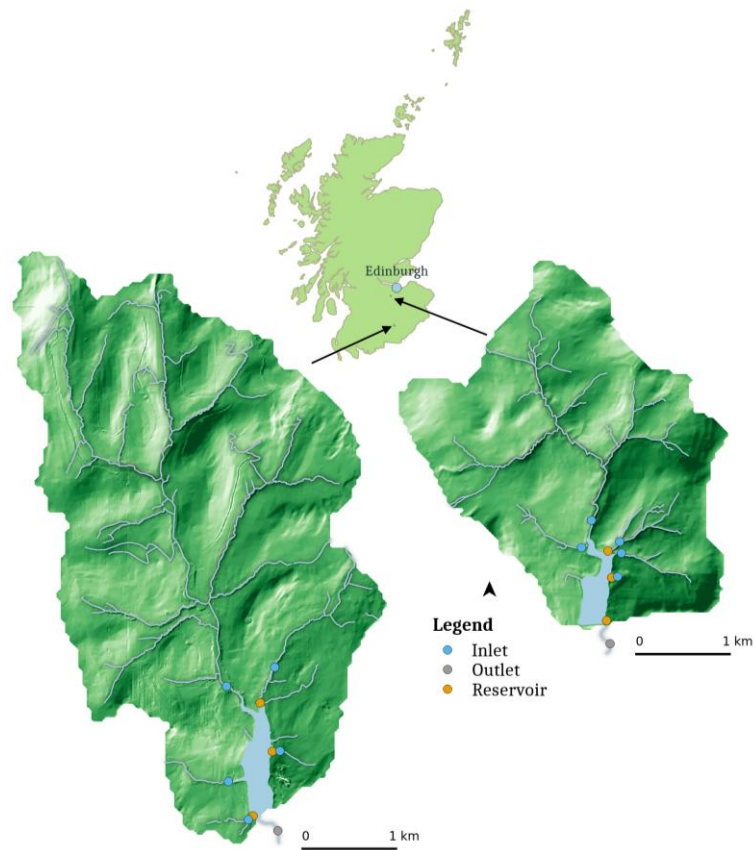
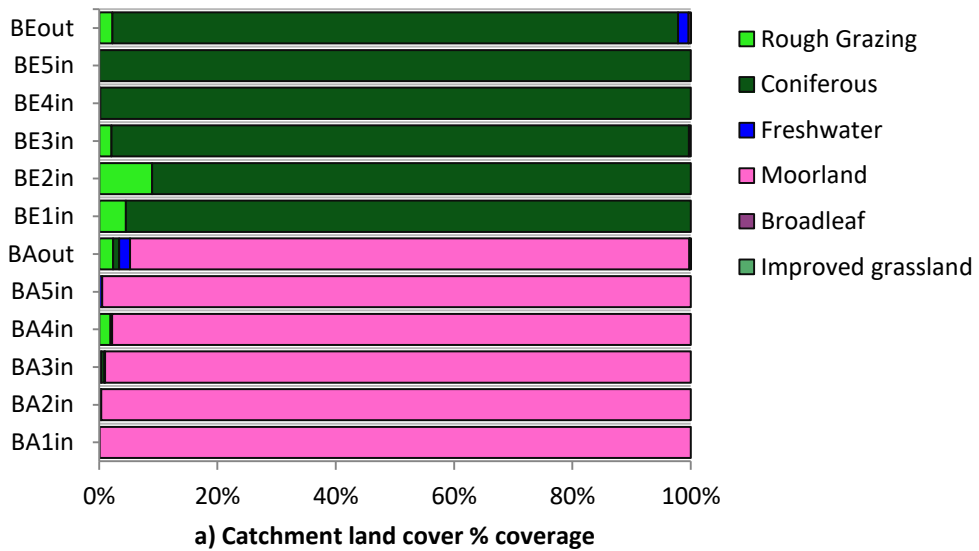


Figure 2.8 Inlet, reservoir and outlet sampling sites and location of Baddingsgill and Black Esk reservoirs in Scotland.



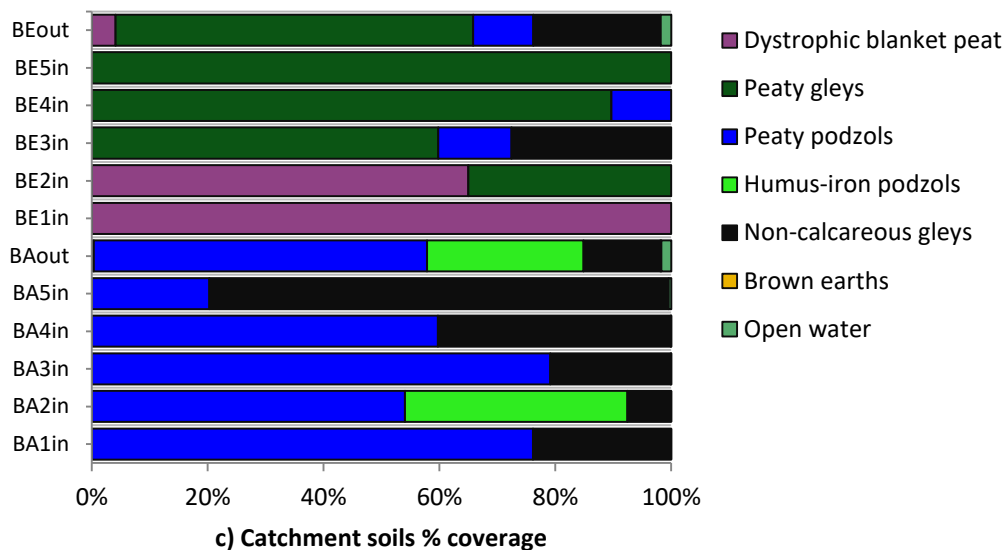
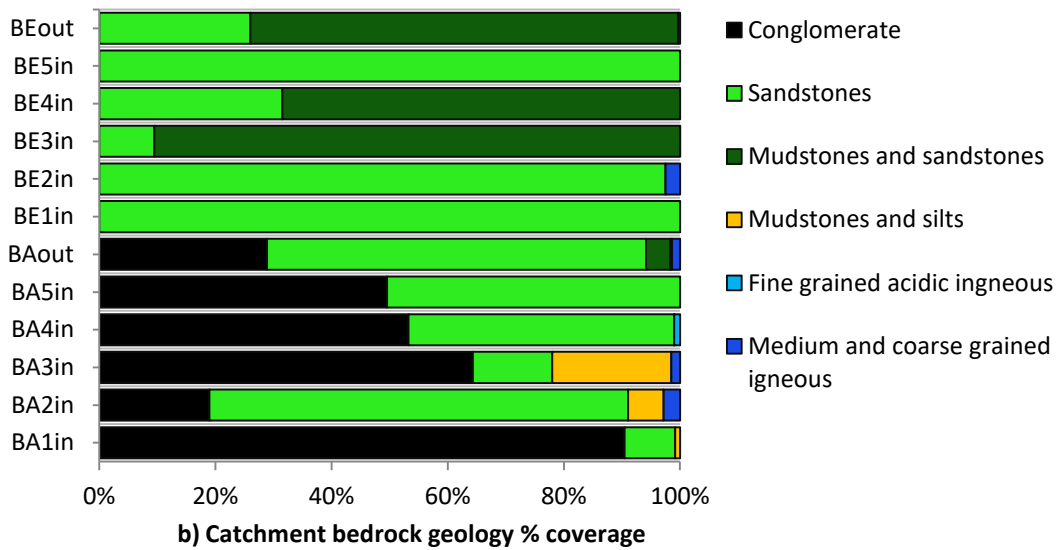


Figure 2.9 Sub-catchment characteristics at Baddinsgill and Black Esk reservoirs of land cover (a), geology (b) and soil (c).

2.1.1.3 Waltersmuir

The study was conducted from January 2016 to January 2017 at Waltersmuir reservoir, near Dunblane, Central Scotland (N 56° 10' 54", W 03° 55' 11") (Figure 2.1). The climate is temperate maritime, with an average annual rainfall of 1019 mm, monthly average maximum air temperature of 12.9°C and monthly average minimum temperature of 5.6°C for the period 1981-2010 (Met Office, 2015). The reservoir is situated in a sheltered area surrounded by trees which contributes to low wind speeds and wave height.

Waltersmuir was constructed as a drinking water reservoir in the 1950s, but since 1993 has been actively used as an aquaculture holding facility for Atlantic salmon (*Salmo salar*) smolt,

and is owned and operated by Howietoun Fishery, University of Stirling. During the sampling period ~160,000 smolt aged 0+ to 1+ were stocked. Howietoun aim to have the reservoir stocked by the last week in August and then removed from mid to late March, with all fish being removed before the start of April. During the stocking period fish were fed on a commercial EWOS (EWOS Ltd, Westfield, Near Bathgate, Scotland) diet (EWOS Micro LR 15P and 40P with average phosphorous = 1.4%, nitrogen = 7.9% and carbon = 45.2%), and a total of ~12 tonnes was used during the whole production time from August-April. No other product or supplements were added to the reservoir during the sampling period. Since 1998, Waltersmuir reservoir has been subject to an annual drawdown event. During 2016, the reservoir was drained from the bottom outlet valve on the dam for an extended period of time (11 weeks) to allow maintenance work at the dam. This provided an opportunity to access the reservoir sediments to measure biogeochemical properties of the exposed sediment.

At full capacity, Waltersmuir reservoir has a surface area of 32,600 m², a maximum depth of 12 m, mean depth 4.4 m, and storage capacity of 123,900 m³. The reservoir catchment is 1169 ha with an elevation range of 171-460 m (mean 352 m) above sea level. The mean slope across the catchment is 9° (gently rolling topography) and slopes are on average, easterly facing. Waltersmuir reservoir has one outlet and one main inlet, the Wharry Burn, which is 10.33 km in length, and is classified as having 'high' ecological status according to the Water Framework Directive (Nutt and Perfect, 2011).

The catchment land cover is comprised of rough grazing (68%) for sheep, alongside improved grassland (19%), coniferous (9%) and broadleaf (1%) woodlands, moorland (2%) and arable (1%). The vegetation surrounding the reservoir consists of shrubs, grasses, sedges, bryophytes and lichens amongst managed woodland of *Betula pendula*, *Quercus petraea*, *Fagus sylvatica*, and *Sorbus aucuparia*. Directly downstream of the dam, the outlet flows through Kippenrait Glen a Site of Special Scientific Interest (SSSI) designated for its ancient woodlands.

The underlying geology of Waltersmuir catchment is predominantly Early Devonian Old Red Sandstones (28%), with basaltic lavas (basaltic-andesite and olivine basalt) in the catchment headwaters (56%) and areas of conglomerates (15%). Overlain are superficial Quaternary glaciofluvial and river terrace deposits (clay, silt, sand and gravel) with small areas of peat (4%). The surface soils overlying these superficial layers are peaty podzols (31%), non-calcareous gleys (23%), brown forest soils (22%) and blanket peats (19%) in the headwaters of the Wharry Burn. The dominant HOST classes occurring in the Waltersmuir catchment are 15 (31%), 18 (26%), 29 (22%) and 24 (14%). Classes 15 and 29 correspond to peaty soils which

suggest these areas are waterlogged, with classes 18 and 24 corresponding to slowly permeable soils with seasonal waterlogging that have moderate storage capacity.

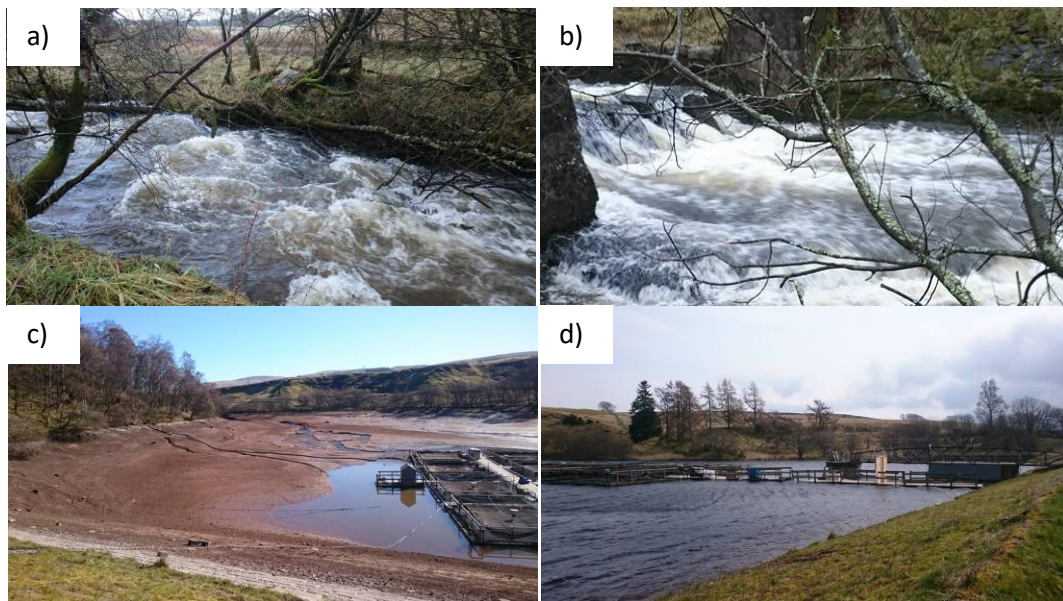


Figure 2.10 Field photographs at Waltersmuir reservoir during a high flow event at the a) inlet and b) outlet. Photograph c) shows the exposed reservoir sediment during drawdown and d) the typical reservoir water level outside the drawdown period.

2.2 Field and laboratory methods

2.2.1 Dissolved CO₂, CH₄ and N₂O concentrations – headspace method

The headspace method was originally developed by Kling et al. (1991) to determine the concentration of gas dissolved in a liquid and has since been widely used in aquatic biogeochemistry (e.g. Billett et al., 2004; Dinsmore et al., 2010, Wallin et al., 2011). The method involves equilibrating a known volume of water with a ‘headspace’ of air taken from the surrounding atmosphere (Hope et al., 1995). For this research, a 40 mL water sample (collected from approximately 10 cm water depth) was equilibrated with 20 mL ambient air at water temperature by shaking vigorously underwater for one minute in a luer-lock syringe with attached 3-way tap. Duplicate headspace samples were collected at each sampling point (percentage differences in duplicate samples are shown in Table 2.4. The headspace samples, along with a separately collected sample of ambient air from the sampling location are then immediately transferred into 12 mL pre-evacuated Exetainer® vials (Labco, Lampeter, UK) using a small needle for later analysis using gas chromatography.

Headspace samples from 16/06/2015 to 17/01/2016 were analysed on an HP5890 Series II gas chromatograph (Hewlett-Packard, Palo Alto, CA USA) with a flame ionisation detector (FID)

and attached methaniser. Detection limits were 7 ppmv for CO₂, 84 ppbv for CH₄ and <0.2 ppmv for N₂O. Samples collected from 27/01/2016 to 07/06/2017 (end of field period) were analysed on a 7890B gas chromatograph (Agilent Technologies) with flame ionization detector (FID) for CH₄ and attached methaniser for CO₂, and the micro electron capture detector (μECD) for N₂O. These detectors were set up in parallel allowing simultaneous analysis of all three GHGs. Peak detection and integration was performed using the OpenLAB CDS ChemStation software (Agilent Technologies). A set of four certified standards (BOC Special Gases, UK) were used for calibration for each gas during each analysis run (Table 2.3).

The dissolved concentrations of CO₂, CH₄ and N₂O in the water column from the ambient and headspace concentrations were then calculated (Equation 2.1) based on Henry's Law (Dawson, 2000; Hope et al., 1995) $GHG_{[aq]}$ is the original gas concentration in the water sample (mg L⁻¹), P_i and P_f are the initial and final partial pressure of the gas in the syringe (atm), corrected for the head of water and atmospheric pressure at time of sampling, P_{wa} is the total ambient pressure (atm) at the depth of sampling, with Y_f the concentration in the equilibrated headspace (ppmv), and Y_i is the concentration of the headspace prior to equilibration (ppmv) (Equations 2.2, 2.3) K_H is Henry's law constant i.e. the solubility coefficient, V_{hs} is the headspace volume (L), V_w is the water volume (L), r is the universal gas constant (0.082057) and T is the stream or reservoir temperature (°K). Gas solubility in water is dependent on both temperature and salinity, and the values of K_H are adjusted for temperature according to (Weiss and Price, 1980), (Wiesenburg and Guinasso, 1979) and (Weiss, 1974) for CO₂, CH₄ and N₂O, respectively. Air temperature and barometric pressure were obtained using a hand-held weather meter (Kestrel 2500, accuracy 3% of reading) at ~1 m above the water surface from each sampling location.

$$GHG_{[aq]} = \left[P_f \times \left(K_H + \left(\frac{V_{hs}}{V_w} \right) \times \left(\frac{1}{r} \right) \times T \right) \right] - \left[P_i \times \left(\frac{V_{hs}}{V_w} \right) \times \left(\frac{1}{r} \right) \times T \right] \quad (2.1)$$

$$P_f = Y_f \times P_{wa} \quad (2.2)$$

$$P_i = Y_i \times P_{wa} \quad (2.3)$$

Table 2.3 Concentrations of certified standards used during GC analysis.

Standard	CO ₂ (ppm)	CH ₄ (ppm)	N ₂ O (ppb)
1	200	1.26	199.5
2	344	1.83	285
3	678	5.16	490
4	4941	101.1	975

Table 2.4 Overall percentage differences between collected duplicate headspace samples for each sampling campaign and chapter across all three GHGs.

Location and chapter	Mean	Median
Scotland (Chapter 3)	8.4%	4.8%
Wales (Chapter 3)	17%	6.4%
Baddingsgill (Chapter 4)	11%	4.8%
Black Esk (Chapter 4)	16%	5.9%
Waltersmuir (Chapter 5)	11%	6.6%
All headspace samples	13%	5.5%

2.2.2 CO₂, CH₄ and N₂O emissions – static chambers

Measurements of CO₂, CH₄ and N₂O fluxes were made from the sediment of Waltersmuir reservoir over a three month period using the static chamber method (Clayton et al., 1994; Livingston and Hutchinson, 1995). The sediment-atmosphere flux is calculated by measuring the concentration change over time in a known volume of air inside a closed chamber. There are a variety of chamber types and measurement protocols across the literature (e.g. Clayton et al., 1994). Consideration also needs to be made in terms of the number of chambers deployed, layout across the study site, measurement frequency and time of day measurements are taken. The chambers used in this study are based on a design by Clayton et al. (1994) and have been extensively tested and used in other research (Cowan et al., 2016; Dinsmore et al., 2009; Drewer et al., 2010) and a full description is presented in Chapter 5.

In total, nine chambers were positioned along a transect from the middle of the reservoir to the bank edge to cover a range of areas of different slope and sediment moisture regimes. Due to wetness of bottom sediment from water level drawdown, locations of deployment were restricted to a certain side of the reservoir for health and safety concerns. Throughout the sampling period, measurements were carried out within a 1 hour window between 10:30 and 15:00. During flux measurements, the lids were placed onto circular stainless steel collar bases and fastened with 4 clips. The collars had been inserted approximately 5 cm into the sediment two days before the first sampling event and were left in situ for the remainder of the study period (Figure 2.11). Wooden pallets were also used to reach three chambers positioned in very soft wet sediment in order to avoid the inadvertent release of gases during flux measurements

All static chamber gas samples were analysed on the 7890B gas chromatograph (Agilent Technologies) with FID and μ ECD (see above). The flux was calculated by measuring the concentration change (ΔC) over time (Δt), relative to the chamber volume (V) and surface area (A) (Equation 2.4).

$$Flux = \frac{V\Delta C}{A\Delta t} \quad (2.4)$$



Figure 2.11 Static chamber transect installation at Waltersmuir reservoir during first week of water-level drawdown.

2.2.3 Water quality sampling procedure

Both reservoir and stream water samples were collected by drawing up 60 ml of water at ~10 cm depth using a syringe which was pre-rinsed three times between sites. Samples were filtered in the field by injection through 0.45 µm syringe-driven filters (Whatman®) and stored in 30 ml Nalgene® water bottles that had been pre-soaked in Decon® solution and rinsed thoroughly with deionised water. The bottles were also rinsed three times with filtered sample water in the field before a sample was taken. Samples were kept cool and dark in a cool box whilst in the field. On return (typically less than 5 hours), one filtered water sample was placed immediately in the refrigerator at 4-5 °C for DOC and DIC analysis within two weeks of collection whilst the other filtered sample was placed in the freezer at -18 to -21 °C for analysis of ammonium, nitrite and nitrate (NH_4^+ , NO_2^- and NO_3^-) at a later date.

2.2.3.1 Determination of DOC and DIC concentrations

There are three forms of carbon commonly identified in freshwater; i) particulate carbon, ii) dissolved, i.e. dissolved organic carbon (DOC), bicarbonate (HCO_3^-) or carbonate ions (CO_3^{2-}) or iii) gaseous such as free CO_2 or CH_4 (Dawson et al., 2004). Although gaseous CO_2 and CH_4 are a form of dissolved inorganic carbon (DIC), for clarity they have been separated throughout the thesis due to the different methods of calculating concentrations; therefore any reference to DIC in the remainder of the text does not include CO_2 or CH_4 .

DOC and DIC concentrations were determined for sediment, stream and reservoir water samples using a LabTOC TOC analyser (Pollution & Process Monitoring Ltd., UK) connected to a PPM PSA auto sampler. The detection range was 0.1-4000 mg L⁻¹ and concentrations were calculated based on a three-point calibration curve with standard of 50 mg L⁻¹. It has a limit of detection equivalent to 1% of the calibration standard concentration (50 mg L⁻¹). This instrument converts the sample to CO_2 using UV promoted persulphate oxidation and the CO_2 is then analysed by an infra-red gas analyser (IRGA). The method combines the samples with an acid solution (5% sodium persulphate and 5% orthophosphoric acid in deionised water), lowering the pH. Acid sparging with N_2 allows removal of acidified inorganic carbon and organic constituents to be determined. DIC is then determined from the Total Carbon (TC) minus the Total Organic Carbon (TOC) concentrations, with DIC being determined as CO_2 released from the sample by acidification followed by sparging. As all water sampled were in-field filtered (0.45 µm) prior to analysis, the particulate organic carbon (POC) is removed and

therefore the LabTOC instrument outputs for TC and TOC are therefore interpreted as the dissolved portion only as they do not include POC, e.g. the TOC output constitutes the DOC component. For further quality control, the 50 ppm standard solution and ultra pure deionised water were placed at the start and the deionised water also placed in the middle and end of each run to monitor potential instrument drift.

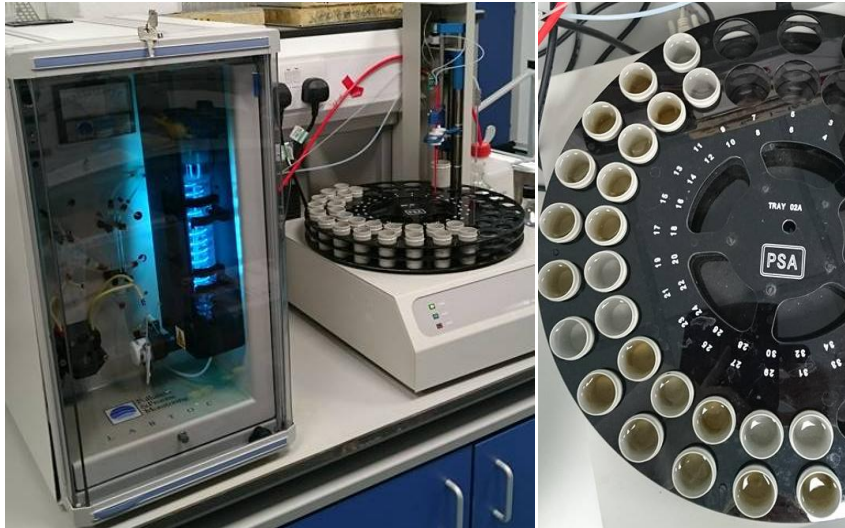


Figure 2.12 LabTOC analyser with autosampler.

2.2.3.2 Colorimetric analysis

Concentrations of NH_4^+ , NO_2^- and NO_3^- in the water and sediment extracts (only NH_4^+ and NO_3^-) were measured using a SEAL AQ2 discrete analyser (SEAL Analytical, Southampton, UK) fitted with a cadmium coil. The widely used phenol-hypochlorite (for NH_4^+) and sulfanilamide (NO_2^- & NO_3^- after cadmium coil reduction) methods were used to provide the relevant colorimetry reactions (EPA 350.1 v2 and EPA 353.2 v2, USEPA, 1993). Detection limits are $0.002 \text{ mg N L}^{-1}$, $0.0005 \text{ mg N L}^{-1}$ and $0.003 \text{ mg N L}^{-1}$, for NH_4^+ , NO_2^- and NO_3^- , respectively. For further quality control within each analytical batch, standards and deionised water samples were added at the start and end of each analysis run.

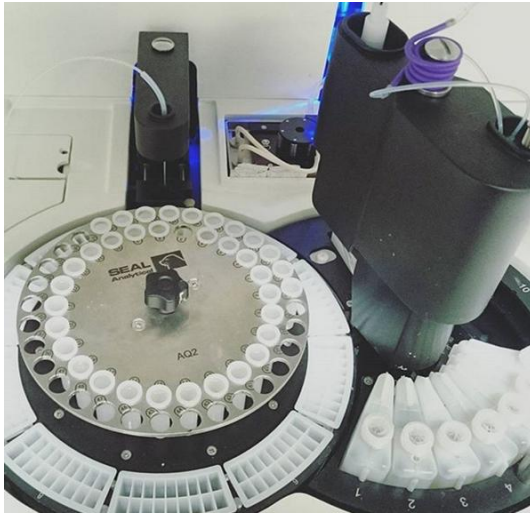


Figure 2.13 Water samples being run on the SEAL AQ2 discrete analyser for determination of nitrogen species.

2.2.3.3 General water chemistry

Simultaneously to dissolved gas sampling, dissolved oxygen (DO), pH, temperature and electrical conductivity (EC) were measured in situ using handheld multi-meters (Hanna Instruments HI-9145, HI-9124, HI-0933). The meters were calibrated every two weeks using their recommend calibration solutions.

2.2.4 Stage height, river discharge measurements and export

2.2.4.1 Formation of stage-discharge relationships

An estimation of discharge (volume per time, 'Q') in rivers and streams at Baddingsgill and Black Esk catchments was required to determine input and export (mass per time) of aquatic C and N concentrations to and from the reservoirs. Rates of flow were measured over a range of water levels at all major inlets ($n = 5$) and outlets ($n = 1$) at both Baddingsgill and Black Esk reservoirs to provide data for the construction of stage-discharge calibration curves (Carter and Davidian, 1989; Turnipseed and Sauer, 2010). A number of small drainage channels were not sampled due to time and cost constraints, and practicalities in that they often ran dry throughout much of the year due to their small size and were difficult to sample due to in-channel vegetation. Reliable estimates of the amount of water entering the reservoir from these channels would have been difficult to quantify. Cross-sectional area of the stream channel is calculated using the 'mid-section' method (Turnipseed and Sauer, 2010). Flow velocity measurements are generally made at each segment using a two-point method where the depth of water column is >0.76 m and using a six-tenths depth method where the depth is

<0.76 m, the latter of which was applicable to all streams at Baddinsgill and Black Esk reservoirs.

A Valeport Ltd. 801 single axis flow meter was used to measure water velocity. Stream flow was determined using the velocity (V), area (A) method. Firstly, the cross sectional area (CSA) of the river reach was divided into one to four segments depending on the width of the stream. The mean velocity at 0.6 of the water depth and the CSA of the stream channel was measured (Equation 2.5). The stream flow at each segment was calculated as the product of V and A (Equation 2.6). Total flow was the sum of the flows in each segment. A ratings curve was then constructed using measures of stream flow regressed against gauge height at the time of measurement. Discharge rates were then used to create individual stream rating curves by plotting a series of concurrent measurements of stage height and discharge, across the various flow conditions. The relationship between stage height and discharge was expressed by applying a line of 'best-fit' either power or order-two polynomial, to the observed measurements (Appendix I). The resulting relationship allowed an estimation of discharge when only stage data was available.

$$CSA = \frac{\sum D}{2} \times d \quad (2.5)$$

Where:

CSA = cross sectional area of channel, m^2 .

D = water depths bounding segment, m. (e.g. $D1+D2$, $D2+D3$ etc).

d = distance between depth measurements, m.

$$Q = V \times A \quad (2.6)$$

Where:

Discharge (Q) = stream flow, $m^3 \text{ sec}^{-1}$,

V = average water velocity in channel, $m \text{ sec}^{-1}$.

A = cross section area of channel, m^2 .

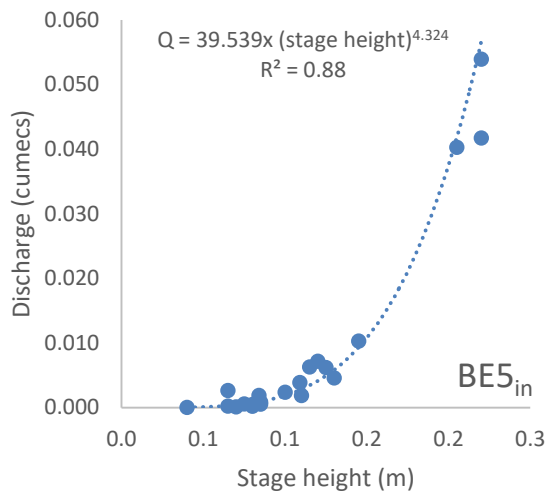


Figure 2.14 Example of a discharge-stage relationship curve for Black Esk inlet (BE5_{in}), alongside goodness of fit and the equation used to describe the relationship between stage height and discharge. Rating curves for other inlets and outlets are displayed in Appendix I.

2.2.4.2 Export and flow weighted concentrations

In order to calculate annual C and N loads in the inlets and outlets of Baddingsill and Black Esk reservoirs, 'Method 5' of (Walling and Webb, 1985) (Equation 2.7) was followed. Daily fluxes were estimated based on the dissolved concentrations, on sampling day, multiplied by the mean stream discharge, on sample day.

$$\text{Total load} = \frac{K \sum_{i=1}^n (C_i Q_i)}{\sum_{i=1}^n Q_i} \bar{Q}_r \quad (2.7)$$

K = Conversion factor to take account of period of record.

C_i = Instantaneous concentration associated with individual samples.

Q_i = Instantaneous discharge at time of sampling.

\bar{Q}_r = Mean discharge for record period.

n = Number of samples.

The standard error of flux estimates based on 'Method 5' was calculated following Equation 2.8 (Hope et al., 1997), where F is the total annual discharge and C_F is the flow-weighted mean concentration.

$$SE = F \times \sqrt{\text{var}(C_F)} \quad (2.8)$$

The variance of C_F ($\text{var}C_F$) is estimated from Equation 2.9 (Hope et al., 1997), where Q_n is the sum of all individual Q_i values.

$$\text{var}(C_F) = \left[\sum (C_i - C_F)^2 \times \frac{Q_i}{Q_n} \right] \times \left[\sum Q_i^2 / Q_n^2 \right] \quad (2.9)$$

2.3 Data analysis

Various stages of data processing, quality checks and statistical analysis, were required to produce and analyse the data during this study. R Studio statistical software was used for the all final statistical analysis, calculation of p-values, f-values, standard errors and histograms. Both ArcGIS and QGIS were used for catchment analysis and map making, with study specific details provided in the associated Chapters, 3-5.

2.3.1 Reservoir and stream evasion flux calculations

Evasion from the water surface of the reservoirs was calculated indirectly using wind speed to predict gas transfer velocity, combined with the partial pressure difference across the air-water interface. The method is based on established relationships between wind speed and gas transfer velocity (Wanninkhof, 1992; MacIntyre et al., 1995). This method is based on evasion from lake or ocean surfaces and is not applicable to fast flowing streams where stream banks shelter the water surface and turbulence is generated primarily from stream-bank and stream-bed friction. Gas fluxes ($\text{FCO}_2/\text{FCH}_4/\text{FN}_2\text{O}$) are calculated using Equation 2.10, Fick's first law, as described in Borges et al. (2004), where k is the gas transfer velocity (cm h^{-1}), a is the solubility coefficient and Δp_{gas} is the difference in partial pressure between the surface water and the atmosphere. The solubility coefficient a is temperature and salinity dependent. Values of a for CO_2 , CH_4 and N_2O were derived from Weiss (1974), Weisenburg and Guinasso (1979), and Weiss and Price (1980), respectively. The transfer velocity k is a function of turbulence, the kinematic viscosity of the water and the molecular diffusion coefficient of the gas. In Equation 2.11 (Cole and Caraco, 1998), wind speed (m s^{-1}) at 10 m above the water surface U_{10} is used to describe turbulence, and the Schmidt number Sc is a function of the latter two terms. $k(600)$ refers to the transfer velocity normalised to $Sc = 600$, the Schmidt number of CO_2 at 20°C in freshwater. This is then adjusted using the Schmidt number for the particular gas in freshwater at measured temperature using figures from Table 3.1 in MacIntyre et al. (1995) and then using Equation 2.12. The exponent in Equation (2.10) varies from $-\frac{2}{3}$ to $-\frac{1}{2}$ as wind speed increases and waves become present (Jähne et al., 1987). The exponent of $-\frac{1}{2}$ was selected due to the onset of wave action within

the reservoirs. Wind speed at 10 m (U_{10}) is calculated using Equation 2.13 (Erkkilä et al., 2018).

$$F_{gas} = k\alpha\Delta p_{gas} \quad (2.10)$$

$$k(600) = 2.07 + 0.215u_{10}^{1.7} \quad (2.11)$$

$$k = k(600) \left(\frac{Sc}{600} \right)^{\frac{1}{2}} \quad (2.12)$$

$$U_{10} = 1.22U_z \quad (2.13)$$

Stream evasion was calculated following largely the same procedure as reservoir evasion but with a different procedure to calculate $k(600)$. A number of measurements of stream width, depth and flow velocity were taken across different field visits to cover a range of flow conditions. As per section 2.2.4.1, discharge-stage relationship curves were established, and these were used to infer flow velocity and discharge for dates at which only depth measurements were available. The flow velocity and stream slope (calculated using GIS) were then used to find the gas transfer coefficient at a Schmidt number of 600 (i.e. $k(600)$) (Butman and Raymond, 2011; Magin et al., 2017; Raymond et al., 2012) using Equation 2.14, where S is the stream slope and v is the flow velocity.

$$k(600) = 2841.6 \times S \times v + 2.03 \quad (2.14)$$

In the U_{10} model, wind is the only factor considered for causing water turbulence and driving the gas exchange (Erkkilä et al., 2018). One shortcoming of this model is that it does not consider buoyancy flux driven turbulence during periods of cooling e.g. buoyancy flux is positive when the lake is heating and negative when cooling. Erkkilä et al. (2018) evaluated different models for calculating gas transfer velocity (k) and found that including the effect of lake cooling improves flux estimates but the models are not as simple to use as the wind-speed-based models and requires data which was not available for this study e.g. mixing layer depth, moisture, radiation data.

2.3.2 Statistical analysis

The normality of data is examined throughout the thesis with appropriate transformations made if required for particular statistical tests. Multiple linear regression analysis is applied in Chapters 3 and 4, which attempts to model the relationship between multiple explanatory variables and a response variable (e.g. CO_2 , CH_4 and N_2O) by fitting a linear equation to the observed data. This approach is typically used in the thesis to investigate relationships between water quality and catchment characteristics, and dissolved greenhouse gas

concentrations. Multiple linear regression was conducted on statistical software R (3.3.4, 2016) using the 'lm' function. Linear mixed effects modelling is applied in Chapter 5 to determine drivers of both aquatic and sediment GHG concentrations and fluxes. Mixed effects models have both fixed effects (i.e. influences the mean of y) and random effects (i.e. influences the variance of y).

Mixed effects models take care of non-independence of errors by modelling the covariance structure introduced by grouping the data. They are also useful when there is temporal and/or spatial pseudoreplication (e.g. repeated measurements) in the data as was the case here. Separate linear mixed effects model was built for each GHG, due to the different processes driving their production. Variables which would form terms in the model were identified, and an exploratory analysis carried out to identify appropriate transformations, and to highlight obvious relationships or potential problems for statistical analysis such as collinearity that can lead to artificially inflated p-values. GHGs in particular exhibited a high degree of positive skew, and were transformed by taking the log or principal cube root, which has a similar effect to log-transformation but accounts for the presence of zero and negative values. For each GHG, a small number of independent models were fitted, each using a subset of predictors and the maximal random effect structure justified by the design. Care was taken to fit uncorrelated random slope and intercept for each variable.

After a maximal model was fitted, an iterative procedure similar to that proposed by Bates, et al. (2015) was used to simplify it. Fixed and random effects were removed one-by-one, starting with high-order interactions and later guided by visualisation of the model and dataset. At each stage, an F-test based on the Kenward-Roger approximation was used to determine the significance of the removed terms, and whether they should remain in the model. All statistical analysis was carried out in R 3.2.3, using lme4 (Bates et al., 2015) to fit linear mixed effects models, pbkrtest (Halekoh and Højsgaard, 2014) to perform the Kenward-Roger approximate F-test, and MuMIn (Barton, 2018) to compute conditional and marginal coefficients of determination ('pseudo- R^2 ') for the final models.

3 The role of catchment characteristics in determining spatial variation of reservoir biogeochemistry

3.1 Introduction

Globally, inland waters are well known sources of greenhouse gases (GHG) to the atmosphere (Cole et al., 2007; Prairie et al., 2017; Tranvik et al., 2009), and in relation to their area, are important zones of nitrogen (N) and carbon (C) cycling (Whitfield et al., 2011). Biogeochemical processes in lakes and reservoirs are closely linked to their surrounding catchment as they receive allochthonous C and nutrient inputs via catchment runoff, streams and groundwater (Huttunen et al., 2003). Reservoirs are usually viewed as systems that are more tightly coupled with their catchment than most natural lakes due to relatively short residence times (Straskraba et al., 1993; Rinke et al., 2013). Reservoir GHG production rates are spatially and temporally variable, and are dependent on a wide variety of factors: i) between reservoirs e.g. catchment characteristics, latitude, altitude, lake morphology; ii) within reservoirs e.g. dissolved organic matter quantity and quality, water temperature, nutrient and pH levels, and along environmental gradients from inputting tributaries to the dam; and iii) over time e.g. as reservoirs age, seasonal variability, and change in catchment activities and dam operations (e.g. Sobek et al., 2003; Soumis et al., 2004; Tranvik et al., 2009; Barros et al., 2011; Mendonça et al., 2012; Prairie et al., 2017)

Inland water bodies are typically supersaturated with carbon dioxide (CO₂), leading to net emissions (Tranvik et al., 2009), particularly for those with large allochthonous C inputs or dissolved inorganic carbon (DIC) from carbonate weathering (Del Giorgio et al., 1999; Gómez-Gener et al., 2016). Many surface waters also emit methane (CH₄) which is mainly produced by microbes in anoxic sediments. Surface water CH₄ emissions vary depending on factors such as methanogenic and methanotrophic activities, in addition to dissolved oxygen concentrations (Rich and Wetzel, 1978), temperature (DelSontro et al., 2010; Ostrovsky et al., 2008), and organic and nutrient inputs. In-reservoir processes are important for gas consumption and production, and are regulated by factors including C sources and concentrations, N concentrations, as well as sediment type and lake morphology (Striegl and Michmerhuizen, 1998; Wang et al., 2006). Spatial variation also occurs within reservoirs along longitudinal gradients. GHG production, particularly CH₄ ebullition, is more common in shallower regions e.g. in littoral zones or in upper deltaic river environments rather than in deeper water zones near the dam (Bastviken et al., 2008; Beaulieu et al., 2014; Galy-Lacaux et al., 1999). Emissions of GHGs also vary spatially among reservoirs distributed along wide geographical gradients

(Mosher et al., 2015). Reservoir age affects organic matter and nutrient supplies, where (Kelly et al., 1997) found GHG emissions to negatively correlate with reservoir age as newer reservoirs often contain larger pools of labile organic C derived from freshly inundated terrestrial vegetation. This can drive both autochthonous and bacteria production, which can promote oxygen consumption and sediment anaerobic metabolism (Huttunen et al., 2003). Regional climate also influences GHG dynamics via differences in temperature, rainfall and wind speed. Mean annual air temperature has been found to affect GHG emissions, with low-latitude tropical reservoirs typically emitting more GHGs per unit area than high-latitude boreal and temperate systems (Barros et al., 2011). Temporally, reservoir GHGs also vary among seasons and years due to changes in temperature, hydrology, nutrient dynamics and stratification turnover dynamics (Beaulieu et al., 2014; Kankaala et al., 2006).

A growing body of work is highlighting the importance of nutrient status and associated primary productivity play in determining reservoir GHG dynamics (Deemer et al., 2016). For example, Li et al. (2015) found a negative correlation between nutrient enrichment, primary productivity and CO₂ fluxes. Supplementary nutrients support atmospheric C sequestration by increased photosynthesis which leads to accelerated organic C sedimentation and burial (Deemer et al., 2016). Eutrophication can also support greater CH₄ emissions by increasing organic matter quality and reducing reservoir bottom water oxygen concentrations. Despite greater uncertainty around reservoir nitrous oxide (N₂O) controls, strong positive correlations have been found between nitrate (NO₃⁻) concentrations and N₂O concentrations across aquatic systems (Baulch et al., 2011; Beaulieu et al., 2015). Current evidence suggests that there are different drivers for the production of different GHGs, for example, in a recent study by Deemer et al. (2016), CH₄ emissions were positively correlated with air temperature and chlorophyll a concentrations. CO₂ emissions were positively correlated with mean annual precipitation, while N₂O emissions were positively related to NO₃⁻ concentrations. Rantakari and Kortelainen (2005) observed precipitation flushing terrestrial C into surface waters, which in turn enhanced CO₂ concentrations and emissions by degradation of organic matter.

Catchment land-use has also been found to impact aquatic systems. For example, areas with agriculture are often sites of N₂O emissions (Seitzinger and Kroeze, 1998) as production is stimulated via fertilization with mineral and organic N compounds (Whitfield et al., 2011). Rawlins et al. (2014) found partial pressure of CO₂ (pCO₂) values in streams draining agricultural catchments to be greater than those in less managed or semi-natural environments. Similarly, Beaulieu et al. (2014) found reservoir GHG variation to be linked to catchment nutrient loading, particularly water bodies that received drainage from agricultural

areas versus natural land-cover. Land-use has also been strongly related to area-normalised C fluxes in a variety of catchments across the US (Butman and Raymond, 2011). Inland waters show positive correlations between CO₂ and allochthonous dissolved organic carbon (DOC) concentrations (Premke et al., 2016). High DOC concentrations are particularly associated with catchments containing large proportions of peat (Aitkenhead et al., 1999). Significant correlations have been found between DOC and nitrate concentration in upland streams (Harriman et al., 1998), along with percentage wetland cover and sub-catchment drainage area (Frost et al., 2006). Catchment slope can account for GHG variation as it influences contact time between soil and water percolation (Rawlins et al., 2014).

Given the global variation in reservoir age, size, geomorphology and catchment characteristics, there is a growing need for additional studies, to provide insight into factors that drive the differences in GHG dynamics among reservoir type and locations. Identifying both spatial and temporal GHG drivers within and among reservoirs is an important step in developing a predictive framework that could be used to forecast future GHG emissions of both existing reservoirs as well as ones being constructed or planned (Mosher et al., 2015). Identification of environmental drivers of GHGs requires data from geographic regions and environments that lack current study. For example, the temperate climate zone accounts for ~40% of total reservoirs (Barros et al., 2011) but quantification remains sparse (DeSontro et al., 2010; Soumis et al., 2004) with only a couple of studies investigating UK reservoir GHG dynamics. Such studies do exist for other aquatic systems such as natural lakes, rivers, streams and peatland systems. In addition, very few studies have concurrently investigated the three major biogenic GHGs (CO₂, CH₄, N₂O), critical for understanding the net role of reservoirs in GHG balances (C. Whitfield et al., 2011).

Here we present baseline results from a synoptic sampling survey that aims to quantify aquatic C and N concentrations from a variety of temperate freshwater reservoirs (n = 30) within geographically distinct regions of the UK. Quantification of GHG concentrations and evasion from reservoirs in Scotland and Wales are needed to better constrain GHG budgets, which is particularly important for CH₄ and N₂O due to limited data. We specifically aim to improve understanding of catchment controls on aquatic GHGs, in order to elucidate how pressures in the future may impact these systems (Whitfield et al., 2011). Accordingly, the specific objectives of this research were threefold: 1) to quantify aquatic C and N concentrations, and estimate emissions via evasion from Welsh and Scottish reservoirs; 2) to explore the influence of catchment and reservoir morphological and biophysical characteristics

on observed GHG concentrations; and 3) to determine whether there are regional spatial differences between concentrations.

3.2 Methods

The UK experiences a humid maritime climate, which is moderated by the North Atlantic Ocean. The 30 year (1981-2010) annual average temperature is 14.3 °C (Met Office, UK), ranging from 0.9-6.4 °C in January to 10.9-19.4 °C in July. Average annual UK precipitation (1981-2010) is 1154 mm, ranging between 70 mm in May to 122 mm in January and with highest precipitation levels observed at higher elevations. For the 2015-2016 sampling period, the majority of months were at least slightly warmer than average for the UK, most notably September, with both April and November cooler than average, and most places were within 10% of the yearly average for rainfall. For both 2015 and 2016, Wales had a higher mean temperature (9.5°C and 9.7°C, respectively) than Scotland (7.6 °C and 7.8 °C, respectively). Yearly rainfall for 2015 was higher in Wales (1493 mm) than in Scotland (1250 mm), whilst 2016 saw higher rainfall in Scotland (1499 mm) than Wales (1370 mm) (Met Office, 2016, 2015).

To capture spatial variability in water physico-chemistry, nutrient and GHG concentrations, 30 reservoirs were selected in coordination with associated water companies to exhibit a wide variation in catchment properties, including elevation, precipitation, soil, geology and land use. The majority of the reservoir catchments are located in remote upland locations in Scotland and Wales but some are affected by anthropogenic disturbances such as forestry, agriculture and sheep grazing. The catchments were generally characterised as having rough grazing and moorland land cover, dominated by podzols and peaty gleys, with numerous catchments also having areas of deeper blanket peat.

Four field campaigns were conducted seasonally over a one year period between September 2015 and October 2016 where 30 drinking water reservoirs in Scotland and North Wales were sampled for diffusive greenhouse gas concentrations and water chemistry variables (Figure 3.1). Seasons were defined in accordance to the hydrological year (autumn = September to November; winter = December to February; spring = March to May; Summer = June to August). Reservoirs were sampled over a two week period per season between 0830 and 1830 GMT each day with a precise time recorded at each site. The location and elevation of the sampling sites were recorded using a global positioning system (Garmin™). Sampling took place at two locations per reservoir, with samples being taken in duplicate (n = 4). Locations were determined based on the following criteria: i) away from feeder inlets where incoming

water might be more concentrated as it is not properly mixed with reservoir water; ii) avoiding isolated bays or narrow inlets of the reservoir as they way also be poorly mixed and contain water of a different quality; iii) where possible, sampling from opposite ends of the reservoir where wind could influence spatial water quality concentrations; and iv) as access was via foot, safety was also an important consideration and locations were scoped out on Ordnance Survey (OS) maps beforehand and adjusted in the field if necessary. Water samples were collected in areas that were free of littoral and/or macrophyte vegetation, apart from in one Welsh reservoir, which could not be avoided due to the reservoir also being surrounded by wetland, trees or thick vegetation limiting access.

3.2.1 Reservoir characteristics and field sampling



Figure 3.1 Catchment locations of sampled reservoirs in Scotland and North Wales.

3.2.2 Measurement of water physico-chemistry, nutrient and GHG concentrations

Surface water and headspace samples (including replicate and ambient) were collected from two locations on each of the thirty reservoirs. Dissolved CO₂, CH₄ and N₂O gas samples were collected using the headspace technique which is fully described by Kling et al. (1991), Billett et al. (2004) and Dinsmore et al. (2010). A 40 ml water sample, collected from ~10 cm water depth, was equilibrated with 20 ml headspace of ambient air in a 60 ml polypropylene syringe at water temperature by shaking vigorously underwater for one minute. The equilibrated 20

ml headspace was then injected into a 12 ml pre-evacuated gas-tight borosilicate Exetainer[®] (Labco, Lampeter, UK). Ambient air samples (20 ml) were collected from a height of ~2 m and stored in Exetainers[®] from each sampling point. Septum-capped Exetainer[®] vials have been proven to be suitable for long-term storage and transport (Bastviken et al., 2004; Glatzel and Well, 2008). Wind speed, air temperature and barometric pressure were also obtained from each sampling location with a Kestral 2500 hand-held weather meter (KestrelMeters.com, Pennsylvania, USA, accuracy 3% of reading) at 1 m above the water surface.

Headspace and ambient samples were analysed on a 7890B gas chromatograph (Agilent Technologies, UK Ltd, Stockport, UK) with flame ionization detector (FID) and attached methaniser for CH₄ and CO₂, and micro electron capture detector (μ ECD) for N₂O. These detectors were setup in parallel allowing the analysis of the GHGs at the same time. The peak detection and integration were performed using OpenLAB CDS ChemStation (Agilent Technologies). Dissolved concentrations of CO₂, CH₄ and N₂O in the reservoir surface water were calculated (as per Chapter 2, section 2.2.1) from the headspace and ambient concentrations according to Henry's Law using temperature dependent solubility (Weiss, 1974; Weiss and Price, 1980). The Bunsen solubility coefficient, corrected for temperature and salinity (Yamamoto et al., 1976), was used for dissolved CH₄ concentrations. Equilibrium concentrations were also calculated with the solubility equations using measured air concentration, barometric pressure and water temperatures for individual reservoirs. In order to evaluate the overall importance of the three GHG in terms of global warming potential (GWP) over the 100 year horizon, concentrations of CH₄ and N₂O were multiplied by 34 and 298, respectively (IPCC, 2014). Excess partial pressure values are also used, where the term 'ep' refers to the partial pressure of the gas in solution divided by the partial pressure in equilibrium with the atmosphere; hence an 'ep' of >1 suggests the reservoir surface water was consistently oversaturated with respect to the atmosphere.

Evasion rates were calculated (as per Chapter 2, section 2.3.1) indirectly using wind speed to predict gas transfer velocity, combined with the partial pressure difference across the air-water interface, using established relationships between wind speed and gas transfer velocity (Wanninkhof, 1992; MacIntyre et al., 1995). Evasion gas fluxes were then calculated following Billett and Moore (2008); Borges et al. (2004). The solubility coefficient values for CO₂, CH₄ and N₂O were derived from Weiss (1974), Weisenburg and Guinasso (1979), and Weiss and Price (1980), respectively. Wind speed at 10 m above the water surface was calculated according to (Cole and Caraco, 1998) and Erkkilä et al. (2018).

Duplicate water samples were collected from the two locations chosen on each reservoir to optimise spatial coverage ($n = 4$). Samples were collected using a 60 ml syringe at ~ 10 cm depth in the water column and filtered in the field by passing through $0.45 \mu\text{m}$ syringe-driven filters (Watmann®). They were stored in 30 ml and 100 ml Nalgene bottles that were thoroughly cleaned (Decon soaked and rinsed with deionised (DI) water) before being taken into the field, and were further rinsed with the filtered sample. The samples were kept in a dark cool box during transport, and on return to the field base all samples were refrigerated at $\sim 4^\circ\text{C}$. On return to the Centre for Ecology & Hydrology (CEH) in Edinburgh, the 30 ml water samples were immediately placed in a refrigerator at $\sim 4^\circ\text{C}$ for DOC and DIC analysis within one week of collection whilst the 100 ml samples were frozen at -18 to -21°C for nutrient analysis at a later date. At the same time as water sample collection, dissolved oxygen (DO), pH, temperature and electrical conductivity (EC) were measured in-situ using handheld multi-meters (Hanna Instruments HI-9145, HI-9124, HI-0933 respectively). The multi-meters were calibrated each time before being taken into the field using water saturated air, buffer solutions (pH 4 and 7) and a conductivity standard with thermometer. The refrigerated sample was analysed for DOC and DIC on a PPM LabTOC (Pollution & Process Monitoring, UK) and a PPM PSA auto sampler. Organic carbon in the sample was converted to CO_2 by UV-persulphate oxidation and then measured using an infrared detector. Samples were reacted with a solution of 5% sodium persulphate, 5% orthophosphoric acid in DI water. Detection range is $0.1\text{--}4000 \text{ mg L}^{-1}$ and concentrations were calculated based on a three point calibration curve with a maximum of 50 mg L^{-1} (analytical accuracy of the instrument is 1% of standard concentration i.e. $\pm 0.5 \text{ mg C L}^{-1}$ for the 50 ppm standard). For further quality control within each analytical batch, standards (50 ppm) and blank DI samples were added at the start and end of a run. The filtrate from the frozen sample bottle was analysed for ammonium (NH_4^+) by phenate colorimetry, nitrite (NO_2^-) by reaction with N-(1-Naphthyl)ethylenediamine and sulfanilamide and measurement of absorption at 540 nm, and nitrate (NO_3^-) using the Cd-reduction method on a Seal AQ2 Discrete Analyser (SEAL Analytical, Ltd) following Methods: EPA 350.1 v2 and EPA 353.2 v2 (USEPA, 1993). The instrument was calibrated immediately before analysis and verified for quality using analysis of laboratory duplicates, fortified blanks and method blanks. Freezing of samples was necessary because of the time required between collection and analysis. However, freezing has been shown to reduce concentrations (Fellman et al. 2008). Short-term cold storage in a refrigerator has similar effects as single freezing and thawing (Hudson et al. 2009), hence stronger long-term effects of cold storage were avoided by

freezing and thawing the samples only once and processing them identically. It is therefore assumed that this impacted all samples similarly and minimally.

3.2.3 GIS and statistical analysis

Geographic Information Systems (GIS) was used to quantify catchment characteristics based on catchment boundaries obtained from the UK Lakes Portal and inland water bodies downloaded from EDINA Digimap. Land cover was derived from the Land Cover 2015 map (Centre for Ecology & Hydrology), where the 15 broad habitat classes occurring in the catchments were re-coded into 9 classes following (Porter et al., 2017): coniferous woodland, broadleaf woodland, arable, improved grassland, rough grazing, bog, moorland, freshwater and suburban.

A digital database of Hydrology of Soil Types (HOST; Boorman et al. 1995) which classifies UK soils into 29 groups according to their hydrological characteristics was also used. Of the 29 HOST classes, 16 classes were present across the reservoir catchments. Following Chiverton et al. (2015), four different HOST groups were created based on the depth to the gleyed layer (reduced from the 16 occurring HOST classes). HOST no gleying is the % of catchment made up of classes 4-7 & 17; HOST gleyed between 40 cm and 100 cm is the % of catchment made up of classes 18-19 & 22; HOST gleyed within 40 cm is made up of classes 14 & 24-25. HOST peat total is the % of catchment made up of peat (classes 11, 12, 15 & 26-29). These were re-coded further to identify what catchment percentage was made up of peaty gleys (classes 11, 12, 15, 26), peaty rankers (class 27) and blanket peats (class 29). HOST class 98 representing lakes were not identifiable by GIS analysis for every catchment (Figure 3.4) and this category was excluded from further statistical analysis. Underlying catchment geology was also downloaded (British Geological Survey 50k Bedrock map; EDINA Digimap) where bedrock classes were aggregated to form new groups as shown in Figure 3.3. Each land cover, geology and HOST class was then expressed as a percentage of its respective catchment area using QGIS. Elevation, slope and aspect summary statistics were derived from a Digital Terrain Model (OS Terrain 5 DTM; EDINA Digimap). Slope was calculated using the Zevenbergen Thorne formula within QGIS (Zevenbergen and Thorne, 1987). Summary statistics (min, max, average, median and standard deviation (SD)) were calculated for slope and elevation, with a directional average computed for aspect.

Statistical analysis

Principal component analysis (PCA) was carried out to identify the main parameters that explain data variation of the observed groupings at the reservoir sites. The analysis aimed to

link the observed variability in dissolved GHG concentrations with the water quality, geomorphic and biophysical variables. PCA is a data reduction technique that transforms the variables into principle components (uncorrelated/independent variables that are linear combinations with observable variables) which explain the variance observed in the original data. As concentrations were used for the analysis, water temperature was excluded as temperature is attributed to gas solubility. Reservoir sites were grouped considering similarities in water quality and catchment characteristics using hierarchical cluster analysis (CA) with Ward method of association (Chiverton et al., 2015; Ward, 1963). The distance between two groups depends on the sum of the sum of the squares of the analysis of variance, resulting in a dendrogram that summarised the clustering processes.

A comprehensive suite of water quality (pH, conductivity, dissolved oxygen, EC, DIC, DOC, CH₄, CO₂, N₂O, NO₂⁻, NO₃⁻, and NH₄⁺), geomorphic (reservoir area, catchment area, elevation, slope, reservoir area: catchment area ratio) and biophysical landscape variables (percentage HOST, geology and LCM classes) were tested for correlation with dissolved gas concentrations using multiple linear regression models. The majority of the HOST, geology and land use percentage data was sparse and did not meet assumptions of normality so was excluded from linear regression models. To improve normality, variables were natural log transformed and cubed-root transformed (Table 3.3). Due to the non-normal nature of the non-transformed data, medians, 1st and 3rd quartiles (25th and 75th percentiles) representing the interquartile range (IQR) since means and standard deviations would not be robust. All statistics were performed in R 3.4.4 (R Core Team, 2018) using the tidyverse package, `kruskal.test`, `wilcox.test` and `lm()`, `hclust()`, `prcomp()` and `ggbiplot()` functions.

3.3 Results

3.3.1 General reservoir water quality and catchment characteristics

The studied reservoirs represent a large gradient in environmental and geographic factors, showing spatial variability across the reservoirs (Table 3.1). The majority of the study catchments were located above 360 m, with gentle slopes of a rolling to hilly topography (median 8.3°) (Table 3.1). There was a wide range in both reservoir (4 to 1330 ha; median 40 ha) and catchment areas (106 to 10900 ha; median 1241 ha). Reservoir area significantly correlated to catchment area (Pearson's $r = 0.70$; $p < 0.001$, $n = 30$).

The dominant catchment land cover were 'rough grazing' (0-93%; median = 52%, occurring across $n = 30$ catchments), 'moorland' (0-94%; median = 6%, occurring across $n = 27$ catchments) and 'coniferous woodland' (0-96%; median = 2%, occurring across $n = 21$

catchments) (Figure 3.2). 'Arable' was present in a number of catchments ($n = 10$) but at <3% maximum coverage. Similarly, 'suburban' also had low maximum coverage (<2%) across catchments ($n = 9$).

The dominant bedrock geology in the catchments were sandstones (0-100%; median = 12%, occurring across $n = 23$ catchments), and mudstones and silts (0-100%; median = 1% and occurring across $n = 18$ catchments) (Table 3.1). The class breakdown of geology across all 30 catchments is shown in Figure 3.3, with key differences seen between Scotland and Wales. The Scottish reservoirs have a larger percentage of mudstones and sandstones, granites and metamorphic rock types, with Welsh catchments being more homogeneous with sandstones, mudstones and silts.

The prevalent HOST type was Total Peat (0-100%; median = 83% and occurring at $n = 27$ catchments) (Figure 3.4). Within this category, peaty gleys were the dominant HOST type (0-100%; median = 45%, at $n = 24$ catchments), followed by blanket peats (0-100%; median = 8%, at $n = 17$) and peaty rankers (0-57%; median = 0% at $n = 3$ catchments). This implies that the hydrological conditions of these catchments were mostly poorly draining.

Reservoir water chemistry exhibited considerable variation for most variables (Table 3.1). The vast majority of reservoirs had a circumneutral pH (median = 6.9) but ranged widely from acidic (minimum = 4.6) to alkaline (maximum = 8.5). Conductivity also ranged widely but was generally low across all reservoirs (median = $42 \mu\text{S cm}^{-1}$). Concentrations of NH_4^+ , NO_2^- and NO_3^- were low, with greatest variability seen across reservoir NO_3^- concentrations (Table 3.1). Median concentrations of DOC and DIC were 5.8 and 3.4 mg L^{-1} , respectively. There was also high DOC and DIC variability between reservoirs and seasons, with concentrations as high as 29.6 and 33.5 mg L^{-1} , respectively.

The study reservoirs tended to be on average, oversaturated with all of the biogenic gases. Median concentrations for the 30 reservoirs for CO_2 , CH_4 and N_2O were $1396 \mu\text{g L}^{-1}$, $1 \mu\text{g L}^{-1}$ and $0.7 \mu\text{g L}^{-1}$, respectively (Table 3.1). Nitrous oxide showed the least variability of the three gases with dissolved concentrations being close to saturation (average 1.3 times saturation). Average saturation was higher for CO_2 (2.2 times saturation). Methane concentration had more variability than the other gases with an average epCH_4 of 63.9. When split between the campaigns, reservoirs in Scotland had higher overall median concentrations across all three gases compared to Wales ($\text{CO}_2 = 1791$ vs. 1031 ; $\text{CH}_4 = 1.2$ vs 0.9 and $\text{N}_2\text{O} = 0.8$ and $0.6 \mu\text{g L}^{-1}$, respectively). Statistically significant differences (ANOVA) at the 95% confidence level between

the Scotland and Wales campaigns were found for concentration of CO₂ ($p < 0.001$) and N₂O ($p = 0.015$), but not CH₄ ($p = 0.905$).

Table 3.1 Reservoir and catchment characteristics for the study sites (n = 30), including water quality, geomorphic and biophysical properties. The median, 1st and 3rd quartiles (25th and 75th percentiles) representing the interquartile range (IQR) are shown.

Variable	Units	Q1	Q2	Q3
Catchment area	ha	257	1241	2495
Reservoir area	ha	13	40	139
Catchment:Lake ratio		13	22	42
Elevation	m	263	359	420
Slope	°	6	8	16
HOST - no gleying	%	0	0	24
HOST - gleying between 40-60 cm	%	0	0	2
HOST - gleying below 40 cm	%	0	0	2.1
HOST - Total Peat	%	53	83	100
HOST - Peaty Gleys	%	7	45	72
HOST - Peaty Rankers	%	0	0	0
HOST - Blanket Peat	%	0	8	29
LCM - Rough Grazing	%	10	52	76
LCM - Coniferous woodland	%	0	2	7
LCM - Suburban	%	0	0	0
LCM - Freshwater	%	3	5	8
LCM - Moorland	%	1	6	23
LCM - Bog	%	0	0.2	4
LCM - Broadleaf woodland	%	0	0	1
LCM - Improved	%	0	0.4	9
LCM - Arable	%	0	0	0.1
Geology - Basalts	%	0	0	0
Geology - Granites	%	0	0	0.1
Geology - Conglomerates	%	0	0	0
Geology – Sandstone	%	0.3	12	65
Geology - Mudstones and sandstones	%	0	0	14
Geology - Mudstones and silts	%	0	1.2	57
Geology – Limestone	%	0	0.0	0.0
Geology - Basic igneous	%	0	0.0	0.0
Geology - Fine grained acidic igneous	%	0	0.0	0.3
Geology - Medium and coarse grained igneous	%	0	0.0	0.3
Geology – Metamorphic	%	0	0.0	0.0
DOC	mg L ⁻¹	3.5	6.0	9.8
DIC	mg L ⁻¹	1.2	3.4	9.9
NH ₄ ⁺	µg L ⁻¹	9.0	22	46
NO ₂ ⁻	µg L ⁻¹	1.0	2.0	3.0
NO ₃ ⁻	µg L ⁻¹	65	112	194
pH		6.4	6.8	7.2
DO	%	37	47	58

Variable	Units	Q1	Q2	Q3
Conductivity	$\mu\text{S cm}^{-1}$	28	42	75
Water temperature	$^{\circ}\text{C}$	6.0	11	176
CH ₄	$\mu\text{g L}^{-1}$	0.37	0.99	3.0
CO ₂	$\mu\text{g L}^{-1}$	998	1362	2163
N ₂ O	$\mu\text{g L}^{-1}$	0.59	0.74	0.88

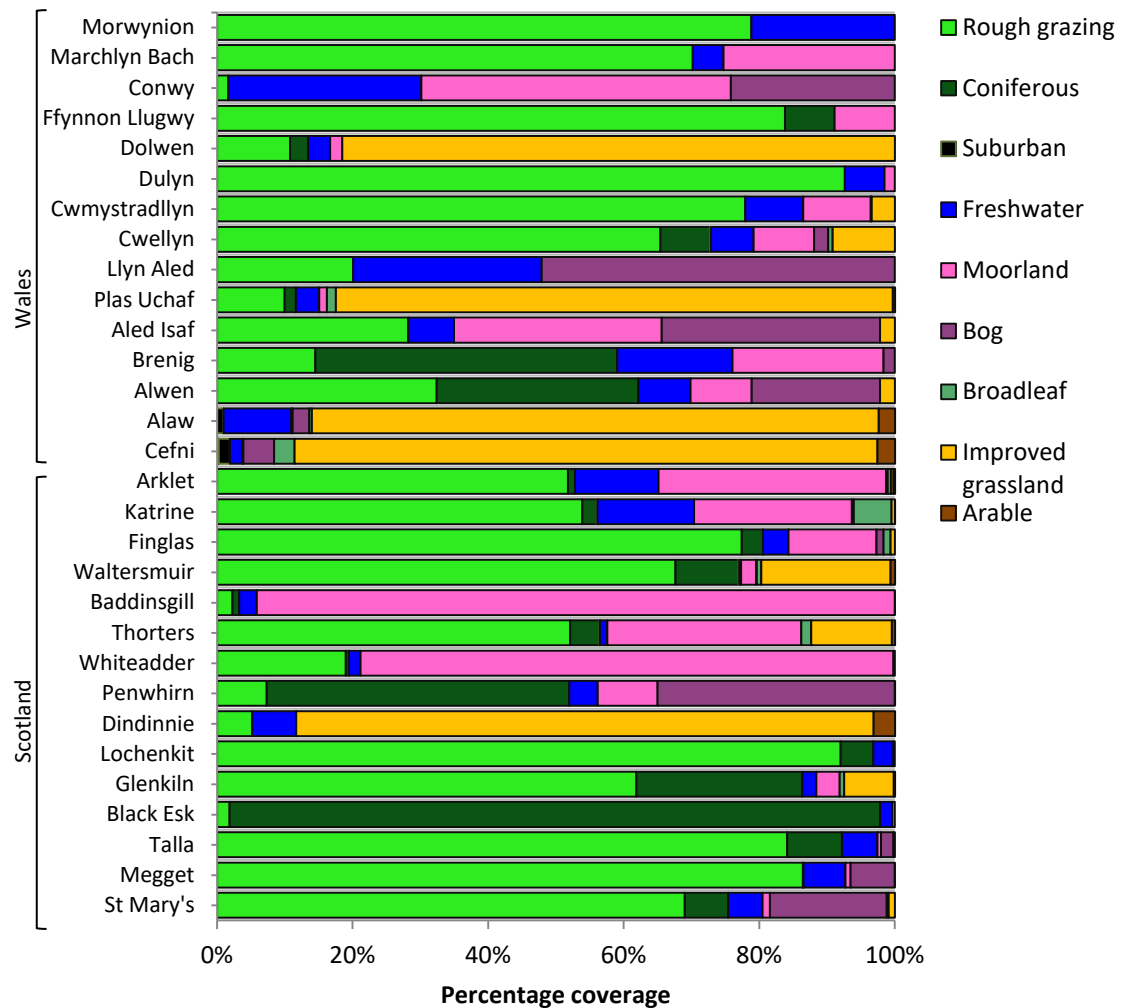


Figure 3.2 Bar plot showing the proportion of land cover classes associated with each catchment.

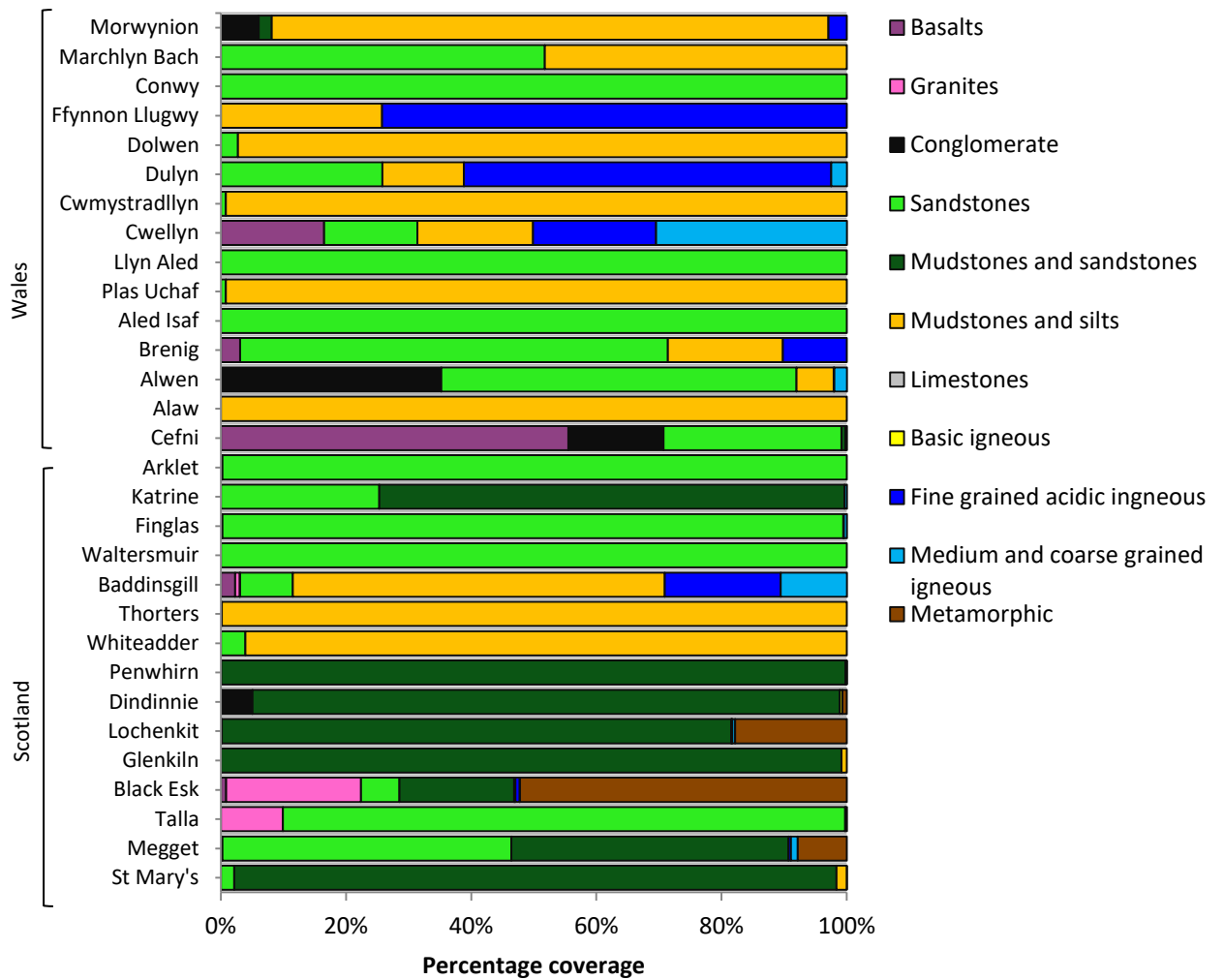


Figure 3.3 Bar plot showing the proportion of geology classes associated with each catchment.

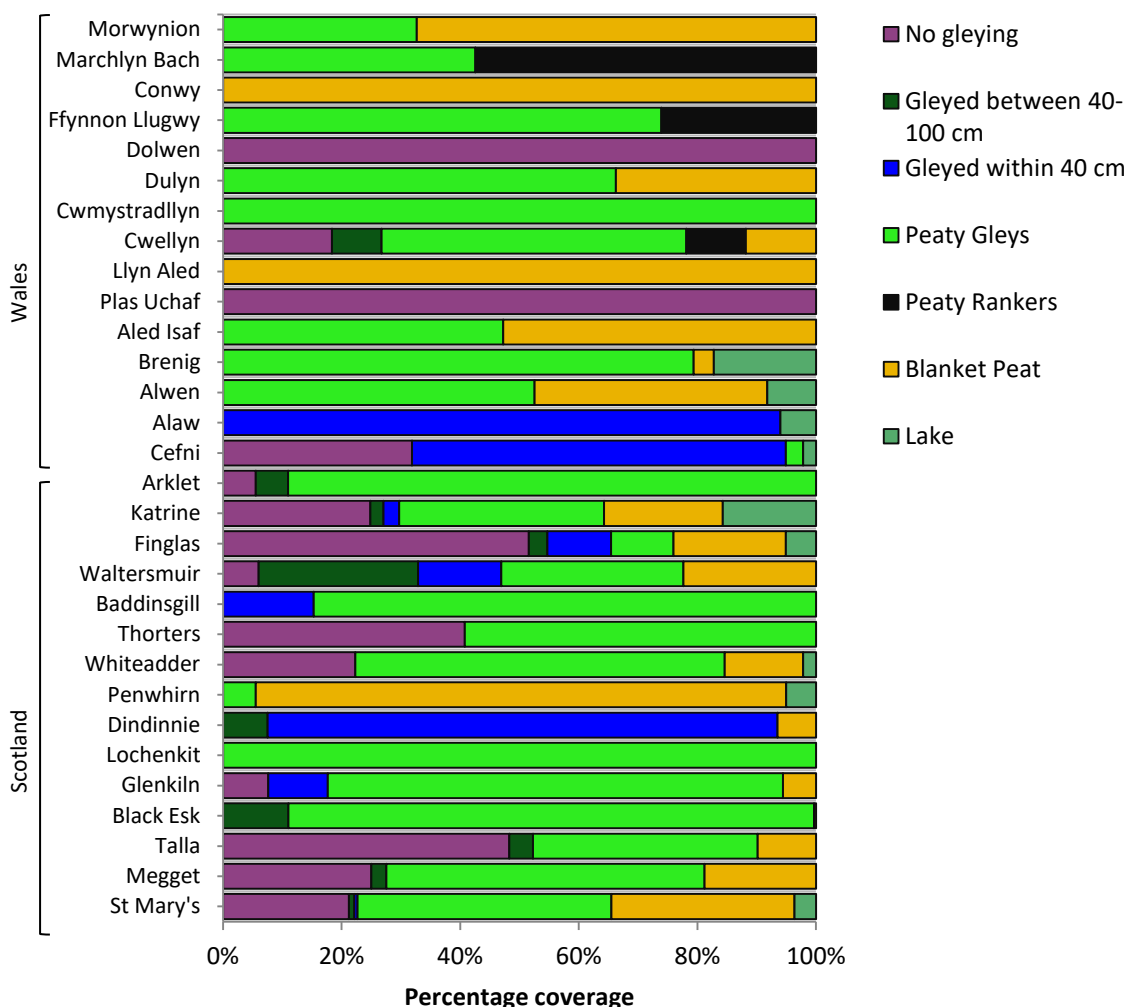


Figure 3.4 Bar plot showing the proportion of HOST categories within the catchments, with total peat split into categories representing peaty gleys, peaty rankers and blanket peat.

3.3.2 Seasonal variability in C and N concentrations

Both median CO_2 ($2110 \mu\text{g L}^{-1}$) and CH_4 ($1.7 \mu\text{g L}^{-1}$) concentrations were highest during the autumn sampling for Scottish reservoirs, whilst Welsh reservoirs had higher concentrations in winter for CO_2 ($1384 \mu\text{g L}^{-1}$) and spring for CH_4 ($1.1 \mu\text{g L}^{-1}$) (Figure 3.7). Both Scotland and Wales saw highest median N_2O concentrations in winter (0.94 and $0.89 \mu\text{g L}^{-1}$, respectively). Dissolved organic carbon concentrations for both Scotland and Wales were higher in autumn (10.5 and 5.0 mg L^{-1} , respectively), while highest DIC concentrations occurred in summer (9.0 and 9.5 mg L^{-1} , respectively). Concentrations of NO_3^- for both Scotland and Wales were higher in spring (0.15 and 0.18 mg L^{-1} , respectively). There was little seasonal variability in NO_2^- concentrations across both Scotland and Wales, with NH_4^+ being higher in winter for Wales (0.06 mg L^{-1}), with again, little seasonal variation across the Scottish sites. A Holm-Bonferroni

corrected Wilcoxon signed rank test to compare seasons found statistically significant differences ($p < 0.01$) across all three GHGs in winter's aquatic concentration vs. each of the other seasons. For N_2O only, there were also statistically significant ($p < 0.001$) differences in summer's aquatic concentration vs. each of the other seasons.

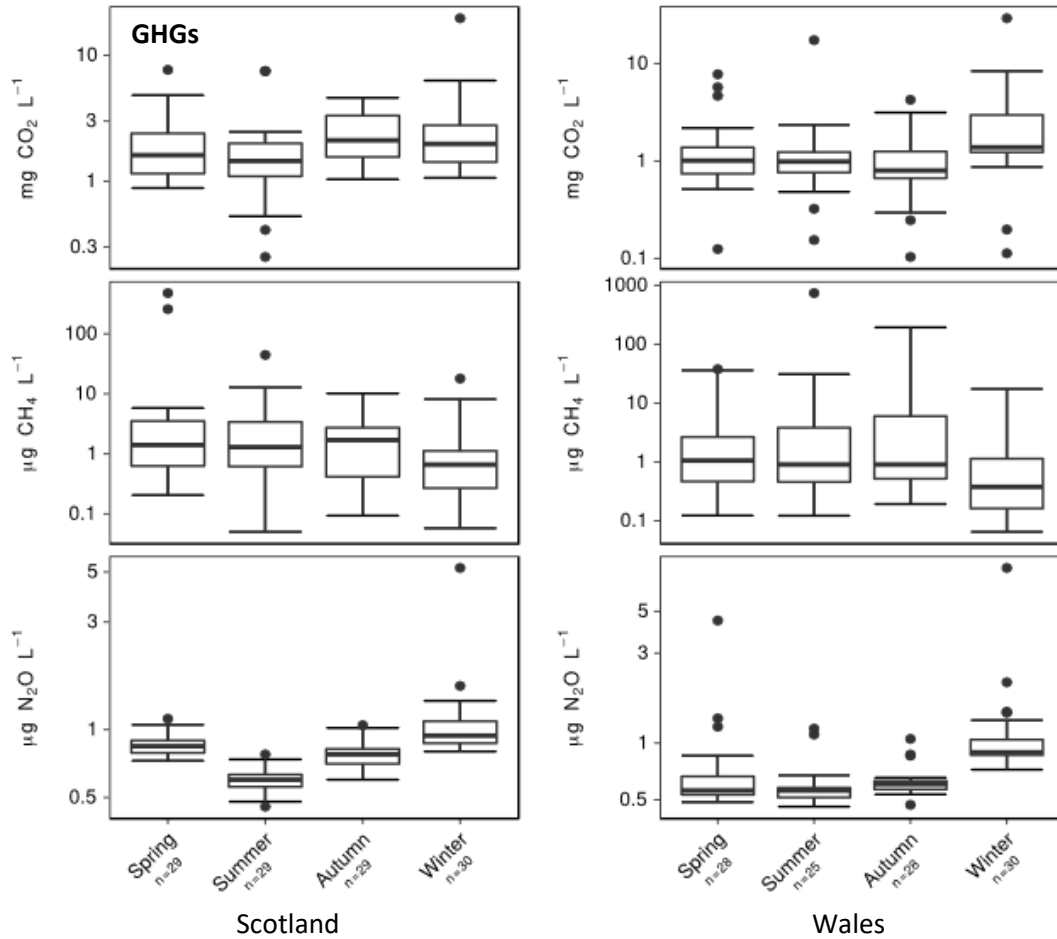


Figure 3.5 Seasonal variability in concentrations of CO_2 , CH_4 and N_2O , across the 30 Scottish and Welsh reservoirs.

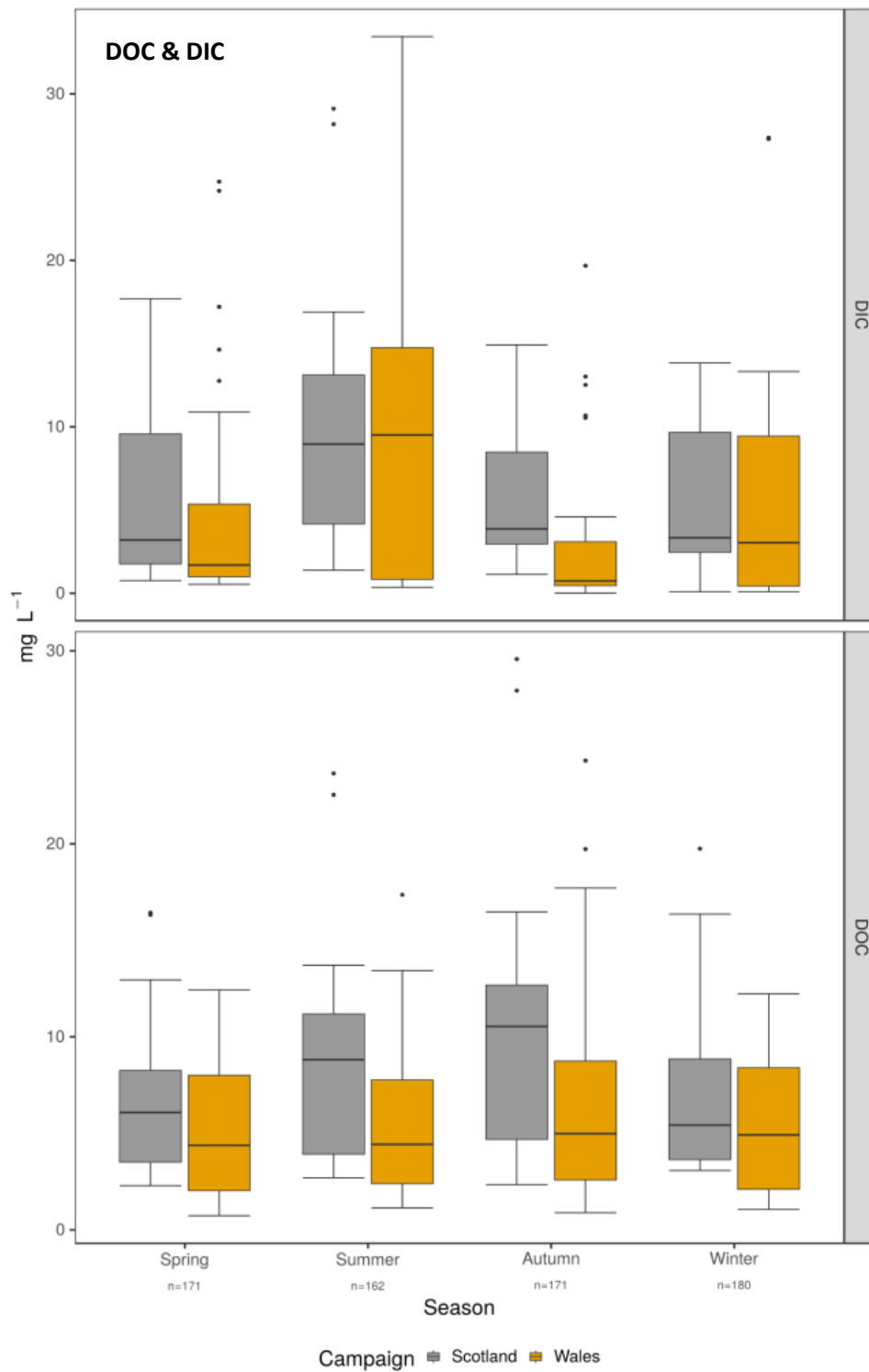


Figure 3.6 Seasonal variability in concentrations of DOC and DIC across the 30 Scottish and Welsh reservoirs.

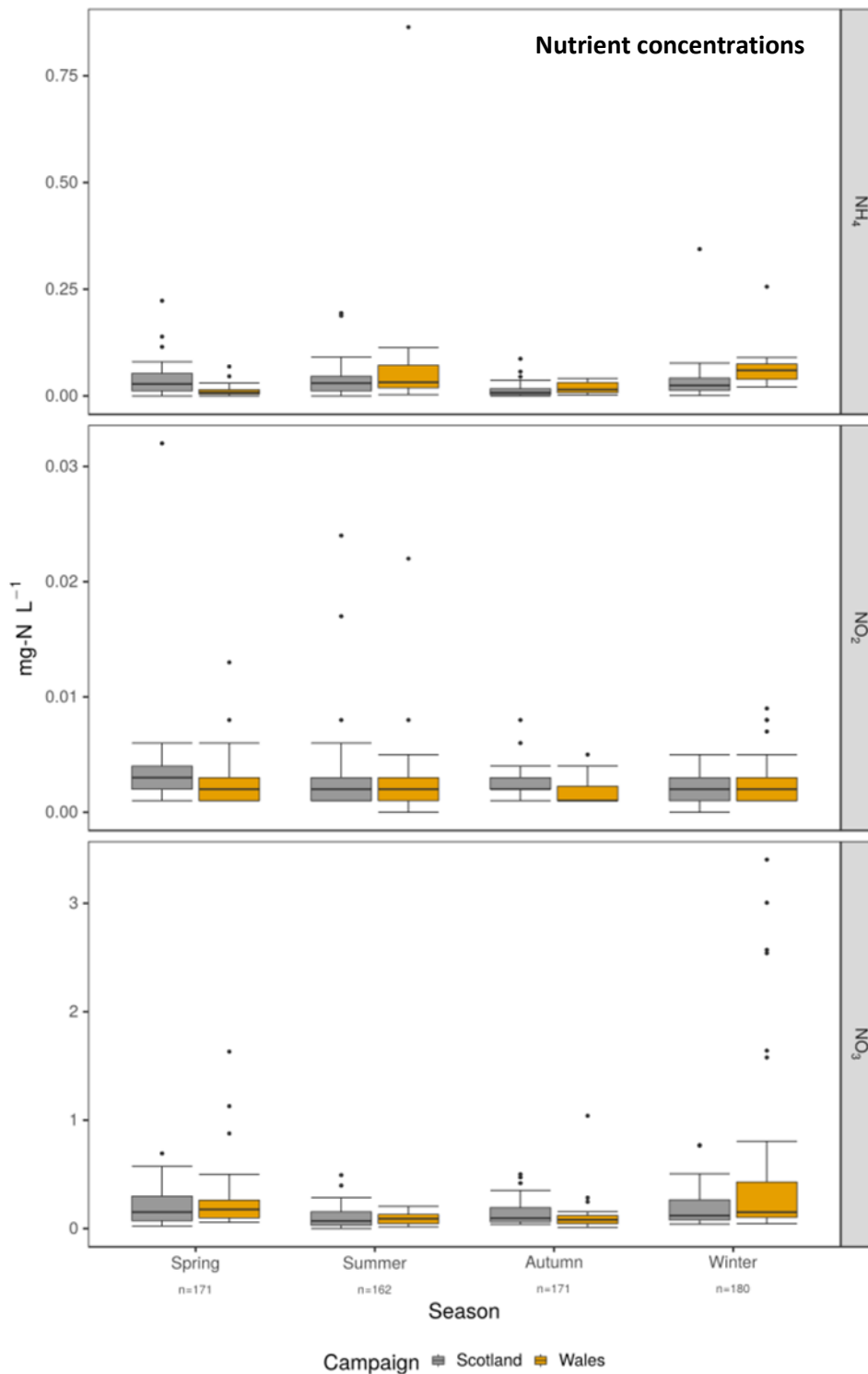


Figure 3.7 Seasonal variability in concentrations of NH_4^+ , NO_2^- , NO_3^- across the 30 Scottish and Welsh reservoirs.

3.3.3 Spatial variability in evasion and excess partial pressure by reservoir

The median CO_2 evasion across the 15 reservoirs in Scotland was $4.34 \text{ mg C m}^{-2} \text{ h}^{-1}$ (range -3.36 to 71) and was higher compared to median evasion rates of $1.58 \text{ mg C m}^{-2} \text{ h}^{-1}$ (range -17.2 to

126) from the 15 reservoirs in Wales (Table 3.2). Scotland reservoirs had a median $epCO_2$ of 1.79 (range 0.31 to 20.1) and reservoirs in Wales had a median $epCO_2$ of 1.29 (range 0.04-20.3), indicating that overall, the reservoirs were supersaturated in CO_2 . In Scotland, reservoirs with the highest evasion rates for CO_2 -C were Glenkiln ($8.74 \text{ mg C m}^{-2} \text{ h}^{-1}$), Lochokit ($8.13 \text{ mg C m}^{-2} \text{ h}^{-1}$) and Black Esk ($7.98 \text{ mg C m}^{-2} \text{ h}^{-1}$). In Wales, similar high evasion rates were observed in Cefni ($12.9 \text{ mg C m}^{-2} \text{ h}^{-1}$) and Aled Isaf ($8.33 \text{ mg C m}^{-2} \text{ h}^{-1}$). Dolwen reservoir in Wales was the only reservoir to have an overall negative median evasion of $-0.06 \text{ mg C m}^{-2} \text{ h}^{-1}$, and an $epCO_2$ of 0.99 which suggests it is in equilibrium with atmospheric CO_2 .

Both $epCH_4$ (range 0.78-540) and CH_4 evasion (-0.49 to $11700 \text{ } \mu\text{g C m}^{-2} \text{ h}^{-1}$) showed a higher variability between sites, particularly when compared to CO_2 (Table 3.2). Scotland had a higher median CH_4 evasion rate than Wales, 18.2 vs. $12.6 \text{ } \mu\text{g C m}^{-2} \text{ h}^{-1}$, respectively. Reservoirs in Wales showed a greater range in CH_4 evasion, with maximum rates of $11700 \text{ } \mu\text{g C m}^{-2} \text{ h}^{-1}$, compared with $6040 \text{ } \mu\text{g C m}^{-2} \text{ h}^{-1}$ across the Scotland sites. In Scotland, Dindinnie and Waltersmuir have the highest median evasion rates of 85.4 and $67.0 \text{ } \mu\text{g C m}^{-2} \text{ h}^{-1}$, respectively. Both these sites were consistently supersaturated with median $epCH_4$ of 36.5 and 70.2, respectively. In Wales, both Cefni and Dolwen had highest median CH_4 evasion at 274 and 119, $\mu\text{g C m}^{-2} \text{ h}^{-1}$, respectively. Both sites were highly supersaturated with median $epCH_4$ of 226 and 102, respectively.

Evasion of N_2O across Scotland and Wales saw less variability than the other gases, particularly in Scotland (range -1.09 to $42 \text{ } \mu\text{g N m}^{-2} \text{ h}^{-1}$) (Table 3.2). In terms of saturation, epN_2O ranged from 0.94-7.47 in Scotland to 0.88-10.3 in Wales. Cefni reservoir in Wales, had the highest median evasion ($6.06 \text{ } \mu\text{g N m}^{-2} \text{ h}^{-1}$) and an epN_2O of 1.68, whilst in Scotland, Black Esk reservoir had the largest median epN_2O of 1.46.

Table 3.2 Open water evasion flux and excess partial pressure across the study reservoirs. Results shown are median with min and max values given for Scotland Wales overall. Note smaller units for N₂O evasion.

	Evasion rate			Excess partial pressure		
	CO ₂ (mg C m ⁻² h ⁻¹)	CH ₄ (µg C m ⁻² h ⁻¹)	N ₂ O (µg N m ⁻² h ⁻¹)	epCO ₂	epCH ₄	epN ₂ O
Arklet	3.14	21.70	0.71	1.76	27.23	1.10
Baddinsgill	6.06	11.94	1.29	2.42	14.82	1.20
Black Esk	7.98	56.23	3.12	2.68	66.15	1.46
Dindinnie	1.83	85.37	5.84	1.23	36.52	1.30
Finglas	3.02	30.28	1.42	1.64	29.59	1.21
Glenkiln	8.74	13.01	1.75	2.56	14.83	1.24
Katrine	1.80	3.35	0.39	1.44	4.91	1.06
Lochenkit	8.13	18.89	1.16	2.45	18.50	1.13
Megget	1.13	5.02	0.69	1.15	3.53	1.09
Penwhirn	7.43	42.13	2.58	1.71	28.55	1.20
St Mary's	1.33	2.28	1.33	1.15	3.01	1.17
Talla	2.11	1.48	0.88	1.19	2.74	1.11
Thorters	3.19	14.22	2.04	1.73	14.99	1.26
Waltersmuir	7.17	67.01	1.54	2.61	70.17	1.23
Whiteadder	7.31	14.54	1.64	2.64	15.03	1.16
Scotland total		18.17				
median	4.34 (-3.36	(-0.49 to	1.46	1.79 (0.31 to	19.89 (0.78	1.18 (0.94
(range)	to 71)	6040)	(-1.09 to 42)	20.07)	to 539.50)	to 7.47)
Alaw	0.41	93.30	1.46	1.09	105.66	1.16
Aled Isaf	8.33	232.67	1.36	2.81	93.97	1.16
Alwen	3.33	11.52	0.73	1.76	12.04	1.09
Brenig	3.10	43.33	1.30	1.72	44.75	1.18
Cefni	12.87	273.79	6.06	4.01	226.41	1.68
Conwy	1.20	5.39	0.94	1.19	6.24	1.11
Cwellyn	0.68	14.64	1.19	1.16	14.58	1.16
Cwmystradllyn	0.58	15.47	0.98	1.11	15.56	1.14
Dolwen	-0.06	119.38	2.90	0.99	102.37	1.40
Dulyn	0.95	7.10	1.20	1.17	6.84	1.14
Ffynnon						
Llugwy	0.76	2.72	0.67	1.14	3.01	1.10
Llyn Aled	2.67	12.97	0.99	1.52	14.21	1.12
Marchlyn Bach	0.66	6.28	0.56	1.14	7.99	1.09
Morwynion	3.66	7.21	2.53	1.39	6.52	1.22
Plas Uchaf	0.98	79.24	3.30	1.35	87.24	1.48
Wales total	1.58	12.62				
median	(-17.16 to	(-0.04 to	1.26	1.29 (0.04 to	15.01 (0.95	1.14 (0.88
(range)	126)	11,700)	(-1.26 to 80)	20.31)	to 507.01)	to 10.31)

3.3.4 Relationships of CO₂, CH₄ and N₂O with catchment characteristics

Principle component analysis

The PCA highlights how CO₂, CH₄ and N₂O concentrations co-varied with landscape properties and water chemistry (Figure 3.8). The PCA suggests that across the study, concentrations of CH₄ and N₂O, and to a lesser extent CO₂, are associated with broadly similar catchment types. The total cumulative variance explained by the first three principal components was 46% (Table 3.3). Many of the potential controls on CO₂ in the study reservoirs are negatively loaded on PC1, whilst CH₄ and N₂O are better explained by the positive loadings on PC3 (Table 3.3). PC1 explained 26% of the total variance and represented a gradient for 'elevation' (0.32), 'improved grassland' (-0.32), 'HOST total peat' (0.30), 'arable' (-0.30), 'conductivity' (-0.30), and to a lesser extent 'HOST gleying below 40 cm', 'DIC' and 'suburban' (Table 3.3). Carbon dioxide concentrations had a negative loading on PC1, consistent with catchments with higher DOC, sandstone geology and coniferous woodland. Methane and N₂O concentrations negatively loaded on PC1 suggest that they are consistent with catchments with higher conductivity, DIC and dissolved oxygen (Figure 3.8).

An additional 11% of the variance was explained by PC2, with 'slope' (0.36) and 'rough grazing' (0.33) positively loaded, and 'DOC' (-0.36), 'HOST total peat' (-0.24) and 'coniferous woodland' (-0.21) all negatively loaded. Loadings of 'CO₂' (-0.07) and 'N₂O' (-0.01) were lower than for PC1, indicating that these variables explained less of the variance in the dissolved gas concentrations, whereas CH₄ had a higher loading on PC2 (-0.15) than PC1. PC3, explaining 9% of total variance, had the strongest loadings for both 'CH₄' (0.40) and 'N₂O' (0.29) compared to PC1 and PC2. This variance was also explained with positive loadings for 'catchment:lake ratio' (0.41), 'HOST gleying between 40-60 cm' (0.33), 'coniferous woodland' (0.24) and 'DIC' (0.20), and 'mudstones/silts' and 'bog' negatively loaded. Together, PC1 to PC3 explained nearly half of the variability in the data (Table 3.3).

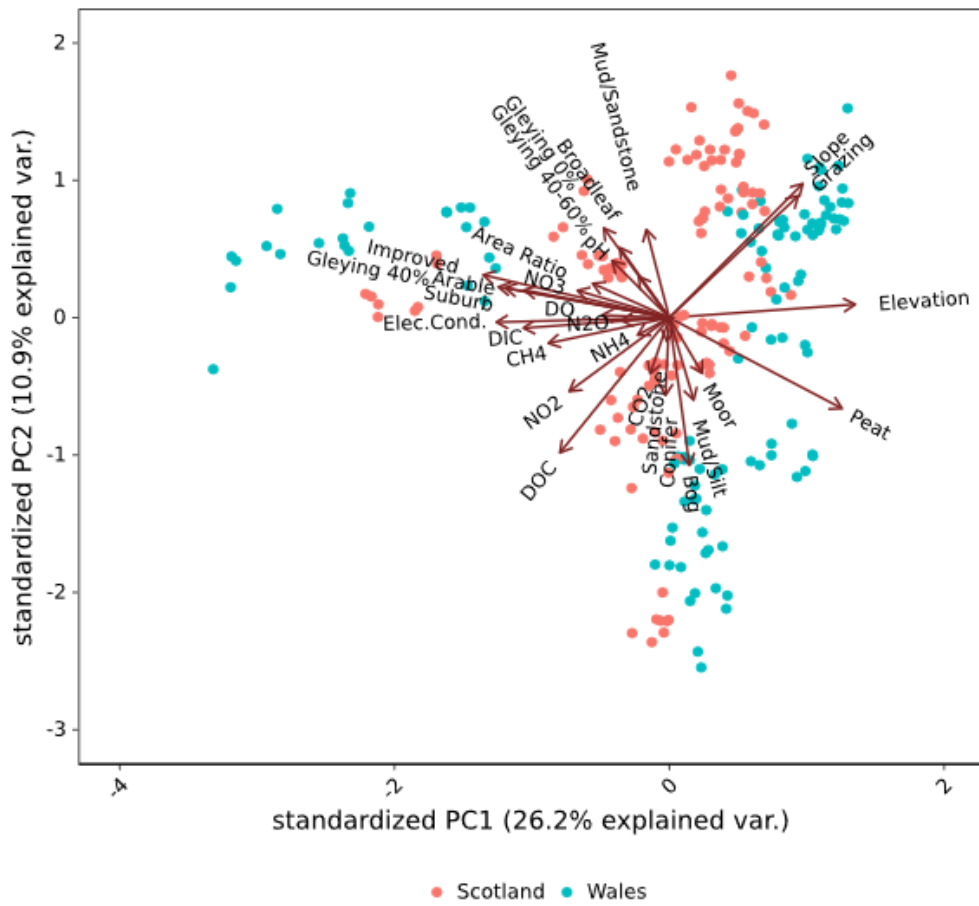


Figure 3.8 Correlation biplot displaying the orientation of the environmental variables from Table 3.3 on the first two principle components.

Table 3.3 Eigenvectors, eigenvalues and variance explained by principle component (PC) analysis of water quality, geomorphic and biophysical variables for the study lake catchments (n = 30).

Eigenvectors	PC1	PC2	PC3	PC4
HOST - No gleying	-0.11	0.24	0.00	0.40
HOST - Gleying between 40-60 cm	-0.05	0.11	0.33	0.02
HOST - Gleying below 40 cm	-0.28	0.08	-0.13	-0.28
HOST - Total Peat	0.30	-0.24	0.05	-0.09
LCM - Rough Grazing	0.22	0.33	0.07	-0.03
LCM - Coniferous woodland	-0.01	-0.21	0.24	0.09
LCM - Suburban	-0.25	0.07	-0.14	-0.12
LCM - Moorland	0.06	-0.15	0.11	-0.12
LCM - Bog	0.03	-0.40	-0.21	0.06
LCM - Broadleaf woodland	-0.09	0.19	0.02	-0.06
LCM - Improved	-0.32	0.11	-0.15	0.03
LCM - Arable	-0.30	0.08	-0.11	-0.26
Geology - Sandstones	0.00	-0.06	0.27	-0.40
Geology - Mudstones/Sandstones	-0.04	0.24	0.00	0.06
Geology - Mudstones/Silts	0.04	-0.22	-0.28	0.40
pH (centered)	-0.10	0.15	-0.08	0.01
DO (fraction)	-0.12	0.01	-0.14	0.00
log(DOC)	-0.19	-0.36	0.11	-0.07
log(DIC)	-0.25	-0.03	0.20	0.05
³ V(NH ₄)	-0.05	-0.05	0.09	0.23
³ V(NO ₂)	-0.17	-0.20	0.08	0.16
³ V(NO ₃)	-0.16	0.07	0.07	0.38
log(conductivity)	-0.30	-0.01	-0.01	0.13
log(Catchment:Lake ratio)	-0.13	0.09	0.41	0.07
log(mean elevation)	0.32	0.04	0.06	0.17
log(mean slope)	0.23	0.36	0.12	0.01
log(CO ₂)	-0.21	-0.07	0.12	0.03
log(CH ₄)	-0.03	-0.15	0.40	0.00
log(N ₂ O)	-0.08	-0.01	0.29	0.17
Standard deviation	2.76	1.78	1.63	1.50
Variance explained (%)	26.2	10.92	9.12	7.80
Variance explained (cumulative, %)	26.22	37.14	46.26	54.07

Cluster analysis

The cluster analysis grouped the 30 reservoir sampling sites into five clusters (Figure 3.9) which gave two catchments in cluster 5, three catchments in cluster 3, five catchments in cluster 2, six catchments in cluster 4 and fourteen catchments in cluster 1. There is a spatial difference between the clusters, with all reservoirs in cluster 5 and 4 in North Wales, and cluster 2 in Scotland. Cluster 1 is dominated by catchments with large areas of 'HOST total peat', land uses of rough grazing and moorland and sandstone geology. Cluster 4 is also dominated by catchments with large areas of 'HOST total peat', with land uses of bog and moorland, and geology of mudstone and silts more common. Cluster 3 is dominated by catchments with 'HOST gleying below 40 cm', improved grasslands, sandstone and mudstone geology. Cluster 2 is similar in terms of having catchments with rough grazing, coniferous forests, moderate percentages of 'HOST total peat', and mudstone/sandstone geology. Cluster 5 is characterised by catchments with higher percentages of 'HOST no gleying', improved grasslands, and mudstones/silt geology. Box plots were used to investigate the possible catchment characteristics of land use, geology and HOST driving concentrations of CO₂, CH₄ and N₂O differences between the five identified clusters (Figure 3.10). There was a statistically significant difference (Kruskal-Wallis, $H = 9.794$, $p = 0.044$) in CH₄ concentrations between the five different catchment clusters, but not with CO₂ or N₂O concentrations. This suggests that the catchment characteristics are more important drivers of CH₄ concentrations than CO₂ and N₂O. When geology, land use and HOST were clustered individually with the three greenhouse gases, a significant difference was found between CH₄ concentration for both the land use clustering (Kruskal-Wallis, $H = 8.655$, $p = 0.032$) and HOST clustering (Kruskal-Wallis, $H = 8.537$, $p = 0.036$) but not geology.

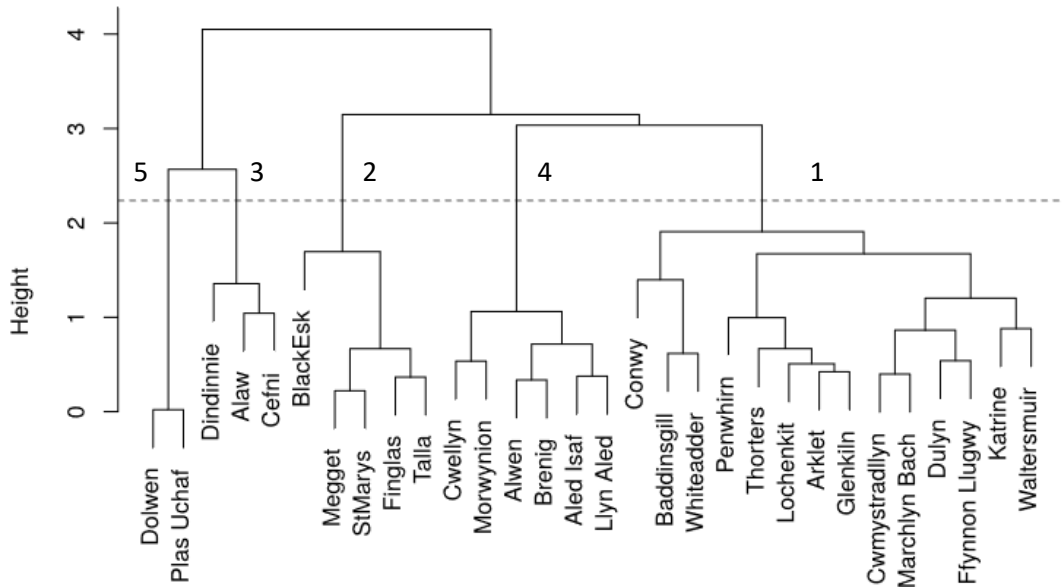


Figure 3.9 Hierarchical clustering by catchment characteristics for land use, geology and soil HOST categories. The number of each cluster (1-5) is shown representing each individual cluster below the dotted line.

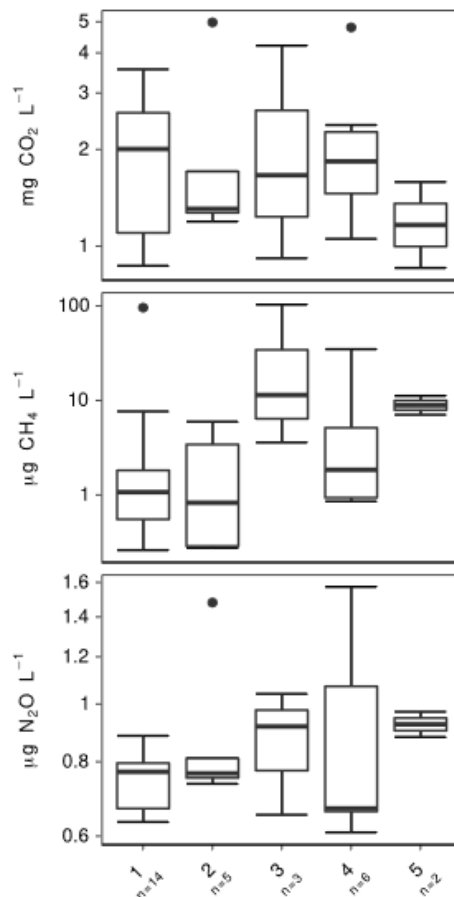


Figure 3.10 Boxplot showing concentration of CO₂, CH₄ and N₂O by the five catchment clusters (1-5) as shown in Figure 3.9.

Multiple linear regression

Drivers of surface reservoir concentrations of CO₂, CH₄ and N₂O were modelled using multiple linear regressions (Table 3.4), indicating a number of significant relationships between dissolved gases and the environmental variables. Carbon dioxide concentrations were positively correlated with DOC, HOST total peat, NH₄⁺, conductivity, and catchment:lake ratio, and were negatively correlated with pH, and dissolved oxygen. Methane had positive correlations with only DIC and catchment:lake ratio. Concentrations of N₂O were positively correlated with NO₃⁻ and conductivity, whilst negatively correlated with dissolved oxygen.

Table 3.4 Multiple linear regression coefficient results between greenhouse gas concentrations of CO₂, CH₄, N₂O and biophysical variables. Significant correlations are marked by an asterisk* for p < 0.05, a double asterisk** for p < 0.01 or triple asterisk*** for p < 0.001.

Variable	CO ₂ Adj. r ² = 0.307		CH ₄ Adj. r ² = 0.328		N ₂ O Adj. r ² = 0.235	
	Coefficient	P value	Coefficient	P value	Coefficient	P value
ln(DOC)	0.259	0.009**	-0.088	0.656	0.062	0.190
ln(DIC)	0.098	0.059	0.220	0.036*	-0.020	0.417
³ V(NH ₄ ⁺)	0.777	0.042*	0.608	0.426	0.315	0.088
³ V(NO ₂ ⁻)	-0.486	0.761	2.396	0.457	0.245	0.752
³ V(NO ₃ ⁻)	0.261	0.397	-1.170	0.060	0.439	0.004**
pH (centered)	-0.194	0.016*	-0.099	0.535	-0.064	0.097
DO (fraction)	-0.849	0.002**	0.727	0.175	-0.535	<0.001***
ln(conductivity)	0.265	0.049*	0.454	0.094	0.128	0.049*
ln(catchment:lake ratio)	0.126	0.030*	0.272	0.019*	0.047	0.093
ln(mean elevation)	-0.196	0.193	-0.584	0.054	-0.087	0.235
ln(mean slope)	0.197	0.139	-0.088	0.743	0.092	0.155
³ V(HOST - Total Peat)	1.334	<0.001***	-0.170	0.771	0.156	0.270

3.4 Discussion

The study sought to understand spatial variability of C and N concentrations across different reservoirs in Scotland and North Wales and associated controls relating to key landscape, reservoir and water quality characteristics. There were large differences in water chemistry and landscape features between Scotland and North Wales, which translated into a wide range in the concentrations of dissolved carbon species, however, less variation was seen across nitrogen species. There were different patterns of covariation across the landscape and water quality variables for different GHGs, ranging from relatively moderate coupling to spatial decoupling, suggesting that each GHG has distinct sets of environmental drivers.

3.4.1 Variables controlling spatial variability in GHG concentrations

Carbon dioxide

Carbon dioxide concentrations were positively correlated to five variables and negatively correlated to two (Table 3.4). The positive relationships between CO₂ and DOC are consistent with results from other studies (e.g. Premke et al., 2016) and suggest that organic matter decomposition is an important source of CO₂ in the reservoirs from allochthonous organic carbon (Sobek et al., 2003), particularly peatland derived C as HOST total peat is correlated with CO₂. Many studies reporting DOC as a predictor of CO₂ do not always evaluate the relationship between CO₂ and dissolved oxygen (Roehm et al., 2009). When DO is included, studies found a significant negative correlation (Cole et al., 2010; Zhang et al., 2013), and similar to here, other studies found dissolved oxygen to be a better predictor (Kortelainen et al., 2006; Rantakari and Kortelainen, 2005). A correlation between O₂ and CO₂ can be indicative of respiration, often from the sediments (Jonsson et al., 2003; Kortelainen et al., 2006) and can be stronger in lakes with high DOC, likely from high sedimentation of allochthonous carbon (Jonsson et al., 2003). Many of the reservoirs studied here have peatland soils in their catchments, promoting export of organic carbon through runoff and erosion into the reservoirs.

Over an 18 month period from January 2010, Hughes et al. (2013) measured DOC concentrations in four lakes in North Wales, three of which were also used in this study, Cefni (mean monthly DOC across the study was 5.5-12.7 mg L⁻¹), Cwellyn (1.4-3.8 mg L⁻¹) and Conwy (3.1-5.6 mg L⁻¹). Such results from Hughes et al. (2013) match very closely with mean DOC concentrations from the same reservoirs used in this research despite the differences in sampling year and frequency (Cefni = 9.0, Cwellyn = 2.0 and Conwy = 4.0 mg L⁻¹). Hughes et al. (2013) found Cefni to have higher DOC concentrations due to rainfall events flushing DOC out of the fen (although no significant relationship with rainfall/DOC was found) and correlations with temperature. As results between their study and here were similar, this could also be a plausible explanation for the higher DOC concentrations observed.

A significant positive relationship with CO₂ and NH₄⁺ was observed, which has also been reported in other lake studies (e.g. Rantakari and Kortelainen, 2008) and also emphasises the importance of the quality of organic matter and nutrient availability for decomposition processes. High DOC concentrations have been associated with catchments with large proportions of peat (Aitkenhead et al., 1999), but no significant relationship ($p = 0.196$) between DOC and 'HOST total peat' was found despite multiple catchments having large

areas. Boothroyd et al. (2015) found DOC concentration to vary significantly with slope position, supporting findings of a significant negative relationship of both DOC ($p < 0.001$) and DIC ($p < 0.01$) with catchment slope in this study.

A significant positive relationship ($p < 0.001$) was found between CO_2 and % of 'HOST peat'. Studies have found peat to be a significant source of dissolved CO_2 to freshwaters (e.g. Dawson et al., 2002; Johnson et al., 2010; Dinsmore et al., 2009), and results here suggest that the organic rich soils of the catchments are releasing carbon into the reservoirs, e.g. via surface inflows or percolation through organic catchment soils. There was also no significant relationship between CO_2 and DIC concentrations, despite overall CO_2 supersaturation occurring in all but one of the sampled reservoirs (Table 3.1). Waters with large DIC inputs from carbonate weathering are often supersaturated with CO_2 (e.g. Del Giorgio et al., 1999). Median DIC concentrations across all but one reservoir was low to moderate ($< 15.4 \text{ mg L}^{-1}$), with Cefni reservoir in North Wales having both the highest median DIC (24.7 mg L^{-1}) and epCO_2 (4.0). Dolwen reservoir (Wales) experienced negative evasion and undersaturation of CO_2 , with low concentrations also seen in Alaw and Cefni. During summer and autumn sampling, cyanobacteria were visible (and warming signs were present) in these reservoirs, which can account for the undersaturation of CO_2 . Previous research on lakes in Wisconsin, USA (Cole et al., 2000) and Finland (Cole et al., 2000; Huttunen et al., 2003a) suggests that CO_2 uptake during photosynthesis by large aquatic plants and algae has similar results.

The sources of CO_2 in the reservoirs were more likely from decomposition of organic matter due to identified correlations with DOC and NH_4^+ than from weathering processes in the catchment as supported by the lack of correlation with CO_2 and DIC, and the cluster analysis showing no correlation with catchment geology. This is reflected particularly in Welsh reservoirs where CO_2 concentrations were highest in winter and in-lake processes are expected to dominate. In Scotland, by contrast, highest concentrations were observed in autumn when the influence of the catchment is more important due to increasing rainfall events flushing in C at the end of drier summer periods. It is also worth noting that groundwater can be an important aquatic CO_2 source (Humborg et al., 2010) but is unlikely to play a major role in the majority of these reservoirs as conductivity was low (median = $42 \mu\text{S/cm}$), indicating that reservoirs are predominantly precipitation fed (Brooks et al., 1998). A positive relationship between CO_2 and conductivity was found across the sites.

Carbon dioxide, CH_4 , DOC ($p < 0.001$) and DIC ($p < 0.001$) all correlated positively with the drainage ratio (catchment:lake ratio; Table 3.4) indicating that the flow of water through the

reservoir and residence time is important for these C species. Lake size has been known to influence biogeochemical and hydrological processes (Hanson et al., 2007), with typical decreasing trend in lake CO₂ concentrations with increasing lake area (e.g. Holgerson and Raymond, 2016; Rocher-Ros et al., 2017). Lakes with large surface areas and those with large fetches have greater potential for degassing, allowing faster CO₂ equilibration with the atmosphere; however, no significant relationship was found between reservoir area and epCO₂ in this study CO₂ concentrations show a significant negative correlation with pH, a common relationship in aquatic systems (e.g. Holgerson and Raymond, 2016).

Reservoirs in this study had a median pH of 6.8. Higher pH causes CO₂ to dissolve in water to form carbonate and reduce the pCO₂ in surface waters, whilst low pH can promote CO₂ emission to the atmosphere. Our results suggest that slope does not account for GHG variability despite other studies finding it to influence contact time between soil and water percolation (Rawlins et al., 2014), or influence evaporative enrichment of water routing through a catchment (Gibson et al., 2005). Likewise, no relationship was found with elevation which is often seen as a proxy for temperature (Pighini et al., 2018). This suggests that the range of elevation and slope gradients were either too small to pick up trends in GHG concentrations and/or hidden by other factors.

Methane

Methane had only two significant positive relationships with DIC (p <0.05) and catchment:lake ratio (p <0.05) in the multiple regression models (Table 3.4). Dinsmore et al. (2009) also found a negative relationship between CH₄ and DIC in a Scottish peatland catchment. In turn, DIC exhibited positive correlations with NO₂⁻ (p <0.05), pH (p <0.001), conductivity (p <0.05), lake-to-catchment ratio (p <0.001), and negative relations with NO₃⁻ (p <0.05), dissolved oxygen (p <0.001), slope (p <0.01), and HOST peat (p <0.01). In aquatic systems, DIC is determined by four main processes: i) inputs from gas loaded waters from soils and ground water; ii) within lake respiration by aquatic plants and through organic matter; iii) from products of carbonate dissolution and weathering of silicate materials; and iv) atmospheric exchange through outgassing and drawdown depending on equilibrium between the water and atmosphere (Hope et al., 1994; Jones and Mulholland, 1998; Billett et al., 2004; Jarvie et al., 2017). Cefni supported the highest observed CH₄ concentrations of the sampled reservoirs. One potential explanation for this, was the presence of aquatic plants around the shore, particularly cattails, which were not observed at the other reservoirs and have been found to decompose in the littoral sediments and contribute to large CH₄ emissions through the decomposition of old cattail biomass (Emilsson et al., 2018). As no significant relationships were found between

greenhouse gas concentrations and catchment geology, and only a handful of catchments had carbonate- and silicate-rich bedrock, DIC sourced from dissolution and weather is less important for the reservoirs measured here and the in-lake processes and soil and/or ground water inputs would seem more relevant. For example, Black Esk has the largest percentage of limestone at 8% and had a high epCH₄ of 66, but other reservoirs showed much higher supersaturation.

The positive correlation between CH₄ concentrations and catchment:lake ratio suggests hydrologic connectivity between the reservoirs and landscape is important for controlling CH₄. High catchment:lake ratios can promote more catchment connectivity, which in turn gives more opportunity for higher allochthonous inputs and sedimentation rates (Van Geest et al., 2003). The reservoirs with highest rates of evasion and epCH₄ (Table 3.2) all are drainage, as opposed to seepage lake types as catchment:lake ratios are >30. Many studies have found CH₄ to correlate significantly with peatland soils as they release high concentrations of CH₄ due to lack of oxygen and resulting methanogenesis. However, this was not found in this study despite large peatland areas in the majority of catchments i.e. 23 out of 30 catchments have >50% 'HOST Total Peat'. Higher CH₄ concentrations (e.g. Huttunen et al., 2002) have also been reported in near shore areas only. The Scotland and Wales reservoirs were sampled in near shore littoral zones, therefore, an over approximation of the reservoir CH₄ concentrations could have been made and should be evaluated in future work through sampling away from the bank edge.

Results from the cluster analysis also showed that there were significant differences in CH₄ between clusters, with HOST and land use being the main factors causing the differences (Figure 3.10). Results from the clustering also showed that geology was not a significant factor in controlling any of the three greenhouse gases. Highest and most variable CH₄ concentrations are seen in cluster 3 (Figure 3.10), which is composed of HOST gleying below 40 cm (81%), improved grassland (85%) and arable (3%) land uses. The reservoirs in this cluster are Dindinnie (median epCH₄ = 37), Alaw (epCH₄ = 106) and Cefni (epCH₄ = 226) which are all highly supersaturated in CH₄. Animal deposition is likely a factor contributing to the high DOC concentrations here.

High CH₄ emissions have been reported from agricultural lake catchments in Finland with high nutrient loads and well-developed soils (Huttunen et al., 2003). Nutrient enriched temperate lakes have also had high CH₄ emissions (Casper et al., 2000) and N₂O concentrations (Mengis et al., 1997). Our study supports these findings; the Dindinnie and Cefni reservoirs had the

highest median N₂O concentrations and epN₂O and their CH₄ concentrations were the highest amongst the Scottish and Welsh reservoirs tested (Table 3.2). Increased availability of degradable autochthonous organic matter, presumably from dung deposits and soil disturbance mediated by the grazing animals, increases decomposition and oxygen consumption. This in turn, promotes the depletion of water column and sediment oxygen. The anoxic conditions can promote CH₄ emissions from lake sediments by enhanced production and/or decreased oxidation of CH₄ (Kiene, 1991) and N₂O production, supported by runoff from fertiliser and organic matter be supported by low oxygen (Huttunen et al., 2003). In this study in Scottish and Welsh reservoirs, a significant negative relationship between N₂O and dissolved oxygen was found.

Nitrous oxide

Nitrous oxide concentrations saw highest saturation in winter for both Scotland and Wales (Table 3.2) and only three variables were found to be significantly correlated to reservoir concentrations (Table 3.4). Evasion fluxes were low in the majority of reservoirs, and epN₂O saw concentrations closer to saturation levels. The shallow regions of reservoirs in Scotland and Wales do not seem to contribute significantly to the atmospheric N₂O budget, particularly when compared to CO₂ and CH₄, which supports previous studies in finding freshwater lakes as only moderate sources of N₂O (Mengis et al., 1997).

The significant positive relationship ($p < 0.01$) between N₂O and NO₃⁻ has been observed in other studies (e.g. Beaulieu et al., 2008). Both NO₃⁻ and organic carbon availability are important controlling factors of denitrification (Seitzinger and Kroeze, 1998; Kroeze et al., 2010). However, no relationship was found between N₂O and DOC which was also observed in Beaulieu et al. (2009) and attributed to considerable variation in overall carbon availability in DOC (Kaplan and Newbold, 2003). Denitrification and N₂O production could have been limited by oxygen, which are important when process rates are not limited by NO₃⁻. In this study, a negative correlation was found between N₂O and dissolved oxygen. DOC, as a carbon source, and DO as indicator of the presence/absence of O₂ are key factors determining denitrification rates. Whilst oxygen is the main regulator of denitrification, pH is also a key factor (Sun et al., 2012) with pH values > 7 tend to promote larger rates of denitrification to N₂, compared to the opposite in acid soils.

The generally lower concentrations of N₂O, compared to concentrations reported in the literature (e.g. Beaulieu et al., 2015) could be limited by the low NO₃⁻ concentrations seen across the majority of the reservoirs (medians of <0.11 mg L⁻¹), and overall low inorganic N

potentially limiting the capacity for denitrification and suggesting the dominant N source in the upland reservoirs would be from atmospheric deposition. Despite higher median N₂O concentrations occurring in winter, the highest NO₃⁻ concentrations were observed in spring (median = 0.15 and 0.18 mg L⁻¹ for Scotland and Wales, respectively). Nitrate concentrations have also been shown to positively correlate in a study on Scottish streams with the percentage cover of improved grasslands, brown forest soils and negatively with peat (Chapman et al., 2001). Similarly, a significant negatively relationship ($p = 0.005$) was found between NO₃⁻ and HOST peat. The cluster analysis and Kruskal-Wallis tests found no significant relationship with catchment land-use and N₂O concentrations despite areas of agriculture often being sites of N₂O emission (Seitzinger and Kroeze, 1998; Beaulieu et al., 2015) but was likely down to the small sample size of agricultural catchments.

Only a handful of sampled reservoirs had arable land in their catchments (max catchment coverage = 3.1% of which Dindinnie, Cefni and Alaw have between 2.4 to 3.1%). However, improved grassland had greater presence (max catchment coverage = 86% with Dindinnie, Thorters, Waltersmuir, Cefni, Alaw, Plas Uchaf and Dolwen having >12%) and could further aid explanation of the lower N₂O concentrations seen across the majority of reservoirs. Cefni in North Wales, which has 3% of arable land and 86% of improved grasslands in the catchment, had the highest median N₂O concentration (1.1 µg L⁻¹ or 0.7 µg N L⁻¹). The Cefni catchment and surrounding area has a history of cattle and sheep farming where agro-chemicals are used (Hughes et al., 2013) which is a likely N source to the reservoir. A marshy wetland also immediately surrounds the reservoir, which likely stores some of the catchment run-off. The reservoir also has a history of eutrophication which can support growths of potentially toxic cyanobacteria during summer. Plas Uchaf and Dolwen are two shallow connected reservoirs and previous water quality monitoring have indicated that nitrogen concentrations are high (TN = 2.90 mg L⁻¹) (Hatton-Ellis, 2015). Llyn Alaw catchment also consists of intensive agriculture, with slightly elevated nitrogen concentrations (TN = 1.03 mg L⁻¹ and winter nitrate at 0.66 mg L⁻¹) (Hatton-Ellis, 2015). The reservoirs sampled were also more typical of upland UK drinking water catchments, which have reduced nutrient pressures that would typically relate to higher intensity agricultural land use and population pressure. Future work should include reservoirs in areas with more productive agriculture land to assess the evasion and concentrations of N₂O in these types of catchments.

3.4.2 Seasonal variability

Seasonality plays a role in controlling lake temperatures which influence nutrient concentrations and microbial activity, oxygen availability (e.g. lake stratification), time of

fertiliser application, along with organic matter availability (e.g. flushing of carbon). Results demonstrate seasonal differences in GHG concentrations across regions, with highest median CO₂ and CH₄ concentrations for Scotland in autumn (Figure 3.7). Reservoirs receive CO₂ produced and derived from their catchment area as a result of rainfall events when large amounts of C are transported into the water bodies (Rantakari and Kortelainen, 2005). Dinsmore et al. (2013) have also found CO₂ concentrations in Scottish catchments to strongly link to discharge. The Scottish reservoirs were sampled over a wider spatial gradient compared to the Welsh sites and the limited resolution of available rainfall data does not provide a true reflection of the rainfall for each catchment or a clear east-west rainfall gradient. Therefore, rainfall was excluded from the models. To provide some insight for the sampling year, rainfall at Eskdalemuir weather station (near four of the Scottish catchments) was highest in winter (446 mm) followed by autumn (240 mm) (Met Office, 2018). In North Wales, the nearest weather station (Valley on Anglesey) also showed highest rainfall over winter (1135 mm) for the sampling year, followed by summer (376 mm). Greater fall of leaf litter in autumn (Scholz et al., 2016), could also partially explain the higher autumn CO₂ and CH₄ concentrations in Scotland where catchments include broadleaf and coniferous woodlands (drop of needles also increased during autumn) in contrast to Welsh sites (Figure 3.2).

Welsh reservoirs saw higher median concentrations for CO₂ in winter and CH₄ in spring (Figure 3.7). The higher spring CH₄ concentrations could be linked to highly oxygen depleted conditions that are typical of shallow eutrophic lakes with soft sediments (Huttunen et al., 2003). A further explanation of the spring CH₄ concentrations relate to the February snowfall, resulting in melt water running into the catchments. Snow melt has also been shown to be an important period for the export of both DOC (Nilsson et al., 2008) and gaseous carbon (Dyson et al., 2011). The higher winter CO₂ concentrations could be attributed to lower temperatures and reduced photosynthetic activity within the reservoirs (e.g. Striegl et al., 2001). The most likely cause, however is linked to increased rainfall promoting runoff and leaching of organic material into the reservoirs from already highly saturated soils (Striegl et al., 2001). Both Scotland and Wales saw higher N₂O concentrations during winter. Nitrate, a main predictor of N₂O concentration, (Figure 3.8) typically increases during winter and declines during growing seasons as NO₃⁻ catchment export is mediated by inorganic N uptake by plants, which is decreasing during the non-growing season (Lee et al., 2012).

3.4.3 Comparison with other lakes and reservoirs

Carbon dioxide

Dissolved CO₂ concentrations (range 2.36 to 663.6 μmol L⁻¹) were in the same order of magnitude as Diem et al. (2012) when supersaturated with CO₂. They were also comparable to Casper et al. (2000) where concentrations ranged from 27-326 μmol L⁻¹ in a small lake with fen catchment in England, UK. An assessment of global lake CO₂ by Sobek et al. (2005) found 93% of lakes (n = 4902) were supersaturated in CO₂ with respect to the atmosphere and ranged between 17 and 65,250 μatm. In this study, the reservoirs ranged between 42 and 10,748 μatm. An earlier global lake study by Cole et al. (1994) found 87% of lakes (n = 1835) to be supersaturated in CO₂, with North American temperate lakes having a mean of 1087 μatm, with reservoirs in this study having a mean of 934 and 879 μatm in Scotland and Wales, respectively. Tropical reservoirs are regarded as having higher CO₂ and CH₄ concentrations than temperate systems. For example, in a reservoir in French Guiana, Guérin et al. (2006) found CO₂ concentrations to range from 50-400 μmol L⁻¹. The same order of magnitude of CO₂ (mean 0.80 mg L⁻¹), DOC (mean 5.05 mg L⁻¹) and DIC (mean 1.55 mg L⁻¹) concentrations were measured at Loch Katrine during 2014 by Pickard et al. (2017), which is also a reservoir sampled in this research, highlighting consistency in findings between the two studies.

A study on constructed wetlands measuring C and N inflow/outflow concentrations were measured at Cefni reservoir during 2014 (weekly from Mar-Oct) (Scholz et al., 2016) providing results from a similar period and a reservoir also used in this research. In the outflow of the reservoir, Scholz et al. (2016) reported mean concentrations of DOC, DIC and CO₂ to be lower than results from this study, but higher NO₃⁻ concentrations (the latter values are from this study): DOC = 1.4 vs. 9.0 mg L⁻¹, DIC = 16.2 vs. 25.8 mg L⁻¹, NO₃⁻ = 1.2 vs. 0.5 mg L⁻¹, and this study median GHG concentrations against their means were CO₂ 1129 vs. 4107 μg L⁻¹ and CH₄ 20.1 vs. 17.1 μg L⁻¹. Such differences are likely due to the higher frequency (weekly) sampling over spring, summer and early autumn when concentrations are typically higher compared to just seasonal sampling across Scotland and North Wales. Cefni, Marchlyn Bach and Llugwy reservoirs in North Wales were sampled monthly over a one year period by Jones (2006), with average concentrations of DOC (9.3, 2.8 and 3.2 mg L⁻¹, respectively) and showed little seasonal variation. Dissolved CH₄ concentrations at Marchlyn Bach and Llugwy (mean 0.001 mg L⁻¹) were low, with Cefni having a maximum of 0.01 mg L⁻¹. Carbon dioxide concentrations showed significant (p<0.001) seasonal variation for Cefni (range 13.2 μmol l⁻¹ to 65.7 μmol l⁻¹), Llugwy (max 64.9 μmol l⁻¹) and Marchlyn Bach (max <40 μmol l⁻¹). Marchlyn Bach and Llugwy were also reported to have low nitrate concentrations (mean <1 mg L⁻¹), with a maximum of

11.9 mg L⁻¹ in Cefni during winter with large seasonal change. Marchlyn Bach and Llugwy have both peat/bog dominated catchments but the concentrations in these two reservoirs are lower than typical concentrations in such catchment types.

In a study of Irish lakes (n = 121) Whitfield et al. (2010) also found the majority of lakes to be supersaturated with CO₂, with a mean estimated flux of 14 mmol CO₂ m⁻² d⁻¹ and median surface concentration of 21 µmol L⁻¹. Reservoirs in Scotland had a mean evasion rate of 13.7 mmol CO₂ m⁻² d⁻¹ and a median surface concentration of 41 µmol L⁻¹, with reservoirs in Wales having a mean evasion rate of 11.7 mmol CO₂ m⁻² d⁻¹ and a median surface concentration of 23 µmol L⁻¹. In Scotland and Wales, a wider range across reservoirs was observed, emphasising the wide spatial variability in GHG concentrations and the difficulties that could emerge from up-scaling emissions from a few select reservoirs in different regions as they could over or under estimate emissions. However, results from the Irish study are quite comparable to this research, albeit a higher median surface CO₂ concentration was observed in Scotland, but the agreement between the two studies provides increased confidence in the estimates of GHG concentration and evasion from Scotland and North Wales, and provides potential for up-scaling. Future work could also investigate GHGs in reservoir catchments which have become degraded or are actively eroding, which could complement the C work of Stimson et al. (2017). Their carbon budget study (DOC, POC, aqueous CO₂) at Kinder reservoir, located in a degraded upland catchment in the South Pennines, UK (Stimson et al., 2017) found this POC rich reservoir to be a net fluvial C sink, with mean DOC concentrations of 6 mg L⁻¹ at the reservoir outlet (Stimson et al., 2017). This could also help future up-scaling research.

Methane

The range of measured surface concentrations of CH₄ (0.003-46 µmol L⁻¹, or 0.04-554 µg C L⁻¹) in this study were on the same order of magnitude as other temperate lakes and reservoirs (e.g. Bastviken et al., 2008; Diem et al., 2012; Tang et al., 2014). All reservoirs were supersaturated in surface dissolved CH₄ with respect to the atmospheric concentration, which supports findings by Tang et al. (2014). Schulz et al. (2001) found CH₄ concentrations at Lake Constance (Germany) to be oversaturated as much as forty times, with results here showing oversaturation between 3 and 226 times. Greater within site variation was seen across some of individual sampled reservoirs in this study compared to Priest Pot lake, England UK, where CH₄ concentrations ranged from 0.31 to 4.8 µmol L⁻¹ (Casper et al., 2000). Similarly, Whitfield et al. (2010) also found all lakes to be above saturation in CH₄, with a mean estimated flux of 0.36 (0-4.5) mmol m⁻² d⁻¹ and median surface concentration of 0.06 µmol L⁻¹. Reservoirs in Scotland had a mean CH₄ evasion rate of 0.23 (0-12.1) mmol m⁻² d⁻¹ and a median surface

concentration of $0.07 \mu\text{mol L}^{-1}$, with reservoirs in Wales having a mean evasion rate of 0.44 ($0-23.7$) $\text{mmol m}^{-2} \text{d}^{-1}$ and a median surface concentration of $0.05 \mu\text{mol L}^{-1}$. Compared to the study in Ireland, mean and median concentrations were similar but maximum concentrations and evasion were higher. According to Wang et al. (2017) this methane-enriched surface zone causing oversaturation could be produced by phototrophs and with methanogens, whereas Fernández et al. (2016) believe CH_4 surface concentrations would more likely originate from methane-rich shallow zones. Ebullition, which was not measured here, could also be contributing to the high supersaturation of CH_4 in some of the reservoirs (e.g. Sobek et al., 2012; Maeck et al., 2013).

Nitrous oxide

Nitrous oxide concentrations ranged from 0.29 to $5.41 \mu\text{g C L}^{-1}$ (mean 0.019 , range $0.001-0.19$ in $\mu\text{mol L}^{-1}$). Overall, reservoirs showed N_2O supersaturation and low evasion rates, but variability was high across the sites. The reservoirs either were close to atmospheric equilibrium or showed supersaturation (Table 3.2). This is similar to previous findings of small N_2O fluxes in boreal and semi-alpine lakes and reservoirs (Huttunen et al., 2002; Huttunen et al., 2003; Diem et al., 2012). In two lowland Swiss lakes, Diem et al. (2012) found supersaturation and low levels of emission of N_2O at $72 \mu\text{g N}_2\text{O m}^{-2} \text{day}^{-1}$ (Lake Wohlen) and $50 \mu\text{g N}_2\text{O m}^{-2} \text{day}^{-1}$ (Lake Lungern). Surface concentrations at Lake Wohlen were $23 \pm 4 \text{ nmol L}^{-1}$, with Lake Lungern varying from $17-20 \text{ nmol L}^{-1}$ across four sampling dates. Mean evasion from the reservoirs across Scotland was $117 \mu\text{g N}_2\text{O m}^{-2} \text{day}^{-1}$ and for Wales $85 \mu\text{g N}_2\text{O m}^{-2} \text{day}^{-1}$ which is comparable. Similar to results here, Whitfield et al. (2010) found the majority of Irish lakes ($n = 121$) to be supersaturated with N_2O with an average flux of $1.3 \mu\text{mol m}^{-2} \text{d}^{-1}$, ranging from -3.8 to $6.9 \mu\text{mol m}^{-2} \text{d}^{-1}$ and median surface concentration of 11 nmol L^{-1} . Mean evasion were on the same order of magnitude but both Scotland and Wales saw higher evasion at some reservoirs. Scotland had a mean of $1.9 \mu\text{mol m}^{-2} \text{d}^{-1}$, ranging from -0.9 to $35.9 \mu\text{mol m}^{-2} \text{d}^{-1}$ and Wales had a mean of $2.6 \mu\text{mol m}^{-2} \text{d}^{-1}$, ranging from -1.1 to $68.1 \mu\text{mol m}^{-2} \text{d}^{-1}$. Beaulieu et al. (2015) measured N_2O concentrations in temperate reservoirs ($n = 17$) in the Ohio River Basin, USA and found 80% to be supersaturated in the surface waters, indicating most reservoirs were a source of N_2O to the atmosphere. 13 of these US reservoirs had a median N_2O saturation of 1.6 (suggesting production), 3 were at equilibrium (mean saturation = 1.04) and 1 showed consumption (mean = 0.65). Using the N_2O saturation ratios in Beaulieu et al. (2015), where production is >1.2 , 18 (60%) reservoirs in Scotland and Wales showed production and 12 reservoirs were at equilibrium. Results here were much lower than in a hyper-eutrophic lake in China where littoral zones were found to be N_2O emission hotspots

(-265.1 to 2101.4 $\mu\text{g N}_2\text{O m}^{-2} \text{h}^{-1}$) (Wang et al., 2006). The evasion range across Scotland and Wales were -2.0 to 124.9 $\mu\text{g N}_2\text{O m}^{-2} \text{h}^{-1}$. Currently IPCC methods for N_2O emissions do not consider lakes, therefore more research is required to determine whether agricultural and urban N enrichment contributes to changing N_2O dynamics in lakes and determine if they are significant in global N_2O budgets.

3.5 Conclusions

There have been few studies on C and N concentrations, and even fewer, which have measured dissolved CO_2 , CH_4 and N_2O concentrations and evasion fluxes from reservoirs in the UK. Despite the coarse sampling frequency, comparison with other temperate lakes and reservoirs indicates that the surface estimates give useful first approximations of GHG concentrations and evasion in drinking water reservoirs in North Wales and upland regions of Scotland, particularly for catchments with large areas of peatland. The main result of this study is that the surface waters of sampled reservoirs were overall, supersaturated with CH_4 and N_2O . All reservoirs, except one, were also overall supersaturated in CO_2 . This suggests that reservoirs in Scotland and North Wales tend to act as sources of CO_2 , CH_4 and N_2O to the atmosphere. Results also illustrate the large spatial variability of GHG concentrations and evasion among reservoirs in two areas of the UK, which represent typical upland areas for drinking water reservoirs. Results also showed there were regional spatial differences between concentrations. The exchange of these GHGs between water and atmosphere also depends on the transfer velocity across the water and air interface (Wanninkhof, 1992). Studies that quantified both dissolved concentration and fluxes report supersaturation levels similar to this study (e.g. Sobek et al., 2005; Cole et al., 2007; Diem et al., 2012), and the evasion rates reported earlier from in-direct wind speed measurements, support that reservoirs in Scotland and North Wales, would act as carbon sources to the atmosphere. Reservoirs were to a much lesser extent a source of nitrogen (evasion across most of the sites was small and many reservoirs close to atmospheric equilibrium) and those which did show greatest supersaturation, were in catchments with managed grazed grasslands. From a GWP perspective over the 100-year time horizon (IPCC, 2014), CO_2 is still an order of magnitude larger and accounts for the majority of emissions compared to CH_4 and N_2O , and emissions of CH_4 and N_2O are of the same order of magnitude. Scotland has a median CH_4 flux of 20 $\text{mg CO}_2\text{-equivalents m}^{-2} \text{d}^{-1}$ (5% of total Scotland reservoir emissions) and Wales has 14 $\text{mg CO}_2\text{-equivalents m}^{-2} \text{d}^{-1}$ (8% of total reservoir emissions for Wales). For N_2O , this equates to a median of 16 (4%) and 14 (9%) $\text{mg CO}_2\text{-equivalents m}^{-2} \text{d}^{-1}$ for Scotland and Wales, respectively. Efforts to develop flooded land emission inventories in the UK also suggest more

studies are required to allow regional upscaling, given the variability seen in GHG concentrations and evasion, particularly of CH₄ at some of the reservoirs.

Despite significant correlations, principle component analysis showed approximately half of the variance was explained by the top three principle components, suggesting that critical explanatory factors were not included from the field sampling or GIS analysis, particularly for CH₄ given the high concentrations and variability seen across the reservoirs. Future research should attempt to clarify the drivers for the unexplained variance (e.g. precipitation and hydrological dynamics) and additionally attempt to make in-situ flux measurements to better quantify the water-atmosphere exchange. This would be particularly beneficial if samples are collected from the middle of the reservoir and, away from littoral areas with potentially higher CH₄ fluxes due to ebullition.

Acknowledgements

This work was funded by the UK Natural Environment Research Council (NERC) from the IAPETUS Doctoral Training Programme. We are very grateful to Scottish Water and Dwr Cymru for permitting access to reservoir sites and providing background site information. We also thank Angus Lepper, Jennifer Williamson, Fraser Leith and Song Ling for field assistance; Nick Cowan for training and assistance with SEAL AQ2 analysis; and Philip Taylor for advice on GIS analysis.

4 Spatio-temporal patterns in carbon dioxide, methane and nitrous oxide emissions from moorland and forested reservoir catchments in Scotland, UK

4.1 Introduction

Carbon dioxide (CO₂), methane (CH₄) and nitrous oxide (N₂O) are well-mixed greenhouse gases (GHGs), adding 80% of the positive radiative forcing that drives climate change (IPCC, 2014). These GHGs have been reported in the literature as important fluxes in global lentic and lotic GHG budgets (Marescaux et al., 2018). Inland waters are globally recognised as significant systems for carbon (C) transport and processing, although the degree of which is under debate (Cole et al., 2007; Aufdenkampe et al., 2011; Tranvik et al., 2009). Recent research efforts have also resulted in the inclusion of inland waters in global C models (IPCC, 2014). Inland waters can regulate landscape C balances acting as C sources through evasion of GHGs, but also as sinks through C burial in reservoir and lake sediments (Bastviken et al., 2011).

Streams and rivers have low areal coverage (~20% of global inland water surface area) but are considered important contributors (particularly small-order streams of strahler order 1-4) to aquatic CO₂ emissions, with 1.8 Pg C yr⁻¹ estimated globally from streams and rivers, which exceeds an estimated 0.3 Pg C yr⁻¹ from reservoirs and lakes (Raymond et al., 2013). This combined estimate from global inland waters is of similar magnitude to terrestrial ecosystem net uptake of ~2.6 Pg C yr⁻¹ (IPCC, 2014). Stream CH₄ and N₂O emissions are less well understood but there is increasing understanding of their significance (e.g. Beaulieu et al., 2011; Campeau et al., 2014). Global inland water CH₄ emissions have been estimated at 2-27 Tg CH₄ yr⁻¹ (Bastviken et al., 2011; Borges et al., 2015; Sawakuchi et al., 2014; Stanley et al., 2016) and research has highlighted that stream CH₄ emissions could show greater spatial and temporal variability than CO₂ (Wallin et al., 2011; Stanley et al., 2016). River N₂O emissions are estimated between 47-1980 Gg N₂O yr⁻¹ (Beaulieu et al., 2011; Hu et al., 2016; Kroeze et al., 2010). Stream emissions are often neglected in landscape level C budgets due to limited data, despite being shown to be large contributors with high per area emissions (Teodoru et al., 2012).

Lakes and streams are typically studied independently due to limited collaborated research efforts and systems having different emission drivers and physical gas exchange, which restricts landscape scale integrative understanding of GHG dynamics (Kokic et al., 2015). Past research focus has been on lakes due to larger surface areas (Algesten et al., 2004) but an

increasing number of studies have shown that streams have an important landscape scale impact (Campeau et al., 2014; Crawford et al., 2013). Integrative inland water studies tend to be at larger spatial scales (Aufdenkampe et al., 2011) with only a few in recent years at catchment scale (Kokic et al., 2015; Marescaux et al., 2018). There are also only a handful of studies which evaluate all three GHG emissions together for lakes and reservoirs (Huttunen et al., 2002, Zhao et al., 2013) or streams and rivers (Borges et al., 2018; Schade et al., 2016; Teodoru et al., 2015), with even fewer studies combining GHG measurements across lentic and lotic systems (e.g. Kokic et al., 2015, Marescaux et al., 2018).

Dissolved GHG concentrations and emissions in inland water networks are highly variable in space and time due to gas input e.g. affected by land-use, ground water inputs and soil characteristics (Jones et al., 1998, Hope et al., 2004, Wallin et al., 2014) and gas loss e.g. dependent on k , regulating vertical gas exchange (Wallin et al., 2014). Evasion from inland waters is driven by supersaturation of GHGs in the water and controlled by the gas transfer velocity (k) (Cole et al., 1994) which in streams will vary as a result of e.g. water velocity and discharge, channel slope and morphology (Dinsmore et al., 2013; Long et al., 2015; Wallin et al., 2011). For example, varying discharge from precipitation, snow melt events and ground water level changes can influence GHG concentrations and emissions due to either dilution or increased supply (Billett et al., 2004; Billett and Harvey, 2013; Dinsmore and Billett, 2008).

Supersaturation of CO_2 in lakes can be caused by organic matter mineralisation by photochemical and microbial processes, producing a net heterotrophic system when these processes outweigh photosynthetic consumption (Pace et al., 2004). Net lake heterotrophy is also supported by the flushing of terrestrial organic matter into the system (e.g. Sobek et al., 2003). DIC input from stream inflow and groundwater have also been shown to influence lake CO_2 supersaturation (Molot and Dillon, 1996). Stream CO_2 supersaturation has also been linked to catchment wetland coverage (Wallin et al., 2014). Through conversion to CO_2 and CH_4 by photodegradation and biodegradation, DOC can also be lost from the water column to the atmosphere and is likely to show seasonal variation (Huttunen et al., 2002, Cole et al., 2007).

Lakes and reservoirs are found in many forested and peatland catchments in the UK uplands yet there are no in-depth studies considering GHG emissions in and out of lakes or reservoirs, with only a handful of studies focussing on DOC export (e.g. Evans et al., 2017; Stimson et al., 2017) or reservoir sedimentation (Holliday et al., 2008). Fluvial C losses from peatland dominated catchments are particularly high, with stream export ranging from 2-50 $\text{g C m}^{-2} \text{ yr}^{-1}$

(Billett et al., 2004; Dinsmore et al., 2013; Leach et al., 2016; Wallin et al., 2015). This is greater from degraded peatlands, extensive across the UK, and characterised by gullyng, artificial drainage ditch presence and loss of vegetation and moisture (Evans and Lindsay, 2010). DOC is frequently the prevailing C species in water bodies draining peatland catchments where CO_2 can be consumed through primary production, although DIC has also been reported at the same order of magnitude (Wallin et al., 2013, Billett et al., 2015). Peatland derived discharge is typically supersaturated in CO_2 and CH_4 , with rapid evasion occurring when this soil water is exposed to the atmosphere.

Forested catchments receive greater atmospheric N inputs than moorland catchments as forest vegetation, especially coniferous species, have a better ability to capture N (Fowler et al., 1989). N sources are also derived from forest felling debris (brash) which can contain over 70% of the N in above ground tree biomass (Hyvönen et al., 2000). Brash can increase rates of N mineralisation and denitrification from increasing underneath soil temperature and moisture (Emmett et al., 1991). This has been shown to increase N concentrations in UK streams N (Cummins and Farrell, 2003) and could likely lead to eutrophication (Correll, 1998) and potentially an increase in microbial respiration, resulting in greater CO_2 efflux (Waldron et al., 2009). There have been catchment studies in the UK that have shown afforestation and felling to elevate NO_3^- concentrations in upland lakes and streams (e.g. Allott et al., 1995).

To address these knowledge gaps, both comparative and integrative studies investigating catchment scale GHG dynamics in lakes and streams are required (Kokic et al., 2015). In this study we investigate spatial and temporal patterns in aquatic C and N concentrations and fluxes within two temperate reservoir catchments with different land covers (coniferous forest and moorland peat) in Scotland, UK. The aim is to quantify the annual variability of C and N inputs and export to/from the reservoirs via the catchment streams, allowing inferences to be made about the overall C and N balance of the reservoirs. Also to evaluate the differences in GHG concentrations and export from catchments with different managed land uses, moorland and coniferous forestry, commonly found in upland reservoirs in Scotland.

4.2 Materials and methods

4.2.1 Study sites

The study was conducted within the catchments of Black Esk (BE) and Baddinsgill (BA) reservoirs, both used for drinking water supply situated in Scotland, UK (Figure 4.1). At each catchment, five inlets ($\text{BA}_{1-5_{\text{in}}}$ and $\text{BE}_{1-5_{\text{in}}}$) and the outlet (BA_{out} and BE_{out}) were sampled,

along with three locations at the edge of the reservoir (BA1-3_{res} and BE1-3_{res}) covering a spatial gradient from top to the bottom dam end of the reservoir (n = 9 sampling locations for each reservoir). Black Esk was sampled from June 2015 to July 2017, whilst Baddingsgill was sampled from July 2015 to January 2017.

Black Esk reservoir is located ~5km from Eskdalemuir, Dumfries and Galloway, south-west Scotland (55° 15' N, 03° 15' W). The climate is temperate, with mean maximum annual temperature of 11.2 °C, mean minimum annual temperature of 3.9 °C and mean annual rainfall of 1742 mm (1981 – 2010; Eskdalemuir station 7 km north east of the reservoir dam, Met Office, 2016). The reservoir has a catchment area of 18.1 km², surface area of 0.4 km² and a maximum depth of 17.3 m. During 2014, the dam was raised by 2.5 m which resulted in flooding of land immediately surrounding the reservoir perimeter and further felling of trees. The catchment has mean elevation of 331 m (range 247-536 m) and a mean slope of 8°. The catchment land cover is dominated by coniferous forestry (96%) plantations with small areas of rough grazing (acid grassland) and moorland (heather grassland). Sitka spruce (*Picea sitchensis*) and Norway spruce (*Picea abies*) are the main tree species and were actively felled throughout the sampling period in the headwaters of sub-catchment BE3_{in}. Restocking of broadleaf trees also occurred in spring of 2017. The main catchment soil type is peaty podzols (72%) and peaty gleys (26%). Based on the Hydrology of Soil Type (HOST) classification system (Boorman et al., 1995) which classifies UK soils into 29 groups based on hydrological characteristics, classes 19 (11%), 15 (89%) and 29 (<1%) are dominant in the catchment. This suggests that the majority of the catchment (89%) has wet, peaty topped upland soils over relatively free draining permeable rocks. In terms of catchment geology, the bedrock was comprised of metasandstones and mudstones (74%), wacke (25%) and quartz-microgabbro (<1%), with superficial deposits of diamicton (51%), peat (9%) and silt, sand and gravel (5%).

Baddingsgill is an upland water supply reservoir located in the Pentland Hills near West Linton, in the Scottish Borders region of Scotland, UK (55° 47' N, 03° 23' W). The climate is temperate with mean maximum annual temperature is 11.8 °C, mean minimum annual temperature is 4.2 °C and mean annual rainfall is 980 mm (1981 – 2010; Penicuik station, 13 km north west of Baddingsgill dam, Met Office, 2016). The reservoir has a catchment area of 9.6 km², surface area of 0.25 km² and maximum depth of 22.6 m. Mean catchment elevation is 420 m (range 314-565 m) with a mean slope of 9° of which the majority are south facing. The catchment land use is predominately moorland (heather and heather grassland, 94%), with small areas of rough grazing (acid grassland 2%), coniferous woodland (1%) and improved grassland (<1%). The main catchment soil type is peaty podzols (59%), peaty gleys (20%) and non-calcareous

gleys (18%). Based on the Hydrology of Soil Type (HOST) classification system (Boorman et al., 1995), classes 24 (15%) and 15 (85%) are the most dominant. The catchment has largely (85%) permanently wet, peaty topped upland soils over relatively free draining permeable rocks. The catchment bedrock is composed of sandstones (57%), conglomerates (35%), mudstones and silts (6%) and has small areas (2%) of igneous rocks (quartz-diorite and mafite). Diamicton (25%), peat (22%) and small areas of clay, silt, sand and gravel make up the superficial deposits. The catchment also has a history of sheep farming, small-scale plantation felling, grouse shooting and managed heather burning, with the former three occurring during the sampling period. A large portion of the catchment is artificially drained via open cut ditches and areas of exposed eroded peatland are present, particularly between BA1_{in} and BA2_{in}.

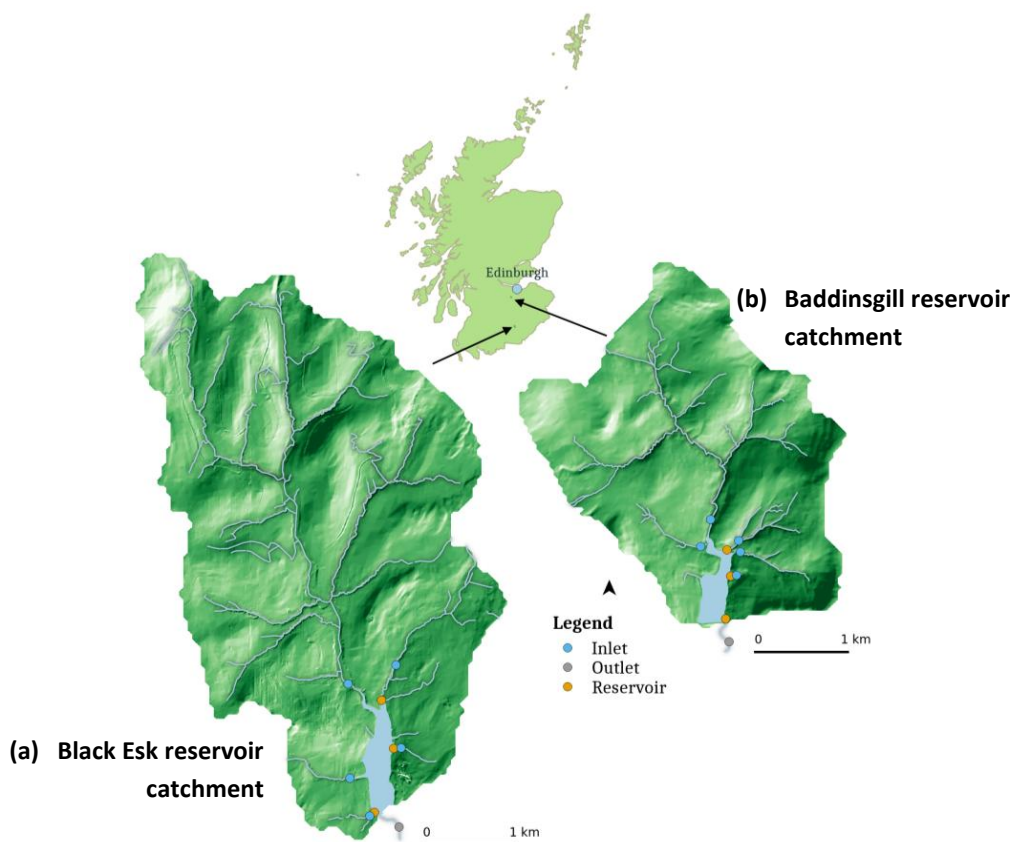


Figure 4.1 Location map of (a) Baddingsgill and (b) Black Esk reservoir catchments in Scotland, UK. The locations of the inlet, reservoir and outlet sampling points are highlighted.

4.2.2 Measurement of C, N and water chemistry parameters

Stream and reservoir surface water and headspace samples were collected from the sample sites ($n = 18$) in Figure 4.1 approximately every fortnight. Sampling at Black Esk ran from June 2015 to June 2017, whilst sampling at Baddingsgill was from July 2015 to January 2017. Water samples were collected and analysed for dissolved organic carbon (DOC), dissolved inorganic

carbon (DIC), ammonium (NH_4^+), nitrite (NO_2^-) and nitrate (NO_3^-). At the same time, a headspace sample was collected for the determination of dissolved CO_2 , CH_4 and N_2O . Water temperature, pH, dissolved oxygen (DO), and electrical conductivity (EC) were recorded in situ using handheld multi-meters (Hanna Instruments HI-9145, HI-9124, HI-0933).

All water samples were collected approximately 10 cm below the water surface using 60 ml syringes and in-field filtered through 0.45 μm syringe-driven filters (Whatman®) and stored without headspace in 30 ml bottles. Samples for DOC and DIC were stored in the dark at ~ 4 °C before analysis (within two weeks of collection) on a PPM LabTOC Analyser (detection range 0.1-4000 mg L^{-1} ; Pollution & Process Monitoring, UK) and concentrations calculated based on a three-point calibration curve with a maximum of 50 mg L^{-1} . Samples for NH_4^+ , NO_2^- and NO_3^- were stored in the freezer at approximately -21 °C for later analysis on a Seal Analytical AQ2 discrete analyser (Methods: EPA 350.1 v2 and EPA 353.2 v2 (USEPA, 1993)).

Dissolved CO_2 , CH_4 and N_2O gas samples were collected (including replicate and ambient) from each sampling site using the headspace technique (e.g. Kling et al., 1991; Billett et al., 2004; Dinsmore et al., 2010). A 40 ml water sample was equilibrated with 20 ml ambient air (collected from approximately 10 cm water depth) at water temperature by shaking underwater for one minute. The equilibrated headspace and ambient samples were then injected into 12 ml pre-evacuated Exetainer® vials (Labco, Lampeter, UK) and analysed on a 7890B gas chromatograph (Agilent Technologies) with flame ionization detector (FID) for CH_4 and attached methaniser for CO_2 , and the micro electron capture detector (μECD) for N_2O . Detection limits were <199 ppmv for CO_2 , <1.26 ppmv for CH_4 and <0.2 ppmv for N_2O . Henry's Law was then used to determine dissolved concentrations of CO_2 , CH_4 and N_2O in the water column from the ambient and headspace concentrations (e.g. Hope et al., 1995). Concentrations are also expressed in units of excess partial pressure (e.g. epCO_2 , epCH_4 , epN_2O), which is the partial pressure of the gas in solution divided by the partial pressure of the gas in equilibrium with the atmosphere. Wind speed, air temperature and barometric pressure were also obtained using a hand-held weather meter (Kestrel 2500, accuracy 3% of reading) at ~ 1 m above the water surface from each sampling location. Kruskal-Wallis rank sum tests were conducted to establish if there were significant statistical differences between GHG concentrations between inlets, reservoirs and outlets.

4.2.3 Calculation of reservoir and stream GHG evasion rates

Evasion rates were calculated indirectly using wind speed to predict gas transfer velocity, combined with the partial pressure difference across the air-water interface, using established relationships between wind speed and gas transfer velocity (MacIntyre et al., 1995; Wanninkhof, 1992). Evasion gas fluxes ($F_{CO_2}/F_{CH_4}/F_{N_2O}$) were then calculated using Eq. (2), Fick's first law, as described in Borges et al. (2004), where k is the gas transfer velocity ($cm\ h^{-1}$), a is the solubility coefficient and Δp_{gas} is the difference in partial pressure between the surface water and the atmosphere. The solubility coefficient a is temperature and salinity dependent. Values of a for CO_2 , CH_4 and N_2O were derived from Weiss (1974), Weisenburg and Guinasso (1979), and Weiss and Price (1980), respectively. The transfer velocity k is a function of turbulence, the kinematic viscosity of the water and the molecular diffusion coefficient of the gas. In Eq. (3) (Cole and Caraco, 1998) wind speed ($m\ s^{-1}$) at 10 m above the water surface U_{10} is used to describe turbulence, and the Schmidt number Sc is a function of the latter two terms. $k(600)$ refers to the transfer velocity normalised to $Sc = 600$, the Schmidt number of each gas at $20^\circ C$ in freshwater. This is then adjusted using the Schmidt number for the particular gas in freshwater at measured temperature (MacIntyre et al., 1995) using Eq. (4). The exponent in Eq. (4) varies from $-\frac{2}{3}$ to $-\frac{1}{2}$ as wind speed increases and waves become present (Jähne et al., 1987). Wind speed at 10 m (U_{10}) is calculated using Eq. (5) (Erkkilä et al., 2018).

An estimate of stream evasion was also made following Eq. (2) and the gas transfer velocity at $20^\circ C$ (k_{600} , in $m\ d^{-1}$) was predicted as a product of stream slope (S) and velocity (V) and calculated following Eq. (6) (Raymond et al., 2012; Eq. 5) and adjusted to stream temperature (k) following Eq. (4). A number of measurements of stream width, depth and flow velocity were taken across different field visits to cover a range of flow conditions. As per Chapter 2 (section 2.2.4.1), discharge-stage relationship curves were established, and these were used to infer flow velocity and discharge for dates at which only depth measurements were available. The flow velocity and stream slope (calculated using GIS) were then used to find the gas transfer coefficient at a Schmidt number of 600 (i.e. $k(600)$) (Raymond et al., 2012; Butman and Raymond, 2011; Magin et al., 2017) using Eq. (6).

$$F_{gas} = k\alpha\Delta p_{gas} \quad (2)$$

$$k(600) = 2.07 + 0.215u_{10}^{1.7} \quad (3)$$

$$k = k(600) \left(\frac{Sc}{600} \right)^{-\frac{1}{2}} \quad (4)$$

$$U_{10} = 1.22U_z \quad (5)$$

$$K_{600} (\text{m d}^{-1}) = S \times V \times 2841.6 + 2.03 \quad (6)$$

4.2.4 Estimating catchment areas

Data from a 5 m digital terrain model (DTM) and the hydrological tool extension in ArcGIS Pro were used to determine reservoir areas, total catchment areas, sub-catchment inlet and outlet areas and percentage of different land uses, soil, geology, along with slope and elevation. The analysis resulted in a total catchment area for Black Esk reservoir of 1810 ha with surface water area of 34 ha, and sub-catchment drainage areas for BE1in of 21 ha, BE2in of 44 ha, BE3in of 1370 ha, BE4in of 176 ha, BE5in of 11 ha and BEout of 1850 ha. Baddingsgill has a reservoir surface area of 25 ha and total catchment area of 962 ha. The sub-catchment drainage areas of the catchment areas at Baddingsgill were 79 ha at BA1in, 640 ha at BA2in, 72 ha at BA3in, 77 ha at BA4in, 12 ha at BA5in and BAout had a total area of 1360 ha.

It was discovered at the later stages of the project that there is an abstraction point on another stream in an adjacent catchment that was not sampled but feeds into Baddingsgill Reservoir via an underground route. The area of this catchment is 387 ha, which gives Baddingsgill Reservoir a 'true' catchment area of 1350 ha. The stream has an impoundment across it with differential height weirs and overspill so abstraction can only occur during certain flow conditions (i.e. this catchment does not enter the reservoir constantly), where a raw water main takes the stream water into the reservoir via an underground pathway. This stream also has a water abstraction licence in place that permits abstraction of up to 27,280 m³ per day (vs. 37,070 m³ per day from Baddingsgill reservoir) (Scottish Water, pers.comm). From field work and GIS analysis, there was nothing to believe that this additional catchment would be uniquely different from the inlets naturally feeding the reservoir. As this additional catchment is used as just a top-up water source under certain flow conditions, and is located adjacent to Baddingsgill, the study assumed a constant C and N flux per unit area in each of the measured catchments but uncertainty estimates become unbounded. As the catchments cover a small area with little spatial variation in areal runoff, taking a whole catchment approach assumes that water out is equal to water in. As budgets for full years were only calculated, it avoids issues such as storage changes in the reservoir and seasonal fluctuations and/or lags. To evaluate the impact of this additional water supply, the predicted catchment

export was removed from the overall balance, and results showed that the reservoir continued to act as a net sink for areal fluxes.

4.2.5 Aquatic C and N export

Rating curves were developed from manual discharge measurements made over a range of flow conditions. Total annual load of each C and N species were calculated as the product of flow-weighted mean concentration and mean annual discharge. Areal mean C and N fluxes were then calculated as annual loads divided by sub-catchment area to normalise exports (Aitkenhead-Peterson et al., 2005). Full details are provided in Chapter 2 (section 2.2.4) with ratings curves and equations used presented in Appendix I.

4.3 Results

4.3.1 Spatial and temporal variability in C and N concentrations

Inlet, reservoir and outlet water chemistry across the full sampling period at Baddingsgill and Black Esk catchments are shown in (Table 4.1) as mean, standard error and range. Discharge across both reservoir catchments is shown in Figure 4.6. At Baddingsgill, mean water temperatures for all sites over the study period varied from 7.4°C to 9.7°C with higher mean temperatures seen at the reservoir sites than inlets. A similar pattern of higher reservoir temperatures was seen at Black Esk, with mean temperatures across all sites varying from 8.7°C to 11°C. Mean conductivity in both catchments was highly variable across sites from 41 to 183 $\mu\text{S cm}^{-1}$. All sites in both catchments had a mean circumneutral pH (6.7 to 7.5) but ranged widely from acidic (minimum pH = 4.7 at BE1in) to alkaline (maximum pH = 8.6 at BE3in). Mean dissolved oxygen varied from 59% to 76% across both inlet and reservoir sites. Differences in catchment characteristics of land cover, soil and geology are also shown for each sub-catchment in . Land cover at Baddingsgill is dominated by moorland, whilst Black Esk is coniferous forestry. Bedrock geology shows great percentage of conglomerates at Baddingsgill whilst Black Esk has more mud- and sandstones. Catchment soil at Baddingsgill is largely peaty podzols and non-calcareous gleys, whilst Black Esk has peaty gleys and blanket peats.

Carbon dioxide

Carbon dioxide concentrations at both Baddingsgill and Black Esk catchments were on average, above atmospheric equilibrium with oversaturation of CO₂ occurring as indicated by the excess partial pressure 'ep' values >1 in (Table 4.1). Baddingsgill dissolved CO₂-C concentrations in the inlets ranged from 0.27 to 2.1 mg C L⁻¹, with a wider range (0.18 to 12 mg C L⁻¹) observed in the

reservoir (as illustrated by the spikes in CO₂ concentrations in (Figure 4.3), and from 0.26 to 0.96 mg C L⁻¹ at the outlet (Figure 4.3). Apart from the spikes in CO₂ (Dec-15 to Feb-16), Baddingsgill showed no strong temporal or seasonal pattern. Concentrations of CO₂-C in the reservoir were on average 15% higher than the inlets and 72% higher than the outlet. Spatial variability was also seen within the reservoir across the three sampling locations, with a 71% increase in CO₂ concentrations at BA2res (i.e. half way up the reservoir) compared to BA1res and BA3res (0.71 ± 0.071 and 0.73 ± 0.22 mg C L⁻¹, respectively). CO₂-C concentrations at Black Esk had a smaller range than Baddingsgill with 0.14 to 1.2 mg C L⁻¹ observed in the inlets, 0.37 to 6.7 mg C L⁻¹ in the reservoir and 0.13 to 1.5 mg C L⁻¹ at the outlet. A much larger increase in reservoir CO₂-C concentrations was observed at Black Esk with the reservoir being on average 111% higher than the inlets and 132% higher than the outlet. The reservoir also showed strong temporal variability in CO₂ concentrations with multiple spikes occurring throughout the sampling period across different seasons (Figure 4.3). A Kruskal-Wallis rank sum test found concentrations to be significantly different between the inlets and reservoirs for CO₂ (p < 0.001) and between the reservoirs and outlets (p<0.001) at both Baddingsgill and Black Esk.

Four of the five sampled inlets at Baddingsgill saw consistent CO₂ oversaturation with epCO₂ values ranging from 1.1 to 7.1, along with two of the three reservoir sampling locations (epCO₂ ranged from 1.1 to 34 at BE2res and BA3res, respectively). Minimum epCO₂ values of 1.0, 0.9 and 0.8 suggest that an inlet (BA3in), reservoir sampling sites (BA1res) and outlet (BAout) were occasionally in atmospheric equilibrium or undersaturated in CO₂. However, this was observed only once at each location during the sampling period. At Black Esk, all reservoir sampling locations were consistently oversaturated in CO₂ (epCO₂ ranged from 1.3 to 19) and on average, the reservoir was 33% higher than Baddingsgill. Like Baddingsgill, undersaturation and equilibrium with atmospheric CO₂ occurred at the outlet (BEout; minimum = 0.4 on four sampling dates i.e. 9% of total sampling) and at inlet BE2in (minimum = 1.0 on two sampling dates) and BE3in (minimum = 0.6 and on eight sampling occasions i.e. 19% of total sampling).

Methane

At both Baddingsgill and Black Esk catchments, all water bodies were also on average, oversaturated in CH₄, with mean epCH₄ ranging from 3.3 ± 0.45 to 154 ± 41. Dissolved CH₄-C concentrations at Baddingsgill ranged from 0.031 to 10 µg C L⁻¹, whilst a higher range was observed at the Black Esk catchment (0.018 to 69 µg C L⁻¹) (Figure 4.3). Temporal and seasonal variability was more apparent in CH₄ concentrations at Baddingsgill, rising in late summer and early autumn (Sep-Oct) in both 2015 and 2016 at Baddingsgill and can be seen at the reservoir

sampling sites at Black Esk (Figure 4.3). At Baddingsgill, three inlets (BA1in, BA3in, BA5in), a reservoir sampling location (BA1res) and outlet (BAout) were consistently oversaturated in CH₄ (minimum epCH₄ = 1.8 and maximum = 159) whilst BA3in, BA4in, BA2res and BA3res showed periods of undersaturation (i.e. 9% of total sampling across these sites) with a minimum epCH₄ of 0.27 observed at BA3res. At Black Esk, the reservoir sampling locations were consistently oversaturated in CH₄ (epCH₄ range = 7.1 to 1236), with inlets BE3in and BE4in also showing oversaturation, whilst BE1in, BE2in, BE5in and BEout also showed periods of undersaturation (minimum epCH₄ of 0.31 at BE5in). A Kruskal-Wallis rank sum test also found concentrations at both Baddingsgill and Black Esk to be significantly different between the inlets and reservoirs for CH₄ ($p < 0.001$) and between the reservoirs and outlets ($p < 0.001$). Mean epCH₄ across all three Baddingsgill reservoir sampling locations was 80% lower than at Black Esk. Within reservoir spatial variability was also seen for CH₄ concentrations at Baddingsgill and Black Esk. At Baddingsgill, lower CH₄ concentrations were observed at BA3res (mean $0.87 \pm 0.23 \mu\text{g C L}^{-1}$; located near the dam), with similar concentrations at BA2res and BA1res (mean $1.3 \pm 0.35 \mu\text{g C L}^{-1}$ and $1.4 \pm 0.35 \mu\text{g C L}^{-1}$, respectively) resulting in a 61% increase in CH₄ concentrations between the opposite ends of the reservoir. Similarly at Black Esk, lowest in-reservoir CH₄ concentrations were observed at the dam end (BE3res; mean $5.2 \pm 0.93 \mu\text{g C L}^{-1}$), with highest concentrations at BE2res ($7.4 \pm 2.1 \mu\text{g C L}^{-1}$). At BE2res, CH₄ concentrations were 43% and 23% higher compared to BE3res and BE1res, respectively.

DOC and DIC

There was pronounced spatial variability in DOC concentration in the catchment inlets with mean concentrations ranging from 6.0 ± 0.76 to $15 \pm 1.8 \text{ mg L}^{-1}$ between the inlets at Baddingsgill and 8.3 ± 0.84 to $31 \pm 1.8 \text{ mg L}^{-1}$ at Black Esk (Figure 4.4). Both reservoirs showed little spatial variability with mean DOC concentrations of 13.0 mg L^{-1} at all three of the Baddingsgill reservoir sampling locations, and Black Esk mean concentrations ranged from 9.7 ± 0.37 to $12.0 \pm 0.63 \text{ mg L}^{-1}$. DOC concentrations were also highly temporally variable in both catchments, ranging from 0.93 to 37 mg L^{-1} at Baddingsgill and from 2.0 to 58 mg L^{-1} at Black Esk (Figure 4.4).

Pronounced spatial variability was also seen in DIC concentrations in the inlets of both catchments (Figure 4.4). At Baddingsgill, mean inlet concentrations ranged from $12 \pm 1.3 \text{ mg L}^{-1}$ (BA1in) to $34 \pm 2.1 \text{ mg L}^{-1}$ (BA5in). At Black Esk, mean inlet DIC concentrations ranged from $5.8 \pm 1.1 \text{ mg L}^{-1}$ (BE5in) to $19 \pm 1.6 \text{ mg L}^{-1}$ (BE2in). Similarly to DOC, there was little DIC spatial variability between the reservoir sampling locations. At Baddingsgill, mean DIC reservoir

concentrations ranged from $10 \pm 1.0 \text{ mg L}^{-1}$ (BA1res) to $12 \pm 1.6 \text{ mg L}^{-1}$ (BA2res) and from $12 \pm 0.84 \text{ mg L}^{-1}$ (BE3res) to $13 \pm 0.95 \text{ mg L}^{-1}$ (BE1res) at Black Esk. There was a small increase (5%) between reservoir and outlet DIC concentrations at Baddinsgill and a 10% decrease at Black Esk. DIC concentrations were also highly temporally variable in both catchments, ranging from 0.6 mg L^{-1} (BA2in) to 59 mg L^{-1} (BA5in) at Baddinsgill, and 0.3 mg L^{-1} to 42 mg L^{-1} at Black Esk (Figure 4.4). There is however, no clear seasonal pattern in either DOC or DIC concentrations at either catchment.

Nitrous oxide, NH_4^+ , NO_2^- and NO_3^-

Concentrations of $\text{N}_2\text{O-N}$ at Baddinsgill (range 0.29 to $2.5 \text{ } \mu\text{g N L}^{-1}$) and Black Esk (0.22 to $3.3 \text{ } \mu\text{g N L}^{-1}$) catchments were on average oversaturated in N_2O but values were much closer to atmospheric equilibrium than the other measured gases with lowest mean epN_2O values of 1.1 ± 0.022 at BEout to a highest mean of 1.8 ± 0.042 at BA5in (Table 4.1). An epN_2O range of 0.69 to 6.4 was seen across the two catchments with 21% of sampled undersaturated at Baddinsgill and 22% at Black Esk. Temporal variability at Baddinsgill catchment is low (with spikes in N_2O seen within the reservoir during Mar-Apr 2016), with Black Esk showing greater temporal variability also within the reservoir across the full sampling period (Figure 4.3). At Baddinsgill catchment, all inlets had a mean N_2O concentration of $0.5 \text{ } \mu\text{g N L}^{-1}$ apart from BA5in, which was at least 56% larger at $0.78 \pm 0.017 \text{ } \mu\text{g N L}^{-1}$ (Figure 4.3, Figure 4.8). Spatial variability within the reservoir saw highest mean concentrations at BA2res (0.61 ± 0.088) which was 30% higher than BA1res and 20% higher than BA3res. Mean outlet N_2O concentrations (0.48 ± 0.015) were lower than the inlets by 4-38%. At Black Esk, similar patterns are seen with mean inlet concentrations varying from 0.47 ± 0.014 (BE4in) to 0.52 ± 0.016 (BE1in). Spatial variability was also seen within the reservoir; highest mean concentrations were observed at BE3res (0.67 ± 0.099) and BE2res saw a 16% decrease in mean concentrations. The Kruskal-Wallis rank sum test found no significant difference in N_2O concentrations between the inlets and reservoirs ($p = 0.522$) or the reservoirs and outlets ($p=0.084$) at both Baddinsgill and Black Esk.

Ammonium concentrations at Baddinsgill were spatially variable across sites where mean values ranged from $8.4 \pm 2.1 \text{ } \mu\text{g N L}^{-1}$ (BA3in) to $62 \pm 26 \text{ } \mu\text{g N L}^{-1}$ (BA5in) (Table 4.1). At Black Esk mean NH_4^+ concentrations across sites ranged from $39 \pm 8.1 \text{ } \mu\text{g N L}^{-1}$ (BEout) to $94 \pm 16 \text{ } \mu\text{g N L}^{-1}$ (BE5in). NO_2^- concentrations in both catchments were low, with mean concentrations ranging from $2.8 \pm 0.48 \text{ } \mu\text{g N L}^{-1}$ at BA4in to $8.7 \pm 4.0 \text{ } \mu\text{g N L}^{-1}$ at BE3res across the sites. Concentrations of NO_3^- at Baddinsgill were highly spatially variable where mean

concentrations ranged from $160 \pm 22 \mu\text{g N L}^{-1}$ at BA2in to $511 \pm 105 \mu\text{g N L}^{-1}$ at BA5in. There was also a wide temporal concentration range during the sampling period from 8 to $2750 \mu\text{g N L}^{-1}$. At Black Esk, mean concentrations across sites ranged from $137 \pm 23 \mu\text{g N L}^{-1}$ (BE2in) to $293 \pm 39 \mu\text{g N L}^{-1}$ (BE3in).

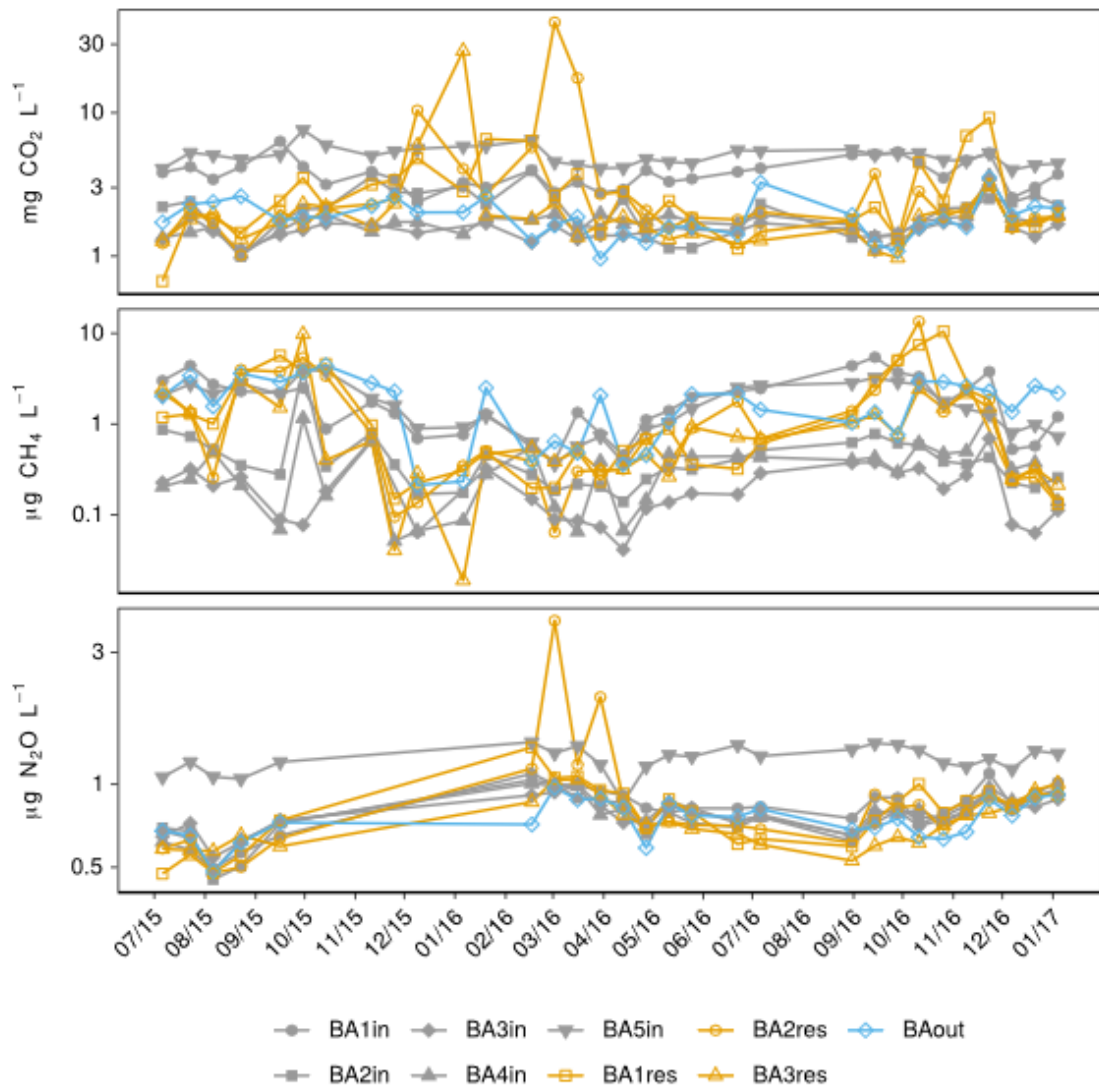


Figure 4.2 Temporal variability in inlet (gray), reservoir (orange) and outlet (blue) GHG concentrations at Baddingsill (BA) reservoir catchments from July 2015 to January 2017.

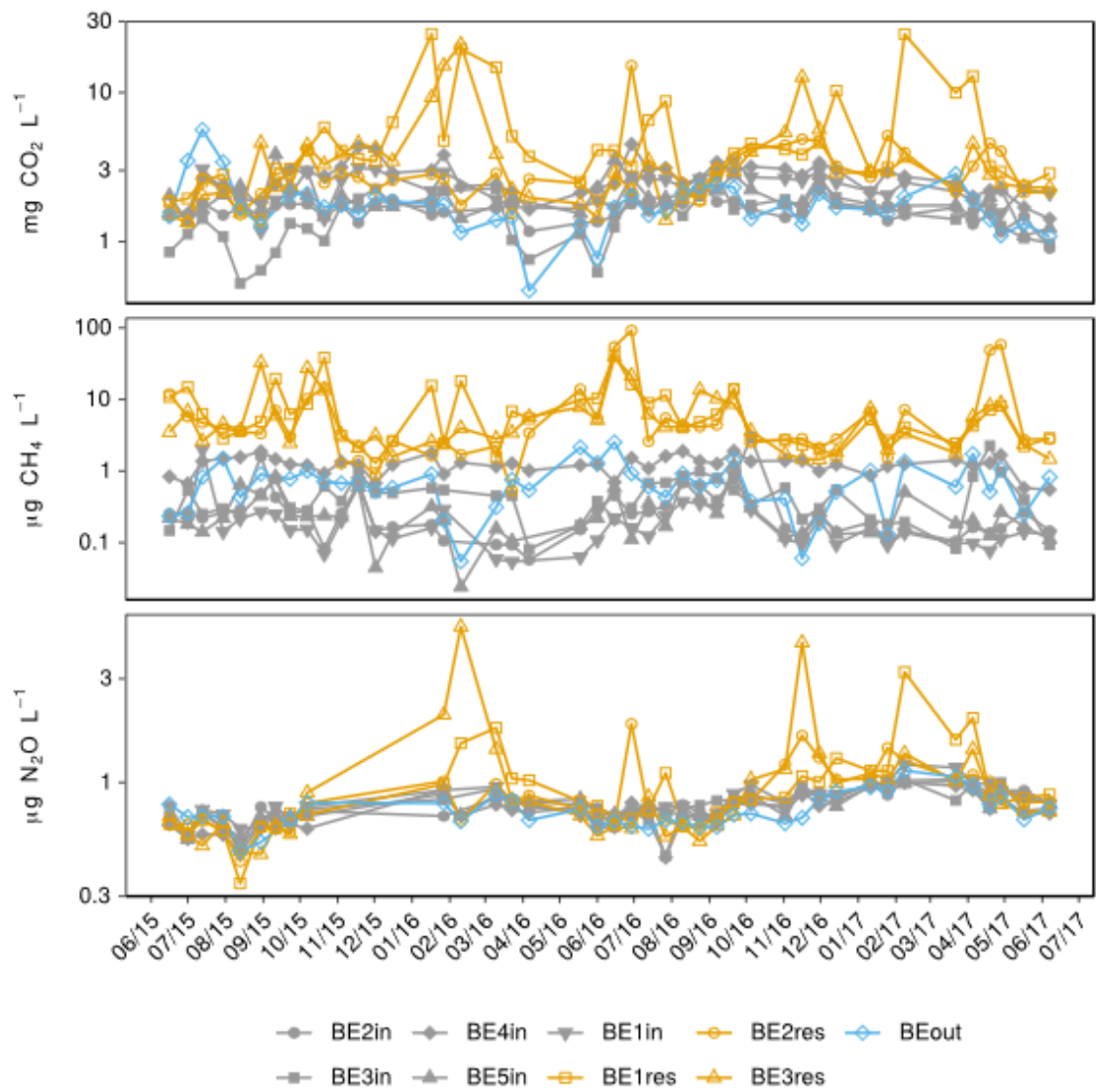


Figure 4.3 Temporal variability in inlet (gray), reservoir (orange) and outlet (blue) GHG concentrations at Black Esk (BE) catchments from June 2015 to July 2017.

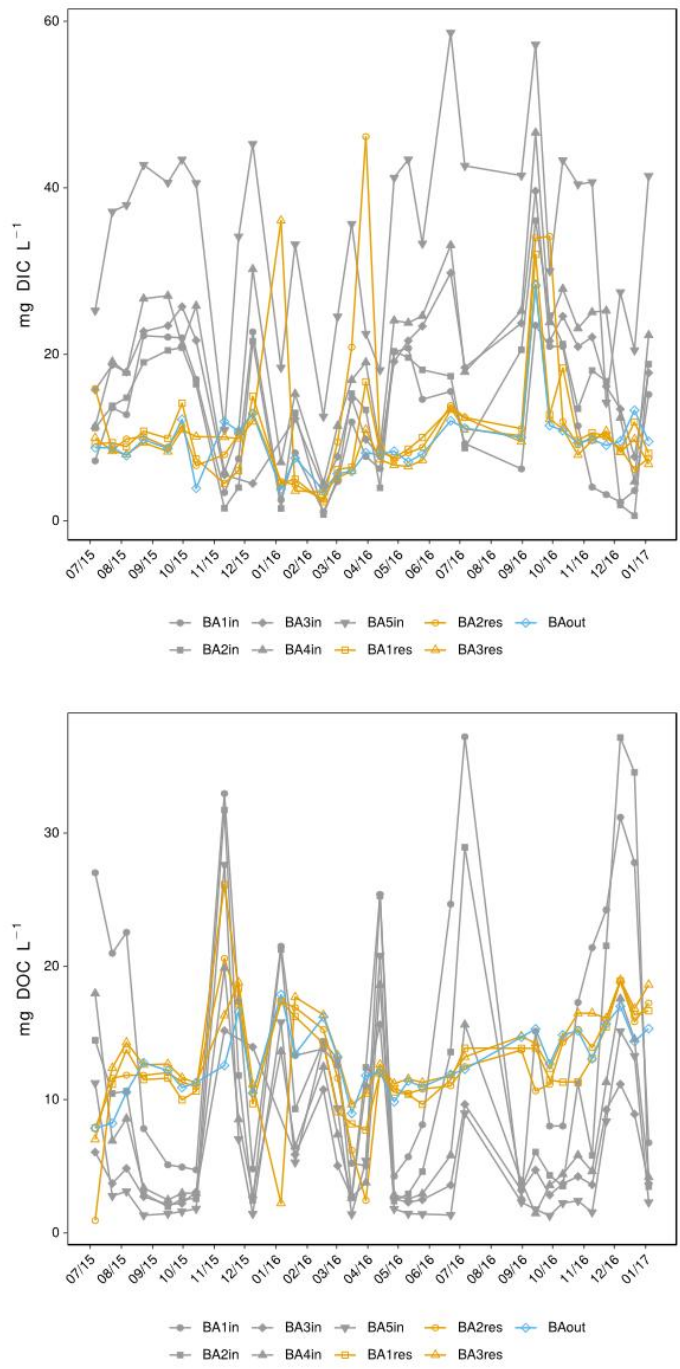


Figure 4.4 Temporal variability in inlet (gray), reservoir (orange) and outlet (blue) DIC and DOC concentrations at the sampling locations of Baddinsgill (BA) reservoir from July 2015 to January 2017.

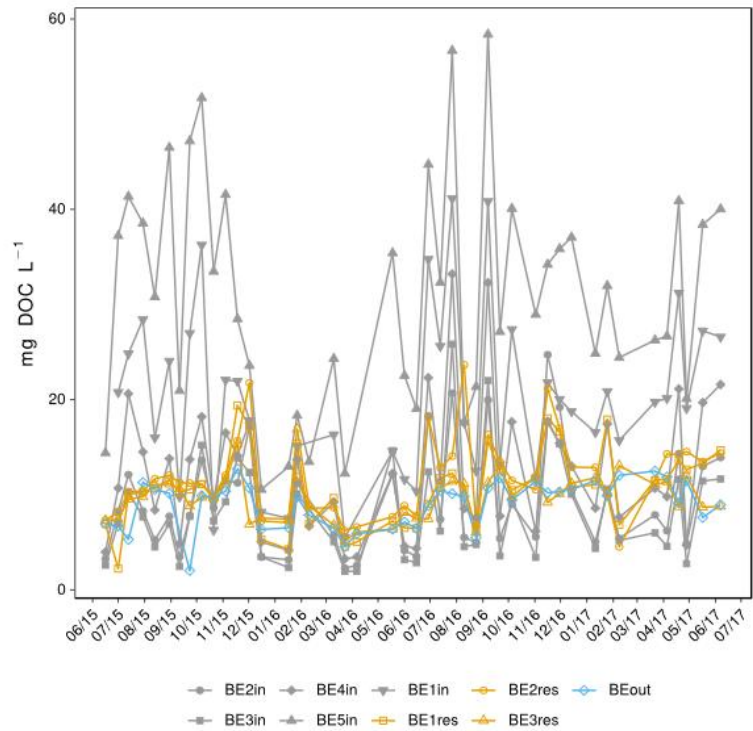
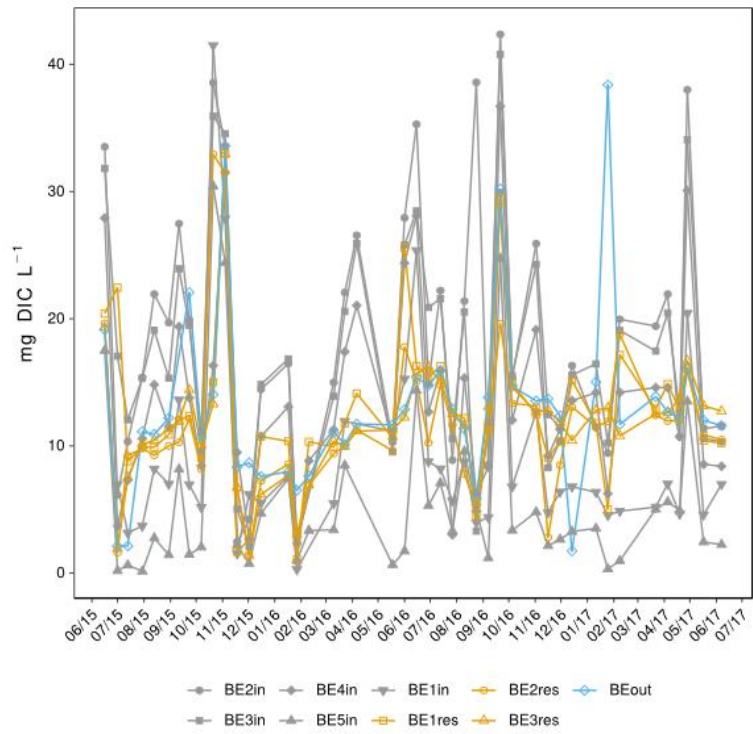


Figure 4.5 Temporal variability in inlet (gray), reservoir (orange) and outlet (blue) DIC and DOC concentrations at the sampling locations of Black Esk (BE) reservoir from June 2015 to July 2017.

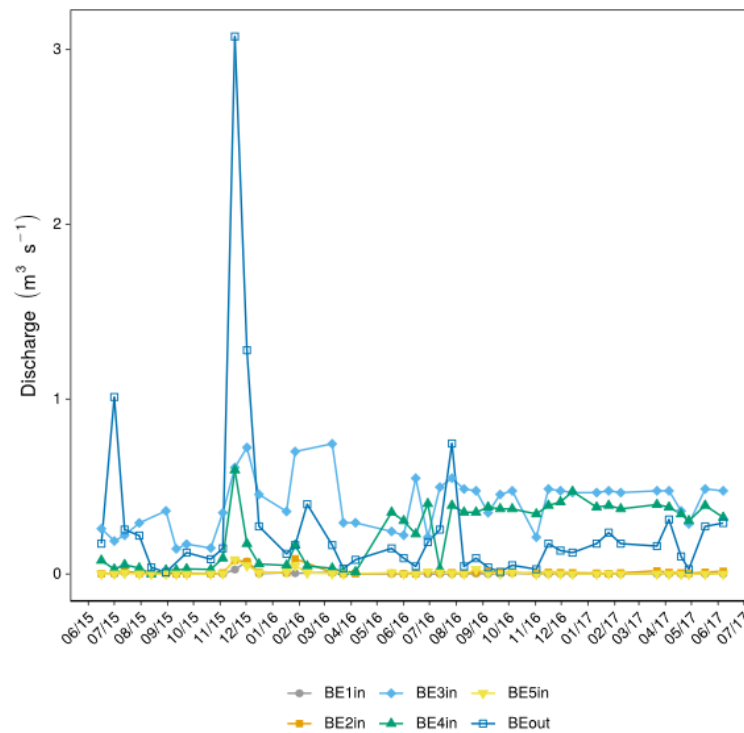
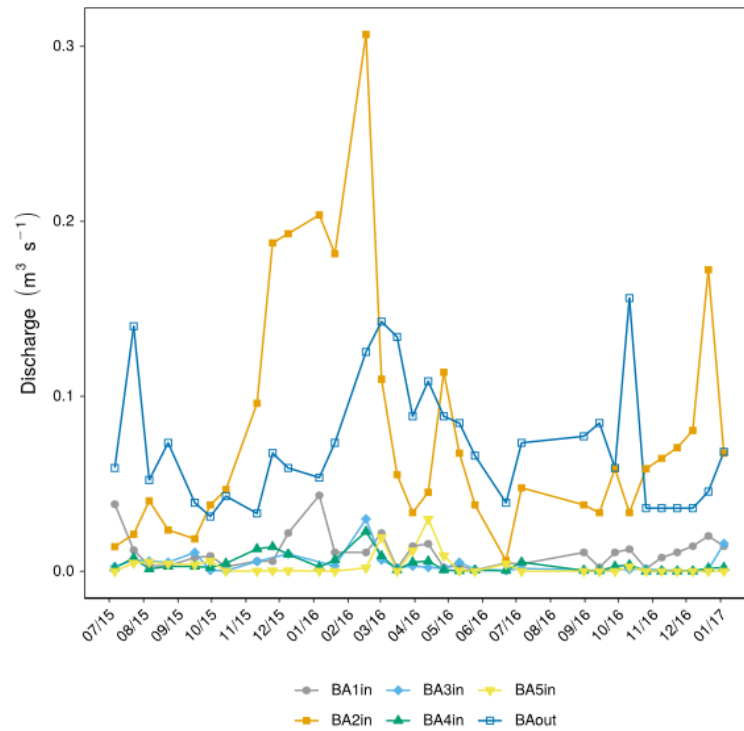


Figure 4.6 Spatial variability in discharge at Baddingsgill and Black Esk catchment inflows and outflows.

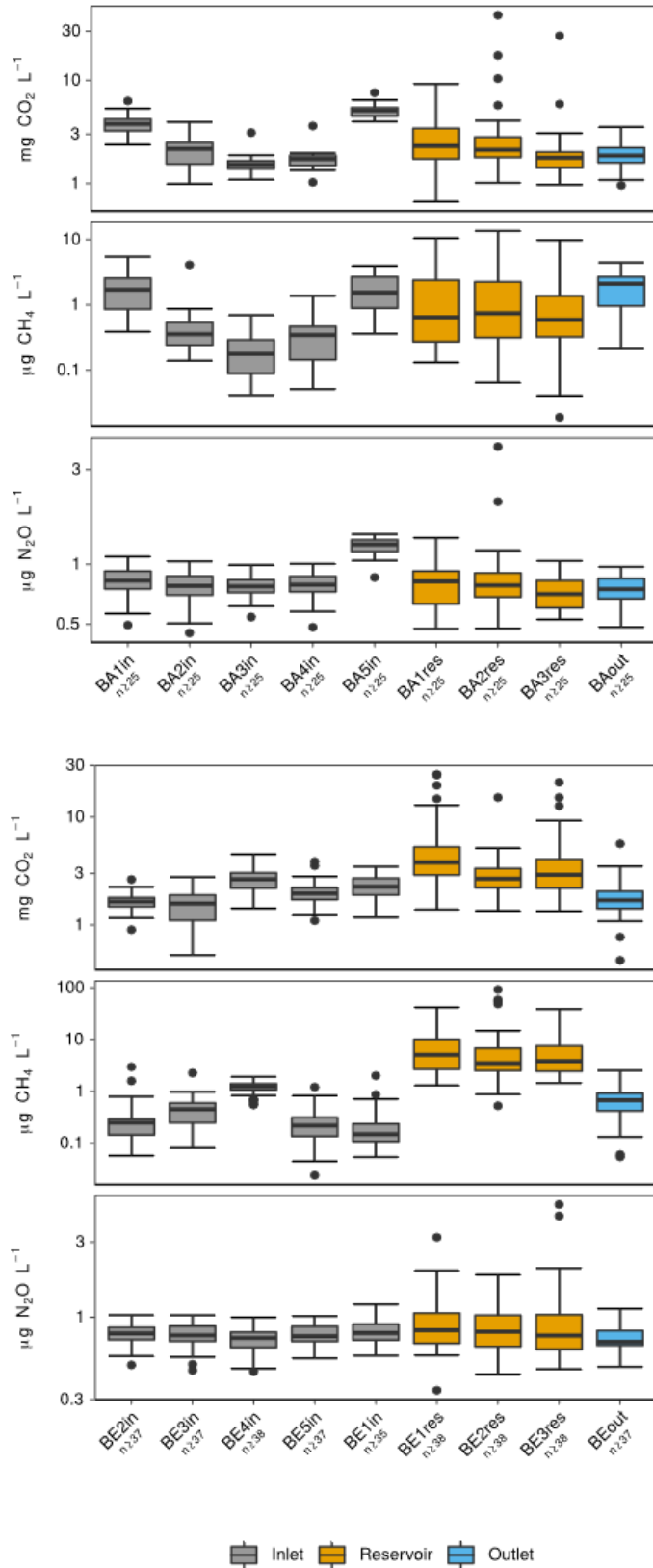


Figure 4.7 Spatial variability inlet (gray), reservoir (orange) and outlet (blue) GHG concentrations at Baddingsgill and Black Esk catchments during the full sampling period.

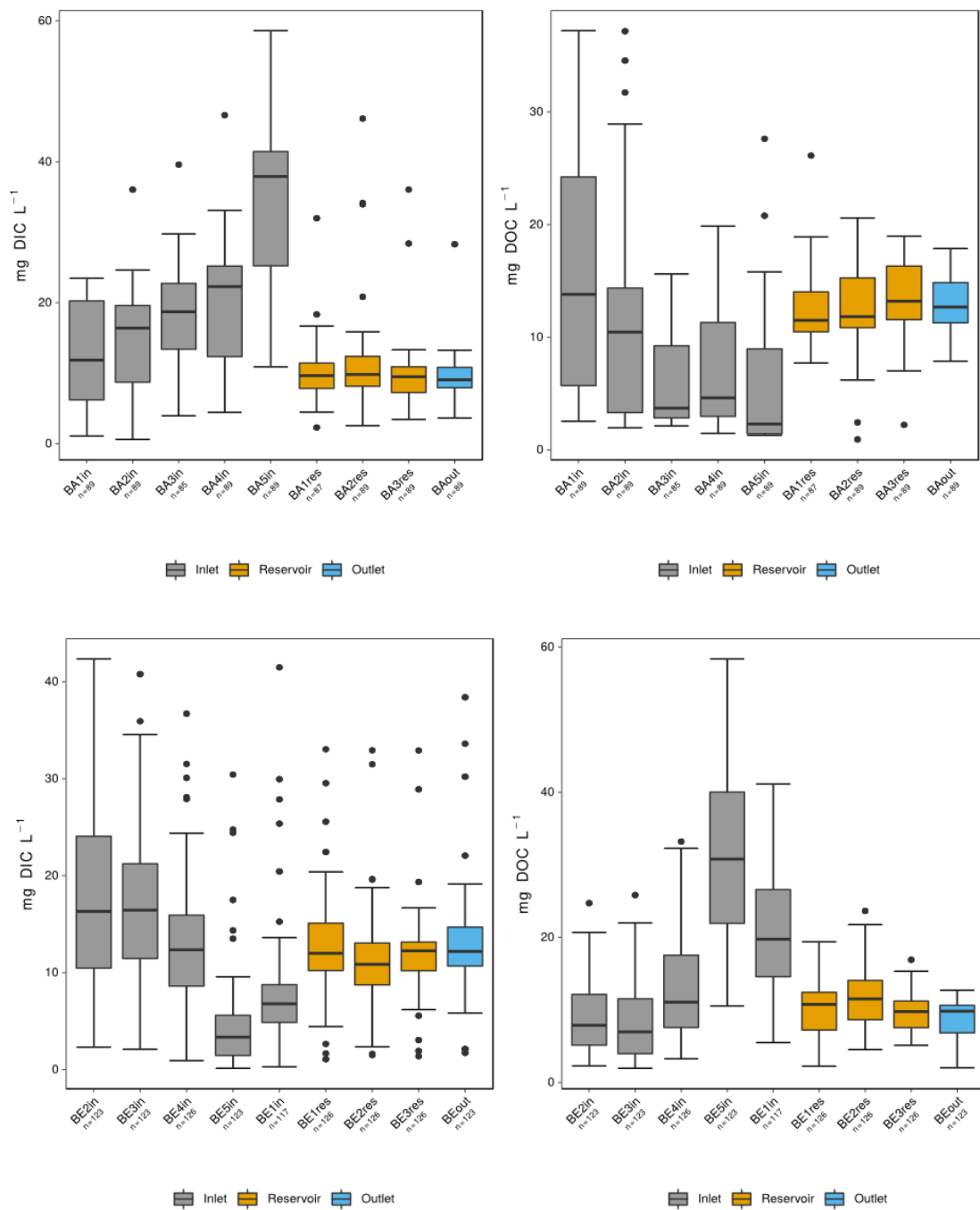


Figure 4.8 Spatial variability in inlet (gray), reservoir (orange) and outlet (blue) DOC and DIC concentrations at Baddingsgill and Black Esk catchments during the full sampling period.

Table 4.1 Variability in concentrations and excess partial pressure of different C and N species at Baddinsgill inlet, reservoir and outlet surface waters. Values are reported to two significant figures as mean \pm standard error (minimum-maximum).

Location	CO ₂ (mg C L ⁻¹)	CH ₄ (μ g C L ⁻¹)	N ₂ O (μ g N L ⁻¹)	epCO ₂	epCH ₄	epN ₂ O	DOC (mg L ⁻¹)	DIC (mg L ⁻¹)	NH ₄ ⁺ (μ g L ⁻¹)	NO ₂ ⁻ (μ g L ⁻¹)	NO ₃ ⁻ (μ g L ⁻¹)
BA1in	1.0 \pm 0.044 (0.65-1.7)	1.5 \pm 0.18 (0.29-4.1)	0.53 \pm 0.02 (0.32-0.7)	3.6 \pm 0.2 (2-6.4)	31 \pm 3.9 (5-90)	1.2 \pm 0.03 (0.83-1.5)	15 \pm 1.8 (2.5-37)	12 \pm 1.3 (1.1-23)	30 \pm 9.9 (0-185)	6.7 \pm 2.6 (1-62)	188 \pm 41 (24-827)
BA2in	0.57 \pm 0.034 (0.27-1.1)	0.39 \pm 0.09 (0.1-3.1)	0.5 \pm 0.018 (0.29-0.66)	1.9 \pm 0.097 (1.1-3.6)	7.8 \pm 1.8 (1.9-59)	1.1 \pm 0.025 (0.75-1.3)	12 \pm 1.8 (2-37)	14 \pm 1.5 (0.61-36)	19 \pm 5.1 (0-77)	6.1 \pm 1.9 (0-46)	160 \pm 22 (5-407)
BA3in	0.42 \pm 0.017 (0.3-0.85)	0.16 \pm 0.022 (0.031-0.52)	0.5 \pm 0.014 (0.35-0.63)	1.5 \pm 0.057 (0.96-2.7)	3.3 \pm 0.45 (0.58-10)	1.1 \pm 0.02 (0.89-1.3)	6 \pm 0.76 (2.1-16)	18 \pm 1.5 (4-40)	8.4 \pm 2.1 (0-34)	6.1 \pm 3.7 (0-80)	226 \pm 31 (8-683)
BA4in	0.48 \pm 0.02 (0.28-0.98)	0.27 \pm 0.039 (0.038-1)	0.5 \pm 0.017 (0.31-0.64)	1.6 \pm 0.058 (1.2-3.1)	5.5 \pm 0.76 (0.72-19)	1.1 \pm 0.026 (0.8-1.3)	7.6 \pm 1 (1.5-20)	20 \pm 1.6 (4.5-47)	25 \pm 18 (0-432)	2.8 \pm 0.48 (1-11)	220 \pm 18 (14-373)
BA5in	1.4 \pm 0.037 (1.1-2.1)	1.3 \pm 0.14 (0.27-3)	0.78 \pm 0.017 (0.55-0.9)	4.7 \pm 0.13 (3.5-7.1)	27 \pm 2.8 (5-58)	1.8 \pm 0.042 (1.1-2.1)	6.2 \pm 1.2 (1.3-28)	34 \pm 2.1 (11-59)	62 \pm 26 (0-404)	3.4 \pm 0.89 (0-17)	511 \pm 105 (153-2750)
BA1res	0.71 \pm 0.071 (0.18-1.8)	1.4 \pm 0.35 (0.098-7.9)	0.51 \pm 0.029 (0.3-0.87)	2.5 \pm 0.2 (0.89-5.1)	31 \pm 7.5 (1.8-159)	1.2 \pm 0.039 (0.87-1.6)	13 \pm 0.72 (7.7-26)	10 \pm 1 (2.3-32)	25 \pm 6.7 (0-139)	4.1 \pm 0.41 (2-12)	281 \pm 37 (85-662)
BA2res	1.2 \pm 0.37 (0.28-12)	1.3 \pm 0.35 (0.048-10)	0.61 \pm 0.088 (0.3-2.5)	3.8 \pm 1.1 (1.3-34)	29 \pm 7.6 (0.85-215)	1.4 \pm 0.16 (0.85-4.8)	13 \pm 0.74 (0.93-21)	12 \pm 1.6 (2.6-46)	21 \pm 5 (0-94)	3.5 \pm 0.39 (0-10)	258 \pm 37 (56-935)
BA3res	0.73 \pm 0.22 (0.26-7.4)	0.87 \pm 0.23 (0.014-7.3)	0.47 \pm 0.02 (0.34-0.66)	2.5 \pm 0.69 (1.1-24)	19 \pm 5.4 (0.27-169)	1.1 \pm 0.017 (0.97-1.3)	13 \pm 0.62 (2.2-19)	10 \pm 1.1 (3.4-36)	20 \pm 5.2 (0-86)	5.4 \pm 1.7 (1-41)	243 \pm 29 (75-589)
BAout	0.52 \pm 0.028 (0.26-0.96)	1.4 \pm 0.15 (0.16-3.3)	0.48 \pm 0.015 (0.31-0.62)	1.8 \pm 0.1 (0.84-3.3)	29 \pm 3.3 (3-73)	1.1 \pm 0.026 (0.82-1.3)	13 \pm 0.45 (7.9-18)	9.6 \pm 0.75 (3.6-28)	28 \pm 8.3 (1-168)	5.5 \pm 2 (2-52)	271 \pm 55 (123-1349)

Table 4.2 Variability in concentrations and excess partial pressure of different C and N species at Black Esk inlet, reservoir and outlet surface waters. Values are reported to two significant figures as mean \pm standard error (minimum-maximum).

Location	CO ₂ (mg C L ⁻¹)	CH ₄ (µg C L ⁻¹)	N ₂ O (µg N L ⁻¹)	epCO ₂	epCH ₄	epN ₂ O	DOC (mg L ⁻¹)	DIC (mg L ⁻¹)	NH ₄ ⁺ (µg L ⁻¹)	NO ₂ ⁻ (µg L ⁻¹)	NO ₃ ⁻ (µg L ⁻¹)
BE1in	0.63±0.023 (0.32-0.95)	0.18±0.038 (0.041-1.5)	0.52±0.016 (0.36-0.77)	2.2±0.088 (1.3-3.4)	3.6±0.8 (0.72-32)	1.2±0.022 (0.93-1.5)	20±1.4 (5.5-41)	9.4±1.3 (0.29-41)	52±8.2 (0-160)	7.2±2.9 (1-72)	138±27 (9-629)
BE2in	0.44±0.012 (0.25-0.72)	0.26±0.056 (0.043-2.2)	0.5±0.012 (0.32-0.66)	1.5±0.051 (0.96-2.8)	5.3±1.1 (0.77-45)	1.1±0.021 (0.77-1.4)	9.3±0.85 (2.3-25)	19±1.6 (2.3-42)	41±12 (0-352)	6.1±4.4 (0-147)	137±23 (24-601)
BE3in	0.42±0.022 (0.14-0.76)	0.37±0.043 (0.061-1.7)	0.5±0.015 (0.29-0.66)	1.4±0.075 (0.57-3)	7.4±0.84 (1.1-32)	1.1±0.023 (0.76-1.4)	8.3±0.84 (2-26)	18±1.4 (2.1-41)	47±15 (0-409)	8.3±5.4 (0-179)	293±39 (45-1022)
BE4in	0.73±0.029 (0.39-1.2)	0.93±0.038 (0.41-1.4)	0.47±0.014 (0.29-0.64)	2.5±0.1 (1.4-4.5)	19±0.81 (9.3-31)	1.1±0.023 (0.75-1.2)	12±1.1 (3.3-33)	14±1.2 (0.93-37)	51±16 (0-475)	4.1±1.2 (0-31)	140±34 (0-976)
BE5in	0.54±0.022 (0.3-1.1)	0.21±0.027 (0.018-0.91)	0.5±0.013 (0.35-0.65)	1.9±0.098 (1.1-4)	4.3±0.56 (0.31-19)	1.1±0.02 (0.85-1.3)	31±1.8 (11-58)	5.8±1.1 (0.14-30)	94±16 (0-326)	6.5±0.75 (1-21)	155±42 (2-1039)
BE1res	1.6±0.23 (0.38-6.7)	6±0.97 (0.97-31)	0.62±0.052 (0.22-2)	5.3±0.64 (1.7-19)	131±22 (18-753)	1.5±0.087 (0.69-3.9)	11±0.6 (2.2-19)	13±0.95 (1.1-33)	67±15 (0-403)	4.8±1.7 (0-56)	216±28 (41-773)
BE2res	0.86±0.086 (0.37-4.1)	7.4±2.1 (0.39-69)	0.56±0.032 (0.28-1.2)	3.1±0.25 (1.3-12)	154±41 (7.1-1236)	1.3±0.051 (0.8-2.3)	12±0.63 (4.5-24)	12±0.94 (1.5-33)	50±12 (0-336)	5.9±3.3 (1-116)	233±22 (72-585)
BE3res	1.1±0.15 (0.37-5.7)	5.2±0.93 (1.1-29)	0.67±0.099 (0.3-3.3)	3.8±0.45 (1.6-17)	114±22 (20-727)	1.6±0.19 (0.83-6.4)	9.7±0.37 (5.1-17)	12±0.84 (1.4-33)	45±8.7 (0-223)	8.7±4 (1-113)	264±41 (9-1178)
BEout	0.5±0.034 (0.13-1.5)	0.57±0.06 (0.041-1.9)	0.48±0.015 (0.31-0.72)	1.8±0.13 (0.39-5.7)	12±1.3 (0.72-44)	1.1±0.022 (0.81-1.3)	9±0.37 (2-13)	13±1.1 (1.7-38)	39±8.1 (0-170)	2.9±0.44 (1-15)	276±23 (86-722)

Table 4.3 Variability in water chemistry (pH, conductivity, dissolved oxygen and temperature) at Baddingsgill and Black Esk inlet, reservoir and outlet surface waters. Values are reported to two significant figures as mean \pm standard error (minimum-maximum).

Location	pH	Conductivity ($\mu\text{S cm}^{-1}$)	DO (%)	Temperature ($^{\circ}\text{C}$)	Location	pH	Conductivity ($\mu\text{S cm}^{-1}$)	DO (%)	Temperature ($^{\circ}\text{C}$)
BA1in	6.7 \pm 0.092 (5.6-7.7)	65 \pm 6.8 (22-174)	58 \pm 3.5 (34-121)	7.4 \pm 0.62 (1.4-14)	BE1in	6.8 \pm 0.1 (4.7-8)	64 \pm 5.6 (18-167)	53 \pm 2.3 (32-101)	8.7 \pm 0.5 (1.9-14)
BA2in	6.8 \pm 0.12 (5.5-8)	84 \pm 8.2 (21-186)	64 \pm 4.7 (25-170)	7.6 \pm 0.66 (2-17)	BE2in	7.3 \pm 0.076 (5.5-8.3)	107 \pm 8.7 (30-290)	67 \pm 2.5 (47-132)	8.8 \pm 0.45 (2.8-15)
BA3in	7.3 \pm 0.098 (6.2-8.1)	105 \pm 8.9 (44-198)	62 \pm 3.8 (36-152)	7.8 \pm 0.6 (2.5-14)	BE3in	7.5 \pm 0.091 (5.3-8.6)	111 \pm 8.6 (32-265)	69 \pm 4.3 (25-146)	9.3 \pm 0.5 (2.9-16)
BA4in	7.4 \pm 0.099 (6.2-8.1)	110 \pm 9.9 (35-214)	61 \pm 4.1 (37-159)	7.8 \pm 0.56 (2.7-14)	BE4in	7.2 \pm 0.083 (5-7.9)	89 \pm 7.2 (28-238)	64 \pm 3.1 (26-135)	9.5 \pm 0.53 (3.4-17)
BA5in	7.5 \pm 0.067 (6.6-8)	183 \pm 17 (55-371)	62 \pm 5.1 (12-176)	7.5 \pm 0.31 (3.1-10)	BE5in	6.9 \pm 0.12 (4.1-7.8)	41 \pm 3 (10-81)	49 \pm 2.1 (24-99)	8.8 \pm 0.53 (1.9-15)
BA1res	7 \pm 0.092 (5.9-7.7)	63 \pm 4.2 (38-117)	55 \pm 4.1 (23-134)	9.7 \pm 0.92 (2.1-18)	BE1res	7.1 \pm 0.077 (5.4-7.9)	83 \pm 6 (20-170)	50 \pm 2.3 (5.2-103)	11 \pm 0.75 (2.4-21)
BA2res	7.3 \pm 0.092 (6.2-8.2)	66 \pm 4.3 (31-136)	51 \pm 3.8 (18-117)	9.3 \pm 0.82 (2.8-16)	BE2res	7 \pm 0.085 (4.7-7.7)	82 \pm 5.1 (38-161)	49 \pm 2.3 (22-120)	11 \pm 0.75 (3.4-20)
BA3res	7.5 \pm 0.068 (6.7-8.1)	63 \pm 5 (30-148)	53 \pm 3.4 (27-124)	9.4 \pm 0.85 (1.9-17)	BE3res	6.9 \pm 0.089 (5.1-8)	81 \pm 5.8 (29-202)	52 \pm 2.6 (1.5-106)	11 \pm 0.77 (0-19)
BAout	7.2 \pm 0.069 (6.1-7.8)	67 \pm 5 (29-147)	58 \pm 4.1 (34-137)	8 \pm 0.57 (2.6-13)	BEout	6.9 \pm 0.087 (5.6-7.9)	70 \pm 4.6 (24-143)	76 \pm 3.5 (22-163)	9.6 \pm 0.61 (2.6-15)

4.3.2 Greenhouse gas evasion from reservoirs and catchment streams

The mean CO₂ evasion from Baddingsgill reservoir was estimated at $0.2 \pm 0.1 \text{ g C m}^{-2} \text{ d}^{-1}$ (range -0.02 to 0.6), which was comparable to Black Esk reservoir at $0.3 \pm 0.09 \text{ g C m}^{-2} \text{ d}^{-1}$ (range 0.04 to 2.1) (Table 4.2). Evasion of CO₂ from the inlets was considerably higher than evasion from the lakes (Figure 4.9). Mean inlet evasion at Baddingsgill was spatially variable across sites and estimated between $0.7 \pm 0.06 \text{ g C m}^{-2} \text{ d}^{-1}$ at BA4in to $19 \pm 1.0 \text{ g C m}^{-2} \text{ d}^{-1}$ at BA5in. Mean Black Esk inlet evasion showed less spatial variability than Baddingsgill and was estimated between 0.4 ± 0.05 at BE2in to $5 \pm 1 \text{ g C m}^{-2} \text{ d}^{-1}$ at BE4in. Estimated CO₂ outlet evasion at Baddingsgill was lower than the inlets and reservoir sites at $0.2 \pm 0.02 \text{ g C m}^{-2} \text{ d}^{-1}$, whereas mean outlet evasion at Black Esk was estimated higher ($5.4 \pm 1.1 \text{ g C m}^{-2} \text{ d}^{-1}$) than evasion from the inlets and reservoir.

Baddingsgill saw similar patterns in estimated CH₄ evasion to CO₂. Mean CH₄ evasion from Baddingsgill reservoir was $0.5 \pm 0.2 \text{ mg C m}^{-2} \text{ d}^{-1}$ (range -0.5 to 64) with mean evasion rates across inlets considerably higher than the reservoir and estimated between $0.8 \pm 0.2 \text{ mg C m}^{-2} \text{ d}^{-1}$ at BA4in to $22 \pm 2.7 \text{ mg C m}^{-2} \text{ d}^{-1}$ at BA5in (Figure 4.9). Mean outlet CH₄ evasion at Baddingsgill was lower than the inlets but higher than the reservoir at $1.0 \pm 0.1 \text{ mg C m}^{-2} \text{ d}^{-1}$. At Black Esk, mean CH₄ evasion ($2.7 \pm 1.0 \text{ mg C m}^{-2} \text{ d}^{-1}$) from the reservoir was higher than Baddingsgill and of a similar order of magnitude to mean evasion into the reservoir via the inlets ($2.9 \pm 0.5 \text{ mg C m}^{-2} \text{ d}^{-1}$). Mean BEout CH₄ evasion was an order of magnitude higher than the inlets and reservoir at $11 \pm 1.4 \text{ mg C m}^{-2} \text{ d}^{-1}$.

Estimated mean N₂O evasion at Baddingsgill reservoir was low at $0.04 \pm 0.03 \text{ mg N m}^{-2} \text{ d}^{-1}$ (range -0.005 to 0.7). Greater spatial N₂O variability occurred at the inlets with mean evasion between $0.2 \pm 0.05 \text{ mg N m}^{-2} \text{ d}^{-1}$ at BA4in to $5.8 \pm 0.4 \text{ mg N m}^{-2} \text{ d}^{-1}$ at BA5in (Figure 4.9). Mean outlet N₂O evasion was lower than both inlets and reservoir locations, estimated at $0.03 \pm 0.009 \text{ mg N m}^{-2} \text{ d}^{-1}$. At Black Esk, estimated mean N₂O evasion from the reservoir sites was $0.08 \pm 0.04 \text{ mg N m}^{-2} \text{ d}^{-1}$ which is lower than mean evasion across all five inlets ($0.4 \pm 0.2 \text{ mg N m}^{-2} \text{ d}^{-1}$) and the outlet ($0.9 \pm 0.2 \text{ mg N m}^{-2} \text{ d}^{-1}$).

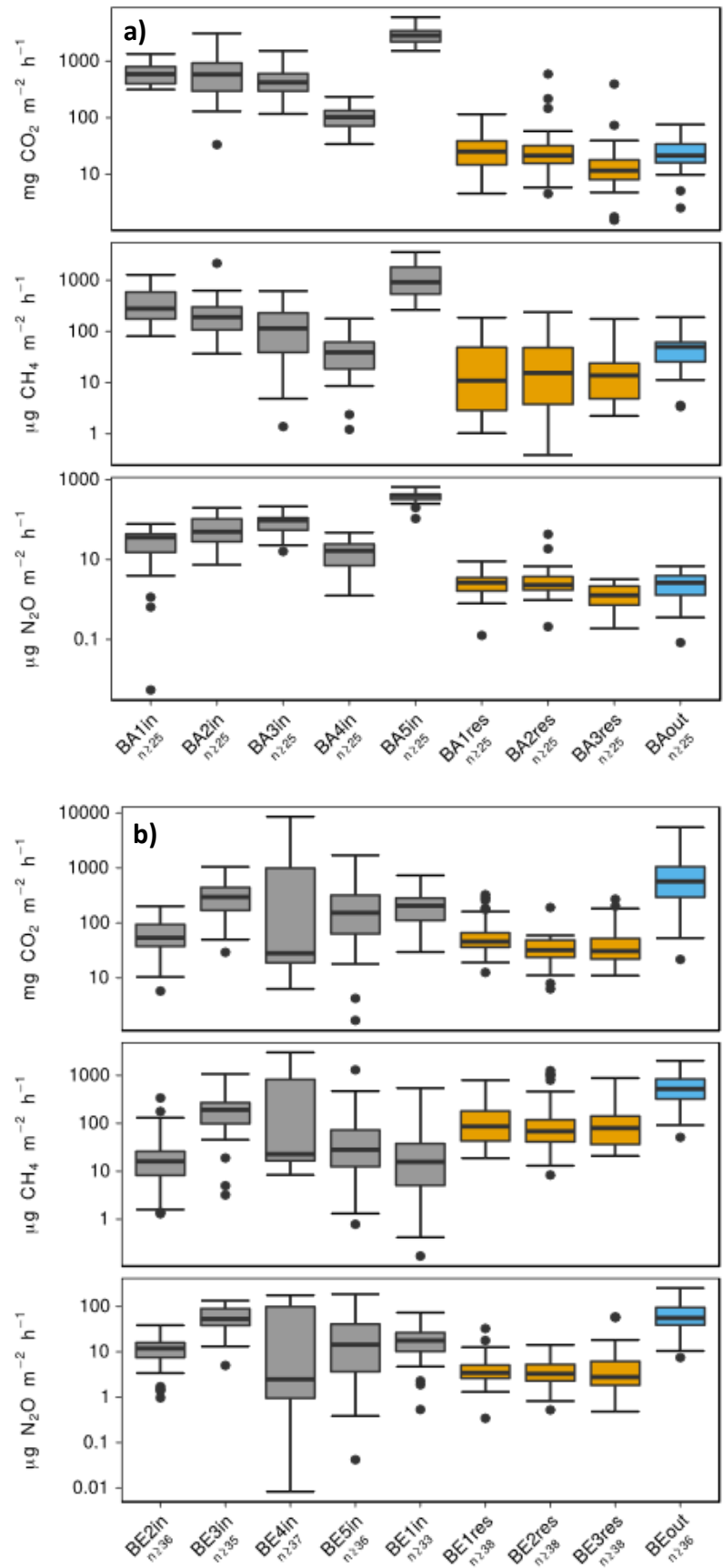


Figure 4.9 Boxplots show GHG evasion across all sampled inlets (gray), the reservoir (orange) and outlet (blue) sampling sites at Baddingsgill (a) and Black Esk (b) reservoirs.

Table 4.4 Mean \pm standard error (range) for stream and open water evasion in the Baddinsgill and Black Esk catchments. Note different units (g) for CO₂ evasion. Mean, minimum and maximum slope and elevation are also shown.

Site	Elevation (m)	Slope (°)	CO ₂ Evasion (g C m ⁻² d ⁻¹)	CH ₄ Evasion (mg C m ⁻² d ⁻¹)	N ₂ O Evasion (mg N m ⁻² d ⁻¹)
BA1in	391 (330-464)	6.7 (0.0-26.7)	4.3 \pm 0.35 (2.1-8.8)	8.5 \pm 1.2 (1.5-23)	0.46 \pm 0.073 (-0.33-1.2)
BA2in	431 (330-566)	8.8 (0.0-38.8)	5.1 \pm 0.81 (0.22-20)	5 \pm 1.2 (0.66-39)	0.83 \pm 0.19 (-1.4-3)
BA3in	428 (330-531)	10.4 (0.0-42.4)	2.9 \pm 0.35 (-0.28-10)	2.5 \pm 0.5 (-0.46-11)	1.2 \pm 0.2 (-1.1-3.3)
BA4in	432 (330-535)	12.1 (0.0-36.2)	0.67 \pm 0.055 (0.22-1.5)	0.79 \pm 0.15 (-0.097-3.2)	0.21 \pm 0.046 (-0.29-0.72)
BA5in	391 (330-469)	10.9 (0.0-31.9)	19 \pm 1.0 (10-39)	22 \pm 2.7 (4.7-64)	5.8 \pm 0.35 (1.6-10)
BA1res	NA	NA	0.18 \pm 0.025 (-0.019-0.58)	0.62 \pm 0.16 (0.018-3.3)	0.038 \pm 0.0076 (-0.033-0.14)
BA2res	NA	NA	0.33 \pm 0.12 (0.03-3.9)	0.6 \pm 0.15 (-0.0028-4.3)	0.067 \pm 0.027 (-0.041-0.66)
BA3res	NA	NA	0.18 \pm 0.079 (0.01-2.6)	0.37 \pm 0.1 (-0.014-3.2)	0.02 \pm 0.0031 (-0.0046-0.049)
BAout	424 (304-566)	8.9 (0.0-42.5)	0.16 \pm 0.022 (-0.04-0.5)	0.99 \pm 0.14 (0.061-3.4)	0.025 \pm 0.0089 (-0.079-0.1)
BE1in	281 (258-300)	3.2 (0.1-10.0)	1.5 \pm 0.17 (0.19-4.8)	0.68 \pm 0.26 (-0.085-9.8)	0.27 \pm 0.041 (-0.17-1.1)
BE2in	295 (248-360)	5.8 (0.0-26.7)	0.43 \pm 0.049 (-0.042-1.3)	0.6 \pm 0.17 (-0.022-6.1)	0.16 \pm 0.028 (-0.25-0.59)
BE3in	348 (250-536)	8.3 (0.0-44.0)	1.7 \pm 0.27 (-1.3-6.9)	4 \pm 0.54 (0.057-19)	0.79 \pm 0.12 (-1.3-2)
BE4in	294 (250-348)	4.3 (0.0-26.1)	5 \pm 1.5 (0.041-56)	7.8 \pm 1.9 (0.15-54)	0.53 \pm 0.16 (-2.2-2.7)
BE5in	296 (251-311)	4.9 (0.02-20.4)	2.1 \pm 0.46 (0.011-11)	1.5 \pm 0.59 (-0.8-24)	0.41 \pm 0.11 (-0.74-2.8)
BE1res	NA	NA	0.48 \pm 0.071 (0.082-2.1)	2.6 \pm 0.44 (0.34-14)	0.079 \pm 0.015 (-0.051-0.5)
BE2res	NA	NA	0.24 \pm 0.027 (0.041-1.2)	3.1 \pm 0.79 (0.15-23)	0.057 \pm 0.0086 (-0.032-0.22)
BE3res	NA	NA	0.32 \pm 0.051 (0.072-1.8)	2.4 \pm 0.48 (0.38-16)	0.095 \pm 0.032 (-0.032-0.9)
BEout	330 (228-536)	7.4 (0.0-56.3)	5.4 \pm 1.1 (-3.3-36)	11 \pm 1.4 (-0.43-36)	0.86 \pm 0.22 (-2.6-3.9)

4.3.3 Annual, catchment-scale and retained fluvial C and N fluxes

Calculated fluvial C and N annual and areal fluxes and associated standard errors for Baddinsgill (2015-2016) and Black Esk (2015-2017) reservoirs are shown in Table 4.5. Loads of all carbon forms were highly variable, likely reflecting between-stream discharge variations. DIC represents the greatest C input to Baddinsgill reservoir in terms of annual C loads at 67 t C yr⁻¹. DIC is 6% greater than DOC input and 94% larger than CO₂ flux. Of the three GHGs, CO₂ represents the largest annual load at 4.1 t C yr⁻¹, compared to 2.1 kg C yr⁻¹ for CH₄ and 2.6 kg N yr⁻¹ for N₂O. In terms of areal mean fluxes at Baddinsgill, DIC also represents the largest input to the reservoir at 5.3 g C m⁻² yr⁻¹, which is 7% greater than DOC and 15.5× greater than CO₂. Carbon dioxide is also the dominant areal GHG flux species at 0.32 g C m⁻² yr⁻¹, whilst fluxes of CH₄ (0.16 mg C m⁻² yr⁻¹) and N₂O (0.26 mg N m⁻² yr⁻¹) more similar. The dominant areal mean N input to Baddinsgill reservoir is NO₃⁻ (105 mg N m⁻² yr⁻¹). The catchment of BA2in (6.4 km²) accounts for 50% of the area of the five measured input streams plus the abstraction inlet not sampled. It drains predominately peaty podzols (54%) and humus-iron podzols (38%) soils. This inlet accounts for between 36-56% of the annual C loads entering the reservoir across the different C species (51% of total annual C load) and between 29-63% across the N species. Measured fluvial C and N species show that they are retained at Baddinsgill reservoir, with only the annual CH₄ load acting as a source (20% increase between inlets and outlet). 57% and 52% of the measured C and N loads entering Baddinsgill were retained within the reservoir (i.e. they did not leave the reservoir via the outlet) and therefore, Baddinsgill was acting as a net C and N sink during the sampling period.

At Black Esk reservoir, the greatest annual C load into the reservoir was DIC at 321 ± 30 t C yr⁻¹, which is 23% greater than DOC input and 96% greater than CO₂. Carbon dioxide was also the largest of the gas flux loads at 13.4 ± 0.36 t C yr⁻¹, compared to 13 ± 0.46 kg C yr⁻¹ for CH₄ and 10.5 ± 0.26 kg N yr⁻¹ for N₂O. The greatest catchment-scale input at Black Esk is also DIC, with an average areal flux of 19.8 ± 2.45 g C m⁻² yr⁻¹, which is 30% greater than DOC and 23× greater than CO₂. Carbon dioxide is the largest input to Black Esk reservoir, with an average areal flux of 0.82 ± 0.04 g C m⁻² yr⁻¹, followed by 0.80 ± 0.04 mg C m⁻² yr⁻¹ of CH₄ and 0.64 ± 0.02 mg N m⁻² yr⁻¹ for N₂O. The dominant N input to Black Esk reservoir is also NO₃⁻ (344 ± 50 mg N m⁻² yr⁻¹). The catchment of BE3in (13.7 km²) accounts for 84% of the area of the five input streams combined and drains predominantly peaty gleys (60%) and peaty podzols (13%). This inlet accounts for 44% to 68% of the annual loads of different C species (60% of total annual C load) and 62-73% of the different N species into the reservoir. 61% and 47% of the measured C and N loads entering Black Esk were retained within the reservoir, with Black Esk acting as a sink

for each C and N species measured (Figure 4.10, Table 4.5). The C and N species entering Baddinsgill reservoir via the inlets is estimated at 134 t C yr^{-1} ($10.6 \text{ g C m}^{-2} \text{ yr}^{-1}$) and 1.6 t N yr^{-1} ($127 \text{ mg N m}^{-2} \text{ yr}^{-1}$) respectively. At Black Esk, total C entering the reservoir via the inlets is estimated at $581 \pm 35 \text{ t C yr}^{-1}$ ($36 \pm 3 \text{ g C m}^{-2} \text{ yr}^{-1}$) and $7.3 \pm 0.6 \text{ t N yr}^{-1}$ ($451 \pm 55 \text{ mg N m}^{-2} \text{ yr}^{-1}$), respectively. A breakdown of total C and N flux for individual streams is presented in Figure 4.10.

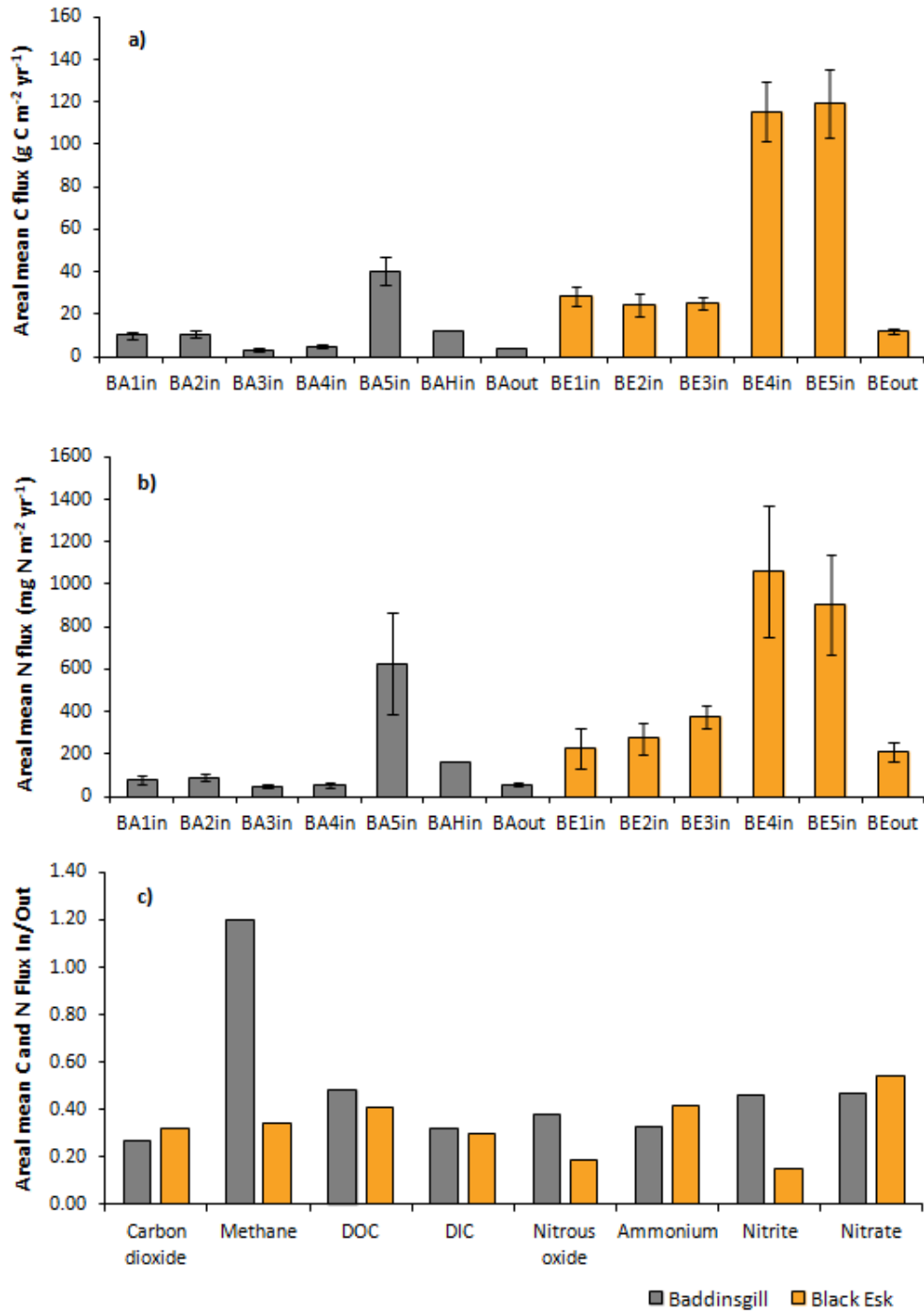


Figure 4.10 Areal mean C flux (CO_2 , CH_4 , DOC, DIC combined) (a) and areal mean N flux (N_2O , NH_4^+ , NO_3^- , NO_2^- combined) for each inlet and outlet at Baddingsgill and Black Esk reservoirs. Error bars represent the minimum and maximum cumulative standard errors for each C or N species and annual discharge calculated from Equations 2.8 and 2.9 in Chapter 2; and b) shows the input-output balance based on areal mean fluxes in (Table 4.5) for all measured C and N species at Baddingsgill and Black Esk reservoirs. Both reservoirs are net sinks as $\text{Out}/\text{In} < 0.9$.

Table 4.5 GHG, DOC and DIC exports during a 1 year sampling period for Baddingsill (2015-2016) and a 2 year period for Black Esk (2015-2017), expressed as annual loads (based on measured discharge from flow rating curves at each location) and areal mean fluxes assuming spatially uniform run-off. Note different units. *Balance +/- = OUT – IN; **Out/In = output divided by the sum of the inputs. Net sinks = Out/In <0.9; approximately balanced = 0.9< Out/In <1.1; net sources = Out/In >1.1.

Site	Annual C and N load (kg/t C or N yr ⁻¹)							
	CO ₂ (kg C yr ⁻¹)	CH ₄ (kg C yr ⁻¹)	DOC (t C yr ⁻¹)	DIC(t C yr ⁻¹)	N ₂ O (kg N yr ⁻¹)	NH ₄ ⁺ (kg N yr ⁻¹)	NO ₂ ⁻ (kg N yr ⁻¹)	NO ₃ ⁻ (kg N yr ⁻¹)
BA1in	304±22	0.35±0.09	4.7±0.83	3±0.73	0.14±0.0054	11±5.4	2.6±1.3	49±16
BA2in	2080±194	0.75±0.11	35±6.8	31±7.4	1.2±0.067	69±21	19±6	490±83
BA3in	50±2.7	0.018±0.0065	1.2±0.24	1.1±0.39	0.065±0.0029	2.2±0.64	0.5±0.5	33±6.7
BA4in	74±2.3	0.039±0.0092	1.6±0.29	2±0.45	0.066±0.0036	6.6±5.1	0.51±0.086	36±5.4
BA5in	148±8.1	0.064±0.028	1.4±0.45	3.2±0.66	0.11±0.0099	19±10	0.3±0.14	55±26
BAHin	1429±NA	0.87±NA	19±NA	27±NA	1±NA	132±NA	7.3±NA	478±NA
IN	4085	2.1	63	67	2.6	240	30	1140
BAOut	1183±87	2.5±0.43	33±1.4	24±3	1.4±0.053	85±25	15±6.1	670±132
Balance +/-	-2902	0.41	-30	-43	-1.2	-155	-15.21	-471
	Sink	Source	Sink	Sink	Sink	Sink	Sink	Sink
Out/In	0.29	1.20	0.52	0.36	0.54	0.35	0.50	0.59
BE1in	177±16	0.045±0.02	4.1±0.57	1.6±0.69	0.047±0.0026	8.6±5.1	0.83±1.2	38±19
BE2in	232±14	0.14±0.071	6.3±0.95	4.3±2.1	0.17±0.0058	19±13	4.4±6.3	97±29
BE3in	6711±417	5.7±0.56	120±21	220±35	6.7±0.31	958±341	125±114	4065±615
BE4in	6013±398	7±0.46	105±17	94±18	3.4±0.16	512±156	43±14	1320±523
BE5in	227±14	0.1±0.029	11±1.6	1.3±0.63	0.14±0.0064	49±14	2.7±0.62	45±21
IN	13,400±355	13±0.46	246±18	321±30	11±0.26	1550±288	176±96	5560±523
BEout	4792±394	5.1±1.2	114±11	108±21	2.2±0.087	418±173	30±6	3418±775
Balance +/-	-8568	-7.885	-132.4	-213.2	-8.257	-1128.6	-145.93	-2147
	Sink	Sink	Sink	Sink	Sink	Sink	Sink	Sink
Out/In	0.36	0.39	0.46	0.34	0.21	0.27	0.17	0.61

Site	Areal mean C and N flux (mg/g C or N m ⁻² yr ⁻¹)							
	CO ₂ (g C m ⁻² yr ⁻¹)	CH ₄ (mg C m ⁻² yr ⁻¹)	DOC (g C m ⁻² yr ⁻¹)	DIC (g C m ⁻² yr ⁻¹)	N ₂ O (mg N m ⁻² yr ⁻¹)	NH ₄ ⁺ (mg N m ⁻² yr ⁻¹)	NO ₂ ⁻ (mg N m ⁻² yr ⁻¹)	NO ₃ ⁻ (mg N m ⁻² yr ⁻¹)
BA1in	0.38±0.028	0.44±0.11	5.9±1	3.8±0.93	0.18±0.0068	14±6.8	3.3±1.7	62±20
BA2in	0.33±0.03	0.12±0.017	5.4±1.1	4.9±1.2	0.19±0.01	11±3.2	3±0.93	77±13
BA3in	0.069±0.0037	0.024±0.009	1.7±0.33	1.6±0.54	0.09±0.004	3±0.88	0.69±0.69	46±9.3
BA4in	0.096±0.003	0.05±0.012	2.1±0.38	2.6±0.59	0.085±0.0047	8.5±6.6	0.67±0.11	46±7
BA5in	1.3±0.068	0.54±0.23	12±3.8	27±5.5	0.94±0.084	161±88	2.5±1.2	461±223
BAHin	0.37±NA	0.23±NA	4.9±NA	6.9±NA	0.26±NA	34±NA	1.9±NA	124±NA
IN	0.32	0.16	5.0	5.3	0.26	18.9	2.4	105
BAOut	0.087±0.0064	0.19±0.032	2.4±0.1	1.7±0.22	0.099±0.0039	6.3±1.8	1.1±0.45	49±9.6
Balance +/-	-0.23	0.03	-2.6	-3.6	-0.16	-13	-1.3	-56
	Sink	Source	Sink	Sink	Sink	Sink	Sink	Sink
Out/In	0.27	1.2	0.48	0.32	0.38	0.33	0.46	0.47
BE1in	0.86±0.078	0.22±0.097	20±2.8	7.6±3.3	0.23±0.013	42±25	4±5.6	183±91
BE2in	0.53±0.031	0.32±0.16	14±2.2	9.8±4.8	0.38±0.013	43±29	10±14	221±67
BE3in	0.49±0.03	0.42±0.041	8.8±1.5	16±2.6	0.49±0.023	70±25	9.1±8.3	296±45
BE4in	3.4±0.23	4±0.26	59±9.7	53±10	1.9±0.091	290±89	24±7.7	748±296
BE5in	2.1±0.13	0.96±0.27	105±15	12±5.9	1.3±0.059	453±128	25±5.8	423±198
IN	0.82±0.04	0.80±0.04	15.2±1.65	19.8±2.45	0.64±0.02	95±23.3	11±7.1	344±50
BEout	0.26±0.021	0.27±0.066	6.2±0.6	5.9±1.1	0.12±0.0047	23±9.4	1.6±0.32	185±42
Balance +/-	-0.56	-0.53	-9	-13.9	-0.52	-72	-9.4	-159
	Sink	Sink	Sink	Sink	Sink	Sink	Sink	Sink
Out/In	0.32	0.34	0.41	0.30	0.19	0.42	0.15	0.54

4.4 Discussion

4.4.1 Spatial and temporal variability in C and N concentrations and fluxes

Carbon

This study found streams and reservoirs in both catchments to be on average, oversaturated with CO₂ which is in agreement with the literature (e.g. Cole et al., 2007; Tranvik et al., 2009). Aquatic systems are frequently assumed to be sources of CO₂ to the atmosphere (e.g. Tranvik et al., 2009) and although the sites in this research mainly behaved as such, there were some occasions of influx. For example, Dolwen reservoir as sampled in Chapter 3, had an overall negative median rate of evasion (-0.06 mg C m⁻² h⁻¹). This suggests that the surface waters can shift from sources to sinks, and that longer term, more frequent monitoring is likely important to pick up such trends.

Lake CO₂ supersaturation is partly caused by organic matter mineralisation by photochemical and microbial processes (Pace and Prairie, 2005) and also by the flushing in of terrestrial organic matter (Sobek et al., 2003). Surface waters associated with peat have repeatedly been shown to be supersaturated in both CO₂ and CH₄ with respect to the atmosphere (e.g. Kling et al., 1991; Cole et al., 1994; Hope et al., 1995) with both reservoir catchments showing high proportions of peaty soil types (peaty gleys, peaty podzols and blanket peats;), promoting input of CO₂-rich drainage water into the streams and reservoirs (Billett et al., 2004).

Lake supersaturation has also been linked to DIC input via inlets (e.g. Molot and Dillon, 1996). Results at both Baddingsgill (67 t C yr⁻¹) and Black Esk (321 ± 30 t C yr⁻¹) showed DIC to be the dominant annual C load into the reservoirs. High proportions of blanket peat are present at both BE1in (100%) and BE2in (65%); however, they do not represent the highest areal DOC flux into the reservoir which occurs at BE4in (59 ± 9.7 g C m⁻² yr⁻¹) and BE5in (105 ± 15 g C m⁻² yr⁻¹) which have peaty gley soil types. Reservoir DOC concentrations at Baddingsgill (median 11.9 mg L⁻¹, range 0.93 to 26 mg L⁻¹) and Black Esk (median 10.6 mg L⁻¹, range 2.2 to 24 mg L⁻¹) were approximately double the median concentration (5.7 mg L⁻¹) reported by Sobek et al. (2007) from an analysis of 7,500 lakes around the world. In the global study, only 4.2% of lakes had DOC concentrations between 20 and 40 mg L⁻¹, suggesting both reservoirs have high DOC concentrations. Both reservoirs also correspond to being net heterotrophic systems as DOC is > 5 mg L⁻¹ (e.g. Prairie et al., 2002) which is also reflected in the high input DOC fluxes containing allochthonous organic matter (Santana et al., 2015). At Baddingsgill, managed burning is practiced (albeit not during the sampling period) to enhance moorland productivity and forage quality, and promote nutritious new growth to improve grazing for game and

livestock (Webb, 1998). Managed burning has been found to contribute to other C losses such as increase DOC production, altering C in nearby aquatic ecosystems (Ramchunde et al., 2013). The burned moorland and limited vegetation in parts of the catchment could enhance run-off into the streams and reservoirs, affecting the loads.

Results showed spatial variability within the reservoirs across the three sampling locations at both Baddinsgill and Black Esk. Estimated CO₂ evasion at Black Esk reservoir was higher than Baddinsgill. Both reservoirs are old, however the capacity at Black Esk was increased in 2014, resulting in newly flooded land and the decomposition of submerged fresh and labile organic matter (Barros et al., 2011). This is likely the cause of higher CO₂ at BE1res where decaying trees were left behind in the reservoir. At Baddinsgill reservoir, BA2res showed considerably higher CO₂ than the other two locations. This site is located in an area which was more prone to fluctuating water levels leaving sediment exposed, which has been linked to higher CO₂ (Weise et al., 2016).

Results showed both reservoirs to be on average, oversaturated in CH₄ which could be a result of CH₄ production in sediments as it is considered a key emission driver in lakes (Bastviken et al., 2008). Results also showed a spatial gradient within reservoirs, with lower CH₄ concentrations nearer deeper waters close to the dam and is a pattern observed in other studies (e.g. Paranaíba et al., 2018). The dam end also had fewer inflows, and the literature suggests inflow areas show higher CH₄ and linked to the slowing down of water and greater sediment deposition, where degradation of fluvial organic matter via methanogenesis can increase CH₄ production (Sobek et al., 2012). Catchment imported CH₄ may have also contributed to the observed spatial patterns (Mendonça et al., 2012; Paranaíba et al., 2018).

Results also showed seasonal variability in CH₄ concentrations within both reservoirs, with higher concentrations in summer and early autumn which coincide with periods of low rainfall (Figure 4.6). For example, elevated concentrations are seen in both reservoirs during August and October 2015, which was also period of higher temperatures and lower water levels, leaving more sediment exposed. The likely peaty rich reservoir sediments, combined with increased temperatures and fluctuating water levels may have caused the observed increases in CH₄ production within the reservoirs (Beaulieu et al., 2017; Tranvik et al., 2009), which would also help explain why such increases were not also observed at the inlets. The higher range in CH₄ concentrations observed at Black Esk compared to Baddinsgill was also likely attributed to the decomposition of fresh labile organic matter (Barros et al., 2011) from the water volume increase. In addition, hydrological patterns can also affect terrestrial primary

production, influencing C loading in lakes (Tranvik et al., 2009). Black Esk catchment is largely a coniferous forestry plantation which undergoes both felling and re-planting with such activities also attributed to high DOC loads (Creed et al., 2008; Grieve, 1994).

Nitrogen

Nitrate was the dominant N input to both Baddingsill and Black Esk reservoirs, with Black Esk having 3.3× the areal mean flux compared to Baddingsill, likely reflecting the high percentage of coniferous forestry within the Black Esk catchment. Nitrate has been reported in other studies as the dominant soluble N form in surface waters (Neal and Robson, 2000).

Highest mean NO_3^- at Black Esk was seen BE3in which had felling in both 2015 and 2016 within the catchment which has also been used to explain spatial variability in other studies (e.g. Chapman et al., 2001). The stream NO_3^- concentrations in this study were comparable to mean concentrations of less than 1 mg L^{-1} in Scottish upland rivers (Betton et al., 1991) where there is less agricultural activities. Lowest NO_3^- in the Black Esk catchment was at BE1in and BE2in where both sub-catchments have high percentages of blanket peat, which has also been observed in other studies (e.g. Chapman et al., 2001). As observed in other UK upland stream studies, ammonium was present in very small concentrations (Reynolds and Edwards, 1995). Similarly, low NO_2^- concentrations were also observed by Baulch et al. (2011) in Canadian streams.

Nitrogen in the gaseous form as N_2O is derived from allochthonous sources from ground and soil waters, and from in-stream sediment production (Schade et al., 2016). BA5in has both the highest N_2O and NO_3^- concentrations in the catchment, suggesting the additional NO_3^- are being reduced to N_2O through denitrification (Baulch et al., 2011) but to confirm the source of N_2O production in this area, isotopic analysis would need to be performed. Possible causes are the presence of sheep, as observed during field sampling (e.g. McDowell et al., 2009), and the small size of the stream (~60 cm wide) leading to less dilution (Beaulieu et al., 2008). N_2O concentrations in both catchment streams (means 0.47 to $0.78 \mu\text{g N L}^{-1}$) were towards the lower end of the range (means 0.42 to $2.17 \mu\text{g N L}^{-1}$) of USA streams in Beaulieu et al. (2008). The larger range of means in the USA streams might be explained by greater prevalence of agriculture in their catchments. Baddingsill and Black Esk reservoir N_2O concentrations ranged from 0.22 to $3.3 \mu\text{g N L}^{-1}$ and indicated oversaturation. These results are consistent with reports from a variety of lakes and reservoirs. For example, Mengis et al. (1997) found mean surface saturations ranging from 101 to 265% across 15 Swiss lakes, with 11 of those falling within the same range as Baddingsill and Black Esk (110 to 160%). These N_2O results were

comparable to measurements of Ohio (USA) river basin reservoirs (Beaulieu et al., 2015). Although broadly oversaturated, some measurements from sampling points on streams and reservoirs at both reservoirs showed periods of undersaturation (21% of measurements at Baddingsgill, 22% at Black Esk). Other studies have observed both under- and oversaturation in the same system. Despite showing oversaturation overall, streams and reservoirs at Baddingsgill (21% of measurements) and Black Esk (22%) also showed periods of undersaturation which has also been observed in other stream and river studies, even those with high dissolved inorganic N loads (e.g. Beaulieu et al., 2008; Rajkumar et al., 2008). Undersaturation typically reflects denitrifiers ability to use free N_2O as an electron acceptor, and has been associated with low NO_3^- concentrations, low flows and low oxygen (e.g. Rajkumar et al., 2008; Baulch et al., 2011).

4.4.2 Reservoir balance and comparison to other studies

The results from this study show that both Baddingsgill and Black Esk reservoirs are net fluvial carbon and nitrogen sinks as the amounts entering the reservoirs exceeded total output. Results showed a significant portion of C and N load being retained within both reservoirs (the sole exception being CH_4 at Baddingsgill). Previous budget studies in temperate lakes using a mass balance approach have shown lakes to act as both carbon sources (Carpenter et al., 1983) and carbon sinks (Yang et al., 2008). Results here highlight that both reservoirs are active sites of carbon and nitrogen cycling. Net sinks can imply that a large proportion of the C is either being retained in the water column, or being buried within the reservoir sediments (e.g. Molot and Dillon, 1996; Bastviken et al., 2011). Average C burial rates in lakes are estimated to be between 4.5 and 14 $g\ C\ m^{-2}\ yr^{-1}$ (Cole et al., 2007; Tranvik et al., 2009), with higher burial seen in impoundments (average 100 $g\ C\ m^{-2}\ yr^{-1}$, (Downing et al., 2008). DOC can be transformed to POC in the water column and potentially sequestered in lake sediments (Tranvik et al., 2009). Light-driven C removal processes could also be important within the reservoirs e.g. photodegradation and flocculation, increased photo-modified organic matter and autotrophic production (Moran and Zepp, 1997). Further investigations into the fate of organic carbon within the reservoirs are required.

Similarly, Stimson et al. (2017) found Kinder reservoir in a degraded peat catchment in England, UK to be net fluvial carbon sinks for DOC, DIC and particulate organic carbon (POC). POC was found to be the greatest C input to the reservoir (93% greater than DOC) but this species is not sampled at Baddingsgill or Black Esk, with results from Kinder suggesting this to be an important factor in peatland reservoir budgets. Annual budgets over a two-year period

estimated DOC input flux at 35 and 89 t C yr⁻¹ being inputted, and 40 and 72 t C yr⁻¹ being outputted from the reservoir. Kinder reservoir is showing similar annual DOC loads to Baddingsgill at 63 t C yr⁻¹ (7.4 g C m⁻² yr⁻¹ over a catchment area of 8.5 km², 50% higher than Baddingsgill) inputted and 33 t C yr⁻¹ (3.9 g C m⁻² yr⁻¹, 63% higher than Baddingsgill) outputted but with greater in-reservoir retention of DOC. Evans et al. (2017) found 48 out of 82 lakes and reservoirs were annual net DOC sinks which was strongly influenced by water residence time. Both Baddingsgill (classified as mesotrophic) and Black Esk (oligotrophic) were also included in this study. For Baddingsgill, Evans et al. (2017) estimated DOC_{in} fluxes at 8.14 g C m⁻² yr⁻¹ and DOC_{out} fluxes as 9.38 g C m⁻² yr⁻¹, making Baddingsgill a net DOC source (Out/In = 1.15). At Black Esk reservoir, estimated DOC_{in} fluxes were 9.25 g C m⁻² yr⁻¹ and DOC_{out} fluxes were 7.30 g C m⁻² yr⁻¹, making Black Esk a net DOC sink (Out/In = 0.79). Black Esk flux estimates were similar to the results presented in this chapter and were also found to be a net DOC sink; however, Baddingsgill DOC_{out} was 3× higher, which resulted in the reservoir being an overall net DOC source. The differences in results could potentially be explained by temporal variability of the different sampling years between the two studies and field data was not available for all the inlets included in this chapter, resulting in the study assuming a constant DOC flux per unit area.

Aquatic CO₂ evasion from headwater streams was also found by Kokic et al. (2015) to be the dominant total catchment C loss in a Swedish lake catchment which they mostly attributed to higher gas transfer velocities of streams compared to lakes. Results also supports findings by Raymond et al. (2013) in which rivers and streams were found to evade greater CO₂ (6 times) than reservoirs and lakes. Mean CO₂ evasion from Baddingsgill (200 mg C m⁻² d⁻¹) and Black Esk reservoirs (300 mg C m⁻² d⁻¹) were comparable to mean CO₂ from a global study of hydroelectric temperate reservoirs (~250 mg C m⁻² d⁻¹) but much lower than Lokka reservoir with a peatland catchment which ranged from 1070 to 1972 mg C m⁻² d⁻¹ (Jari. T Huttunen et al., 2002).

DOC export from Baddingsgill outlet (2.4 g C m⁻² yr⁻¹) was lower than DOC export from Lake Gäddejärn in Sweden (6.5 g C m⁻² yr⁻¹) (Jovana. Kokic et al., 2015) but Black Esk was more comparable (6.2 g C m⁻² yr⁻¹). DIC export from the Swedish lake (0.4 g C m⁻² yr⁻¹) was much lower than export from both Baddingsgill (1.7 g C m⁻² yr⁻¹) and Black Esk (6.2 g C m⁻² yr⁻¹). Total C export per inlet at Baddingsgill ranged from 3.4 to 40 g C m⁻² yr⁻¹, comparable to (Leach et al., 2016) where total C exports ranged from 5.9 to 18.1 g C m⁻² yr⁻¹ from streams draining a boreal peatland catchment in Northern Sweden. However, this is much smaller than the total C export range estimated at Black Esk inlets (24 to 119 g C m⁻² yr⁻¹) which is more similar to other

peatland draining streams in the UK (e.g. Billett et al., 2004; Dinsmore et al., 2010) however, in those studies, similar proportions of DOC, dissolved CO₂ and POC are seen, whereas the GHG species in at Black Esk and Baddinsgill are much lower proportion wise.

4.4.3 Limits to calculations of the evasion and export estimates

The GHG fluxes from the inlet and outlet streams, k (gas transfer velocity) were estimated following Eq. 5 in Raymond et al. (2012). In streams, water-air interface turbulence is produced by stream bed shear stresses, where k is typically modelled using channel slope, water depth and velocity (Raymond et al., 2012). This approach has also been widely used in other studies (e.g. Schade et al., 2016) when field measurements are limited. Field based gas tracer methods e.g. using SF₆ were not permitted in this research due to sampling restrictions relating to the reservoir being used for public drinking water supply. Aquatic GHG concentrations are generally well measured; however, the accuracy of the flux estimation is dependent on the k values. A wide range in k values have been estimated in the literature (e.g. Borges et al., 2004; Raymond et al., 2012) due to differences in techniques, tracers and governing processes. For example, Wallin et al. (2018) identified differences in the k estimate from Raymond et al. (2012) and other catchment studies e.g. Natchimuthu et al. (2017) at low velocities and zero to low elevations. Many of the Baddinsgill and Black Esk inlet streams were at times slow flowing, as can be reflected by the low Q values in Appendix 1, which could lead to an under- or overestimation of GHG fluxes. Similarly, storm events resulting in high turbulence and water velocity were not taken into account in some of the larger inlets in this study due health and safety restrictions, which could further bias estimations. There is a need for k measurements in the catchments, which could increase the accuracy of stream GHG emissions in this study.

With regards to the unsampled inlet at Baddinsgill, if the export estimate is removed from the balance, the reservoir continues to act as a sink for areal fluxes. As abstraction from the inlet varied throughout the year depending on flow, it was not possible to quantify this input accurately as information was not available at the time of write up, but future work involving reservoir export should consider the possibility of inputs from outside the true reservoir catchment.

4.5 Conclusions

This study showed pronounced spatial variability in GHG concentrations and fluxes within both catchment inlets, and within the reservoir bodies. By quantifying inlet, reservoir and outlet C and N, this study adds to an increasing knowledge base that small streams are important in

catchment scale budgets (e.g. Cole et al., 2007; Bastviken et al., 2011) but the magnitude and source of GHG emissions is still unclear (Raymond et al., 2013). It also highlights the importance of monitoring inlet streams and not just the lake or reservoir outlet as results highlighted the high variability in export between spatially similar streams. Evasion estimates also showed that C and N loss from streams is higher than reservoirs, which again highlight the importance of streams in the aquatic continuum. The reservoirs had high levels of DIC or DOC influx, with CO₂ being the dominant GHG component and NO₃⁻ being the dominant N species. Both reservoirs were found to be net sinks of fluvial carbon and nitrogen (and of each species, with the exception of CH₄ at Baddinsgill). Increasingly large sums of money are being invested by water companies in catchment management programmes e.g. peatland restoration, with the expectation water quality will be improved and colour and DOC reduced at the water treatment works. To fully understand the sources and fate of C and N within the reservoirs, more comprehensive measurements of C and N processing are required e.g. through isotopic analysis and incorporation of C and N burial rates. Nitrogen loading to aquatic systems is increasing (Beaulieu et al., 2011) which suggests N fluxes from inland waters may become more important, and N₂O a more substantial contributor.

5 The importance of water level drawdown on greenhouse gas emissions from a temperate UK reservoir

5.1 Introduction

Increasing evidence has demonstrated the active role of inland waters in the global carbon (C) cycle, and their capacity to emit substantial amounts of carbon dioxide (CO₂) and methane (CH₄) to the atmosphere (e.g. Cole et al., 2007, Bastviken et al., 2011, Barros et al., 2011). Aquatic systems are also considered to be a source of nitrous oxide (N₂O) emission, but estimates are mainly from rivers and streams (Beaulieu et al., 2008, Venkiteswaran et al., 2014) with fewer studies on reservoir N₂O emissions (Guérin et al., 2008, Beaulieu et al., 2015). A recent global synthesis of global GHG emissions from reservoirs (Deemer et al., 2016) estimate a total flux of 13.3 Tg CH₄-C yr⁻¹, 36.8 Tg CO₂-C yr⁻¹ and 0.03 Tg N₂O-N yr⁻¹. Where emissions occur in lakes or rivers that have not been strongly modified by human activities, they can be considered part of the natural carbon and nitrogen cycle. However, where the hydrology and/or biogeochemistry of drainage networks have been modified by human activities, any subsequent changes in GHG emissions may be considered anthropogenic. In the specific case of constructed reservoirs, this emission may be considerable, due to the mineralisation of soil and biomass organic matter within the reservoir, and creation of hotspots of CH₄ production and transmission to the atmosphere. This has led to the development of methods by the Intergovernmental Panel on Climate Change (IPCC) to account for GHG emissions from 'Flooded Lands'. These emissions have the potential to make a significant contribution to both national and global GHG emissions (Barros et al., 2011, Prairie et al., 2017).

Drawdown (the withdrawal or reduction in water volume during dry periods or due to reservoir maintenance or management) affects reservoir thermal structure, light environment and the area of exposed sediments (Straskraba et al., 1993). Fluctuations in water level also change the hydrostatic head within the water column. Artificial water level fluctuation is a key physical process that distinguishes many reservoirs from lakes in terms of amplitude, frequency and rate of change (Furey et al., 2004; Hirsch et al., 2017). In temperate and boreal regions, an annual water level drawdown in autumn and winter and subsequent spring refill are a common management practice (Carmignani and Roy, 2017; Li and Zhang, 2014). In reservoirs used for aquaculture, drawdown may also be undertaken to help remove undesired fish species and enhance water clarity (Verrill and Berry, 1995). Other common reasons are to

increase flood storage capacity, generate hydropower, or to perform dam maintenance (Harrison et al., 2017; Hayes et al., 2017).

Such water level changes affect biogeochemical processes and their interactions in the open water zone, with even greater effects in nearshore littoral areas (Furey et al., 2004, Yang et al., 2015, Li et al., 2016). The magnitude and frequency of drawdown can determine littoral vegetation presence or absence (Rodhe, 1964), affect the supply of nutrients (i.e. organic and inorganic material from run-off and erosion) and influence sediment structure and distribution (Baxter, 1977; Fahre and Patau-Albertini, 1986). Fluctuating water levels influence GHG release to the atmosphere as the sediment's oxic and anoxic conditions are altered (Billings et al., 1982; Moore and Knowles, 1989). Rewetting and desiccation of sediments can affect microbial community structure, impacting C and N turnover and GHG fluxes (Fromin et al., 2010; Koschorreck and Darwich, 2003; Schimel, 2007; Weise et al., 2016)

Supersaturation of CO₂ in aquatic systems occurs primarily from two main pathways (Prairie et al., 2017); a) the input of CO₂-rich soil water from the surrounding catchment, or b) in-situ degradation of DOC or POC in bottom lake sediments or in the water column by photochemical and microbial processes (Pace and Prairie, 2005). CO₂ emission can also be produced when CH₄ is oxidised to CO₂ by methanotrophs (Guérin and Abril, 2007).

In lakes and reservoirs, CH₄ is primarily produced in anoxic sediments and can be released to the atmosphere via diffusion, ebullition (bubbling) or, plant-mediated transport when emergent vegetation is present (Chanton and Whiting, 1995, Bastviken et al., 2004, Harrison et al., 2017). CH₄ has a 34 times higher global warming potential than CO₂ per mass on a 100-year timescale (IPCC, 2014) meaning a shift from an aerobic to anaerobic degradation pathway in sediments may increase the climatic impact of aquatic systems (Maeck et al., 2013). Sediment CH₄ is produced via anaerobic microbial decomposition of organic matter, where production rates depend on organic C availability, redox conditions, and temperature (Sobek et al., 2012). Under constant hydrostatic pressure, gas produced via microbial activity dissolves in sediment pore-waters, until the collective partial pressure of the dissolved gases surpass the hydrostatic pressure, causing bubble formation (Chanton and Whiting, 1995). Reduced hydrostatic pressure when water level falls can lower compressive stress on sediments, therefore increasing bubble formation and release (Beaulieu et al., 2017; Keller and Stallard, 1994).

In both soil and aquatic systems, denitrification and nitrification are the key N₂O producing pathways (Firestone and Davidson, 1989; Thuss et al., 2014). In surface waters, nitrification is the main N₂O producing pathway, but NH₄⁺ availability can be low, even in eutrophic systems,

due to NH_4^+ absorption by phytoplankton (Tönno et al., 2005). The main controls on denitrification rates include oxygen levels, mineral N and C availability, pH and temperature (Knowles, 1982), while controls on nitrification rates include NH_4^+ , pH, organic C and temperature (Bianchi et al., 1999; Strauss et al., 2004).

A growing number of studies report GHG emissions from the reservoir drawdown zone (Chen et al., 2009; Deshmukh et al., 2016, 2018; Harrison et al., 2017; Li et al., 2016b; Oelbermann and Schiff, 2010; Yang et al., 2012, 2015). These measurements have shown considerable variation, ranging from small to significant CH_4 sources (Chen et al., 2009, Yang et al., 2012, Serça et al., 2016) and, in some cases, even CH_4 sinks (Li et al., 2016). High CO_2 emissions (on the order of $\text{g CO}_2 \text{ m}^{-2} \text{ d}^{-1}$) have been reported from dry sediments in rivers, reservoirs and ponds (Gómez-Gener et al., 2016, 2015; Hyojin et al., 2016; Obrador et al., 2018). Compared to CO_2 and CH_4 , very few studies have measured N_2O emissions from drawdown zones and most of this research is focused on the Three Gorges Reservoir in China. An example of such a study on the Three Gorges Reservoir is by Li et al. (2016) where a mean N_2O sediment flux of $3.6 \text{ mg m}^{-2} \text{ d}^{-2}$ was estimated. Despite large knowledge gaps due to limited data, littoral zones are generally considered 'hot spots' for GHG emissions (Chen et al., 2009, Yang et al., 2015, Deshmukh et al., 2018).

Changes in precipitation patterns are expected due to global warming, affecting both the magnitude and frequency of extreme events like floods and droughts (Bolpagni et al., 2017; Reichstein et al., 2013). Consequently, many European lakes will be subject to higher hydrological variability in their littoral zones which in turn is likely to affect physicochemical characteristics, sediment microbial composition and functioning, the length of desiccation periods, and the use of allochthonous and autochthonous C sources creating changes to biogeochemical cycles (Reichstein et al., 2013; Weise et al., 2016; Zanchettin et al., 2008; Zohary and Ostrovsky, 2011). Due to the potential of inland waters to store and release C, their response to hydrological changes is important, but few studies investigate such impacts (Cole et al., 2007, Tranvik et al., 2009, Aufdenkampe et al., 2011, Hyojin et al., 2016). To address these knowledge gaps, this study aims to quantify CO_2 , CH_4 and N_2O net fluxes across a full year, quantifying the relative importance of key time periods such as water level drawdown, sediment exposure and rewetting at Waltersmuir reservoir, in central Scotland, UK.

5.2 Materials and Methods

5.2.1 Site description

The study was conducted from January 2016 to January 2017 at Waltersmuir reservoir, Central Scotland (56° 10' 89" N, 03° 55' 19" W; Figure 5.1). The climate is temperate maritime, with a mean annual rainfall of 1019 mm, mean monthly maximum air temperature of 12.9°C and mean monthly minimum temperature of 5.6°C for the period 1981-2010 (Met Office, 2015). The reservoir is situated in a sheltered area surrounded by trees which contributes to low wind speeds and wave height. Daily mean, maximum and minimum air temperature and rainfall were obtained from a combination of two nearby weather stations, as complete data for the study period was not available from either one (Met Office stations 62080 and 15486, located 3.4 km south east and 8.4 km south west of the study location, respectively; see Met Office, 2014). The closer station (62080) only began recording on 1st April 2016 so did not cover the start of the sampling period but was used to fill data gaps in the period April-Dec 2016 from station 15486. Total rainfall for the 13-month study period was 1327 mm.

At full capacity, Waltersmuir reservoir has a surface area of 32,600 m², a maximum depth of 12 m, mean depth 4.4 m, and storage capacity of 123,900 m³ (UK Lakes Portal and Pers.Comm, Waltersmuir management). The reservoir catchment is 1169 ha with an elevation range of 171 to 460 m above sea level. Waltersmuir reservoir has one outlet and one main inlet, the Wharry Burn, which is 10.3 km in length, and is classified as having 'high' ecological status according to the Water Framework Directive (Nutt and Perfect, 2011). The catchment land cover consists of rough grazing (68%) for sheep, alongside improved grassland (19%), coniferous (9%) and broadleaf (1%) woodlands, moorland (2%) and arable (1%). The underlying geology of Waltersmuir catchment is predominantly Devonian Old Red Sandstone, with basaltic lavas and overlain with Quaternary glaciofluvial and river terrace deposits (clay, silt, sand and gravel). The surface topography is dominated by sandy and clay-loam brown earth and non-calcareous gley soils, with peaty gleyed podzols and blanket peats in the headwaters of the Wharry Burn.

Waltersmuir was constructed as a drinking water reservoir in the 1950s, and since 1993 has been used as an aquaculture holding facility for Atlantic salmon (*Salmo salar*) smolt and is owned and operated by Howietoun Fishery, University of Stirling. Since 1998, Waltersmuir reservoir has been subject to an annual drawdown event in order to allow the site to fallow, which is not unique to Scottish aquaculture, benefitting water quality and the health of the fish (Waltersmuir management, pers. comm.). It typically takes about 2 weeks for the water levels to drop and 4-6 weeks to refill. However, during 2016 the reservoir was drained for an

extended period of 11 weeks to allow maintenance work on the dam (Figure 5.1). Despite it being used as an aquaculture facility, this extended period of drawdown provided a unique opportunity to be able to conduct in-field sediment sampling in a safe and controlled environment, allowing increased understanding of sediment fluxes and the effects of extreme water level changes to be quantified. The reservoir is drained from the bottom outlet valve on the dam, which is also used to maintain water levels during periods of high inflows. The reservoir can naturally refill within a single day when rainfall is high, as was the case on two occasions during this study. The reservoir cannot be completely emptied due to minimum flow regulations so there was always a pooling of water around the dam area.

During the sampling period ~160,000 smolt aged 0+ to 1+ were stocked. The reservoir is typically stocked by the last week in August and harvested by mid to end of March. The fish weigh ~25 g when put into the reservoir in August and are about 60 to 70 g when removed in March, which equates to ~4 tonnes of fish being stocked during August and approximately 9.6 to 11.2 tonnes being removed in March 2017). Fish were solely fed on a commercial diet provided by EWOS Ltd (Westfield, Scotland). The feed had an average content of 1.4% phosphorous, 7.9% nitrogen and 45.2% carbon and approximately 12 tonnes were used during the stocking period, August-April, which was administered by an automatic release with several releases occurring daily during daylight hours into the reservoir throughout this period.

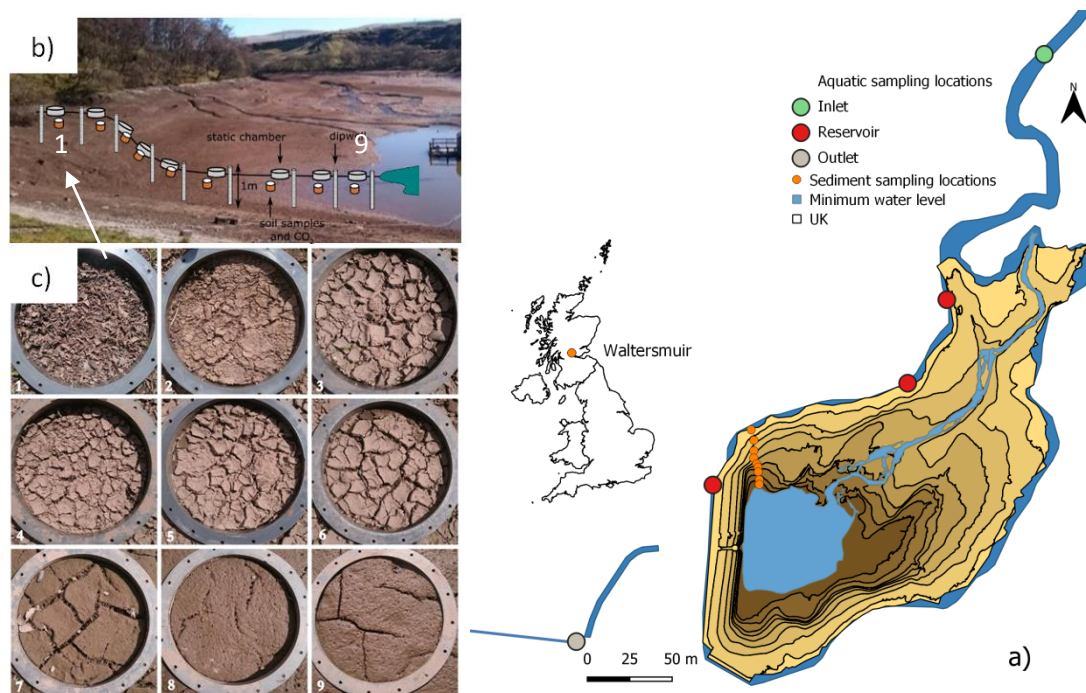


Figure 5.1 a) Location of the Waltersmuir catchment and sampling locations on the digital Elevation Model (DEM) derived from UAV survey. b) Photograph taken in April 2016 during

maximum drawdown, illustrating transect location, with chambers 1 and 9 highlighted. c) Photographs of chambers one (highest elevation) to nine (lowest elevation) illustrating desiccated surface cracks in the sediment and visibly higher moisture levels in chambers seven to nine.

5.2.2 Measurement of dissolved GHG concentrations and aquatic chemistry parameters

Water samples were collected fortnightly from January 2016 to January 2017, but increased to weekly during the 11-week drawdown period (11th April – 14th July 2016). The drawdown period throughout this chapter refers to both time of active water level fluctuations and the period the water is low as a result. Surface water, headspace (including replicate) and air samples were collected from five locations, the main inlet, the outlet downstream of the dam and three locations from the reservoir (Figure 5.1).

At each location, two water samples were collected at ~10 cm depth below the water surface using a 60 ml syringe and filtered in the field using 0.45 µm syringe-driven filters (Whatman®). Water samples were stored in 30 ml bottles, which were rinsed with a small aliquot of the filtered sample and kept cool and dark in a cool box whilst in the field. On return (typically less than 5 hours), one filtered water sample was placed immediately in the refrigerator at 4-5 °C for DOC and DIC analysis within two weeks of collection, whilst the other filtered sample was placed in the freezer at -18 to -21 °C for analysis of ammonium, nitrite and nitrate (NH_4^+ , NO_2^- & NO_3^-) at a later date. At the same time as water sampling, dissolved oxygen (DO), pH, temperature and electrical conductivity (EC) were measured in situ using handheld multi-meters (Hanna Instruments HI-9145, HI-9124, HI-0933).

The refrigerated sample was warmed to room temperature and analysed for DOC and DIC on a PPM LabTOC (Pollution & Process Monitoring, UK) connected to a PPM PSA auto sampler. The LabTOC instrument converts organic carbon to CO_2 via UV-persulphate oxidation, then measures CO_2 using an infrared detector. Samples were mixed with a solution of 5% sodium persulphate and 5% orthophosphoric acid in deionised water. The detection range was 0.1 to 4000 mg l^{-1} and concentrations were calculated based on a three-point calibration curve with a maximum of 50 mg l^{-1} , where all concentrations fell below this level. Ammonium, NO_2^- and NO_3^- concentrations were analysed using a Seal Analytical AQ2 discrete analyser (Methods: EPA 350.1 v2 and EPA 353.2 v2 (USEPA, 1993)). Further quality control within each analytical batch, standards and deionised water samples were added at the start and end of each run to both the DOC, DIC and nitrogen analyses.

Dissolved aquatic CO₂, CH₄ and N₂O concentrations were collected using the headspace technique (Kling et al., 1991, Dinsmore et al., 2010), where a 40 ml water sample, collected from ~10 cm water depth, was equilibrated with 20 ml headspace of ambient air in a 60 ml syringe at water temperature by shaking vigorously underwater for one minute. The equilibrated 20 ml headspace was then injected into a 12 ml pre-evacuated gas-tight borosilicate Exetainer® (Labco, Lampeter, UK). Air samples were also collected at ~1.5 m height at each sampling point. These samples were analysed on a 7890B gas chromatograph (Agilent Technologies) fitted with a flame ionization detector (FID) for CH₄ and attached methaniser for CO₂, and a micro electron capture detector (μECD) for N₂O. These detectors were set up in parallel allowing simultaneous analysis of all three GHGs. Peak detection and integration was performed using the OpenLAB CDS ChemStation software (Agilent Technologies). Dissolved concentrations of CO₂, CH₄ and N₂O in the water column were calculated from the headspace and ambient concentrations using Henry's Law (e.g. Hope et al., 1995). For these calculations, air temperature and barometric pressure were required from each sampling location and were obtained using a hand-held 'Weather Meter' (Kestrel 2500, accuracy 3% of reading) at 1 m above the water surface.

5.2.3 Measurements of sediment GHG fluxes and chemical and physical properties

Fluxes of N₂O, CH₄ and CO₂ were made weekly from the exposed reservoir sediments using the static chamber method (Clayton et al., 1994; Cowan et al., 2016). Nine chambers were positioned along a transect from the middle of the reservoir to the bank edge, covering areas of different slope and sediment moisture (Figure 5.1). The chamber lid consisted of a cylindrical polyvinyl chloride (PVC) plastic pipe of 48 cm inner diameter and 22 cm height with closed cell neoprene sponge strip attached to the underside. Lids were fitted with a pressure compensation plug to maintain ambient pressure in the chambers during and after sample removal and a sample port consisting of a silicon tube (10 cm long, diameter 6 mm) attached to a luer lock. For flux measurements, the lids were placed onto circular stainless steel collar bases and fastened with 4 clips. The collars were inserted approximately 5 cm into the sediment two days before the first sampling event and were left in situ for the remainder of the study period. Wooden pallets were used to reach three chambers positioned into very soft sediment, in order to avoid the inadvertent release of gases during flux measurements.

Manual chamber measurements were carried out between 10:30 and 15:00. Gas samples were collected over a 45 minute period, at t = 0, 15, 30 and 45 minutes, using a 100 ml syringe, and immediately flushed into 20 ml glass vials sealed with butyl rubber plugs using a double needle system. Vials were analysed within approximately one month on a 7890B gas

chromatograph (Agilent Technologies). Samples were analysed together with 4 to 5 sets of certified standards with concentrations ranging from 200 to 4941 ppm for CO₂, 1.26 to 101.1 ppm for CH₄ and 199.5 to 975 ppb for N₂O).

Sediment CO₂ respiration rates (sum of soil and any vegetation present) were measured in situ using a PP-Systems SRC closed dynamic respiration chamber (0.0012 m³ volume, 0.008 m² diameter), attached to an EGM-4 infrared gas analyser, for 120 seconds (IRGA, PP Systems; Hitchin, Hertfordshire, UK). CO₂ respiration measurements are made in-situ, and this standard technique is routinely done over a 2 minute period. A temperature probe attached to the EGM-4 recorded sediment temperature at 10 cm depth simultaneously to respiration measurements. Fluxes were calculated based on the linear increase of CO₂ concentrations and sediment temperature field measurements were used. Three replicate volumetric sediment moisture content (VMC) measurements were taken around each chamber using a Theta probe HH 2 moisture meter (Delta T-Devices, Cambridge, UK).

Two sets of sediment samples (one set was refrigerated and the other frozen) were taken within 50 cm of each chamber immediately after flux measurements using a sharp metal cutting cylinder (7.4 cm diameter, 5 cm deep). It was not possible to take samples from directly inside the chambers until the last week of the experiment, as this disturbance of the sediment would interfere with subsequent flux measurements. The refrigerated samples were used to determine bulk density (BD), total C (TC) and total nitrogen (TN), soil moisture content (via oven drying at 105 °C) and water-filled pore space (WFPS%) (Rowell, 1994). A sub-sample of the refrigerated samples were oven-dried at 105 °C for 48 hours, and the bulk density (g cm⁻³) calculated based on the dry weight that now occupied the cutting ring volume. WFPS% was calculated from the bulk density, the particle density (assumed as 2.65 g cm⁻³) and the volumetric soil moisture content (Rowell, 1994). The frozen samples were used to measure soil pH, gravimetric soil moisture content (via oven drying at 105 °C), DOC, NH₄⁺, NO₂⁻ and NO₃⁻ concentrations.

To determine TC and TN, sediment samples were oven dried at 105 °C and ground with a mixer mill MM200 (Retsch GmbH & Co. KG, Haan, Germany) where 10-15 mg of each sample was transferred to capsules and stored until analysis on a FlashSmart N ORG Elemental Analyzer (Thermo Fisher Scientific, UK). The second sample was analysed for NH₄⁺, NO₂⁻ and NO₃⁻ by mixing 15 g of sediment with 50 ml of a 1 mol L⁻¹ KCl solution in deionised water (Rowell, 1994, p. 226) and placed on a Stuart Orbital Shaker SSL1 (Barloworld Scientific Ltd.,

Stone, UK) set to 100 rpm for 60 minutes. The extracted solution was filtered with Whatman 42 filter papers and stored in 15 ml bottles at -18°C until analysis on a SEAL AQ2. Sediment pH was determined on slurry of 10 g of soil mixed with 30 ml of deionised water and leaving to settle for 1h before measuring with a MP220 pH meter (Mettler-Toledo Ltd. Leicester, UK). Sediment DOC was extracted from a 1:5 (w/v) soil:deionised water mixture which was also left to settle for ~1h followed by filtration using 0.45 µm Whatman® syringe- filters before analysis on the PPM LabTOC (Jones and Willett, 2006).

5.2.4 Instantaneous flux calculation

Fluxes from chambers were calculated using linear regression based on the concentration change as a function of time for the four gas samples according to Eq. (1):

$$F = \frac{dC}{dt_0} \times \frac{\rho V}{A}, \quad (1)$$

where F is the gas flux from the sediment ($\mu\text{mol m}^{-2} \text{s}^{-1}$), $\frac{dC}{dt_0}$ is the concentration (C , μmol) rate of change over time (t , in s) which is calculated by linear regression, ρ is the density of air in mol m^{-3} , V is the volume of the chamber in cubic meters, and A is the ground area enclosed by the chamber in square metres (Levy et al., 2012). In R, the package ‘RCFlux version 2’ was used to calculate the fluxes (Levy et al., 2011) from the linear fit approach.

Evasion rates were calculated indirectly using wind speed to predict gas transfer velocity, combined with the partial pressure difference across the air-water interface, using established relationships between wind speed and gas transfer velocity (Wanninkhof, 1992; MacIntyre et al., 1995). Evasion gas fluxes ($F_{\text{CO}_2}/F_{\text{CH}_4}/F_{\text{N}_2\text{O}}$) were then calculated using Eq. (2), Fick’s first law, as described in Borges et al. (2004), where k is the gas transfer velocity (cm h^{-1}), a is the solubility coefficient and Δp_{gas} is the difference in partial pressure between the surface water and the atmosphere. The solubility coefficient a is temperature and salinity dependent. Values of a for CO_2 , CH_4 and N_2O were derived from Weiss (1974), Weisenburg and Guinasso (1979), and Weiss and Price (1980), respectively. The transfer velocity k is a function of turbulence, the kinematic viscosity of the water and the molecular diffusion coefficient of the gas. In Eq. (3) (Cole and Caraco, 1998) wind speed (m s^{-1}) at 10 m above the water surface U_{10} is used to describe turbulence, and the Schmidt number Sc is a function of the latter two terms. $k(600)$ refers to the transfer velocity normalised to $Sc = 600$, the Schmidt number of CO_2 at 20°C in freshwater. This is then adjusted using the Schmidt number for the particular gas in freshwater at measured temperature (MacIntyre et al., 1995) using Eq. (4). The exponent in Eq. (4) varies

from $-\frac{2}{3}$ to $-\frac{1}{2}$ as wind speed increases and waves develop (Jähne et al., 1987). Wind speed at 10 m (U_{10}) is calculated using Eq. (5) (Erkkilä et al., 2018).

$$F_{gas} = k\alpha\Delta p_{gas} \quad (2)$$

$$k(600) = 2.07 + 0.215u_{10}^{1.7} \quad (3)$$

$$k = k(600) \left(\frac{Sc}{600}\right)^{\frac{1}{2}} \quad (4)$$

$$U_{10} = 1.22U_z \quad (5)$$

5.2.5 Integration and upscaling of GHG fluxes

An aerial survey was conducted during time of maximum drawdown on 21st April 2016 using a custom-built multi-rotor system by a co-author (Simon Gibson-Poole, University of Edinburgh) which is described in full in Maire et al. (2018). The digital elevation model (DEM) produced using photogrammetry and supplied by the co-author, allowed calculation of reservoir water and sediment areas used in up-scaling the point-sampled fluxes. Flying was conducted at 70 and 120 m above ground, and further enhanced by using 13 ground control points positioned across the reservoir sediment to geo-reference the elevation model.

The rate of flux from the reservoir as a whole at a point in time was estimated by multiplying point flux measurements by the area over which these measurements are assumed to be constant. For the sediment evasion, it was assumed that areas within a certain elevation range would have the same net fluxes as the chamber(s) within that range when the sediment was exposed. Figure 5.1 shows contours at the elevation halfway between adjacent chambers, which form areas over which these point measurements are assumed to be constant, and with which they were multiplied, with these products summed to produce a rate of evasion from reservoir sediment. As the water level during drawdown varied with rainfall, the area corresponding to submerged chambers was added to the minimum water extent (also Figure 5.1) to produce a water surface area, which was then multiplied by the mean of the aquatic flux measurements. The estimates of total sediment and aquatic emission were then summed to obtain an estimate of the total emissions from the reservoir as a whole. To assess the contribution of drawdown on reservoir GHG emissions for the year, instantaneous measured rates of evasion were integrated to give cumulative emissions by linear interpolation using the trapezium rule.

5.2.6 Statistical analysis

Box and whisker diagrams were produced to summarise both aquatic and sediment data. A linear mixed effects model (Pinheiro et al., 2015) was built for each GHG to explain flux variations due to the different processes driving their production. Variables to include in respective models were identified, and an exploratory analysis carried out to identify appropriate transformations, and to highlight obvious relationships or potential problems for statistical analysis such as collinearity. For each GHG, a small number of independent models were fitted, each using a subset of predictors and the maximal random effect structure justified by the design.

Variables included as fixed effects in the aquatic models were pH, DOC, DIC, total inorganic nitrogen (TIN, the total mass of N from NH_4^+ , NO_2^- and NO_3^-), water temperature, DO (%), and conductivity. The fixed effects in the sediment models began with pH, DOC, DIC, NO_3^- , NH_4^+ , and moisture availability (a combination of soil bulk density, water filled pore space, field soil moisture, gravimetric soil moisture, and soil water content). pH was transformed to be centred at neutral, GHGs and TIN were (real) cube root transformed, and DOC and DIC were mean-centred, and normalised by their standard deviation. A model could not be fitted using each of the individual measures of moisture availability, as the number of terms led to convergence problems. For each of the fixed effects listed above, a random slope and intercept (uncorrelated with each other) were fit for the random effects of sampling point location and sampling date in both the aquatic and sediment models.

After a maximal model was fitted, an iterative procedure similar to that proposed by Bates et al. (2015) was used to simplify it. Fixed and random effects were removed one-by-one, starting with high-order interactions and later guided by visualisation of the model and dataset. At each stage, an F-test based on the Kenward-Roger approximation was used to determine the significance of the removed terms, and so whether they should remain in the model. All statistical analysis was carried out in R (3.3.2, 2016 R Foundation for Statistical Modelling), using lme4 (Bates et al. 2015) to fit linear mixed effects models, pbkrtest to perform the Kenward-Roger approximate F-test. The function “g.squaredGLMM” in the package MuMIn (Barton, 2018) was used to compute conditional (variance explained by both fixed and random effects) and marginal (variance explained by fixed effects) coefficients of determination ('pseudo- R^2 ') for the final models (Johnson, 2014; Nakagawa et al., 2017; Nakagawa and Schielzeth, 2013).

5.3 Results

5.3.1 Precipitation effects on reservoir water level and surface area

Monthly mean minimum and maximum temperatures were 6.3 °C (-8.4 to 19.7) and 11.2 °C (-4.4 to 27.7), respectively. The minimum air temperature was reached on the 14th February 2016 and maximum on the 19th July 2016. In this study, seasons are defined as autumn (Sep-Nov), winter (Dec-Feb), spring (Mar-May) and summer (Jun-Aug). Precipitation (Figure 5.2) was lowest in spring (198 mm) followed by summer (303 mm), but several rainfall events through April to July caused the water level to rise during the scheduled drawdown, resulting in the partial refilling of the reservoir and therefore limiting access to some of the flux chambers. Similarly, during storm events, the reservoir began to refill. This natural water level fluctuation enabled the role of sediment drying and rewetting on GHG emissions to be investigated. For example, from the 18th to 23rd May 2016, the catchment received 43 mm of rain, causing the water level to rise by ~1.6 m and leaving only chambers 1 to 5 exposed, before draining and re-exposing all chambers by the following sampling week when only 1 mm of rain was recorded. During maximum drawdown when precipitation was low, the reservoir water level decreased leaving ~24700 m² (86%) of exposed reservoir sediment and ~3990 m² (14%) of water surface area as observed during the UAV survey (Figure 5.1).

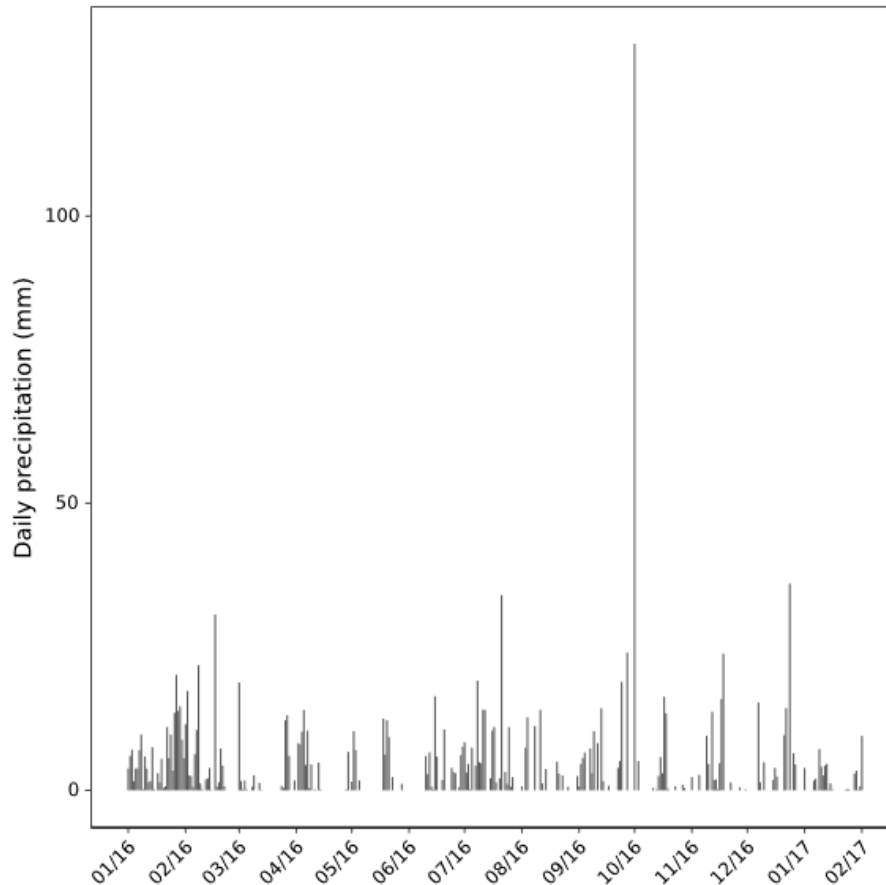


Figure 5.2 Daily precipitation during the sampling period.

5.3.2 The impact of drawdown on aquatic GHGs and water chemistry

Aquatic GHG concentrations and water chemistry data are summarised in Table 5.1. All three greenhouse gases showed considerable temporal variability in aquatic C and N concentrations throughout the reservoir (Figure 5.3). The excess partial pressure ($epCO_2$; extent of oversaturation) of CO_2 showed oversaturation in the inlet (mean = 1.7), reservoir (mean = 3.7) and outlet (mean = 2.6) across the full sampling year. $epCO_2$ indicated saturation or undersaturation on four sampling occasions at the inlet, two at the outlet, and once in the reservoir. Over the sampling period, dissolved CO_2 concentrations on average showed an increase from the inlet ($499 \mu\text{g C L}^{-1}$) to the reservoir ($1050 \mu\text{g C L}^{-1}$), suggesting CO_2 was produced within the reservoir. Concentrations of CO_2 varied considerably between inlet, reservoir and outlet sampling locations (range 212 to $3710 \mu\text{g C L}^{-1}$). A 29% decrease in overall mean CO_2 concentrations was observed from the reservoir to the outlet, implying partial degassing. During the period of drawdown, CO_2 concentrations increased by an average of 38% with a maximum concentration of $3710 \mu\text{g C L}^{-1}$. Following drawdown and the refilling of the reservoir, outlet CO_2 concentrations increased from July to September to values higher than

concentrations observed during the pre-drawdown period (Figure 5.3). A significant relationship ($r = -0.14$, $p = 0.02$) with CO_2 concentration was established only with pH, explaining 66% of variance, with fixed effects explaining 11%.

The excess partial pressure of CH_4 showed consistent oversaturation in the inlet (mean = 53.3), reservoir (mean = 128.2) and outlet (mean = 97.5) across the full sampling year (Table 5.1). The inlet, reservoir and outlet all showed much higher oversaturation levels compared to CO_2 . Over the full year, dissolved CH_4 concentrations on average showed an increase from the inlet ($2.7 \mu\text{g C L}^{-1}$) to the reservoir ($24.8 \mu\text{g C L}^{-1}$), implying in-reservoir production. Methane concentrations varied substantially between sites (Table 5.1) with a 71% reduction from the reservoir sampling sites to the outlet, also implying that partial degassing occurred. During the period of water level drawdown, the reservoir showed on average 371 times saturation, compared to the inlet (ep CH_4 59) and outlet (ep CH_4 165). Figure 5.3 shows two distinct peaks (18th April and 14th June) in CH_4 concentrations during drawdown. Concentrations at the reservoir sampling site (R3) reached $394 \mu\text{g CH}_4\text{-C L}^{-1}$ during the latter, nearly 100 times higher than the mean of $4.0 \mu\text{g C L}^{-1}$ outside the drawdown period. These peaks coincided with reservoir refilling associated with increased rainfall. While there is little change in mean inlet CH_4 concentration during drawdown ($2.3 \mu\text{g C L}^{-1}$ vs. $3.0 \mu\text{g C L}^{-1}$ outside drawdown), there is a more pronounced effect at the outlet ($12.4 \mu\text{g C L}^{-1}$ vs. $3.7 \mu\text{g C L}^{-1}$ outside drawdown). Following drawdown and the refilling of the reservoir, outlet CH_4 concentrations also increased from July to September.

Excess partial pressures of N_2O , especially at the inlet and with the notable exception of the reservoir during drawdown, were much closer to 1 i.e. saturation or equilibrium with respect to the atmosphere (inlet = 1.0, reservoir = 2.2 over the year, but 1.1 outside of drawdown, and outlet = 1.2). On eight of 33 sampling occasions, ep N_2O values were below 1 (i.e. the water was under-saturated in N_2O with respect to the atmosphere) at the inlet, and on four occasions at the outlet. To a lesser extent than both CO_2 and CH_4 , mean N_2O concentrations for the full sampling period also saw an increase from inlet ($0.5 \mu\text{g N L}^{-1}$) to reservoir ($1.3 \mu\text{g N L}^{-1}$), and a decrease from reservoir to outlet ($0.5 \mu\text{g N L}^{-1}$). Minimal temporal or spatial variation, was seen in N_2O concentrations in the inlet (range 0.3 to $0.6 \mu\text{g N L}^{-1}$) and outlet (range 0.4 to $1.3 \mu\text{g N L}^{-1}$), with the exception of two single-sample peaks during drawdown in the reservoir (range 0.4 to $21.6 \mu\text{g N L}^{-1}$), around a month after peaks in CH_4 concentration. The larger of these two N_2O peaks was nearly 40 times larger than the mean reservoir non-drawdown concentration ($0.6 \mu\text{g N L}^{-1}$).

Concentrations of DOC and DIC exhibited a contrasting pattern of increased concentrations from inlet to reservoir, or decrease in concentrations from reservoir to outlet. Across the full sampling year, mean DIC concentrations were highest in the inlet (16.4 mg L^{-1}), followed by the outlet (15.7 mg L^{-1}) and reservoir (14.6 mg L^{-1}). Mean DOC concentrations were highest in the outlet (6.2 mg L^{-1}), with little difference in the reservoir (6.0 mg L^{-1}) and lowest in the inlet (4.6 mg L^{-1}). DOC concentrations at the reservoir and outlet vary together, although the inlet concentration is both consistently lower and more consistent over time following the drawdown (July-November). DIC exhibited much higher temporal than spatial variability, with concentrations ranging from 2.3 to 37.4 mg L^{-1} . A lower range in DOC concentrations was seen across the sites (2.5 to 14.2 mg L^{-1}). Mean reservoir DIC concentrations were lowest in winter (11.3 mg L^{-1}) and highest in late summer and early autumn (18.1 and 15.5 mg L^{-1} , respectively). Concentrations of DIC are elevated in both the reservoir and outflow compared to the inflow post-drawdown and later in the year (Figure 5.3). Mean reservoir DOC concentrations were lowest in spring and winter (4.3 and 4.8 mg L^{-1} , respectively) and highest in summer and autumn (8.0 and 7.7 mg L^{-1} , respectively). There was no clear difference in reservoir mean DIC and DOC concentrations when comparing drawdown and non-drawdown periods (Table 5.1). The only water quality variable showing a significant relationship ($r = 0.58$, $p = 0.02$) with CH_4 concentration was DIC, this model also explaining 66% of variance, with fixed effects explaining 21%.

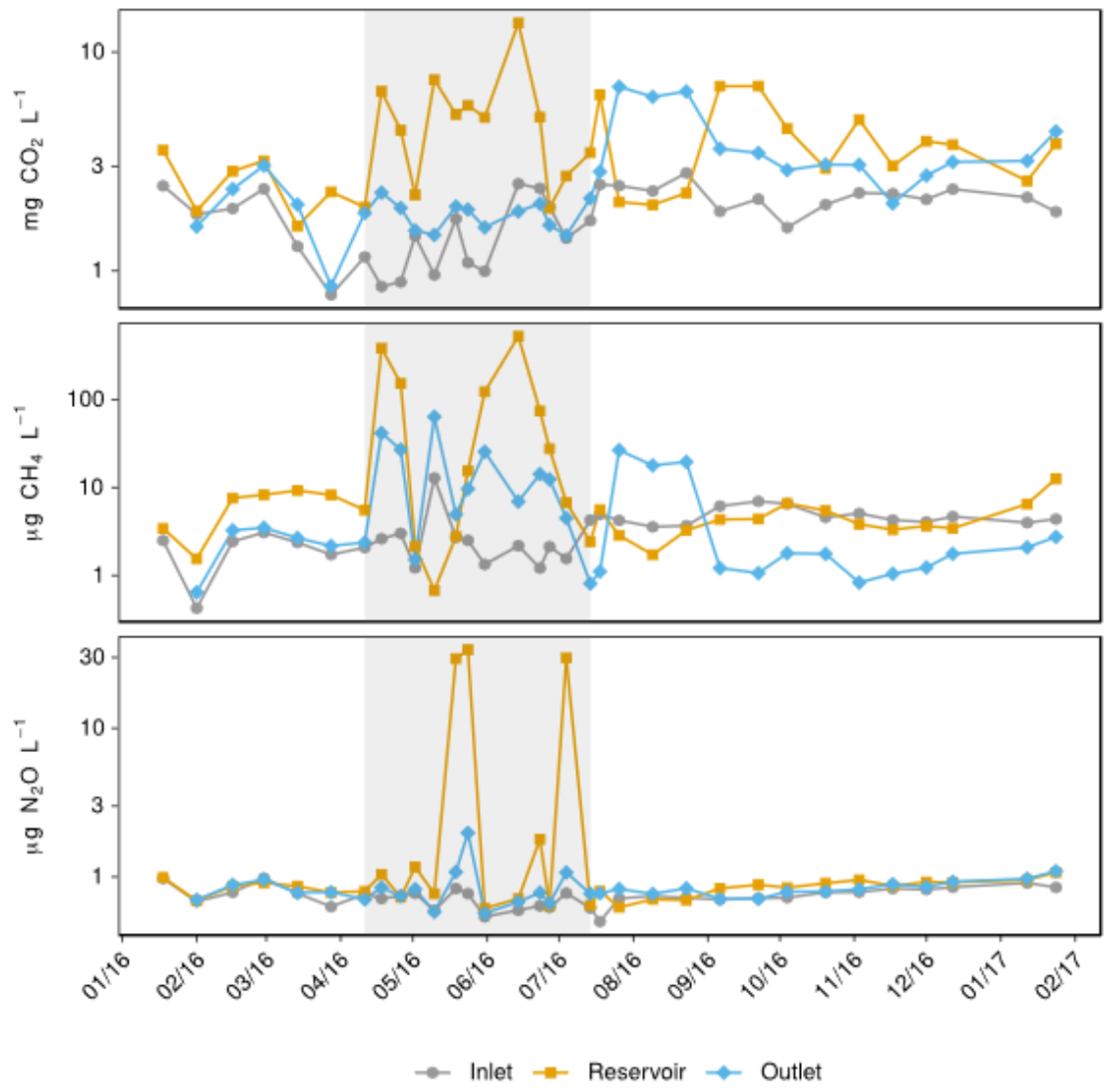
Mean NH_4^+ concentrations across the year were highest in the outlet ($139 \text{ } \mu\text{g N L}^{-1}$), followed by the inlet ($122 \text{ } \mu\text{g N L}^{-1}$) and reservoir ($112 \text{ } \mu\text{g N L}^{-1}$) (Table 5.1). There was a wide range in concentrations (0 to $1300 \text{ } \mu\text{g N L}^{-1}$), with the highest in the outlet post-drawdown. The inlet saw little variation in mean concentrations between the drawdown ($122 \text{ } \mu\text{g N L}^{-1}$) and non-drawdown ($123 \text{ } \mu\text{g N L}^{-1}$) periods. The reservoir had higher mean NH_4^+ concentrations during drawdown compared to non-drawdown (138 vs. $104 \text{ } \mu\text{g N L}^{-1}$), whilst the opposite was observed at the outlet ($82.4 \text{ } \mu\text{g N L}^{-1}$ during drawdown and $177 \text{ } \mu\text{g N L}^{-1}$ for non-drawdown). Concentrations of NO_3^- followed a similar spatial pattern to the three dissolved gases, with an increase in mean concentrations from inlet ($189 \text{ } \mu\text{g N L}^{-1}$) to reservoir ($272 \text{ } \mu\text{g N L}^{-1}$), and a decrease from reservoir to outlet ($215 \text{ } \mu\text{g N L}^{-1}$). There was also a wide range (19 to $2140 \text{ } \mu\text{g N L}^{-1}$) of concentrations across sampling locations, with maximum occurring in the reservoir during drawdown. When comparing drawdown with non-drawdown sampling, mean NO_3^- inlet, reservoir and outlet concentrations were all higher post-drawdown but with least variation seen in the reservoir (267 during drawdown vs. $274 \text{ } \mu\text{g N L}^{-1}$ after). Concentrations of NO_2^- showed the least spatial and temporal variation of N species. The outlet had the highest

mean concentration across the full year (mean 3.9 $\mu\text{g N L}^{-1}$), followed by the reservoir (mean 2.6, range 0 to 53 $\mu\text{g N L}^{-1}$) and lowest concentrations were observed in the inlet (1.7 $\mu\text{g N L}^{-1}$). During drawdown, concentrations were on average higher than the non-drawdown period across all sites this period also showed greatest range in concentrations. The only variable to correlate significantly ($r = 0.57$, $p < 0.01$) with N_2O concentration was TIN, the best fit model explained 74% of variation, with fixed effects explaining 8%. For all other variables and interactions no significant relationships were observed.

Table 5.1 Water chemistry parameters and concentrations of different C and N species for Waltersmuir inlet (a), reservoir (b) and outlet (c). Results show mean, standard error and range, with a comparison provided for the full sampling period (Jan 2016-Jan2017) and drawdown period (April-July 2016).

Waltersmuir Inlet (a)			
Variable measured	Full year	Drawdown	Non-drawdown
CH ₄ (µg C L ⁻¹)	2.71±0.30 (0.32 - 9.66)	2.29±0.64 (0.91 - 9.66)	2.99±0.27 (0.32 - 5.24)
CO ₂ (µg C L ⁻¹)	498.78±27.25 (211.91 - 764.51)	399.78±42.04 (231.22 - 681.74)	563.14±28.01 (211.91 - 764.51)
N ₂ O (µg N L ⁻¹)	0.47±0.01 (0.32 - 0.62)	0.44±0.02 (0.34 - 0.53)	0.49±0.02 (0.32 - 0.62)
epCH ₄	53.26±9.80 (6.80 - 338.08)	58.79±23.56 (18.98 - 338.08)	49.66±6.09 (6.80 - 94.24)
epCO ₂	1.74±0.13 (-0.25 - 2.92)	1.51±0.26 (-0.25 - 2.82)	1.89±0.14 (-0.07 - 2.92)
epN ₂ O	0.95±0.06 (-0.05 - 1.30)	0.96±0.10 (-0.05 - 1.30)	0.94±0.08 (-0.03 - 1.28)
DIC (mg L ⁻¹)	16.44±1.05 (2.63 - 33.04)	18.16±1.17 (13.19 - 26.03)	15.32±1.53 (2.63 - 33.04)
DOC (mg L ⁻¹)	4.57±0.24 (2.45 - 7.09)	4.41±0.43 (2.84 - 7.09)	4.66±0.28 (2.45 - 6.39)
NH ₄ ⁺ (µg N L ⁻¹)	122.18±41.37 (0.00 - 1169.30)	121.04±87.74 (3.20 - 1169.30)	122.93±39.94 (0.00 - 569.50)
NO ₃ ⁻ (µg N L ⁻¹)	188.50±33.33 (19.00 - 839.00)	87.69±28.17 (19.00 - 410.00)	254.03±46.78 (51.50 - 839.00)
NO ₂ ⁻ (µg N L ⁻¹)	1.70±0.33 (0.00 - 10.00)	2.31±0.75 (0.00 - 10.00)	1.30±0.23 (0.00 - 5.00)
Temperature (°C)	9.70±0.72 (3.20 - 18.40)	12.36±1.01 (6.30 - 18.40)	7.97±0.78 (3.20 - 13.90)
pH	6.86±0.07 (6.08 - 7.57)	7.07±0.09 (6.54 - 7.45)	6.73±0.10 (6.08 - 7.57)
Conductivity (µS cm ⁻¹)	81.92±6.13 (39.80 - 159.00)	110.56±9.40 (50.20 - 159.00)	63.30±4.66 (39.80 - 115.90)
DO (mg L ⁻¹)	5.87±0.25 (3.57 - 9.35)	6.08±0.44 (4.04 - 9.35)	5.73±0.29 (3.57 - 8.63)

Waltersmuir Reservoir (b)			
Variable measured	Full year	Drawdown	Non-drawdown
CH ₄ (µg C L ⁻¹)	24.82±8.83 (0.41 - 393.70)	94.73±33.93 (0.51 - 393.70)	3.97±0.28 (0.41 - 9.78)
CO ₂ (µg C L ⁻¹)	1048.65±66.02 (298.50 - 3708.72)	1331.80±201.26 (479.53 - 3708.72)	964.20±58.05 (298.50 - 2161.58)
N ₂ O (µg N L ⁻¹)	1.33±0.44 (0.38 - 21.55)	3.96±1.83 (0.39 - 21.55)	0.55±0.01 (0.38 - 0.69)
epCH ₄	128.17±30.38 (8.49 - 1974.50)	370.56±115.97 (30.53 - 1974.50)	55.88±3.03 (8.49 - 124.85)
epCO ₂	3.68±0.26 (0.67 - 14.18)	5.10±0.76 (1.68 - 14.18)	3.26±0.24 (0.67 - 7.81)
epN ₂ O	2.24±0.61 (-0.09 - 29.83)	6.01±2.48 (0.56 - 29.83)	1.12±0.04 (-0.09 - 1.55)
DIC (mg L ⁻¹)	14.59±0.76 (2.48 - 37.37)	16.56±1.31 (10.52 - 29.79)	14.00±0.89 (2.48 - 37.37)
DOC (mg L ⁻¹)	5.97±0.30 (2.64 - 14.24)	5.32±0.67 (2.64 - 14.24)	6.16±0.33 (2.86 - 12.08)
NH ₄ ⁺ (µg N L ⁻¹)	111.53±15.77 (1.20 - 740.10)	138.32±39.00 (10.30 - 572.50)	103.54±16.92 (1.20 - 740.10)
NO ₃ ⁻ (µg N L ⁻¹)	272.16±31.93 (25.50 - 2140.00)	267.24±120.65 (25.50 - 2140.00)	273.62±22.03 (49.00 - 819.00)
NO ₂ ⁻ (µg N L ⁻¹)	2.59±0.72 (0.00 - 53.00)	4.88±3.03 (1.00 - 53.00)	1.91±0.24 (0.00 - 10.00)
Temperature (°C)	8.83±0.50 (1.10 - 17.80)	12.18±0.89 (6.60 - 17.80)	7.82±0.52 (1.10 - 14.90)
pH	6.68±0.05 (5.72 - 7.58)	6.70±0.09 (5.72 - 7.38)	6.67±0.05 (6.03 - 7.58)
Conductivity (µS cm ⁻¹)	72.61±4.17 (32.00 - 191.00)	115.41±10.06 (39.90 - 191.00)	59.85±2.85 (32.00 - 116.20)
DO (mg L ⁻¹)	5.03±0.13 (2.70 - 7.26)	4.98±0.31 (2.70 - 6.89)	5.05±0.14 (2.91 - 7.26)
Waltersmuir Outlet (c)			
Variable measured	Full year	Drawdown	Non-drawdown
CH ₄ (µg C L ⁻¹)	7.23±1.88 (0.48 - 47.90)	12.43±3.88 (0.61 - 47.90)	3.67±1.29 (0.48 - 19.93)
CO ₂ (µg C L ⁻¹)	746.60±71.15 (232.37 - 1895.05)	495.15±20.14 (395.75 - 621.02)	918.65±102.23 (232.37 - 1895.05)
N ₂ O (µg N L ⁻¹)	0.54±0.03 (0.36 - 1.26)	0.55±0.06 (0.36 - 1.26)	0.53±0.01 (0.45 - 0.69)
epCH ₄	97.50±21.22 (9.65 - 496.19)	164.84±39.01 (13.54 - 496.19)	51.43±17.93 (9.65 - 254.01)
epCO ₂	2.64±0.27 (0.50 - 6.83)	2.06±0.10 (1.54 - 2.87)	3.04±0.44 (0.50 - 6.83)
epN ₂ O	1.15±0.08 (-0.04 - 2.74)	1.29±0.17 (-0.04 - 2.74)	1.05±0.08 (-0.03 - 1.31)
DIC (mg L ⁻¹)	15.72±1.10 (2.34 - 32.58)	17.37±1.49 (4.64 - 25.57)	14.59±1.52 (2.34 - 32.58)
DOC (mg L ⁻¹)	6.24±0.50 (2.84 - 14.18)	5.36±0.86 (2.84 - 14.18)	6.85±0.59 (3.14 - 12.73)
NH ₄ ⁺ (µg N L ⁻¹)	138.49±41.89 (0.80 - 1305.20)	82.39±22.45 (0.80 - 296.40)	176.88±68.25 (5.55 - 1305.20)
NO ₃ ⁻ (µg N L ⁻¹)	215.30±26.65 (59.50 - 640.00)	164.38±41.92 (59.50 - 587.00)	250.13±33.05 (63.00 - 640.00)
NO ₂ ⁻ (µg N L ⁻¹)	3.91±1.21 (1.00 - 38.00)	5.62±2.89 (1.00 - 38.00)	2.74±0.48 (1.00 - 8.00)
Temperature (°C)	9.84±0.74 (2.80 - 18.80)	12.65±0.96 (7.20 - 18.80)	7.92±0.82 (2.80 - 13.00)
pH	7.02±0.07 (6.08 - 7.67)	7.22±0.10 (6.45 - 7.67)	6.88±0.09 (6.08 - 7.66)
Conductivity (µS cm ⁻¹)	78.72±6.54 (36.40 - 163.00)	111.15±9.97 (36.40 - 163.00)	56.52±3.35 (37.70 - 91.20)
DO (mg L ⁻¹)	5.31±0.29 (1.61 - 10.70)	5.96±0.46 (4.06 - 10.70)	4.87±0.34 (1.61 - 7.19)



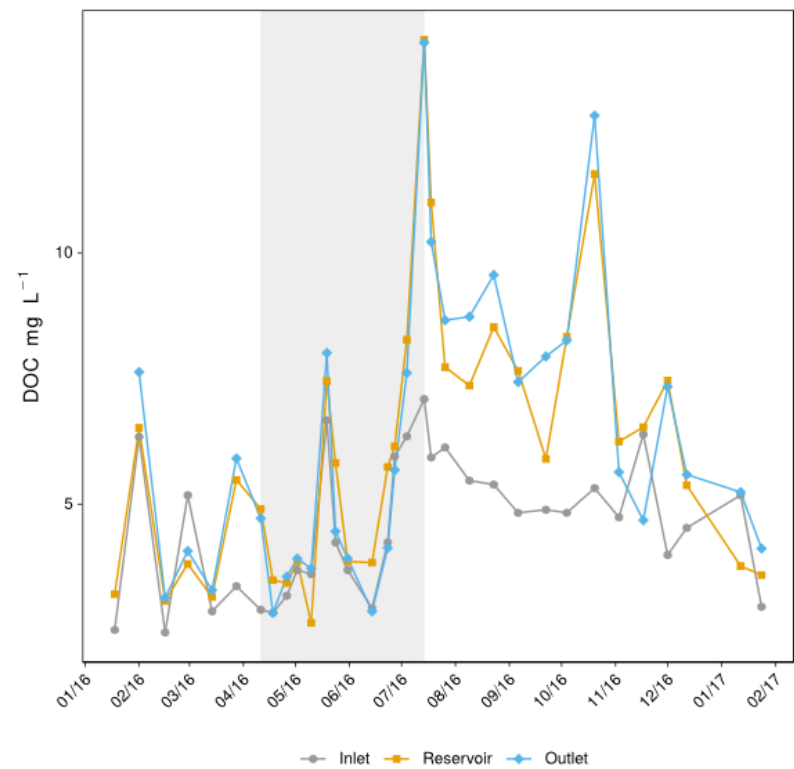
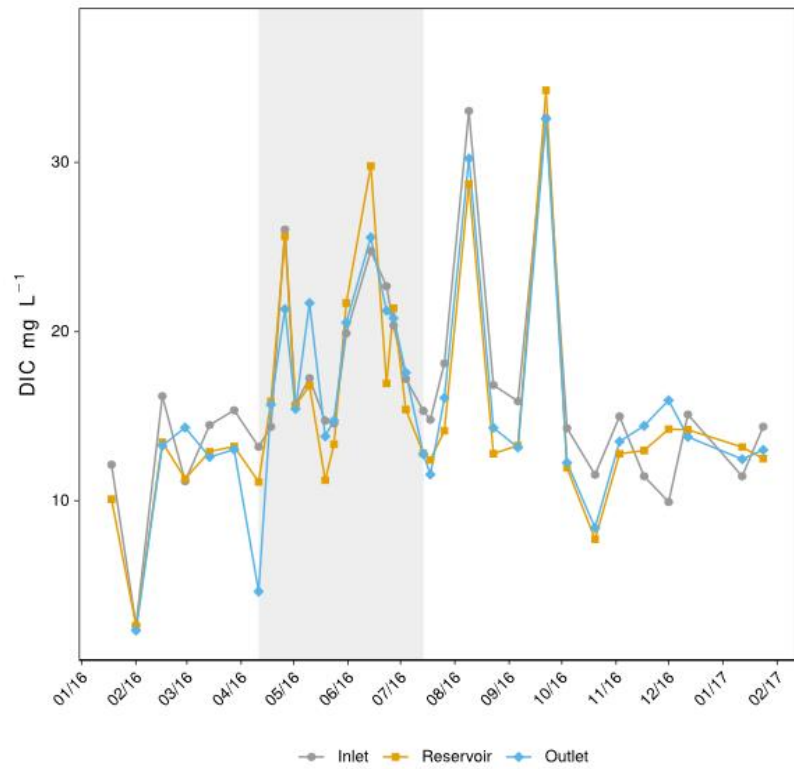


Figure 5.3 Temporal variability of GHG, DOC and DIC concentrations within the Waltersmuir inlet, reservoir and outlet. The shaded area represents the 11 week drawdown period from April-July 2016.

5.3.2.1 GHG evasion from Waltersmuir reservoir water surface

Estimated evasion rates from the water surface are shown in Table 5.1, along with the CO₂ equivalents in terms of 100-year global warming potentials per the IPCC AR5 report (IPCC, 2014). Evasion rates for all three gases increased during the period of drawdown (Figure 5.4), with an almost fourfold increase in CH₄ evasion compared to the full sampling year mean. Although C loss via CO₂ is more than an order of magnitude greater than via CH₄, their CO₂ equivalent values are much more comparable; on the basis the warming impact of open water CO₂ emission exceeds that of CH₄ by a factor of 2.3 over the year, but their contributions are approximately equal (and both considerably higher) during the drawdown period. Despite the low level of supersaturation observed for N₂O, its high CO₂ equivalent value led to it contributing around 10% of total GHG emissions from the water surface on an annual basis, and 16% during the drawdown period.

Table 5.2 Mean, standard error, minimum and maximum values of estimated open water CH₄, CO₂, and N₂O evasion flux at Waltersmuir and global warming potentials, estimated using the IPCC AR5 reported approach (IPCC, 2014).

Water surface evasion		GHG ($\mu\text{g m}^{-2} \text{s}^{-1}$)	Global warming potential (CO ₂ equivalents $\mu\text{g m}^{-2} \text{s}^{-1}$)
CH ₄	Full sampling year	0.16 ± 0.06 (0.002-2.64)	5.48 ± 1.95 (0.08-89.64)
	During drawdown	0.63 ± 0.22 (0.004-2.64)	21.38 ± 7.41 (0.14-89.64)
CO ₂	Full sampling year	12.86 ± 1.28 (0.67-63.89)	12.86 ± 1.28 (0.67-63.89)
	During drawdown	20.43 ± 3.81 (3.41-63.89)	20.43 ± 3.81 (3.41-63.89)
N ₂ O	Full sampling year	0.007 ± 0.003 (0.000-0.16)	1.98 ± 1.00 (-0.09-49.02)
	During drawdown	0.03 ± 0.01 (0.00-0.16)	8.02 ± 4.13 (0.06-49.02)

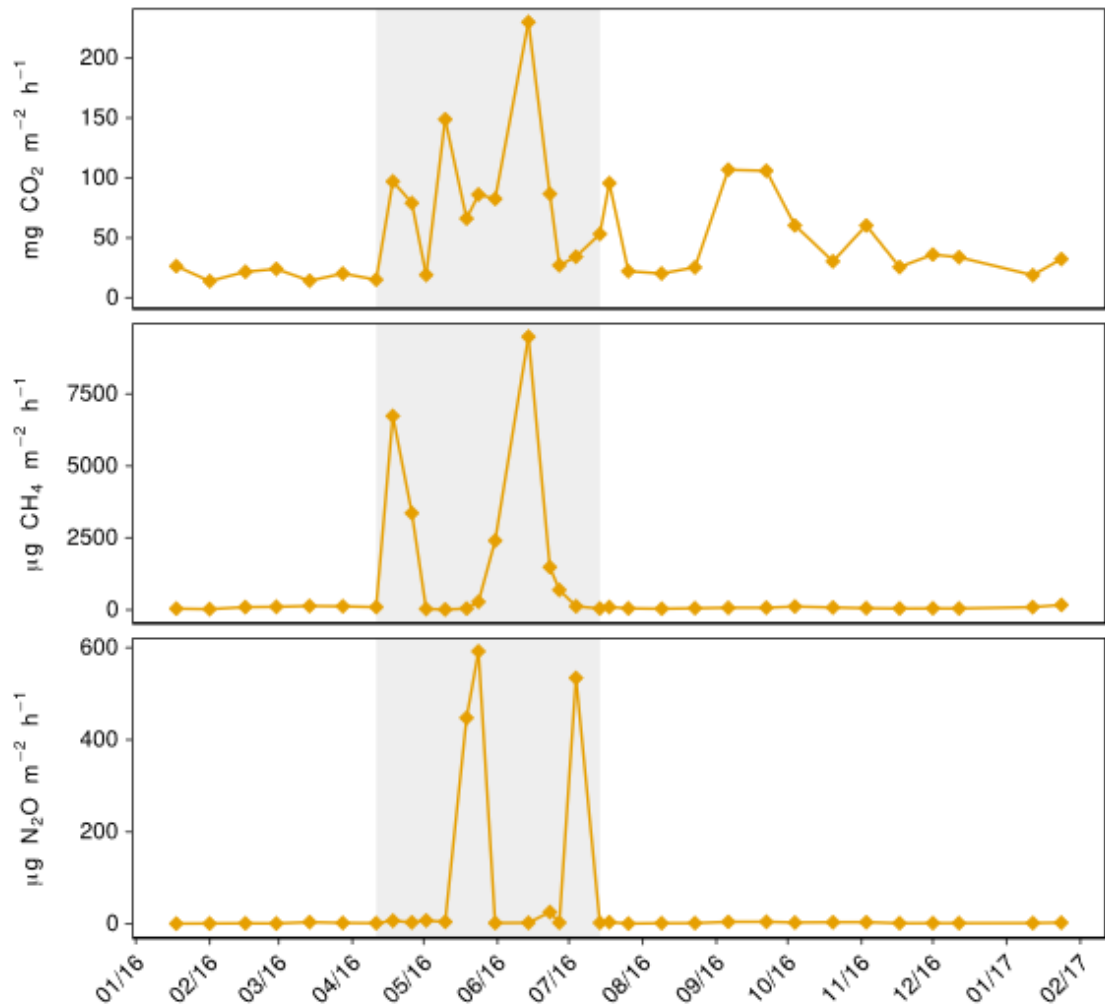


Figure 5.4 Reservoir evasion at Waltersmuir with spikes occurring during the drawdown period (shaded area).

5.3.3 Drawdown area GHG fluxes and sediment properties

There was a visible difference in the appearance of the sediments from the shoreline to the central (middle) area of the reservoir. Terrestrial leaf litter was present in chambers 1 and 2. Chambers 3-6 located on the sloping section were heavily-desiccated from sediment drying out (Figure 5.1), and chambers 7-9 had higher moisture levels (Table 5.3). Chamber 1 also had high moisture levels but also had layers of leaf litter, likely preventing drying out. These spatial observations between chambers reflect a similar trend in the water-filled pore space (Table 5.3), and to some extent also the change in pH from shoreline to central. Sediments from chambers 7-9 were generally more alkaline (pH 6.2 to 6.8) than chambers 1-6.

CO₂ flux rates broadly followed the soil moisture trend and were largest in the littoral zone sediments (chambers 1 to 3, 12.3 ± 1.78 to 10 ± 2.74 g m⁻² d⁻¹), decreasing down the slope

(chambers 4 and 5) and towards the centre of the reservoir basin (chambers 6 to 9) (Figure 5.5). Across all chambers, mean CO₂ flux was $6.54 \pm 0.66 \text{ g m}^{-2} \text{ d}^{-1}$ ranging from -0.96 to $31.7 \text{ g m}^{-2} \text{ d}^{-1}$.

In contrast, CH₄ fluxes were largest in the wettest and central area of the reservoir (chambers 6 to 9, 21.9 ± 19.9 to $291.6 \pm 87.7 \text{ mg m}^{-2} \text{ d}^{-1}$), but close to no net flux in the drier chambers (chamber 1 to 5, 5.4 ± 5.5 to $-0.6 \pm 0.5 \text{ mg m}^{-2} \text{ d}^{-1}$, respectively) (Figure 5.5). The central area experienced cycles of drying and rewetting due to the fluctuating reservoir water level compared to the sediments (chambers 1 to 5) closer to the shore which were able to dry out and desiccate over the 11-week drawdown period. Variation in N₂O fluxes across the transect were considerably smaller than for CO₂ and CH₄, with a mean flux of $15.5 \pm 4.5 \text{ mg m}^{-2} \text{ d}^{-1}$ (range -1.56 to $2504 \text{ mg m}^{-2} \text{ d}^{-1}$). Largest mean N₂O fluxes were measured from chamber 5, 8 and 9.

Ammonium and NO₃⁻ concentrations were larger, but more variable in the sediment compared to the water (Table 5.1, Table 5.3). Sediment NO₃⁻ concentrations decreased from the shore edge (chambers 1 and 2) to the slopes (chambers 3-7) and further to the middle of the reservoir, with mean concentrations at chambers 8 and 9 around 20 times lower than on the slopes (Table 5.3). This trend was much weaker for NH₄⁺. As for NO₃⁻, the sediment TC content decreased from the reservoir edge to the middle of the reservoir, with a marked fall-off from chamber 1 to chamber 2 followed by a steady decrease by chamber 9 (Table 5.3). Although DOC was also highest at chamber 1, it varied non-linearly along the transect, with a decrease through the chambers on the slope followed by an increase of similar scale towards the middle of the reservoir.

Although spatial trends of GHG fluxes from the exposed sediment were observed (Figure 5.5), mixed effects modelling found these were not explained well by the observed sediment variables measured. The only significant relationship ($r = -0.31$, $p < 0.01$) found was between CO₂ flux and pH, where the model explained 45% of the variance, with fixed effects explaining 35%.

Water level fluctuations over the drawdown period exposed between 13% and 86% of sediments from the total reservoir area. The results show the point measurements are most strongly influenced by their position along the transect into the reservoir, suggesting that areas within a certain elevation range can have similar net fluxes. The spatial differences in fluxes could also be explained by variation in sediment erosion, transport and deposition zones across Waltersmuir. Despite Waltersmuir being a small reservoir, differences in

sediment deposition can also influence biological and geochemical cycles, especially in terms of organic matter and nutrient dispersion.

Figure 5.7 shows both pooled cumulative fluxes from the reservoir sediment and evasion rates from the water body. The drawdown period contributed 53% (11200 kg) of CO₂, 77% (69 kg) of CH₄, and 98% (27 kg) of N₂O emissions to the respective annual total emissions. Expressed in CO₂ equivalents, the drawdown period contributed 66% (21600 kg CO₂eq) of CO₂eq-weighted emissions for the year.

Table 5.3 Summary of sediment properties at 5-10 cm depth taken during flux measurements from April – July 2016. The mean values and range (in brackets) of measurements from each variable are included in the table. *For Total C and N, n = 3 from each chamber.

ID (n =)	NH₄⁺ (mg N/L)	NO₃⁻ (mg N/L)	DOC (mg/L)	DIC (mg/L)	pH	Soil Moisture (%)	WFPS (%)	Bulk density (g cm⁻³)	Total nitrogen (%)*	Total carbon (%)*
1 (11)	1.91 (0.67 - 4.50)	3.03 (0.28 - 7.44)	9.51 (1.65 - 17.74)	6.57 (0.23 - 15.99)	5.63 (5.29 - 6.34)	59.36 (19.72 - 116.52)	58.35 (45.55 - 93.82)	0.29 (0.24 - 0.32)	0.53 (0.48 - 0.61)	12.42 (11.39 - 14.28)
2 (10)	1.31 (0.47 - 2.58)	4.00 (1.40 - 7.69)	4.59 (2.49 - 9.44)	8.51 (0.17 - 47.86)	5.79 (5.62 - 6.10)	30.49 (17.23 - 60.32)	51.68 (34.98 - 67.09)	0.54 (0.47 - 0.61)	0.15 (0.12 - 0.17)	5.02 (4.87 - 5.14)
3 (10)	1.01 (0.08 - 1.75)	1.83 (0.35 - 5.03)	4.35 (2.82 - 6.32)	5.46 (0.30 - 16.57)	5.76 (5.51 - 5.87)	25.17 (17.70 - 66.24)	60.99 (48.06 - 78.11)	0.64 (0.51 - 0.71)	0.06 (0 - 0.11)	4.48 (4.45 - 4.49)
4 (10)	1.08 (0.29 - 1.93)	1.59 (0.52 - 4.88)	5.23 (0.29 - 14.81)	4.75 (0.08 - 12.21)	6.00 (5.69 - 7.23)	31.20 (6.06 - 91.51)	54.91 (42.88 - 62.38)	0.65 (0.53 - 0.72)	0.07 (0 - 0.12)	4.36 (4.15 - 4.57)
5 (9)	1.24 (0.10 - 2.75)	1.57 (0.26 - 3.49)	4.85 (2.29 - 10.17)	4.49 (0.15 - 14.80)	5.92 (5.65 - 6.21)	24.13 (9.70 - 49.65)	56.70 (40.79 - 68.07)	0.64 (0.59 - 0.71)	0.03 (0 - 0.09)	4.06 (3.58 - 4.37)
6 (6)	1.31 (0.20 - 2.80)	1.42 (0.54 - 2.06)	4.92 (2.47 - 6.73)	5.94 (0.20 - 15.69)	5.87 (5.62 - 6.00)	29.29 (14.81 - 51.18)	54.78 (37.56 - 67.65)	0.59 (0.42 - 0.67)	0	3.65 (3.18 - 3.92)
7 (6)	1.57 (0.06 - 4.31)	1.02 (0.21 - 3.23)	6.47 (2.41 - 13.18)	12.19 (0.27 - 46.84)	6.39 (6.19 - 6.64)	35.69 (23.73 - 61.15)	72.66 (59.16 - 80.55)	0.66 (0.522 - 0.77)	0.06 (0 - 0.09)	3.98 (3.71 - 4.33)
8 (6)	1.29 (0.26 - 3.29)	0.25 (0.06 - 0.52)	6.68 (3.22 - 13.38)	5.55 (1.39 - 12.88)	6.56 (6.45 - 6.68)	56.59 (43.45 - 100.77)	86.25 (75.99 - 95.17)	0.56 (0.50 - 0.65)	0.04 (0 - 0.11)	3.88 (3.74 - 3.97)
9 (5)	0.91 (0.05 - 1.33)	0.11 (0.01 - 0.18)	7.96 (4.68 - 15.00)	8.90 (1.31 - 14.82)	6.43 (6.21 - 6.76)	59.10 (39.26 - 100.75)	89.21 (72.64 - 110.79)	0.51 (0.45 - 0.60)	0.06 (0 - 0.11)	3.68 (3.41 - 3.99)

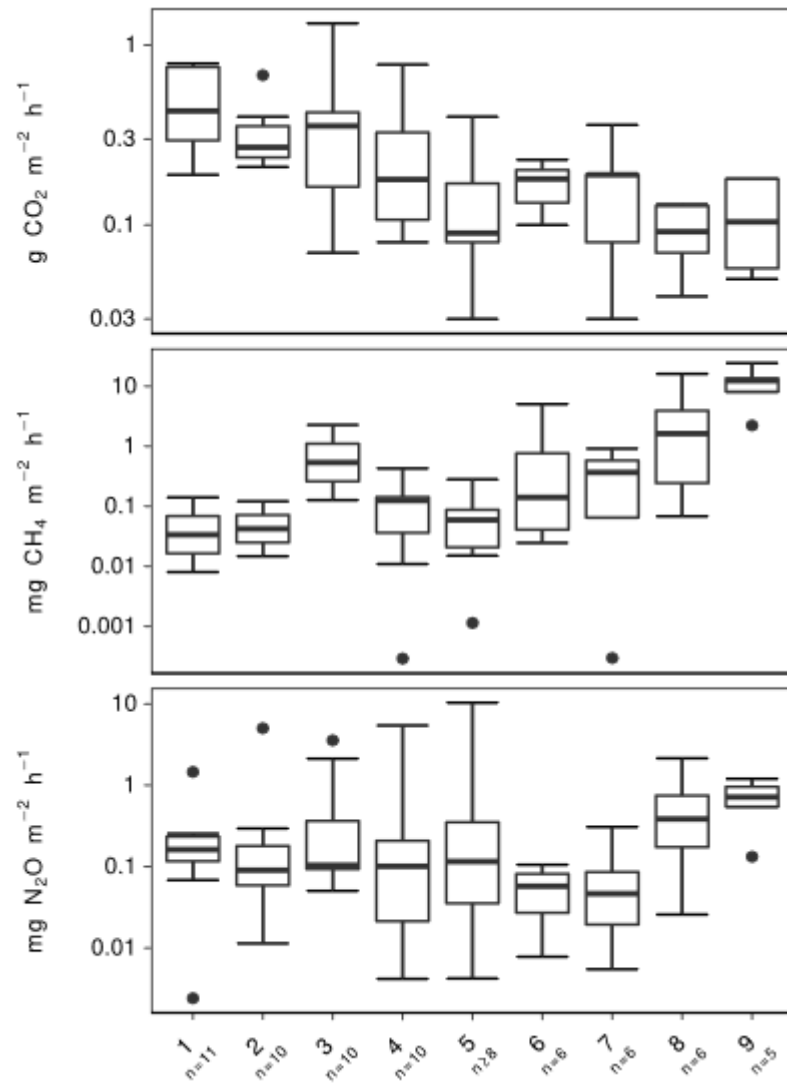
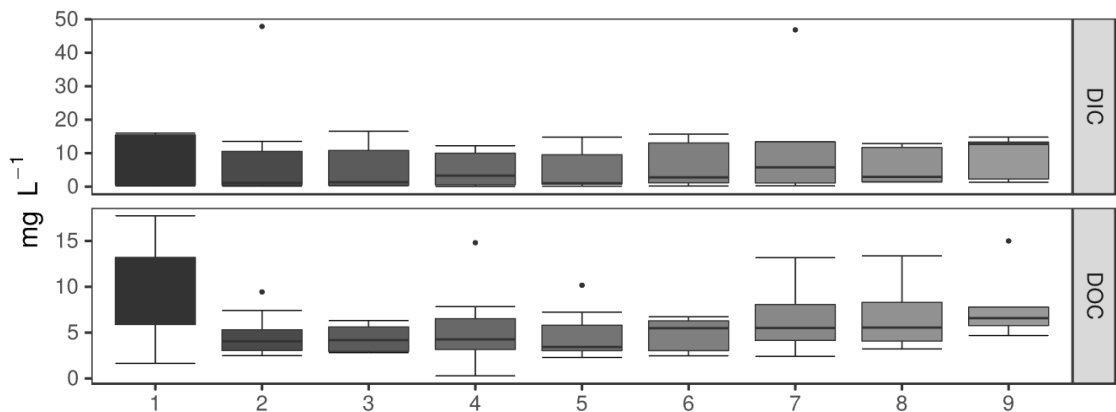


Figure 5.5 Sediment fluxes along the chamber transect (1-9 represent Chamber ID) from the drier reservoir edge (chamber 1) to the wetter centre (chamber 9) during the period of drawdown.



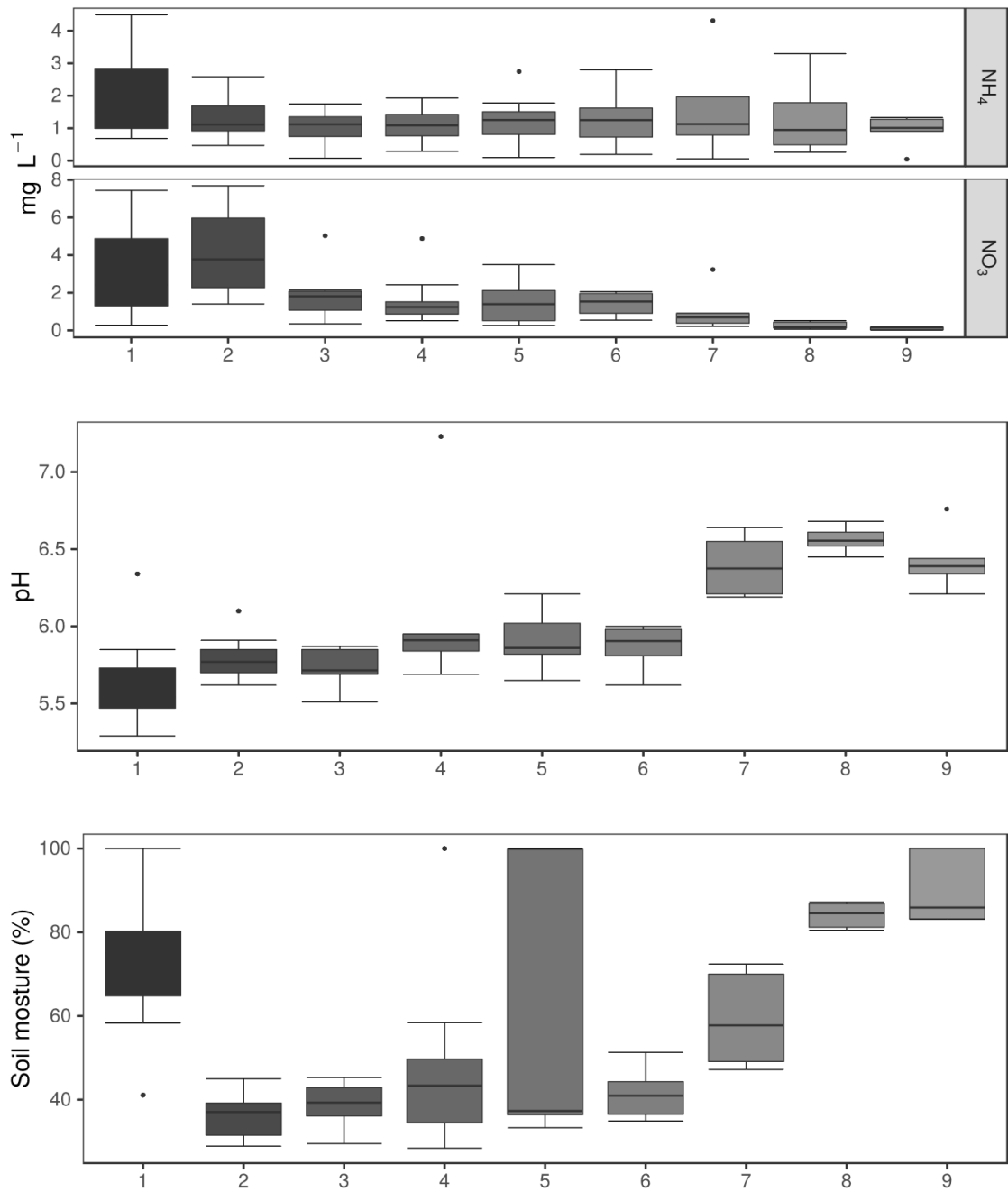


Figure 5.6 Boxplots summarising the main sediment properties measured at 5-10 cm depth simultaneously to sediment flux measurements from April to July 2016 during the period of water level drawdown at chambers 1 (reservoir littoral edge) to 9 (centre of reservoir). Further information on the sediment properties are presented in Table 5.3.

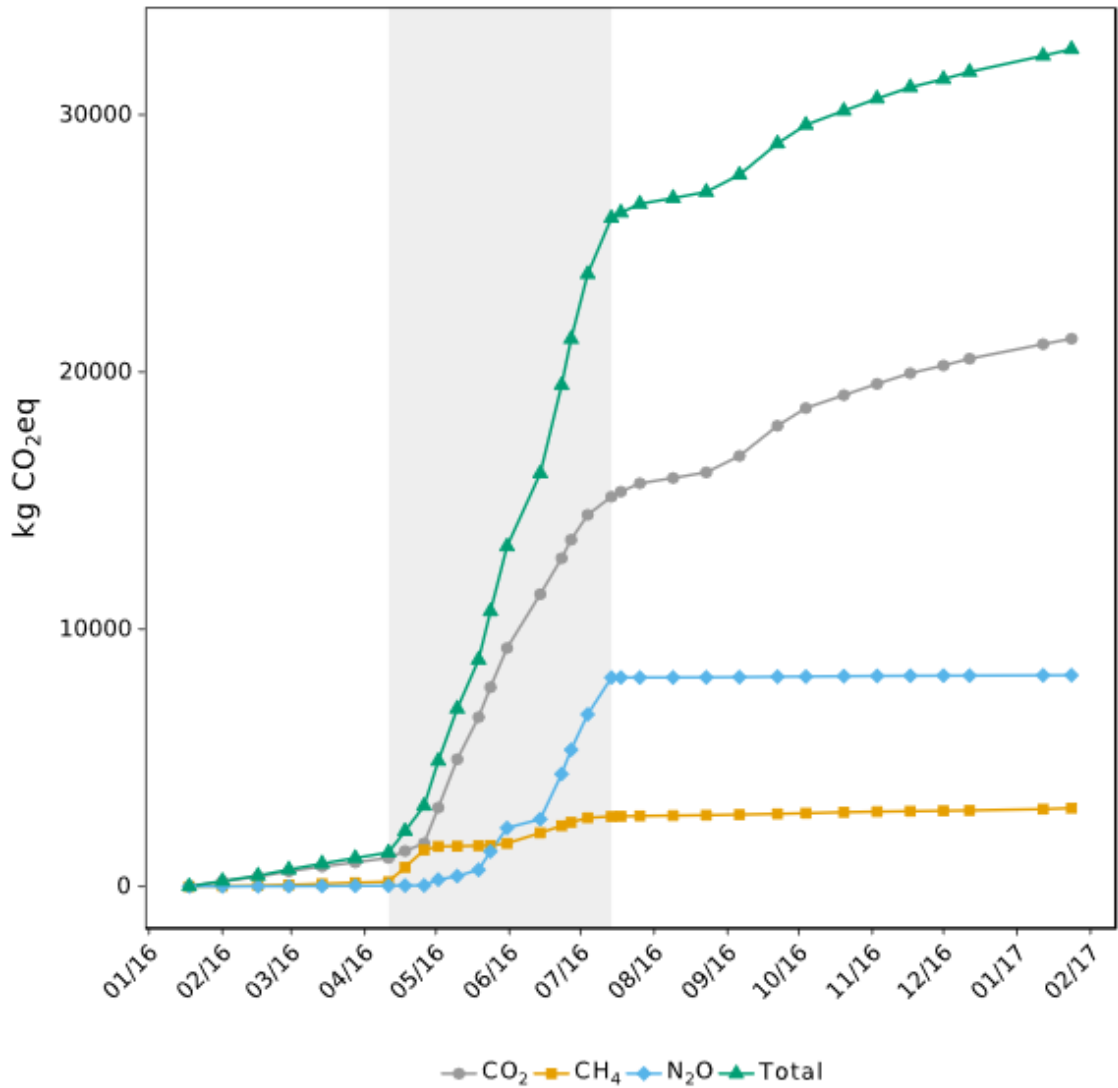


Figure 5.7 Cumulative evasion from upscaled sediment and aquatic evasion from UAV derived DEM (shown in Figure 5.1).

5.4 Discussion

5.4.1 GHG concentrations and evasion rates in the aquatic system

This research presents the first estimate of GHG concentrations and evasion fluxes from a UK reservoir, taking into consideration inputs, outputs and drawdown zone sediments. Waltersmuir reservoir was oversaturated in CO₂, CH₄ and N₂O throughout this 13 month study (Table 5.1), with concentrations greatest during the drawdown period. The oversaturation indicates that continuous release of all three GHGs to the atmosphere is possible, from a smaller water surface area during warmer spring and summer months. Our results show large increases in estimated GHG reservoir surface concentrations during the drawdown period.

5.4.1.1 Carbon dioxide

The origin of CO₂ in the inlet stream has been observed elsewhere as a result of high CO₂ concentrations in soil water, which is released as excess gas when reaching surface waters (Hope et al., 1997; Prairie et al., 2017). This pathway is more important in low order streams such as Waltersmuir's inlet, but is unlikely to influence the reservoir CO₂ balance as the stream is small, and that the mass influx is too small to be equal to the reservoir DIC (Butman and Raymond, 2011; Prairie et al., 2017). Furthermore, the higher CO₂ concentrations in the reservoir compared to the inlet indicate that this could not have been the primary source of CO₂ emissions from the reservoir. The reduction in CO₂ concentration from the reservoir to the outlet can be caused by degassing as water leaves the reservoir (Deshmukh et al., 2016).

The higher concentrations seen in Waltersmuir reservoir compared to the inlet (Table 5.1) is likely explained by in-situ degradation of allochthonous DOC and POC in the bottom sediments or water column by photochemical and/or microbial processes (Pace and Prairie, 2005). In addition, the longer water residence time in the reservoir is also a key factor in the conversion of DOC into CO₂ (Prairie et al., 2017; Sobek et al., 2007; Vachon et al., 2017), along with increased evaporation can also lead to increased CO₂. A reduction in DOC, however, was not observed from inlet to reservoir, which would have corroborated this hypothesis. In fact, DOC concentrations were actually higher in the reservoir and outlet than in the inlet stream, particularly in the post-drawdown period, which is consistent with the general tendency for net DOC production in nutrient-enriched water bodies, resulting from autochthonous primary production (Evans et al., 2017). Primary production would be expected to consume CO₂ from the water column, and could help to explain the lower level of CO₂ supersaturation during the post-drawdown period. A further contributor to both CO₂ emissions and DOC production at this time could be the addition of daily fish feeding in late August, adding both nutrients (P and N) and carbon to the system.

In the absence of higher CO₂ in the inflow compared to the reservoir, or reduced DOC in the reservoir, it appears that another mechanism is required to explain the high rates of CO₂ evasion during the drawdown period. One potential mechanism is that CO₂ is also produced by oxidation of CH₄ by methanotrophs (Guérin and Abril, 2007). This could be an explanation for the co-occurrence of peaks in CH₄ and CO₂ concentrations during drawdown at Waltersmuir. Evasion is also controlled by the concentration gradient and gas transfer velocity, with the inlet and outlet impacted by turbulence, with wind being more important in the reservoir. The gas transfer rate is likely the dominant control in the moving water, whereas the concentration gradient is more important in the reservoir. The observed CO₂ and CH₄ peaks

could also be explained by the gases being forced out the sediment by hydrostatic pressure (DeSontro et al., 2011).

In the last two weeks of drawdown, vegetation began to emerge in the desiccated sediment of the littoral zone, with the potential to retain C and nutrients in the system (Reverey et al., 2016). Following the refilling of the reservoir, an increase in CO₂ concentrations was detected in the reservoir and outlet (but not the inlet), which could be linked to plant dieback and decomposition upon submersion, or increased moisture triggering a microbial response with now more nutrients available.

In a synthesis paper by Aufdenkampe et al. (2011) median areal CO₂ outgassing in temperate zone (25-50°) lakes and reservoirs is estimated at 80 g C m⁻² yr⁻¹, with boreal and arctic (50-90°) lakes and reservoirs estimated at 130 g C m⁻² yr⁻¹. Median CO₂ evasion at Waltersmuir (56°N) is lower than these estimates at 65 g C m⁻² yr⁻¹. Waltersmuir's observed CO₂ concentrations are similar to those from Nam Theun 2 Reservoir, Laos, where concentrations ranged from 1 to 3500 µg C L⁻¹, with 85% of all measurements showing supersaturation (Deshmukh et al., 2018). This might be unexpected, as Waltersmuir is much older (more than half a century vs. a decade) and located in a northern temperate climate rather than the warmer monsoon subtropical climate, both factors linked to lower reservoir C emissions that would be expected at Waltersmuir compared to the Laos reservoir (Barros et al., 2011). There are also a lack of temperate reservoir drawdown studies to make comparisons in more similar climate systems.

Mixed effects modelling found a significant relationship of increased CO₂ with decreased pH. Many previous studies have also reported the same relationship (Crawford et al., 2013; Waldron et al., 2009; Wallin et al., 2013) and, in fact, pH is widely used to estimate pCO₂ when direct measurements are unavailable. Over the pH range observed at Waltersmuir (Table 5.1) most carbon is stored as dissolved CO₂ (Hofmann and Schellnhuber, 2010) and so is readily available for degassing.

5.4.1.2 Methane

Maxima in CH₄ concentrations (Figure 5.3) were coincident with rainfall events (Figure 5.2), which largely refilled the reservoir from near-minimum water levels during drawdown. This is in contrast to the storm event of late September 2016, which had no effect on water level and also no visible effect on GHGs. Variation in hydrostatic pressure with water level plays an important role in regulating CH₄ emissions (Harrison et al., 2017; Beaulieu et al., 2017). A potential explanation of these peaks is that increasing hydrostatic pressure with water level at

Waltersmuir allowed CH₄ to accumulate in sediment, and this was subsequently released to the water column once the water levels dropped (the reservoir still being in drawdown) and the system equilibrated to the restored lower hydrostatic pressure (Beaulieu et al., 2017). This process has been shown to induce ebullition in both reservoirs and tidal estuarine environments (Beaulieu et al., 2017; Deshmukh et al., 2014; Eugster et al., 2011; Harrison et al., 2017).

Whilst ebullition is not accounted for in this study, it was estimated that the drawdown period disproportionately contributes to annual fluxes. It is likely that the relative importance of this period would be even more significant with ebullition included and therefore further study is needed to accurately quantify this important pathway. For example, Beaulieu et al. (2017) found ebullition measured to contribute 94% of CH₄ emissions, including 3% from a 24-hour experimental drawdown, from a eutrophic reservoir in the USA. They also found surface reservoir dissolved CH₄ ranged from 0.4 to 843 µg C L⁻¹ with an overall mean of 18 µg C L⁻¹. Waltersmuir's highest concentration was 47% of their maximum, but Waltersmuir's mean concentration was 37% higher than their reservoir mean surface CH₄ concentration. A broader study of USA reservoirs by Harrison et al. (2017) found ebullition during drawdown alone to contribute to more than 90% of annual CH₄ emissions.

Mixed effects modelling found a significant relationship of increased CH₄ concentration with DIC. Key sources of DIC (dissolved CO₂, H₂CO₃, HCO₃⁻, and CO₃²⁻) in freshwater are bedrock and mineral dissolution, biogenic CO₂ and atmospheric CO₂ (Butman and Raymond, 2011; Wallin et al., 2011). Catchment bedrock at Waltersmuir is dominated by basalt (54%), sandstone (28%) and conglomerate (15%) so bedrock and mineral dissolution is likely not an important factor. (Xiong et al., 2007) also found a positive correlation with CH₄ fluxes and DIC in the water column of a fish farm in China, hypothesising a link with the need for a supply of carbon in order for microbial production of CH₄, and an increase in DIC, POC, and DOC with the decay of organic matter in the sediment. Dinsmore et al. (2013) proposed that observed patterns in stream water DIC and CH₄ could be a product of temperature dependent water solubility, but we did not find a significant relationship between water temperature and DIC or CH₄ concentrations at Waltersmuir. Anaerobic microbial communities in cold, anoxic, and saturated soils degrade organic C, producing both CO₂ and CH₄ through fermentation, anaerobic respiration and methanogenesis (Lee et al., 2012). The correlation between DIC and CH₄ could therefore, be an effect of anaerobic CO₂ production simultaneously to the production of CH₄. Houser et al. (2003) suggested the amount of DIC at depth, in excess of the surface concentration, is a measure of the significance of anaerobic microbial CH₄ production.

They found, past a minimum threshold concentration of excess DIC, CH₄ increased in direct proportion to excess DIC. This Waltersmuir study did not collect measurements of DIC at depth, which would allow evaluation of the relevance of this result. Methane evasion from Waltersmuir reservoir water surface averaged $0.16 \pm 0.06 \mu\text{g m}^{-2} \text{ s}^{-1}$ over the sampling period, with a higher rate over drawdown of $0.63 \pm 0.01 \mu\text{g m}^{-2} \text{ s}^{-1}$. Kling et al. (1991) measured CH₄ evasion from several arctic Alaskan lakes of $0.08 \mu\text{g m}^{-2} \text{ s}^{-1}$, half Waltersmuir's annual figure. Surface evasion from Lake Hallwil (Switzerland) measured between June 2015 and August 2016 averaged $9.6 \text{ mg m}^{-2} \text{ d}^{-1}$ which is comparable to Waltersmuir annual mean of $10.4 \text{ mg m}^{-2} \text{ d}^{-1}$ (Donis et al., 2017).

5.4.1.3 Nitrous oxide

Although many studies of N₂O emissions have focused on lotic systems (Beaulieu et al., 2008; Venkiteswaran et al., 2014), relatively few have examined lakes or reservoirs (e.g. Guérin et al., 2008; Huttunen et al., 2002; Beaulieu et al., 2015). Longer residence times in lentic systems allow more extensive N processing (Beaulieu et al., 2015), suggesting they may be important N₂O sources. Further, reservoirs may support even higher N₂O emissions due to higher N loading and processing rates (Harrison et al., 2009).

Waltersmuir exhibited oversaturation in N₂O throughout the study period, consistent with reports from a variety of lakes and reservoirs (Guérin et al., 2008; Liu et al., 2011), reinforcing the suggestion that many lentic systems are a source of N₂O to the atmosphere. Beaulieu et al. (2015) found 80% of 20 reservoirs surveyed in the USA to be oversaturated with N₂O, with only one being undersaturated.

Mixed effects modelling found a significant relationship of increased N₂O with TIN. Positive correlations between N₂O and NO₂⁻ and NO₃⁻ have been reported for a variety of freshwater ecosystems including small streams (Baulch et al., 2011; Beaulieu et al., 2008) and reservoirs (Liu et al., 2011). A potential explanation for this correlation could be the production of N₂O as a by-product of nitrification (Thuss et al., 2014). Although NO₂⁻ concentrations at Waltersmuir were low, and in-situ nitrification is the most important source of NO₂⁻ in the epilimnion of lakes and reservoirs (Beaulieu et al., 2015), the magnitude of nitrification-driven N₂O also depends on NH₄⁺ concentration (Hu et al., 2013). NH₄⁺ was more available than NO₂⁻, with maximum concentrations occurring during drawdown (Table 5.1). A study by Hu et al. (2013) observed a rapid increase in N₂O concentration with increased fish feed load; but this was not seen at Waltersmuir.

5.4.2 GHG fluxes from exposed sediments

Waltersmuir's sediment flux was not explained well by the measured environmental variables, suggesting flux rates are determined either by a large number of weak mixed model effects, or by variables which were not measured.

5.4.2.1 Sediment CO₂ flux

High CO₂ emissions (on the order of g CO₂ m⁻² d⁻¹) have been reported from dry sediments in rivers, reservoirs and ponds (Gómez-Gener et al., 2016, 2015; Hyojin et al., 2016; Obrador et al., 2018). CO₂ flux at Waltersmuir varied by a factor of almost 6 between the location, from 12.3 g m⁻² d⁻¹ at chamber one to 2.1 g m⁻² d⁻¹ at chamber nine (and a mean of 6.5 g m⁻² d⁻¹). Hyojin et al. (2016) conducted chamber CO₂ flux measurements along a transect in the drawdown area of Soyang reservoir, South Korea. They also found large spatial variation (by more than a factor of 20), but found the reverse pattern of higher fluxes closer to the water: around 100 g m⁻² d⁻¹ for the chamber closest to the water edge, and 44 g m⁻² d⁻¹ for the chamber that was flooded less. Observations from the drawdown area of the Three Gorges Reservoir, China were closer to those at Waltersmuir, averaging 11.0 g m⁻² d⁻¹ (Li et al., 2016). A later study found the drawdown area sediment emitted CO₂ at up to 6 times the rate of diffusion from reservoir surface water (Deshmukh et al., 2018).

Waltersmuir's highest sediment CO₂ fluxes were in the upper littoral zone area, decreasing towards the centre of the reservoir (Figure 5.5). Fluxes also changed from initial exposure to rewetting temporally. During longer desiccation periods, microbial activity is likely to be reduced (Schimel, 2007) and a decreasing pH might further reduce activity (Xiang et al., 2013). This is consistent with Fromin et al. (2010), who found that sites which were drier for longer (as with those situated at the reservoir edge) showed the highest CO₂ flux. However, Weise et al. (2016) found in an experimental study that the highest fluxes were from sediments exposed to cycles of drying and rewetting.

During the last two weeks of drawdown, the emergence of *Persicaria hydropiper* and *Littorella uniflora* could also have contributed to the higher fluxes observed in the littoral zone chambers, as root respiration can account for 55% of surface CO₂ (Andrews et al., 1999). Gas diffusion may also be increased by changes in sediment texture and porosity (Cable et al., 2008). Obrador et al. (2018) found similar patterns in a study of temporary Mediterranean ponds where exposed, vegetated sediments had higher CO₂ fluxes than the exposed, bare sediments during the autumn-spring period where water was present. Although these temporary ponds were overall CO₂ sources (mean 4.74 g m⁻² d⁻¹), they also found negative

fluxes in four ponds during the 'wet' spring. Other recent studies on temporary aquatic systems have found them to be active sites of CO₂ emissions during their dry phases (Gómez-Gener et al., 2016; Schiller et al., 2014).

During drawdown, the Waltersmuir sediments were exposed to cycles of drying and rewetting. When dry, these sediments were more exposed to UV radiation, which can kill large proportions of microbial biomass (Hunting et al., 2013). UV can also cause photo-degradation and -dissolution, which can change the chemical composition of organic matter by degrading recalcitrant fractions and producing CO₂ (Mayer et al., 2011).

Waltersmuir's sediments exhibited desiccation during drawdown (Figure 5.1), and these cracks can enhance O₂ penetration, altering biogeochemical processes and nutrient fluxes (Caraco et al., 1989). Also, release of labile organic material may be enhanced under drier conditions due to higher oxygen availability (Fierer et al., 2003). With desiccation comes reduced CO₂ outgassing, ammonification, and nitrification, leading to an increase in labile organic C and N in the sediment, while anaerobic processes such as methanogenesis and denitrification are inhibited (Arce et al., 2015, 2014; Reverej et al., 2016).

5.4.2.2 Sediment CH₄ flux

Large variations in CH₄ flux measurements have been reported from the few available reservoir sediment drawdown studies. The higher fluxes reported by Chen et al. (2009) were from a newly created drawdown area. The CH₄ sink of -33.2 mg m⁻² d⁻¹ in the drawdown sediment reported by Li et al. (2016) was explained by increased air temperature and solar radiation promoting soil and root respiration. A later study by (Yang et al., 2014) found a similar spatial pattern to Waltersmuir, with CH₄ flux increasing by three orders of magnitude along a transect from dry land to open water (mean of 0.024 mg m⁻² d⁻¹ to 74.4 mg m⁻² d⁻¹). Although comparable to Waltersmuir at the low end, Waltersmuir's chamber 8 exceeded this higher figure by a third, and chamber 9 by almost a factor of 3. Yang et al. (2014) explain this pattern by fluctuating water levels affecting sediment properties such as C, N, bulk density and redox. The littoral zone CH₄ flux of the Miyun Reservoir, China was 6.5 times higher than open water flux (31.2 mg m⁻² d⁻¹ and 4.8 mg m⁻² d⁻¹, respectively) (Yang et al., 2012) and similar to Waltersmuir's mean CH₄ flux across chambers. A study of summer drought in a Mediterranean fluvial network found low (mean 3.2 mg m⁻² d⁻¹) CH₄ fluxes in dry river and impoundment bed sediments, comparable to Waltersmuir's upslope chambers 1-5. Likewise, sediment CH₄ flux in an Amazon lake decreased from mean 14.2 mg m⁻² d⁻¹ to zero when exposed to air (Koschorreck, 2000).

Greater CH₄ flux is seen at chambers 8 and 9 (Figure 5.5) which experienced more frequent inundation and less desiccation, creating more favourable anaerobic conditions for CH₄ production. Net methane production has been found to begin at soil moistures above 60% WFPS in a study on tropical and temperate soils (von Fisher and Hedin, 2007). Both chambers 8 and 9 at Waltersmuir averaged at least 86% WFPS, with chambers 1-6 each averaging below the 60% threshold. Water level fluctuations have also been found to reduce microbial populations and consequently reduce CH₄ production, even after water levels and anoxic conditions recover, as there is a delay in returning to favourable redox conditions (Freeman et al., 1994).

Hotspots of CH₄ emissions have been found in areas of increased sedimentation, caused by promotion of organic matter delivery to anoxic sediments (Beaulieu et al., 2016; DeSontro et al., 2011). Chambers 7-9 were located at the bottom of the reservoir and had higher DOC concentrations than the slope chambers, potentially from increased sediment erosion and organic matter delivery to the bottom of the basin.

CH₄ production can also be inhibited by acidic sediment, particularly below a pH of 5.5 (Achnich et al., 1995). At Waltersmuir, chambers 1-6 each had mean pH below 6, with chambers 7-9 averaging between 6.4 and 6.6. As highlighted in section 5.3.3, chambers 8 and 9 had very low NO₃⁻ concentrations compared to chambers 1-7, around 20 times less. Peters and Conrad (1996) found methanogenic microbial community growth occurs when alternative electron acceptors such as NO₃⁻ are depleted. Following the drop in hydrostatic pressure, CH₄ in the sediments could have been rapidly released through ebullition (Beaulieu et al., 2017; Deshmukh et al., 2014) but not captured at this study's measurement frequency. For example, in an Amazon floodplain lake, CH₄ emissions were only observed during the first few days after drying and became negligible in the dry sediments for the rest of the study period (Koschorreck, 2000).

Another explanation for lack of driving variables in the sediment mixed effects model is that a large proportion (89%) of measured CH₄ fluxes were statistically indistinguishable from zero at the 95% confidence level. In these desiccated sediments, the increased O₂ penetration discussed above can also inhibit methanogenesis (Meronigal et al., 2004), although some studies did find low rates of CH₄ production in dry, oxic soils (von Fischer and Hedin, 2007). Methanogens have also been found to be more sensitive to desiccation than O₂ exposure in an experiment on dry paddy soil (Fetzer et al., 1993).

5.4.2.3 Sediment N₂O flux

When comparing Waltersmuir's sediment fluxes to other studies e.g. Li et al. (2016) also studied sediment N₂O flux from the drawdown zone of the Three Gorges Reservoir, China, finding a mean of 3.6 mg m⁻² d⁻² (less than a quarter of Waltersmuir's mean), and linking a reduction in N₂O emissions to changes in physical sediment properties caused by the varying water levels. At a shallow temperature estuary in the USA, sediments were on average a small net N₂O sink of -0.024 mg m⁻² d⁻¹, but fluxes ranged from negative to positive (-0.105 to 0.082 mg m⁻² d⁻¹) (Foster and Fulweiler, 2016).

As with CH₄, a high proportion (82%) of measured fluxes were statistically indistinguishable from zero (at the 95% confidence level). Although this lack of variance limited our explanatory power, that these values were so low is informative as there are very few reports in the literature of N₂O emissions from drawdown areas and so this makes a contribution. The low NO₃⁻ concentrations in Waltersmuir sediment could reflect insufficient supply from impaired nitrification due to the drying effect on the sediment (Mikha et al., 2005). NO₃⁻ was found to be negligible in the saturated sediment most likely due to anaerobic conditions, increasing as the sediment dries out and mineralisation occurs, and then decreasing again as the sediment desiccates.

5.4.3 Upscaling of sediment and aquatic evasion

Upscaled evasive fluxes suggest that the drawdown period contributed a large percentage (CO₂ 53%, CH₄ 77% and N₂O 98%) of Waltersmuir's total GHG emissions, which is a similar result to other studies (e.g. Chen et al., 2009; Harrison et al., 2017). Methane emissions from a eutrophic USA reservoir during an annual drawdown were found to constitute more than 90% of annual CH₄ emissions (Harrison et al., 2017). In the Three Gorges Reservoir, Yang et al. (2012) estimated that drawdown area CH₄ emissions accounted for 42-54% of the total CH₄ surface water emissions. Beaulieu et al. (2017) found the drawdown period constituted 67% of the annual CH₄ flux also in a eutrophic USA reservoir, and like this study, did not directly account for ebullition. That we did not capture ebullition flux means this research may have underestimated aquatic CH₄ flux. These spikes also suggest that the system is highly-dynamic which will not be well reflected in the weekly sampling regime, with the first initial drop in water level likely to generate an episode of CH₄ efflux. The inclusion of sensors and/or eddy covariance measurements has the potential to improve temporal understanding during these short lived and often missed, episodic events when water levels are changing.

In the Nam Theun 2 Reservoir, Laos, Deshmukh et al. (2018) estimated over a 4-year survey period, that CO₂ emissions from the drawdown area contributed to 40-70% of total reservoir

emissions. Such result is comparable to Waltersmuir's CO₂ contribution (53%) but also highlights the importance of longer-term sampling as GHG emissions are temporally highly variable. Results from Waltersmuir support existing understanding, and adding the first UK drawdown study also suggests that results are similar to CO₂ and CH₄ in other regions, but still little is known about the contribution of drawdown to N₂O emissions. The results from Waltersmuir and other studies also suggest that there could be potential for reservoir management strategies to reduce GHG emissions during periods of water level drawdown, especially if planned as was the case at Waltersmuir. For example, the rate of water level change could be further controlled so that it is low enough to not cause large episodes of ebullition. If CH₄ could be held within the sediment for longer to maximise oxidation, this could result in greater release of CO₂ which is a less potent GHG (Beaulieu et al., 2018).

Although there is no evidence to suggest the chamber transect is atypical (extending from reservoir shoreline to centre, covering changes in elevation and sediment properties), it inevitably only provides partial coverage of the total exposed sediment area of the reservoir, and could only be sampled periodically. Emissions of all three GHGs can be highly variable in both space and time, and uncertainties in estimated total evasion are therefore large. Previous studies have used the average emission rate multiplied by the surface area of the zone where emissions were measured from (Abril et al., 2005). An area that has received relatively little attention is the river-reservoir sediment transition zone. Beaulieu et al. (2017) found diffusive CH₄ fluxes there to be 10 times larger than in the main reservoir body of a eutrophic Midwestern USA reservoir, but few other studies exist.

5.5 Conclusions

This research presents the first estimate of GHG concentrations and evasion fluxes from a UK reservoir, taking into consideration inputs, outputs and drawdown zone sediments. Our results show larger effluxes of reservoir surface GHG are likely during the drawdown period. Such episodic events would occur from physical displacement of accumulated sediment gases, which can contribute significantly to total reservoir emissions. This study only accounted for diffusive fluxes from the reservoir surface, as well as time-averaged fluxes from exposed sediments, but additional contributions by ebullition would likely increase CH₄ fluxes and future studies should account for this pathway (e.g. DelSontro et al., 2010). Upscaled fluxes suggest that the drawdown area was a major component of total reservoir GHGs, contributing 53% of CO₂, 77% of CH₄, and 98% of N₂O. The three-month drawdown contributed to a total of 66% of CO₂eq-weighted emissions for the year. This study adds to the growing body of evidence that suggests reservoir drawdown zones are active areas of biogeochemical cycling

and can stimulate CH₄, CO₂ and N₂O release. This research joins a growing body of literature indicating that temperate zone reservoirs (as well as those of the tropics) could generate globally significant levels of CH₄ emission (DeSontro et al., 2010; Harrison et al., 2017).

This study provides a rare insight into the potential effects of an extreme drawdown event on GHG fluxes and carbon and nitrogen transformations in the sediment, and the effect of sediment drying and rewetting on GHG fluxes. Spatial patterns of the sediment fluxes appear responsive to the chamber position from the edge of the reservoir. This was likely linked to the heterogeneous sediment structure and complex moisture gradients that changed quickly over the 11 week drawdown period, creating both aerobic and anaerobic conditions. Drying sediments produced more CO₂ but less CH₄, with CH₄ emissions occurring at the wetter chambers at the margins of the water surface. As the reservoir is drawn down, there will be a 'fringe' of high CH₄ emissions at the edge of the water surface, which will move as the water level drops, with an expanding area of high CO₂ emissions outside this wet area. These first estimates show that drying reservoir sediments are active sites for respiration and associated CO₂ release to the atmosphere with similar results being found in reservoir drawdown zones and dry streambeds (e.g. Catalan et al., 2014; Gómez-Gener et al., 2016). Future research on drawdown sediments would benefit from studies investigating microbial metabolism in drying sediments through desiccation to rewetting to provide better mechanistic understanding on the gas flux controls. Results also suggested that moisture availability and sediment structure were important factors but further research would be required e.g. investigation of how textural sediment characteristics change moisture, C and N flux under fluctuating water levels. With extreme climate events projected to occur more frequently, affecting terrestrial and aquatic ecosystem C balances (Reichstein et al., 2013) and placing increased demand on water resources, it is even more important to evaluate the effects of drawdown as a mechanism for increased reservoir GHG emissions.

Acknowledgements

This work was funded by the UK Natural Environment Research Council (NERC) from the IAPETUS Doctoral Training Programme. We would like to thank Rob Murray, manager at Waltersmuir reservoir, for granting site access and providing background management information on the reservoir. We are grateful to Ian Washbourne for assistance with % TC and TN laboratory work. We also thank Juliette Maire and Song Ling for field assistance. Thanks also goes to Bryan Spears and Alanna Moore for sediment sampling advice during planning stages, and Iain Gunn for identifying the emerging plant species. Thanks also to Simon Gibson-

Poole for conducting the UAV survey during drawdown and for putting together the DEM used for up-scaling.

6 Overall discussion, synthesis and conclusions

This discussion brings together the findings from Chapters 3 to 5 to address the aims and objectives stated in Chapter 1. The overall aim of this research was to investigate the release of greenhouse gases (CO_2 , CH_4 and N_2O) in temperate freshwater reservoirs across Scotland and North Wales. This was achieved by a field based approach which enabled the modelling of drivers of GHG concentrations from reservoirs. This chapter places the thesis within a wider context, comparing concentration and flux measurements between chapters, and to other temperature studies. Finally, the consequences of the study findings for the management of C and N concentrations in reservoirs and their catchments are outlined, along with recommendations for future research and the wider implications of the results.

6.1 Catchment comparisons: In-depth vs. seasonal sampling

The spatial survey in Chapter 3 also included Baddinsgill, Black Esk and Waltersmuir in the sampling campaigns which were also sampled more frequently as shown in Chapters 4 and 5. The question, is seasonal sampling i.e. only 4 times a year, a good enough measure of GHGs in reservoirs in Scotland and Wales? Table 6.1 shows that epN_2O is well represented in the seasonal survey with similar low concentrations found at Baddinsgill and Black Esk. However, as Waltersmuir underwent a drawdown and fish were then introduced in late summer, N_2O at Waltersmuir is underrepresented. The opposite is the case with CH_4 at Waltersmuir, with higher oversaturation in the spatial survey due to sampling within the drawdown period. Baddinsgill also provides a reasonable comparison across in-depth and spatial campaigns for GHGs. Black Esk however, shows an underestimate in CH_4 within the spatial campaign. As discussed earlier, CH_4 has more episodic release, especially when sampling from the shallow littoral zones. Results suggest that seasonal sampling provides a good estimate of GHG concentrations in relatively stable, more natural reservoirs i.e. without management interference as was the case with drawdown, especially for N_2O and CO_2 . However, CH_4 is captured most poorly in the spatial campaign which highlights the high temporal and spatial variability of CH_4 release.

Table 6.1 Illustrates the differences in seasonal vs. in-depth sampling at Baddinsgill, Black Esk and Waltersmuir reservoirs as mean excess partial pressures.

Spatial	Mean Excess partial pressure		
	epCO ₂	epCH ₄	epN ₂ O
Baddinsgill	3.1	24	1.2
Black Esk	5.0	87	2.2
Waltersmuir	3.4	174	1.3
In-depth			
BA1res	2.5	31	1.2
BA2res	3.8	29	1.4
BA3res	2.5	19	1.1
BE1res	5.3	131	1.5
BE2res	3.1	154	1.3
BE3res	3.8	114	1.6
Waltersmuir	3.7	128	2.2

A summary of mean reservoir GHG fluxes in CO₂-equivalents from the spatial campaign in Scotland and Wales, and also the in-depth reservoirs from Chapters 4 and 5 are provided in Figure 6.1. In terms of CO₂, Black Esk the largest contributor which likely reflects the forest felling, high DOC loads to the catchment and increased capacity of the reservoir providing a fresh labile carbon supply to the system. Waltersmuir shows largest CH₄, N₂O and total flux of all the sampled reservoirs, most likely due to the very different management regime with extreme water level fluctuations, as well as the addition of extra carbon and nitrogen in the aquaculture feed.

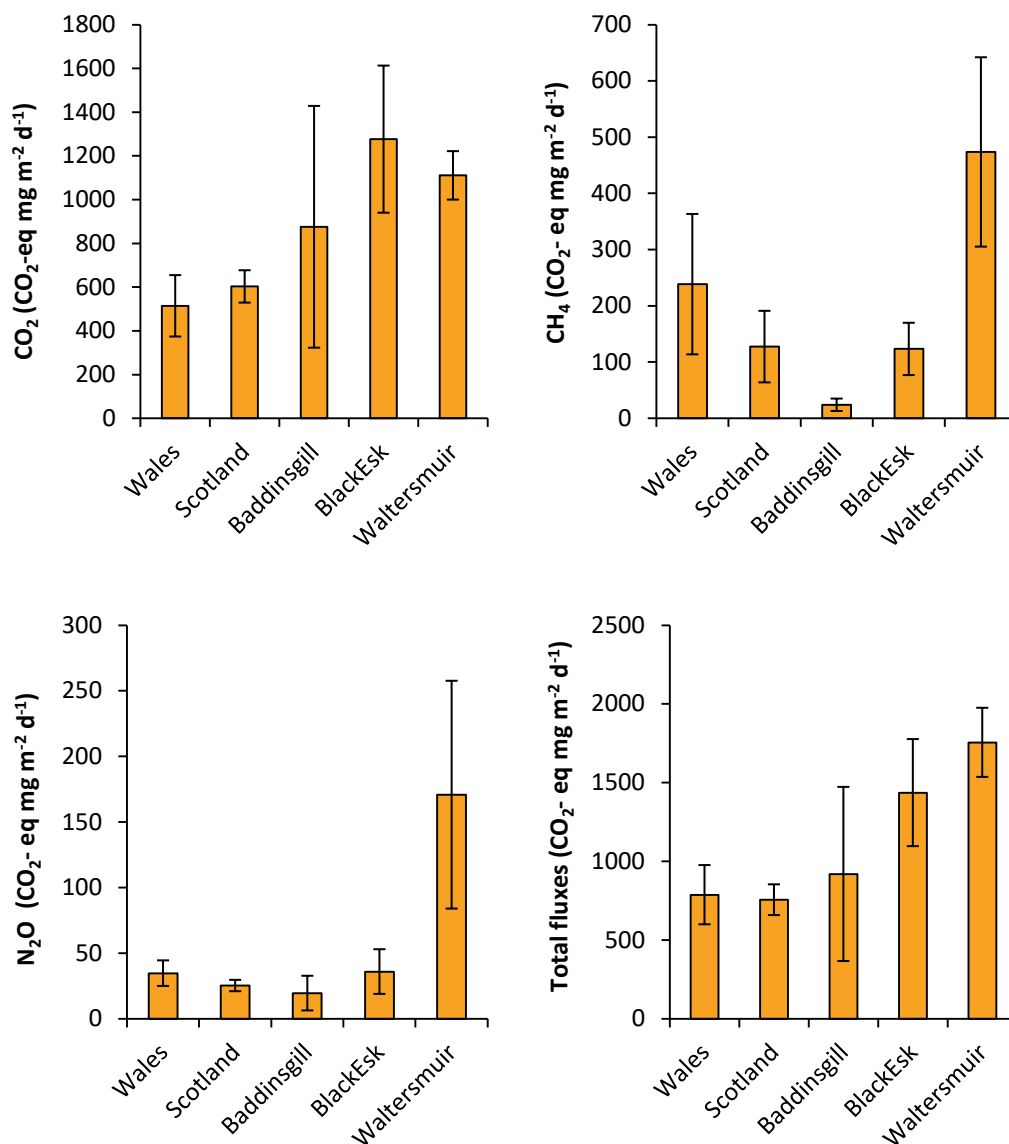


Figure 6.1 Summary of mean reservoir GHG fluxes in CO₂-equivalents from Scotland, Wales and the in-depth sampled reservoirs. N₂O and CH₄ were multiplied by their 100-year GWP, (IPCC, 2014). All values are in mg CO₂-equivalents m⁻² d⁻¹ and expressed as mean ± standard error. Values are only for aquatic evasion within the reservoirs i.e. excluding stream and sediment evasion.

6.2 Recommended further research

Following the results and discussions in this thesis, and to build upon the work accomplished, a number of further field and laboratory based studies could be conducted. Brief descriptions of such recommendations are made below, particularly in relation to improving process understanding of GHG dynamics in UK reservoirs. These future recommendations also recognise the limitations in the current studies methodological approach i.e. lack of ebullition

measurements and sampling from the middle of the reservoir and at depth. As with most studies, this research can also be improved by a greater number of replicates, a more frequent sampling regime and longer time series.

Depth and spatial surveying: As sampling was only permitted from the bank edge of the reservoirs, this research would benefit from boat sampling campaigns to fully capture spatial variability in C and N concentrations and GHG evasion across the surface of the reservoir. This could be achieved through seasonal, or summer and autumn campaigns at both Baddingsgill and Black reservoirs. At the same time, water samples could be collected at different depths to determine if C and N concentrations change, and temperature profiling could be conducted using a thermistor chain to assess stratification. This would also help determine whether the bank samples collected are representative of the reservoir system or only reflect the water quality in the topmost layer if stratified.

Ebullition: The drawdown zone of reservoirs can be important areas of ebullition, for example, due to changes in hydrostatic pressure and increased contributions of terrestrial derived organic matter as discussed previously. An ebullition campaign would be particularly beneficial at Waltersmuir reservoir (Chapter 5) during the drawdown period to further quantify the CH₄ pathway as water levels fluctuate and more accurately quantify the annual reservoir emissions. As ebullition flux is episodic in nature, exclusion of this pathway could lead to an overall underestimation in total reservoir CH₄ flux measured at Waltersmuir reservoir. Future research should determine the importance of ebullition as a conduit of GHGs from UK reservoirs to the atmosphere, especially since it is often poorly quantified and infrequently studied. In doing so, a more complete GHG budget for the reservoirs would be achieved.

This would also require boat work, which could be conducted alongside the above suggestion. The spatial variability in this pathway could be investigated by a series of transects from the littoral edge to the middle of the reservoir (shallow to deeper regions, with greatest ebullition expected to occur in shallower waters i.e. <10 m) (DeSontro et al., 2010). If conducted seasonally, this would provide information on the magnitude of CH₄ through this pathway. The most common method for measuring ebullition is by employing inverted funnels coupled to gas collectors to capture the ascending bubbles. As ebullition is intermittent, funnels should be left out over several days but to avoid CH₄ diffusion from the funnel material and de-dissolution in the water, samples should be collected within 24 hours. If left longer, fluxes could also be underestimated due to microbial oxidation of the trapped CH₄. Alternatively, ebullition could also be measured by hydroacoustic techniques or eddy covariance towers (e.g.

DelSontro et al., 2010, 2011; Eugster et al., 2011). Hydroacoustics quantifies ebullition indirectly based on bubble size and density in the water column. Consideration would need to be given to flux tower placement, i.e. the centre of the reservoir would be optimum, so the flux footprint covers greatest area of bubbling. This would be the least intrusive method to provide near-continuous (30 min scale) to measure total fluxes (Schubert et al., 2012)

Continuous sensor measurements of C species: Results from Chapters 3-5 showed both high spatial and temporal variability in C species from spot sampling. Such measurements are time-consuming to collect and analyse by gas-chromatography but have been very useful in providing a broad interpretation of environmental processes, but it limits comprehension of processes that are highly variable in space and/or time. Concentrations of dissolved CO₂ in two of the Black Esk inlet waters were determined continuously using Vaisala CARBOCAP non-dispersive infra-red (NDIR) CO₂ sensors (e.g. Johnson et al., 2010), along with stage height, water temperature, electrical conductivity, pH and dissolved oxygen. Results are not presented in this thesis due to issues with the equipment and more data quality checks being required beyond the timescale of this PhD project. To provide more insights into C dynamics within aquatic systems, particularly short-lived hydrological events or in the case of water level fluctuations during drawdown, continuous measurements using sensors could be incorporated into future research. Instrumented sensors could be installed at inlet and outlet streams, and within the reservoir itself to determine the concentrations of CO₂ and a range of hydrological parameters. Due to the often remote location of reservoir catchments, thought would need to be given to power supply and site accessibility of sensor equipment. Future work would also be beneficial to develop a method that would allow continuous monitoring of the C pool simultaneously (CO₂, CH₄ and DOC) to allow deeper understanding of variability and processes. For example, steps have been made using an ultraportable GHG analyser which quantifies CH₄ and CO₂ simultaneously (Gonzalez-Valencia et al., 2014) and Boulart et al. (2010) provides a review of in-situ dissolved methane sensors for marine applications that could be adapted to inland waters. Near continuous DOC sampling measurements exist using pump samplers (e.g. Clark et al., 2008) or continuous automated spectrophotometric absorbance methods (e.g. scan and spectrolyser; Koehler et al., 2009) will help capture changes in both DOC quantity and quality from shifting pathways and sources as well as changes due to in-stream biogeochemical transformations at scales that would not be captured using 'grab samples'.

In Chapter 5 at Waltersmuir reservoir, GHG concentrations showed episodic pulsing during the drawdown period as water levels fluctuated. This needs to be considered in greater detail as it may lead to error in emission estimates in up-scaled estimates from infrequent sampling

regimes. Either high-frequency measurements using eddy covariance techniques, sensors or a sampling regime which allows a quick response to rainfall events in addition to standard periodic measurements may therefore provide a basis for further investigation into the peaks in GHG concentrations observed in Waltersmuir during drawdown. The floating walkway surrounding the salmon cages at Waltersmuir would be an ideal location for high frequency measurement equipment to be installed, allowing real time changes in drawdown to be quantified as well as system-level emissions if eddy covariance was used. An extended temporal study (i.e. over at least a 3-year period) would help build a fuller picture of the temporal dynamics of drawdown on C and N fluxes within reservoirs. The longer timescales would permit the inclusion of a more 'normal' drawdown year outside an extended period used for dam wall maintenance in this study. The opportunity to continuously sample from the on start, throughout, and during the full refilling of the reservoir would require closer communication with the water company or reservoir manager to ensure sampling efforts captured specific lowering and refilling events. In addition, data sampling from another reservoir also undergoing planned drawdown in a different geographic location will help account for different catchment characteristics and management regimes, as well as adding to the limited amount of C and N data from drawdown monitoring.

Radiocarbon dating and isotopic signatures: To quantify the role of inland waters on GHG emissions, it is important to understand the hydrological and biological processes that link sources in the terrestrial system to aquatic fluxes (Vonk and Gustafsson, 2013). The differences in concentrations seen between the inlets, reservoirs and outlets in Chapters 4 and 5 suggest that there are different processes occurring within streams and reservoirs. Future work that incorporates radiocarbon (^{14}C) analysis and following the method of e.g. Garnett et al. (2015) would provide a unique tracer that can be used to identify the source of CO_2 , CH_4 and DOC, and quantify the time between C fixation and return to the atmosphere in both reservoirs and streams. This would also help answer questions such as how much DOC is retained within the reservoir, how much carbon is lost to CO_2 or CH_4 , how much to the sediments, and are 'old' C stocks in the reservoir being degraded? An example of such understanding is presented in a study on riverine C release from four UK peatlands by Billett et al. (2007). They found a significant difference between the isotopic signature of DOC and CO_2 lost by surface water evasion, with results indicating that CO_2 and DOC released from peatlands are somewhat decoupled and potentially controlled by different mechanisms (hydrological vs. biogeochemical) and sources (biogenic vs. geogenic). Samples for ^{14}C analysis

of CO₂, CH₄ and DOC could be collected over 3-4 seasons from a range of reservoir types and ages.

Greenhouse gas evasion: Evasion is an important component in catchment carbon and GHG budgets that is controlled by two key factors; the concentration gradient across the water-air boundary and the gas transfer coefficient which represents the physical rate that gas evades across the boundary (Billett et al., 2004; Garnett et al., 2015). Evasion was estimated in Chapters 3-5 but future work should directly measure the gas exchange coefficient (k) for both streams and reservoirs. For example, K could be calculated using sulphur hexafluoride (SF₆) via a whole-reservoir trace-gas spike and/or by the flux rate of SF₆ in flux chambers (Denfeld et al., 2013; Garnett et al., 2015). Further research is also needed to develop methods and models that would allow high temporal resolution of GHG evasion rates to be estimated based on measurable stream morphological and hydrological characteristics (e.g. depth, width, slope, flow, velocity, water temperature, substrate type), and which can be tested at landscape scales to improve annual estimates of evasion loss across multiple sites. Future studies should aim to further bridge GHG exchange knowledge across disciplines, especially integrating the physical limnology component to biogeochemical studies of aquatic systems.

Aquatic plants and algae: Results from Chapter 3 suggested that GHG concentrations were affected by the presence of algae and/or aquatic plants. Future research should investigate the potential influence of plant-mediated GHG transport (e.g. Chanton and Whiting, 1995; Cole et al., 2000). For example, CO₂ absorption has been found to increase through photosynthesis by the presence of aquatic plants. Plants can also fuel CH₄ production if dense mats deplete surface water oxygen. This could be achieved by chamber measurements, similar to those used at Waltersmuir, or by a mesocosm study that can investigate fluxes from individual plant communities present in the reservoir of interest. A mesocosm approach could also allow the control of temperature and water levels to simulate different growing season conditions and under different climate scenarios.

Reservoir management: An increasing number of water companies across the UK are installing ResMix destratification systems (WEARS, Australia) aimed at improving reservoir source water quality and reduce water treatment costs (e.g. Elliott and Swan, 2013). The ResMix pumps warmer oxygen rich surface waters to deeper bottom waters where oxygen is required and can eliminate problems related to reservoir stratification and gradients in dissolved oxygen. A system was installed at Black Esk reservoir (Chapter 4) during the last sampling year but not enough information was available to evaluate, if any, the impact on edge sampling GHG

concentrations. Future work could assess the impact of ResMix operation on C and N dynamics within the reservoir and recommend changes to operation if required.

Up-scaling of GHG emissions to reservoir and UK wide scales: GHG fluxes from the drawdown area were up-scaled based on elevation range of chamber placement which was assumed to have similar sediment moisture gradients from shoreline to the middle of the reservoir spatially across the whole system. Up-scaling of point measurements of fluxes to lake-scale and regional estimates is challenging, particularly when assumptions have to be made. A big weakness of the chamber method is the inability to interpolate measurements over large scales due to the spatial variability in fluxes which can vary by several orders of magnitude over relatively short distances (Chadwick et al., 2014) as seen in Chapter 5. The spatio-temporal variability and the use of different measurements approaches (e.g. headspace, evasion calculations and static chambers) can add multiple levels of uncertainty to flux estimates and is rarely quantified in studies. The accuracy of the emission estimates is also limited by methodological constraints, particularly for CH₄ as ebullition can be the dominant pathway but the ability to accurately measure this flux is hampered by its spatio-temporal variability and difficulty in assessing ebullition rates at the system scale (Beaulieu et al., 2017).

Uncertainty can be considerable in estimating cumulative flux over the experimental period from sparse and variable measurements. Uncertainties need to be properly propagated to provide confidence intervals on emission factors calculated at the local and national scales. The methods most commonly used in the literature to calculate cumulative fluxes are i) simple averaging all measurements (e.g. Skiba et al., 2013) or ii) to interpolate and integrate by trapezoidal rule integration (e.g. Matson et al., 1996) which involved the linear interpolation between data points, calculating the area of each trapezoid formed and summing these areas as used in Chapter 5. Several shortcomings with these methods are highlighted in Levy et al. (2017) such as simple averaging gives equal weight to points, trapezoidal integration is sensitive to noise in the data, there is no straightforward way to quantify introduced uncertainty, and no information such as expectations based on weather, sediment conditions is incorporated. Bayesian approaches are being increasingly taken e.g. Levy et al. (2017) used a Markov Chain Monte Carlo method to provide uncertainties on model parameters, calculated fluxes and can also account for measurement error from chamber measurements, and a similar approach could be used to quantify uncertainties of the up-scaling approach at Waltersmuir (Chapter 5).

Another way to integrate respiration fluxes would be to derive an exponential model of instantaneous CO₂ flux vs. temperature, but due to the variation in moisture content at Waltersmuir, it could be confounded. Similarly, CH₄ and N₂O could be modelled as a function of temperature and water filled pore space. Up-scaling emissions based on predictors of GHG emission rates could result in a more accurate estimate of fluxes and once that can be up-scaled to diverse regions with divergent reservoir size. Predictive models could also include other environmental covariables that predict GHG emission rates, for example, land use and soil variables if empirical relationships with GHG emissions could be demonstrated. However, due to the few data points, and limited significant relationships found between GHGs and variables from the mixed effects modelling (Chapter 5) it was not felt that this would be a reliable approach. Basic linear interpolation between chamber measurement points makes significant assumptions which leaves room for uncertainty, and it would be important to identify areas in the reservoir sediment which may not be well represented by the sampling methodology e.g. the inlet-sediment transition zone. Other interpolation methods e.g. kriging and polynomial will also be affected by the same problem as linear interpolation due to the spatial variability of fluxes. A further advantage of using an eddy covariance method in future research, and especially in drawdown area studies, is that it can measure and integrate flux data directly over larger areas continuously without disturbing the sediment environment. An eddy covariance approach would work well in large homogeneous areas like the exposed drawdown sediment at Waltersmuir, however, it would not be able to address the issue of spatial variability in reported fluxes as seen in Chapter 5 or identify 'hot spot' areas. It is also important to note that eddy covariance also requires sensitive equipment that requires high power supply and so can be expensive (Hensen et al., 2013) which may not be practical for all projects.

Results from Chapter 3 provide insight into the magnitude of GHG concentrations and evasion from a variety of reservoir catchments in Scotland and North Wales. Due to logistical and cost limitations, sampling was restricted to the thirty sites which provided a snapshot of typical drinking water catchments in UK uplands covering a range of geologies, rainfall gradients and catchment land covers. A very similar magnitude in GHG concentrations is reported by Whitfield et al. (2011) for Irish lakes, suggesting the results provide a representative sample of UK reservoir GHG concentrations. This also suggests that up-scaling of GHG concentrations and evasion could be possible in the UK for lakes and reservoirs. Although unlikely representative of all UK reservoir types, future research efforts could be made on quantifying concentrations and evasion from reservoirs in highly degraded peatland catchments (e.g.

Pennines; Stimson et al., 2017), in catchments with limestone and/or chalk geology (e.g. in Yorkshire), and in regions with intensive agriculture (e.g. East Anglia). This further sampling, combined with utilising the GIS-based inventory of UK lake and reservoir catchments, and UK Met Office meteorological stations across different regions could permit reservoir emission up-scaling across the UK.

6.3 Implications for catchment and reservoir management and recommendations

It is important to consider how this research and proposed future research could supplement management practices that could be followed in UK drinking water reservoir catchments to minimise C and N impacts on water quality. Drinking water provision across the UK is heavily reliant on peatland-fed reservoirs, suggesting that peatlands play an important role in UK water security (Xu et al., 2018). Water supply reservoirs in the UK have an estimated storage capacity of 1.8 km³ and 73% (1.3 km³) are peat-fed (Xu et al., 2018). Approximately 1.6 km³ yr⁻¹ of mixed-source peat-fed water is consumed in the UK i.e. supporting 43% of the UK population. Across the 30 reservoirs sampled in Chapter 3, results found a median of 83% of 'HOST – Total Peat' across catchment areas where many of the sampled reservoirs are also peat-fed.

In recent years, water companies across the UK have been adopting integrated catchment management practices to reduce diffuse pollution at source in drinking water supply catchments, which also helps reduce treatment costs and meet regulatory requirements (Spiller et al., 2013). This process relies on local, catchment specific knowledge and data, including stakeholder knowledge (e.g. farmers), land use and hydrogeology. For example, Scottish Water had an ongoing catchment management programme at Black Esk and Baddingsill reservoirs (Chapter 4) prior to and through some of this PhD research looking at colour, DOC and other water quality variables (pers. comm, data not shown). Many catchment management investigations are reactionary and focus on a single pollutant issue in isolation, e.g. increased organic carbon and colour issues, which results in water companies not making the most of an integrated approach to improve drinking water quality (Bloodworth et al., 2015). At Black Esk reservoir, the catchment management and sampling programme focussed efforts at five locations, three of which ran into the main inlet stream (BE3in in this study) and samples from two inlets covered in this PhD were excluded, BE1in and BE5in, which had catchment soils of 100% dystrophic blanket peat and 100% peaty gleys, respectively. Annual mean areal DOC load at BE5in was the highest in Black Esk catchment, estimated at 105 ± 15 g

$\text{C m}^{-2} \text{ yr}^{-1}$ (Chapter 4) which is likely attributed to the high percentage of peaty soils in the catchment. The sampling frequency of the catchment management programme was also low i.e. 8 samples were collected in 2015 which increased to 11 in 2016 for BE2in which may have missed key events. Future catchment management programmes could benefit from exploring the sub-catchment characteristics first via GIS analysis to identify potential dominant pollutant sources which could help focus sampling efforts.

It can be difficult to prioritise areas of catchment management due to catchment heterogeneity and the range of pollutants that should meet the requirements of EU Drinking Water Directive (98/83/EC) and 'good' ecological and chemical status according to the EU Water Framework Directive (WFD; 2000/60/EC). In Scotland, The Public Water Supplies (Scotland) Regulations 2014 ensures high quality water supply and details acceptable levels of elements/substances in drinking water known as the Prescribed Concentration or Value (PCV). For example, pH levels should be in the 6.5-9.5 range, the PCV for conductivity is $2500 \mu\text{S cm}^{-1}$ at 20°C , nitrite is 0.5 mg L^{-1} or 0.10 at the treatment works, nitrate is 50 mg L^{-1} , ammonium 0.50 mg L^{-1} of which median levels and concentrations from the spatial survey of reservoirs in Scotland (Chapter 3) fell below the PCV.

According to Xu et al. (2018), arable and livestock hill farming are common land use activities on water-supply peatlands, especially in the UK. Of the thirty sampled reservoirs in Chapter 3, ten reservoirs had arable activities in their catchments but at very low catchment coverage (<3%), however hill sheep farming was much more common, particularly in North Wales. Cefni catchment in North Wales was found to have highest N_2O concentrations, most likely linked to the improved grassland and arable activities within its catchment from diffuse pollution. A marsh wetland immediately surrounds the reservoir with cattle and sheep farming beyond where agro-chemicals are used (Hatton-Ellis, 2015). At this catchment, riparian buffer strips or setting ponds could be implemented around the catchment. Fertiliser application is commonly used to enhance crop growth but if not managed, excess N and P can leach from soils into waters, which in turn, can induce eutrophication and lead to algal blooms, of which can be toxic. In Chapter 3, five of the reservoirs in North Wales had algae present during summer sampling, including at Cefni, Dolwen and Plas Uchaf which had highest N_2O concentrations. From a drinking water perspective, algae blooms can reduce water quality and negatively affect the treatment process e.g. by clogging filters, producing unwanted odours and tastes (Henderson et al., 2008). Water companies could implement floating constructed wetlands to reduce potential algae bloom formation, which also has the potential to reduce the

contribution of DOC release by algae depending on specific plant species used (West et al., 2017).

Both Black Esk and Baddingsgill reservoirs (Chapter 4) have managed catchments (e.g. forest felling, muirburning, grouse management, sheep farming) which can cause changes to aquatic C and N concentrations at different time periods throughout the year. Although the influence of forest felling was not specifically quantified in this study, the disturbance to the peaty soils in the catchment could potentially increase C release from what was a relatively stable C store, to the water network. Overgrazing can often lead to vegetation and peatland erosion, which can increase fluvial aquatic C loss and downstream water treatment costs (Dawson et al., 2010; Stanley et al., 2012). For example, across Baddingsgill catchment, there were numerous areas of eroding and bare soils, often in areas with high poaching from sheep and cattle and at edges of water courses (e.g. near BA1in and BA2in which saw higher areal mean DOC flux). Poaching has been found to detach sediment from both land and river banks (Skinner et al., 1997). There were many damaged fences around the catchment which allowed sheep and cattle direct access to the water courses, in such areas, fencing should be more regularly checked and maintained.

Removal of peaty sediment and DOC is the largest cost (e.g. chemical usage, labour and waste removal) in raw water treatment for many UK utility companies (Whitfield et al., 2011), and any remaining DOC can react with the disinfectant to produce harmful disinfectant by-products such as regulated carcinogens (Chow et al., 2003) and can also stimulate microbial re-growth in the distribution system (e.g. Niquette et al., 2001). For example, to meet drinking water standards, a water company in England, UK spends ~£150,000 per annum on sediment removal in the 200 km² Bamford catchment (Xu et al., 2018). In temperate regions, degradation of peatlands is thought to be increasing due to rising temperature and drought frequency (Clark et al., 2010) which could also see a rise in future sediment removal activities.

Highest inlet DOC concentrations at Baddingsgill were from BA1in and BA2in which also had high annual loads; however, BA5in had highest areal mean C flux for DOC (Chapter 4). In the UK, the largest DOC source to surface water is from catchments with high percentage of peat soils (Armstrong et al., 2010; Dawson et al., 2002). When walking between sampling locations, the area between BA1in and BA2in had old drainage ditches that were overgrown with moss and vegetation but could still be acting as a conduit for C entering the inlets and reservoirs. A handful of the reservoirs visited in Chapter 3 also had areas of bare peat surface which can contribute to high organic C loads and colour. Also at Baddingsgill, the area around BA1in,

BA3in and BA5in sampling points had exposed peaty soils and large overhanging stream banks which are exposed to wind and rain erosion. On a few sampling occasions, there was evidence of bank collapse which results in large peaty deposits being washed downstream to the reservoir. To prevent this, bank re-profiling and vegetation planting could be one possible solution to protect the peaty soils from erosion. It is recommended that on-foot inspections of the area between these two sub-catchments are carried out to identify potential restoration efforts that could be made e.g. peatland drain blocking has been found to lower DOC and colour values by 60-70% (Wallage et al., 2006).

Catchment officers employed by water companies could work closer with stakeholders (i.e. farmers, land owners, forestry commission) to facilitate local catchment knowledge, especially at a sub-catchment to km² scale where water quality monitoring can be more limited. As discussed earlier, the integration of high frequency sensor measurements into the catchments are more likely to capture water quality impacts at sub-catchment scales from catchment activities that may not be detected from manual sampling at fortnightly to monthly intervals. Water companies should continue working with research institutes and utilising PhD studentships to support the monitoring of problematic catchments to implement more frequent sampling regimes.

Scotland plays a large role in EU and International aquaculture, with being the largest producer of farmed salmon in the EU. In 2016, there were 26 sites of freshwater salmon production around Scotland (Munro and Wallace, 2016), including at Waltersmuir reservoir. Results from Chapter 5 at Waltersmuir reservoir identified increased CO₂ emissions, DIC and DOC concentrations after August which coincided with the time of fish re-stocking and daily feeding of the fish. Approximately 12 tonnes of feed with a composition of 45.2% carbon, 7.9% nitrogen and 1.4% phosphorous was used between August and March. Approximately 4 tonnes of salmon were stocked in August and 10-11 tonnes removed in March. The food conversion ratio (FCR) is commonly used in aquaculture to define the amount of dry food consumed per wet fish biomass produced (i.e. feed given/weight gain) and is an indicator of feed efficiency in fish farming, with an average FCR for salmonids to be 1.0 to 1.2 (Hasan and Soto, 2017). At Waltersmuir, this equates to approximately an FCR of 1.7 to 1.8. Improving the FCR inline with recommendations through better feed management and monitoring could have the potential to reduce GHG emissions and C from aquaculture but more research would be required to verify such changes e.g. through the use of sediment traps under cages (Corner et al., 2006). In this study, Corner et al. (2006) also reported on the carbon assimilation efficiency in farmed marine Scottish, where ~50% of the salmon feed pellet was organic

carbon (similar to the 45% used at Waltersmuir), 3% of feed was assumed uneaten and lost directly to the environment, 14% of the carbon consumed was used for fish growth, and 60% was respired or excreted by the fish, resulting in 74% of the organic carbon in the pellets were digestible. For salmonids, ~35-40% of ingested N is retained for growth, ~50% excreted as ammonia and urea and 10-15% lost in faeces (Talbot and Hole, 1994). The nitrogen content of pellet dry weight is typically ~6-6.5% (Ackefors and Enell, 1990) which is lower than the N content in the Waltersmuir feed. Ackefors and Enell, (1990) also produce a nitrogen load from marine cage-fish farming which shows for every ton of fish produced, 61 kg of nitrogen released is dissolved in water and 17 kg as particulate, and 10-30 kg is estimated to be released from the sediment. The use of fish feed with high N and C content is a major factor for the levels of C and DON observed in Waltersmuir, with additional release likely triggered by the effect of drawdown.

6.4 Research contributions to the wider-knowledge base

This research has added to an existing knowledge base on C and N concentrations and fluxes in temperate inland waters and provided some new information which could be utilised in future studies, as suggested above, or used in industry by utility companies, aquaculture managers and forestry. The main contributions are summarised below:

1. This research provided three novel contributions (Chapters 3 -5) to the study of C and N concentrations and estimates of evasion in upland reservoir catchments, particularly in peatland and forestry dominated catchments. Studies estimating aquatic C and N concentrations and fluxes in temperate reservoirs, but particularly in the UK, are lacking and so this research has created a dataset as detailed as in other temperate regions of Europe, USA and Canada.
2. Chapter 3 quantified C and N concentrations and evasion from thirty reservoirs in Scotland and North Wales, providing the first baseline understanding of spatial variability of C and N from a variety of catchment and reservoir types in the UK. This research showed that the sampled reservoirs are typically oversaturated with CO₂, CH₄ and N₂O, and could act as carbon sources, but to a lesser extent nitrogen sources due to levels closer to atmospheric equilibrium. It was also identified that CO₂ was the dominant GHG, even when GWPs of CH₄ and N₂O were calculated. This spatial understanding illustrates that future research would be beneficial to develop greater process understanding of GHG dynamics in UK reservoirs.
3. Chapter 4 provides the first fluvial C and N export study for lakes and reservoirs in the UK that accounts for CO₂, CH₄ and N₂O, in addition to DOC, DIC and DON. It also provides an

integrated approach, considering changes in C and N fluxes in inlets, reservoirs and outlets. Observational datasets using routinely monitored DOC at catchment outlets are commonly used for assessing variability in concentrations and export (Clark et al., 2010). However, the spatial scale at which hydrological mobilisation and biogeochemical transformations take place is often at much smaller scales which will not always be observed at catchment outlets. As seen in Chapter 4, the input C and N fluxes showed high spatial variability between sub-catchments, and also differences from the inlets to the reservoir and the outlet. Such trends would not have been picked up if monitoring only focussed efforts at the outlet and so this chapter also provides an understanding of the relative role of the sub-catchments to the C and N balance of the reservoirs. This in turn can help the utility company prioritise management activities in specific sub-catchments showing greatest C and N loads, which has the potential to reduce costs at water treatment works, especially for colour and organic carbon.

4. Chapter 5 at Waltersmuir reservoir reports the timing, spatial configuration and magnitude of CO₂, CH₄ and N₂O fluxes, taking account of drawdown impacts. This is a novel, first in the UK study, and makes a valuable contribution to the limited literature in this field and also emphasised that drawdown fluxes are important.
5. The GHG emissions reported in this research have the potential to make a significant contribution to national GHG emissions if up-scaling to UK inland waters was conducted. The development of methods by the IPCC to account for GHG emissions from 'Flooded Lands' could be used to further aid understanding on national emissions from inland waters in the UK, which this research could contribute towards.
6. In addition to an increased understanding of drawdown, results from Waltersmuir reservoir (Chapter 5) shed some insight on the impact aquaculture has on C and N dynamics in freshwaters, of which there are a further 25 freshwater sites in Scotland, with numbers growing globally. The results and data could be of value to the aquaculture sector, particularly if food usage and associated accumulation of C and N in the water body can be reduced, or water level management controlled to lessen the effects of hydrostatic pressure on C and N release from sediments.
7. Greater uncertainty exists over the magnitude of N₂O in aquatic systems and how it varies spatially within catchments (e.g. Beaulieu et al., 2008). Research in this thesis adds to the growing number of studies focussing on reservoir N₂O concentrations and fluxes in recent years. Other studies which investigate N₂O in the UK and globally are more typically conducted in N rich lowland areas which exhibit greater N₂O production and emissions e.g.

Dong et al. (2004) quantified nutrient and N₂O emissions from nutrient rich and oligotrophic rivers in England and Wales. Unsurprisingly, many upland reservoirs and streams sampled in this research had low N₂O concentrations, reflecting the relatively low catchment N loading. Despite the low concentrations of N₂O in the majority of the reservoirs, this is still an important finding, and means future sampling efforts can focus on more nutrient rich environments like Waltersmuir and some of the reservoirs in Wales which had algae blooms.

In summary, this research has led to a greater understanding of GHG release from reservoirs across Scotland and North Wales, with particular reference to the spatial and seasonal variability in C and N concentrations in a variety of reservoir catchments, commonly found across UK uplands. Magnitudes of GHG concentrations and fluxes were in line with other temperate systems and even some tropical reservoirs as was the case with Waltersmuir fluxes. Many reservoirs showed N₂O concentrations to be closer to atmospheric equilibrium, however, higher concentrations were observed in some North Wales reservoirs which had agriculture related land uses in their catchments, and algae visible over summer months. It was shown that CO₂ and CH₄ concentrations and levels of oversaturation can be very different across reservoirs. Evasion of CO₂ and CH₄ ranged from a smaller to significant source, with the high percentage of peat soils in the catchments an important factor.

The in-depth sampling at the managed moorland and coniferous forested catchments of Baddingsgill and Black Esk reservoirs revealed differences in catchment areal fluxes, and emphasised the importance of taking an integrative sampling approach when measuring the reservoir balance and fluvial C and N export. Evasion from inlets was also found to be higher compared to the reservoirs, with a high degree of both spatial and temporal variability seen. The annual balance of areal mean C and N fluxes showed both reservoirs to act as sinks for all measured C and N species compared to inlet and outlet fluxes.

The study at Waltersmuir revealed that drawdown plays an important role in regulating GHG release from reservoir sediments and the water column, and can contribute disproportionately to annual reservoir emissions. Moisture dynamics and slope were important factors in regulating sediment fluxes. With predicted increase in the frequency and intensity of both droughts and extreme rainfall events (IPCC, 2014), the relative importance of fluctuating water levels and exposed sediments is likely to increase. Overall, this research has shown that temperate reservoirs in Scotland and Wales can be quite significant emitters of CO₂ and CH₄, and to a lesser extent, N₂O.

The discussion on future research directions highlights opportunities that could be further explored, enhancing the results from this research. The extent of future research opportunities emphasises the wide range and complexity of C and N dynamics in aquatic systems. In current funding regimes, fully integrated monitoring is more challenging and thus more cost-effective alternatives e.g. automated sensors and remote sensing could be explored. Opportunities surrounding knowledge exchange have not been fully explored in this study but could be a sensible future approach when assessing where to best focus sampling efforts, particularly if other researchers across the UK were utilised, allowing also increased spatial coverage of GHG fluxes. This would also allow needs of stakeholders and scientific interest to be integrated. There is a need for continued catchment wide monitoring at reservoirs across the UK to help understanding longer term impacts on GHG dynamics and any changes in catchment management to water quality and C and N fluxes.

References

- Abe, D.S., Adams, D.D., Galli, C.V.S., Sikar, E., Tundisi, J.G., 2005. Sediment greenhouse gases (methane and carbon dioxide) in the Lobo-Broa Reservoir, São Paulo State, Brazil: Concentrations and diffuse emission fluxes for carbon budget considerations. *Lakes Reserv. Sci. Policy Manag. Sustain. Use* 10, 201–209. <https://doi.org/10.1111/j.1440-1770.2005.00277.x>
- Åberg, J., Bergström, A.-K., Algesten, G., Söderback, K., Jansson, M., 2004. A comparison of the carbon balances of a natural lake (L. Örträsket) and a hydroelectric reservoir (L. Skinmuddselet) in northern Sweden. *Water Res.* 38, 531–538. <https://doi.org/https://doi.org/10.1016/j.watres.2003.10.035>
- Abril, G., Guérin, F., Richard, S., Delmas, R., Galy-Lacaux, C., Gosse, P., Tremblay, A., Varfalvy, L., Dos Santos, M.A., Matvienko, B., 2005. Carbon dioxide and methane emissions and the carbon budget of a 10-year old tropical reservoir (Petit Saut, French Guiana). *Global Biogeochem. Cycles* 19. <https://doi.org/10.1029/2005GB002457>
- Achnich, C., Bak, F., Conrad, R., 1995. Competition for electron donors among nitrate reducers, ferric iron reducers, sulfate reducers, and methanogens in anoxic paddy soil. *Biol. Fertil. Soils* 19, 65–72. <https://doi.org/10.1007/BF00336349>
- Ackefors, H., Enell, M., 1990. Discharge of Nutrients from Swedish Fish Farming to Adjacent Sea Areas. *Ambio* 19, 28–35.
- Aitkenhead-Peterson, J.A., Alexander, J.E., Clair, T.A., 2005. Dissolved organic carbon and dissolved organic nitrogen export from forested watersheds in Nova Scotia: Identifying controlling factors. *Global Biogeochem. Cycles* 19. <https://doi.org/doi:10.1029/2004GB002438>
- Aitkenhead, J.A., Hope, D., Billett, M.F., 1999. The relationship between dissolved organic carbon in stream water and soil organic carbon pools at different spatial scales. *Hydrol. Process.* 13, 1289–1302. [https://doi.org/10.1002/\(SICI\)1099-1085\(19990615\)13:8<1289::AID-HYP766>3.0.CO;2-M](https://doi.org/10.1002/(SICI)1099-1085(19990615)13:8<1289::AID-HYP766>3.0.CO;2-M)
- Algesten, G., Sobek, S., Bergström, A.-K., Ågren, A., Tranvik, L.J., Jansson, M., 2004. Role of lakes for organic carbon cycling in the boreal zone. *Glob. Chang. Biol.* 10, 141–147. <https://doi.org/10.1111/j.1365-2486.2003.00721.x>
- Allott, T.E.H., Curtis, C.J., Hall, J., Harriman, R., Battarbee, R.W., 1995. The impact of nitrogen deposition on upland surface waters in Great Britain: A regional assessment of nitrate leaching. *Water. Air. Soil Pollut.* 85, 297–302. <https://doi.org/10.1007/BF00476845>
- Andrews, J.A., Harrison, K.G., Matamala, R., Schlesinger, W.H., 1999. Separation of Root Respiration from Total Soil Respiration Using Carbon-13 Labeling during Free-Air Carbon Dioxide Enrichment (FACE) This work was completed while the senior author was at the Dep. of Botany, Duke Univ., Durham, NC. *Soil Sci. Soc. Am. J.* 63, 1429–1435. <https://doi.org/10.2136/sssaj1999.6351429x>
- Arce, M.I., Sánchez-Montoya, M. del M., Gómez, R., 2015. Nitrogen processing following experimental sediment rewetting in isolated pools in an agricultural stream of a semiarid region. *Ecol. Eng.* 77, 233–241. <https://doi.org/https://doi.org/10.1016/j.ecoleng.2015.01.035>
- Arce, M.I., Sánchez-Montoya, M. del M., Vidal-Abarca, M.R., Suárez, M.L., Gómez, R., 2014.

- Implications of flow intermittency on sediment nitrogen availability and processing rates in a Mediterranean headwater stream. *Aquat. Sci.* 76, 173–186.
<https://doi.org/10.1007/s00027-013-0327-2>
- Armstrong, A., Holden, J., Kay, P., Francis, B., Foulger, M., Gledhill, S., McDonald, A.T., Walker, A., 2010. The impact of peatland drain-blocking on dissolved organic carbon loss and discolouration of water; results from a national survey. *J. Hydrol.* 381, 112–120.
<https://doi.org/https://doi.org/10.1016/j.jhydrol.2009.11.031>
- Aufdenkampe, A.K., Mayorga, E., Raymond, P.A., Melack, J.M., Doney, S.C., Alin, S.R., Aalto, R.E., Yoo, K., 2011. Riverine coupling of biogeochemical cycles between land, oceans, and atmosphere. *Front. Ecol. Environ.* 9, 53–60. <https://doi.org/doi:10.1890/100014>
- Barros, N., Cole, J.J., Tranvik, L.J., Prairie, Y.T., Bastviken, D., Huszar, V.L.M., del Giorgio, P., Roland, F., 2011. Carbon emission from hydroelectric reservoirs linked to reservoir age and latitude. *Nat. Geosci* 4, 593–596.
<https://doi.org/http://www.nature.com/ngeo/journal/v4/n9/abs/ngeo1211.html#supplementary-information>
- Barton, K., 2018. MuMIn: Multi-Model Inference.
- Bastien, J., Demarty, M., 2013. Spatio-temporal variation of gross CO₂ and CH₄ diffusive emissions from Australian reservoirs and natural aquatic ecosystems, and estimation of net reservoir emissions. *Lakes Reserv. Res. Manag.* 18, 115–127.
<https://doi.org/10.1111/lre.12028>
- Bastviken, D., Cole, J.J., Pace, M.L., de Bogert, M.C., 2008. Fates of methane from different lake habitats: Connecting whole-lake budgets and CH₄ emissions. *J. Geophys. Res. Biogeosciences* 113. <https://doi.org/10.1029/2007JG000608>
- Bastviken, D., Persson, L., Odham, G., Tranvik, L., 2004. Degradation of dissolved organic matter in oxic and anoxic lake water. *Limnol. Oceanogr.* 49, 109–116.
<https://doi.org/doi:10.4319/lo.2004.49.1.0109>
- Bastviken, D., Tranvik, L.J., Downing, J.A., Crill, P.M., Enrich-Prast, A., 2011. Freshwater Methane Emissions Offset the Continental Carbon Sink. *Science* (80-.). 331, 50.
<https://doi.org/10.1126/science.1196808>
- Bates, D., Mächler, M., Bolker, B., Walker, S., 2015. Fitting Linear Mixed-Effects Models Using lme4. *J. Stat. Software; Vol 1, Issue 1* .
- Baulch, H.M., Schiff, S.L., Maranger, R., Dillon, P.J., 2011. Nitrogen enrichment and the emission of nitrous oxide from streams. *Global Biogeochem. Cycles* 25.
<https://doi.org/10.1029/2011GB004047>
- Baxter, R.M., 1977. Environmental Effects of Dams and Impoundments. *Annu. Rev. Ecol. Syst.* 8, 255–283. <https://doi.org/10.1146/annurev.es.08.110177.001351>
- Beaulieu, J.J., Arango, C.P., Hamilton, S.K., Tank, J.L., 2008. The production and emission of nitrous oxide from headwater streams in the Midwestern United States. *Glob. Chang. Biol.* 14, 878–894. <https://doi.org/doi:10.1111/j.1365-2486.2007.01485.x>
- Beaulieu, J.J., Arango, C.P., Tank, J.L., 2009. The Effects of Season and Agriculture on Nitrous Oxide Production in Headwater Streams. *J. Environ. Qual.* 38, 637–646.
<https://doi.org/10.2134/jeq2008.0003>
- Beaulieu, J.J., Balz, D.A., Birchfield, M.K., Harrison, J.A., Nietch, C.T., Platz, M.C., Squier, W.C.,

- Waldo, S., Walker, J.T., White, K.M., Young, J.L., 2018. Effects of an Experimental Water-level Drawdown on Methane Emissions from a Eutrophic Reservoir. *Ecosystems* 21, 657–674. <https://doi.org/10.1007/s10021-017-0176-2>
- Beaulieu, J.J., Balz, D.A., Birchfield, M.K., Harrison, J.A., Nietch, C.T., Platz, M.C., Squier, W.C., Waldo, S., Walker, J.T., White, K.M., Young, J.L., 2017. Effects of an Experimental Water-level Drawdown on Methane Emissions from a Eutrophic Reservoir. *Ecosystems* 1–18. <https://doi.org/10.1007/s10021-017-0176-2>
- Beaulieu, J.J., DelSontro, T., Downing, J.A., 2019. Eutrophication will increase methane emissions from lakes and impoundments during the 21st century. *Nat. Commun.* 10, 1375. <https://doi.org/10.1038/s41467-019-09100-5>
- Beaulieu, J.J., McManus, M.G., Nietch, C.T., 2016. Estimates of reservoir methane emissions based on a spatially balanced probabilistic-survey. *Limnol. Oceanogr.* 61, S27–S40. <https://doi.org/10.1002/lno.10284>
- Beaulieu, J.J., Nietch, C.T., Young, J.L., 2015. Controls on nitrous oxide production and consumption in reservoirs of the Ohio River Basin. *J. Geophys. Res. Biogeosciences* 120, 1995–2010. <https://doi.org/doi:10.1002/2015JG002941>
- Beaulieu, J.J., Smolenski, R.L., Nietch, C.T., Townsend-Small, A., Elovitz, M.S., 2014. High Methane Emissions from a Midlatitude Reservoir Draining an Agricultural Watershed. *Environ. Sci. Technol.* 48, 11100–11108. <https://doi.org/10.1021/es501871g>
- Beaulieu, J.J., Tank, J.L., Hamilton, S.K., Wollheim, W.M., Hall, R.O., Mulholland, P.J., Peterson, B.J., Ashkenas, L.R., Cooper, L.W., Dahm, C.N., Dodds, W.K., Grimm, N.B., Johnson, S.L., McDowell, W.H., Poole, G.C., Valett, H.M., Arango, C.P., Bernot, M.J., Burgin, A.J., Crenshaw, C.L., Helton, A.M., Johnson, L.T., O'Brien, J.M., Potter, J.D., Sheibley, R.W., Sobota, D.J., Thomas, S.M., 2011. Nitrous oxide emission from denitrification in stream and river networks. *Proc. Natl. Acad. Sci.* 108, 214–219. <https://doi.org/10.1073/pnas.1011464108>
- Bergström, I., Mäkelä, S., Kankaala, P., Kortelainen, P., 2007. Methane efflux from littoral vegetation stands of southern boreal lakes: An upscaled regional estimate. *Atmos. Environ.* 41, 339–351. <https://doi.org/https://doi.org/10.1016/j.atmosenv.2006.08.014>
- Betton, C., Webb, D.E., Walling, D., 1991. Recent trends in NO₃-N concentrations and loads in British rivers., in: *Water Quality in a Changing Environment: Trends and Explanation*. IAHS Publication No. 203., Vienna, pp. 169–180.
- Bevelhimer, M.S., Stewart, A.J., Fortner, A.M., Phillips, J.R., Mosher, J.J., 2016. CO₂ is Dominant Greenhouse Gas Emitted from Six Hydropower Reservoirs in Southeastern United States during Peak Summer Emissions. *Water* 8, 15.
- Bianchi, M., Feliatra, Lefevre, D., 1999. Regulation of nitrification in the land-ocean contact area of the Rhone River plume (NW Mediterranean). *Aquat. Microb. Ecol.* 18, 301–312. <https://doi.org/10.3354/ame018301>
- Billett, M.F., Charman, D.J., Clark, J.M., Evans, C.D., Evans, M.G., Ostle, N.J., Worrall, F., Burden, A., Dinsmore, K.J., Jones, T., McNamara, N.P., Parry, L., Rowson, J.G., Rose, R., 2010. Carbon balance of UK peatlands: current state of knowledge and future research challenges. *Clim. Res.* 45, 13–29. <https://doi.org/https://doi.org/10.3354/cr00903>
- Billett, M.F., Garnett, M.H., Dinsmore, K.J., 2015. Should Aquatic CO₂ Evasion be Included in Contemporary Carbon Budgets for Peatland Ecosystems? *Ecosystems* 1–10.

<https://doi.org/10.1007/s10021-014-9838-5>

- Billett, M.F., Garnett, M.H., Harvey, F., 2007. UK peatland streams release old carbon dioxide to the atmosphere and young dissolved organic carbon to rivers. *Geophys. Res. Lett.* 34. <https://doi.org/10.1029/2007GL031797>
- Billett, M.F., Harvey, F.H., 2013. Measurements of CO₂ and CH₄ evasion from UK peatland headwater streams. *Biogeochemistry* 114, 165–181. <https://doi.org/10.1007/s10533-012-9798-9>
- Billett, M.F., Moore, T.R., 2008. Supersaturation and evasion of CO₂ and CH₄ in surface waters at Mer Bleue peatland, Canada. *Hydrol. Process.* 22, 2044–2054. <https://doi.org/10.1002/hyp.6805>
- Billett, M.F., Palmer, S.M., Hope, D., Deacon, C., R., S.-W., Hargreaves, K.J., Flechard, C., Fowler, D., 2004. Linking land-atmosphere-stream carbon fluxes in a lowland peatland system. *Global Biogeochem. Cycles* 18. <https://doi.org/doi:10.1029/2003GB002058>
- Billings, W.D., Luken, J.O., Mortensen, D.A., Peterson, K.M., 1982. Arctic tundra: A source or sink for atmospheric carbon dioxide in a changing environment? *Oecologia* 53, 7–11. <https://doi.org/10.1007/bf00377129> LB - Billings1982
- Bloodworth, J.W., Holman, I.P., Burgess, P.J., Gillman, S., Frogbrook, Z., Brown, P., 2015. Developing a multi-pollutant conceptual framework for the selection and targeting of interventions in water industry catchment management schemes. *J. Environ. Manage.* 161, 153–162. <https://doi.org/https://doi.org/10.1016/j.jenvman.2015.06.050>
- Bolpagni, R., Folegot, S., Laini, A., Bartoli, M., 2017. Role of ephemeral vegetation of emerging river bottoms in modulating CO₂ exchanges across a temperate large lowland river stretch. *Aquat. Sci.* 79, 149–158. <https://doi.org/10.1007/s00027-016-0486-z> LB - Bolpagni2017
- Boorman, D.B., Hollis, J.M., Lilly, A., 1995. Hydrology of Soil types: a hydrologically-based classification of the soils of the United Kingdom. Inst. Hydrol. Rep. No. 126, Wallingford, UK.
- Boothroyd, I.M., Worrall, F., Allott, T.E.H., 2015. Variations in dissolved organic carbon concentrations across peatland hillslopes. *J. Hydrol.* 530, 372–383. <https://doi.org/https://doi.org/10.1016/j.jhydrol.2015.10.002>
- Borges, A.V., Delille, B., Schiettecatte, L.-S., Gazeau, F., Abril, G., Frankignoulle, M., 2004. Gas transfer velocities of CO₂ in three European estuaries (Randers Fjord, Scheldt, and Thames). *Limnol. Oceanogr.* 49, 1630–1641. <https://doi.org/10.4319/lo.2004.49.5.1630>
- Borges, A. V, Darchambeau, F., Lambert, T., Bouillon, S., Morana, C., Brouyère, S., Hakoun, V., Jurado, A., Tseng, H.C., Descy, J.P., Roland, F.A.E., 2018. Effects of agricultural land use on fluvial carbon dioxide, methane and nitrous oxide concentrations in a large European river, the Meuse (Belgium). *Sci. Total Environ.* 610–611, 342–355. <https://doi.org/https://doi.org/10.1016/j.scitotenv.2017.08.047>
- Borges, A. V, Darchambeau, F., Teodoru, C.R., Marwick, T.R., Tamoooh, F., Geeraert, N., Omengo, F.O., Guérin, F., Lambert, T., Morana, C., Okuku, E., Bouillon, S., 2015. Globally significant greenhouse-gas emissions from African inland waters. *Nat. Geosci.* 8, 637. <https://doi.org/10.1038/ngeo2486>
<https://www.nature.com/articles/ngeo2486#supplementary-information>
- Boulart, C., Connelly, D.P., Mowlem, M.C., 2010. Sensors and technologies for in situ dissolved

- methane measurements and their evaluation using Technology Readiness Levels. *TrAC Trends Anal. Chem.* 29, 186–195.
<https://doi.org/https://doi.org/10.1016/j.trac.2009.12.001>
- Brooks, R.T., Stone, J., Lyons, P., 1998. An Inventory of Seasonal Forest Ponds on the Quabbin Reservoir Watershed, Massachusetts. *Northeast. Nat.* 5, 219–230.
<https://doi.org/10.2307/3858622>
- Burford, M.A., Johnson, S.A., Cook, A.J., Packer, T. V, Taylor, B.M., Townsley, E.R., 2007. Correlations between watershed and reservoir characteristics, and algal blooms in subtropical reservoirs. *Water Res.* 41, 4105–4114.
<https://doi.org/https://doi.org/10.1016/j.watres.2007.05.053>
- Butman, D., Raymond, P.A., 2011. Significant efflux of carbon dioxide from streams and rivers in the United States. *Nat. Geosci.* 4, 839. <https://doi.org/10.1038/ngeo1294>
<https://www.nature.com/articles/ngeo1294#supplementary-information>
- Cable, J.M., Ogle, K., Williams, D.G., Weltzin, J.F., Huxman, T.E., 2008. Soil Texture Drives Responses of Soil Respiration to Precipitation Pulses in the Sonoran Desert: Implications for Climate Change. *Ecosystems* 11, 961–979. <https://doi.org/10.1007/s10021-008-9172-x>
- Campeau, A., Lapierre, J.-F., Vachon, D., del Giorgio, P.A., 2014. Regional contribution of CO₂ and CH₄ fluxes from the fluvial network in a lowland boreal landscape of Québec. *Global Biogeochem. Cycles* 28, 57–69. <https://doi.org/10.1002/2013GB004685>
- Caraco, N.F., Cole, J.J., Likens, G.E., 1989. Evidence for sulphate-controlled phosphorus release from sediments of aquatic systems. *Nature* 341, 316–318.
<https://doi.org/10.1038/341316a0>
- Carmignani, J.R., Roy, A.H., 2017. Ecological impacts of winter water level drawdowns on lake littoral zones: a review. *Aquat. Sci.* 79, 803–824. <https://doi.org/10.1007/s00027-017-0549-9> LB - Carmignani2017
- Carpenter, J.W., Green, R.H., Paterson, C.G., 1983. A preliminary organic carbon budget for a small dystrophic lake in Maritime Canada. *Hydrobiologia* 106, 275–282.
<https://doi.org/10.1007/bf00008126> LB - Carpenter1983
- Carter, R.W., Davidian, J., 1989. *Techniques of Water-Resources Investigations of the United States Geological Survey. General procedure for gaging streams.* Denver, CO, USA.
- Casper, P., Maberly, S.C., Hall, G.H., Finlay, B.J., 2000. Fluxes of methane and carbon dioxide from a small productive lake to the atmosphere. *Biogeochemistry* 49, 1–19.
<https://doi.org/10.1023/A:1006269900174>
- Catalan, N., von Schiller, D., Marce, R., Koschorreck, M., Gomez-Gener, L., Obrador, B., 2014. Carbon dioxide efflux during the flooding phase of temporary ponds. *Limnetica* 33, 349–359.
- Chadwick, D.R., Cardenas, L., Misselbrook, T.H., Smith, K.A., Rees, R.M., Watson, C.J., McGeough, K.L., Williams, J.R., Cloy, J.M., Thorman, R.E., Dhanoa, M.S., 2014. Optimizing chamber methods for measuring nitrous oxide emissions from plot-based agricultural experiments. *Eur. J. Soil Sci.* 65, 295–307. <https://doi.org/10.1111/ejss.12117>
- Chanton, J.P., Whiting, G.J., 1995. Trace gas exchange in freshwater and coastal marine environments: ebullition and transport by plants. *Biog. trace gases Meas. Emiss. from soil water.*

- Chao, B.F., Wu, Y.H., Li, Y.S., 2008. Impact of Artificial Reservoir Water Impoundment on Global Sea Level. *Science* (80-.). 320, 212–214. <https://doi.org/10.1126/science.1154580>
- Chapman, P.J., Edwards, A.C., Cresser, M.S., 2001. The nitrogen composition of streams in upland Scotland: some regional and seasonal differences. *Sci. Total Environ.* 265, 65–83. [https://doi.org/https://doi.org/10.1016/S0048-9697\(00\)00650-1](https://doi.org/https://doi.org/10.1016/S0048-9697(00)00650-1)
- Chen, H., Wu, Y., Yuan, X., Gao, Y., Wu, N., Zhu, D., 2009. Methane emissions from newly created marshes in the drawdown area of the Three Gorges Reservoir. *J. Geophys. Res. Atmos.* 114, D18301. <https://doi.org/10.1029/2009jd012410>
- Chiverton, A., Hannaford, J., Holman, I., Corstanje, R., Prudhomme, C., Bloomfield, J., Hess, T.M., 2015. Which catchment characteristics control the temporal dependence structure of daily river flows? *Hydrol. Process.* 29, 1353–1369. <https://doi.org/10.1002/hyp.10252>
- Chow, A.T., Tanji, K.K., Gao, S., 2003. Production of dissolved organic carbon (DOC) and trihalomethane (THM) precursor from peat soils. *Water Res.* 37, 4475–4485. [https://doi.org/https://doi.org/10.1016/S0043-1354\(03\)00437-8](https://doi.org/https://doi.org/10.1016/S0043-1354(03)00437-8)
- Ciais, P., Sabine, C., Bala, G., Bopp, L., Brovkin, V., Canadell, J., Chhabra, A., DeFries, R., Galloway, J., Heimann, M., Jones, C., Quéré, C. Le, Mynen, R., Piao, S., Thornton, P., 2013. Carbon and Other Biogeochemical Cycles. In: *Climate Change 2013: The Physical Science Basis. Contribution of Working Group I to the Fifth Assessment Report of the Intergovernmental Panel on Climate Change.* Cambridge University Press, Cambridge, United Kingdom and New York, NY, USA.
- Clark, J.M., Gallego-Sala, A., Allott, T., Chapman, S., Farewell, T., Freeman, C., House, J., Orr, H., Prentice, I., Smith, P., 2010. Assessing the vulnerability of blanket peat to climate change using an ensemble of statistical bioclimatic envelope models. *Clim. Res.* 45, 131–150.
- Clark, J.M., Lane, S.N., Chapman, P.J., Adamson, J.K., 2008. Link between DOC in near surface peat and stream water in an upland catchment. *Sci. Total Environ.* 404, 308–315. <https://doi.org/https://doi.org/10.1016/j.scitotenv.2007.11.002>
- Clark, J.M., Lane, S.N., Chapman, P.J., Adamson, J.K., 2007. Export of dissolved organic carbon from an upland peatland during storm events: Implications for flux estimates. *J. Hydrol.* 347, 438–447. <https://doi.org/https://doi.org/10.1016/j.jhydrol.2007.09.030>
- Clayton, H.J., Arah, R.M., Smith, K.A., 1994. Measurement of nitrous oxide emissions from fertilized grassland using closed chambers. *J. Geophys. Res. Atmos.* 99, 16599–16607. <https://doi.org/doi:10.1029/94JD00218>
- Cole, J.J., Bade, D.L., Bastviken, D., Pace, M.L., de Bogert, M., 2010. Multiple approaches to estimating air-water gas exchange in small lakes. *Limnol. Oceanogr. Methods* 8, 285–293. <https://doi.org/10.4319/lom.2010.8.285>
- Cole, J.J., Caraco, N.F., 1998. Atmospheric exchange of carbon dioxide in a low-wind oligotrophic lake measured by the addition of SF₆. *Limnol. Oceanogr.* 43, 647–656. <https://doi.org/10.4319/lo.1998.43.4.0647>
- Cole, J.J., Caraco, N.F., Kling, G.W., Kratz, T.K., 1994. Carbon Dioxide Supersaturation in the Surface Waters of Lakes. *Science* (80-.). 265, 1568–1570. <https://doi.org/10.1126/science.265.5178.1568>
- Cole, J.J., Pace, M.L., Carpenter, S.R., Kitchell, J.F., 2000. Persistence of net heterotrophy in lakes during nutrient addition and food web manipulations. *Limnol. Oceanogr.* 45, 1718–

1730. <https://doi.org/10.4319/lo.2000.45.8.1718>
- Cole, J.J., Prairie, Y.T., Caraco, N.F., McDowell, W.H., Tranvik, L.J., Striegl, R.G., Duarte, C.M., Kortelainen, P., Downing, J.A., Middelburg, J.J., Melack, J., 2007. Plumbing the Global Carbon Cycle: Integrating Inland Waters into the Terrestrial Carbon Budget. *Ecosystems* 10, 172–185. <https://doi.org/10.1007/s10021-006-9013-8>
- Corner, R.A., Brooker, A.J., Telfer, T.C., Ross, L.G., 2006. A fully integrated GIS-based model of particulate waste distribution from marine fish-cage sites. *Aquaculture* 258, 299–311. <https://doi.org/https://doi.org/10.1016/j.aquaculture.2006.03.036>
- Correll, D.L., 1998. The Role of Phosphorus in the Eutrophication of Receiving Waters: A Review. *J. Environ. Qual.* 27, 261–266. <https://doi.org/10.2134/jeq1998.00472425002700020004x>
- Cowan, N.J., Levy, P.E., Famulari, D., Anderson, M., Drewer, J., Carozzi, M., Reay, D.S., Skiba, U.M., 2016. The influence of tillage on N₂O fluxes from an intensively managed grazed grassland in Scotland. *Biogeosciences* 13, 4811–4821. <https://doi.org/10.5194/bg-13-4811-2016>
- Crawford, J.T., Striegl, R.G., Wickland, K.P., Dornblaser, M.M., Stanley, E.H., 2013. Emissions of carbon dioxide and methane from a headwater stream network of interior Alaska. *J. Geophys. Res. Biogeosciences* 118, 482–494. <https://doi.org/10.1002/jgrg.20034>
- Creed, I.F., Beall, F.D., Clair, T.A., Dillon, P.J., Hesslein, R.H., 2008. Predicting export of dissolved organic carbon from forested catchments in glaciated landscapes with shallow soils. *Global Biogeochem. Cycles* 22. <https://doi.org/10.1029/2008GB003294>
- Cummins, T., Farrell, E.P., 2003. Biogeochemical impacts of clearfelling and reforestation on blanket peatland streams I. phosphorus. *For. Ecol. Manage.* 180, 545–555. [https://doi.org/10.1016/S0378-1127\(02\)00648-5](https://doi.org/10.1016/S0378-1127(02)00648-5)
- Dai, H.C., Mao, J.Q., Zheng, T.G., 2013. Assessment of greenhouse gas emissions from a large subtropical reservoir in China. *J. Environ. Prot. Ecol.* 14, 430–437.
- Dawson, J.J., 2000. The controls on concentrations and fluxes of gaseous, dissolved and particulate carbon in upland peat dominated catchments. University of Aberdeen.
- Dawson, J.J.C., Billett, M.F., Hope, D., Palmer, S.M., Deacon, C.M., 2004. Sources and sinks of aquatic carbon in a peatland stream continuum. *Biogeochemistry* 70, 71–92. <https://doi.org/10.1023/B:BI0G.0000049337.66150.f1>
- Dawson, J.J.C., Billett, M.F., Neal, C., Hill, S., 2002. A comparison of particulate, dissolved and gaseous carbon in two contrasting upland streams in the UK. *J. Hydrol.* 257, 226–246. [https://doi.org/https://doi.org/10.1016/S0022-1694\(01\)00545-5](https://doi.org/https://doi.org/10.1016/S0022-1694(01)00545-5)
- Dawson, Q., Kechavarzi, C., Leeds-Harrison, P.B., Burton, R.G.O., 2010. Subsidence and degradation of agricultural peatlands in the Fenlands of Norfolk, UK. *Geoderma* 154, 181–187. <https://doi.org/https://doi.org/10.1016/j.geoderma.2009.09.017>
- Dean, W.E., Gorham, E., 1998. Magnitude and significance of carbon burial in lakes, reservoirs, and peatlands. *Geology* 26, 535–538. [https://doi.org/10.1130/0091-7613\(1998\)026<0535:MASOCB>2.3.CO;2](https://doi.org/10.1130/0091-7613(1998)026<0535:MASOCB>2.3.CO;2)
- Deemer, B.R., Harrison, J.A., Li, S., Beaulieu, J.J., DelSontro, T., Barros, N., Bezerra-Neto, J.F., Powers, S.M., dos Santos, M.A., Vonk, J.A., 2016. Greenhouse Gas Emissions from Reservoir Water Surfaces: A New Global Synthesis. *Bioscience* 66, 949–964.

<https://doi.org/10.1093/biosci/biw117>

- Del Giorgio, P.A., Cole, J.J., Caraco, N.F., Peters, R.H., 1999. LINKING PLANKTONIC BIOMASS AND METABOLISM TO NET GAS FLUXES IN NORTHERN TEMPERATE LAKES. *Ecology* 80, 1422–1431. [https://doi.org/10.1890/0012-9658\(1999\)080\[1422:LPBAMT\]2.0.CO;2](https://doi.org/10.1890/0012-9658(1999)080[1422:LPBAMT]2.0.CO;2)
- DelSontro, T., Beaulieu, J.J., Downing, J.A., 2018. Greenhouse gas emissions from lakes and impoundments: Upscaling in the face of global change. *Limnol. Oceanogr. Lett.* 3, 64–75. <https://doi.org/10.1002/lol2.10073>
- DelSontro, T., Boutet, L., St-Pierre, A., del Giorgio, P.A., Prairie, Y.T., 2016. Methane ebullition and diffusion from northern ponds and lakes regulated by the interaction between temperature and system productivity. *Limnol. Oceanogr.* 61, S62–S77. <https://doi.org/10.1002/lno.10335>
- DelSontro, T., Kunz, M.J., Kempter, T., Wüest, A., Wehrli, B., Senn, D.B., 2011. Spatial Heterogeneity of Methane Ebullition in a Large Tropical Reservoir. *Environ. Sci. Technol.* 45, 9866–9873. <https://doi.org/10.1021/es2005545>
- DelSontro, T., McGinnis, D.F., Sobek, S., Ostrovsky, I., Wehrli, B., 2010. Extreme Methane Emissions from a Swiss Hydropower Reservoir: Contribution from Bubbling Sediments. *Environ. Sci. Technol.* 44, 2419–2425. <https://doi.org/10.1021/es9031369>
- Demarty, M., Bastien, J., 2011. GHG emissions from hydroelectric reservoirs in tropical and equatorial regions: Review of 20 years of CH₄ emission measurements. *Energy Policy* 39, 4197–4206. <https://doi.org/https://doi.org/10.1016/j.enpol.2011.04.033>
- Demarty, M., Bastien, J., Tremblay, A., Hesslein, R.H., Gill, R., 2009. Greenhouse Gas Emissions from Boreal Reservoirs in Manitoba and Québec, Canada, Measured with Automated Systems. *Environ. Sci. Technol.* 43, 8908–8915. <https://doi.org/10.1021/es8035658>
- Denfeld, B.A., Frey, K.E., Sobczak, W. V, Mann, P.J., Holmes, R.M., 2013. Summer CO₂ evasion from streams and rivers in the Kolyma River basin, north-east Siberia. *Polar Res.* 32, 19704. <https://doi.org/10.3402/polar.v32i0.19704>
- Descloux, S., Chanudet, V., Serça, D., Guérin, F., 2017. Methane and nitrous oxide annual emissions from an old eutrophic temperate reservoir. *Sci. Total Environ.* 598, 959–972. <https://doi.org/https://doi.org/10.1016/j.scitotenv.2017.04.066>
- Deshmukh, C., Guérin, F., Labat, D., Pighini, S., Vongkhamsoo, A., Guédant, P., Rode, W., Godon, A., Chanudet, V., Descloux, S., Serça, D., 2016. Low methane CH₄ emissions downstream of a monomictic subtropical hydroelectric reservoir (Nam Theun 2, Lao PDR). *Biogeosciences* 13, 1919–1932. <https://doi.org/10.5194/bg-13-1919-2016>
- Deshmukh, C., Guérin, F., Vongkhamsoo, A., Pighini, S., Oudone, P., Sopraseuth, S., Godon, A., Rode, W., Guédant, P., Oliva, P., Audry, S., Zouiten, C., Galy-Lacaux, C., Robain, H., Ribolzi, O., Kansal, A., Chanudet, V., Descloux, S., Serça, D., 2018. Carbon dioxide emissions from the flat bottom and shallow Nam Theun 2 Reservoir: drawdown area as a neglected pathway to the atmosphere. *Biogeosciences* 15, 1775–1794. <https://doi.org/10.5194/bg-15-1775-2018>
- Deshmukh, C., Serça, D., Delon, C., Tardif, R., Demarty, M., Jarnot, C., Meyerfeld, Y., Chanudet, V., Guédant, P., Rode, W., Descloux, S., Guérin, F., 2014. Physical controls on CH₄ emissions from a newly flooded subtropical freshwater hydroelectric reservoir: Nam Theun 2. *Biogeosciences* 11, 4251–4269. <https://doi.org/10.5194/bg-11-4251-2014>
- Diem, T., Koch, S., Schwarzenbach, S., Wehrli, B., Schubert, C.J., 2012. Greenhouse gas

- emissions (CO₂, CH₄, and N₂O) from several perialpine and alpine hydropower reservoirs by diffusion and loss in turbines. *Aquat. Sci.* 74, 619–635.
<https://doi.org/10.1007/s00027-012-0256-5>
- Dinsmore, K.J., Billett, M.F., 2008. Continuous measurement and modeling of CO₂ losses from a peatland stream during stormflow events. *Water Resour. Res.* 44.
<https://doi.org/10.1029/2008WR007284>
- Dinsmore, K.J., Billett, M.F., Skiba, U.M., Rees, R.M., Drewer, J., Helfter, C., 2010. Role of the aquatic pathway in the carbon and greenhouse gas budgets of a peatland catchment. *Glob. Chang. Biol.* 16, 2750–2762. <https://doi.org/doi:10.1111/j.1365-2486.2009.02119.x>
- Dinsmore, K.J., Skiba, U.M., Billett, M.F., Rees, R.M., Drewer, J., 2009. Spatial and temporal variability in CH₄ and N₂O fluxes from a Scottish ombrotrophic peatland: Implications for modelling and up-scaling. *Soil Biol. Biochem.* 41, 1315–1323.
<https://doi.org/https://doi.org/10.1016/j.soilbio.2009.03.022>
- Dinsmore, K.J., Wallin, M.B., Johnson, M.S., Billett, M.F., Bishop, K., Pumpanen, J., Ojala, A., 2013. Contrasting CO₂ concentration discharge dynamics in headwater streams: A multi-catchment comparison. *J. Geophys. Res. Biogeosciences* 118, 445–461.
<https://doi.org/doi:10.1002/jgrg.20047>
- Dong, L.F., Nedwell, D.B., Colbeck, I., Finch, J., 2004. Nitrous Oxide Emission from some English and Welsh Rivers and Estuaries. *Water, Air, Soil Pollut. Focus* 4, 127–134.
<https://doi.org/10.1007/s11267-004-3022-4>
- Donis, D., Flury, S., Stöckli, A., Spangenberg, J.E., Vachon, D., McGinnis, D.F., 2017. Full-scale evaluation of methane production under oxic conditions in a mesotrophic lake. *Nat. Commun.* 8, 1661. <https://doi.org/10.1038/s41467-017-01648-4>
- Downing, J.A., Cole, J.J., Middelburg, J.J., Striegl, R.G., Duarte, C.M., Kortelainen, P., Prairie, Y.T., Laube, K.A., 2008. Sediment organic carbon burial in agriculturally eutrophic impoundments over the last century. *Global Biogeochem. Cycles* 22.
<https://doi.org/10.1029/2006GB002854>
- Downing, J.A., Prairie, Y.T., Cole, J.J., Duarte, C.M., Tranvik, L.J., Striegl, R.G., McDowell, W.H., Kortelainen, P., Caraco, N.F., Melack, J.M., Middelburg, J.J., 2006. The global abundance and size distribution of lakes, ponds, and impoundments. *Limnol. Oceanogr.* 51, 2388–2397. <https://doi.org/10.4319/lo.2006.51.5.2388>
- Drewer, J., Lohila, A., Aurela, M., Laurila, T., Minkkinen, K., Penttilä, T., Dinsmore, K.J., McKenzie, R.M., Helfter, C., Flechard, C., Sutton, M.A., Skiba, U.M., 2010. Comparison of greenhouse gas fluxes and nitrogen budgets from an ombrotrophic bog in Scotland and a minerotrophic sedge fen in Finland. *Eur. J. Soil Sci.* 61, 640–650.
<https://doi.org/10.1111/j.1365-2389.2010.01267.x>
- Driscoll, C.T., Fuller, R.D., Schecher, W.D., 1989. The role of organic acids in the acidification of surface waters in the Eastern U.S. *Water. Air. Soil Pollut.* 43, 21–40.
<https://doi.org/10.1007/BF00175580>
- Duchemin, E., Lucotte, M., Canuel, R., Chamberland, A., 1995. Production of the greenhouse gases CH₄ and CO₂ by hydroelectric reservoirs of the boreal region. *Global Biogeochem. Cycles* 9, 529–540. <https://doi.org/10.1029/95GB02202>
- Dyson, K.E., Billett, M.F., Dinsmore, K.J., Harvey, F., Thomson, A.M., Piirainen, S., Kortelainen, P., 2011. Release of aquatic carbon from two peatland catchments in E. Finland during

- the spring snowmelt period. *Biogeochemistry* 103, 125–142.
<https://doi.org/10.1007/s10533-010-9452-3>
- Elliott, S., Swan, D., 2013. Source Water Management - Deep Reservoir Circulation., in: 7th Annual WIOA NSW Water Industry Operations Conference. pp. 84–91.
- Emilson, E.J.S., Carson, M.A., Yakimovich, K.M., Osterholz, H., Dittmar, T., Gunn, J.M., Mykytczuk, N.C.S., Basiliko, N., Tanentzap, A.J., 2018. Climate-driven shifts in sediment chemistry enhance methane production in northern lakes. *Nat. Commun.* 9, 1801.
<https://doi.org/10.1038/s41467-018-04236-2>
- Emmett, B.A., Anderson, J.M., Hornung, M., 1991. Nitrogen sinks following two intensities of harvesting in a Sitka spruce forest (N. Wales) and the effect on the establishment of the next crop. *For. Ecol. Manage.* 41, 81–93. [https://doi.org/https://doi.org/10.1016/0378-1127\(91\)90120-K](https://doi.org/https://doi.org/10.1016/0378-1127(91)90120-K)
- Erkkilä, K.-M., Ojala, A., Bastviken, D., Biermann, T., Heiskanen, J.J., Lindroth, A., Peltola, O., Rantakari, M., Vesala, T., Mammarella, I., 2018. Methane and carbon dioxide fluxes over a lake: comparison between eddy covariance, floating chambers and boundary layer method. *Biogeosciences* 15, 429–445. <https://doi.org/10.5194/bg-15-429-2018>
- Eugster, W., DelSontro, T., Sobek, S., 2011. Eddy covariance flux measurements confirm extreme CH₄ emissions from a Swiss hydropower reservoir and resolve their short-term variability. *Biogeosciences* 8, 2815–2831. <https://doi.org/10.5194/bg-8-2815-2011>
- Evans, C., Allott, T., Billett, M., Chapman, P., Dinsmore, K., Evans, M., Freeman, C., Goulsbra, C., Holden, J., Jones, T., Moody, C., Palmer, S., Worrall, F., 2013. Greenhouse gas emissions associated with non-gaseous losses of carbon from peatlands – fate of particulate and dissolved carbon. Final Report to the Department for Environment, Food and Rural Affairs. Bangor.
- Evans, C.D., Futter, M.N., Moldan, F., Valinia, S., Frogbrook, Z., Kothawala, D.N., 2017. Variability in organic carbon reactivity across lake residence time and trophic gradients. *Nat. Geosci.* 10, 832.
- Evans, C.D., Page, S.E., Jones, T., Moore, S., Gauci, V., Laiho, R., Hruška, J., Allott, T.E.H., Billett, M.F., Tipping, E., Freeman, C., Garnett, M.H., 2014. Contrasting vulnerability of drained tropical and high-latitude peatlands to fluvial loss of stored carbon. *Global Biogeochem. Cycles* 28, 1215–1234. <https://doi.org/10.1002/2013GB004782>
- Evans, M., Lindsay, J., 2010. High resolution quantification of gully erosion in upland peatlands at the landscape scale. *Earth Surf. Process. Landforms* 35, 876–886.
<https://doi.org/doi:10.1002/esp.1918>
- Evans, M., Warburton, J., Yang, J., 2006. Eroding blanket peat catchments: Global and local implications of upland organic sediment budgets. *Geomorphology* 79, 45–57.
<https://doi.org/https://doi.org/10.1016/j.geomorph.2005.09.015>
- Fahre, A., Patau-Albertini, M.F., 1986. Sediment heterogeneity in a reservoir subject to heavy draw-down. *Hydrobiologia* 137, 89–94. <https://doi.org/10.1007/bf00004176> LB - Fahre1986
- Fearnside, P.M., 2005. Brazil's Samuel Dam: Lessons for Hydroelectric Development Policy and the Environment in Amazonia. *Environ. Manage.* 35, 1–19.
<https://doi.org/10.1007/s00267-004-0100-3>
- Fernández, J.E., Peeters, F., Hofmann, H., 2016. On the methane paradox: Transport from

- shallow water zones rather than in situ methanogenesis is the major source of CH₄ in the open surface water of lakes. *J. Geophys. Res. Biogeosciences* 121, 2717–2726. <https://doi.org/10.1002/2016JG003586>
- Fetzer, S., Bak, F., Conrad, R., 1993. Sensitivity of methanogenic bacteria from paddy soil to oxygen and desiccation. *FEMS Microbiol. Ecol.* 12, 107–115.
- Fierer, N., Allen, A.S., Schimel, J.P., Holden, P.A., 2003. Controls on microbial CO₂ production: a comparison of surface and subsurface soil horizons. *Glob. Chang. Biol.* 9, 1322–1332. <https://doi.org/10.1046/j.1365-2486.2003.00663.x>
- Firestone, M.K., Davidson, E.A., 1989. MICROBIOLOGICAL BASIS OF NO AND N₂O PRODUCTION AND CONSUMPTION IN SOIL, Exchange of Trace Gases between Terrestrial Ecosystems and the Atmosphere.
- Flanagan, K.M., McCauley, E., Wrona, F., Prowse, T., 2003. Climate change: the potential for latitudinal effects on algal biomass in aquatic ecosystems. *Can. J. Fish. Aquat. Sci.* 60, 635–639. <https://doi.org/10.1139/f03-062>
- Forster, P., Ramaswamy, V., Artaxo, P., Berntsen, T., Betts, R., Fahey, D., Haywood, J., Lean, J., Lowe, D., Myhre, G., Nganga, J., Prinn, R., Raga, G., Schulz, M., Van Dorland, R., 2008. Changes in Atmospheric Constituents and in Radiative Forcing. Climate Change 2007: The Physical Science Basis. Contribution of Working Group I to the Fourth Assessment Report of the IPCC, S. Solomon et al. (eds.), Cambridge University Press, Cambridge, UK.
- Foster, S.Q., Fulweiler, R.W., 2016. Sediment Nitrous Oxide Fluxes Are Dominated by Uptake in a Temperate Estuary. *Front. Mar. Sci.* 3, 40. <https://doi.org/10.3389/fmars.2016.00040>
- Fowler, D., Cape, J.N., Unsworth, M.H., 1989. Deposition of atmospheric pollutants on forests. *Biol. Sci. R. Soc.* 324.
- Freeman, C., Hudson, J., Lock, M.A., Reynolds, B., Swanson, C., 1994. A possible role of sulphate in the suppression of wetland methane fluxes following drought. *Soil Biol. Biochem.* 26, 1439–1442. [https://doi.org/https://doi.org/10.1016/0038-0717\(94\)90229-1](https://doi.org/https://doi.org/10.1016/0038-0717(94)90229-1)
- Fromin, N., Pinay, G., Montuelle, B., Landais, D., Ourcival, J.M., Joffre, R., Lensi, R., 2010. Impact of seasonal sediment desiccation and rewetting on microbial processes involved in greenhouse gas emissions. *Ecohydrology* 3, 339–348. <https://doi.org/10.1002/eco.115>
- Frost, P.C., Larson, J.H., Johnston, C.A., Young, K.C., Maurice, P.A., Lamberti, G.A., Bridgman, S.D., 2006. Landscape predictors of stream dissolved organic matter concentration and physicochemistry in a Lake Superior river watershed. *Aquat. Sci.* 68, 40–51. <https://doi.org/10.1007/s00027-005-0802-5>
- Furey, P.C., Nordin, R.N., Mazumder, A., 2004. Water Level Drawdown Affects Physical and Biogeochemical Properties of Littoral Sediments of a Reservoir and a Natural Lake. *Lake Reserv. Manag.* 20, 280–295. <https://doi.org/10.1080/07438140409354158>
- Galy-Lacaux, C., Delmas, R., Jambert, C., Dumestre, J.-F., Labroue, L., Richard, S., Gosse, P., 1997. Gaseous emissions and oxygen consumption in hydroelectric dams: A case study in French Guyana. *Global Biogeochem. Cycles* 11, 471–483. <https://doi.org/10.1029/97GB01625>
- Galy-Lacaux, C., Delmas, R., Kouadio, G., Richard, S., Gosse, P., 1999. Long-term greenhouse gas emissions from hydroelectric reservoirs in tropical forest regions. *Global Biogeochem. Cycles* 13, 503–517. <https://doi.org/10.1029/1998GB900015>

- Garnett, M.H., Gulliver, P., Billett, M.F., 2015. A rapid method to collect methane from peatland streams for radiocarbon analysis. *Ecohydrology* n/a-n/a. <https://doi.org/10.1002/eco.1617>
- Gibson, J.J., Edwards, T.W.D., Birks, S.J., St Amour, N.A., Buhay, W.M., McEachern, P., Wolfe, B.B., Peters, D.L., 2005. Progress in isotope tracer hydrology in Canada. *Hydrol. Process.* 19, 303–327. <https://doi.org/10.1002/hyp.5766>
- Glatzel, S., Well, R., 2008. Evaluation of septum-capped vials for storage of gas samples during air transport. *Environ. Monit. Assess.* 136, 307–311. <https://doi.org/10.1007/s10661-007-9686-2>
- Gómez-Gener, L., Obrador, B., Marcé, R., Acuña, V., Catalán, N., Casas-Ruiz, J.P., Sabater, S., Muñoz, I., von Schiller, D., 2016. When Water Vanishes: Magnitude and Regulation of Carbon Dioxide Emissions from Dry Temporary Streams. *Ecosystems* 19, 710–723. <https://doi.org/10.1007/s10021-016-9963-4> LB - Gómez-Gener2016
- Gómez-Gener, L., Obrador, B., von Schiller, D., Marcé, R., Casas-Ruiz, J.P., Proia, L., Acuña, V., Catalán, N., Muñoz, I., Koschorreck, M., 2015. Hot spots for carbon emissions from Mediterranean fluvial networks during summer drought. *Biogeochemistry* 125, 409–426. <https://doi.org/10.1007/s10533-015-0139-7> LB - Gómez-Gener2015
- Gonzalez-Valencia, R., Magana-Rodriguez, F., Gerardo-Nieto, O., Sepulveda-Jauregui, A., Martinez-Cruz, K., Walter Anthony, K., Baer, D., Thalasso, F., 2014. In Situ Measurement of Dissolved Methane and Carbon Dioxide in Freshwater Ecosystems by Off-Axis Integrated Cavity Output Spectroscopy. *Environ. Sci. Technol.* 48, 11421–11428. <https://doi.org/10.1021/es500987j>
- Grieve, I.C., 1994. Dissolved organic carbon dynamics in two streams draining forested catchments at loch ard, Scotland. *Hydrol. Process.* 8, 457–464. <https://doi.org/10.1002/hyp.3360080508>
- Gruca-Rokosz, R., Tomaszek, J.A., Koszelnik, P., Czerwieniec, E., 2011. Methane and carbon dioxide fluxes at the sediment-water interface in reservoirs. *Polish J. Environ. Stud.* 20, 81–86.
- Gudasz, C., Bastviken, D., Steger, K., Premke, K., Sobek, S., Tranvik, L.J., 2010. Temperature-controlled organic carbon mineralization in lake sediments. *Nature* 466, 478–481. <https://doi.org/http://www.nature.com/nature/journal/v466/n7305/abs/nature09186.html#supplementary-information>
- Guérin, F., Abril, G., 2007. Significance of pelagic aerobic methane oxidation in the methane and carbon budget of a tropical reservoir. *J. Geophys. Res. Biogeosciences* 112. <https://doi.org/doi:10.1029/2006JG000393>
- Guérin, F., Abril, G., Richard, S., Burban, B., Reynouard, C., Seyler, P., Delmas, R., 2006. Methane and carbon dioxide emissions from tropical reservoirs: Significance of downstream rivers. *Geophys. Res. Lett.* 33, L21407. <https://doi.org/10.1029/2006gl027929>
- Guérin, F., Abril, G., Tremblay, A., Delmas, R., 2008. Nitrous oxide emissions from tropical hydroelectric reservoirs. *Geophys. Res. Lett.* 35. <https://doi.org/doi:10.1029/2007GL033057>
- Halbedel, S., Koschorreck, M., 2013. Regulation of CO₂ emissions from temperate streams and reservoirs. *Biogeosciences* 10, 7539–7551. <https://doi.org/10.5194/bg-10-7539-2013>

- Halekoh, U., Højsgaard, S., 2014. A Kenward-Roger Approximation and Parametric Bootstrap Methods for Tests in Linear Mixed Models The R Package pbrtest. *J. Stat. Softw.* 59.
- Hanson, P.C., Carpenter, S.R., Cardille, J.A., Coe, M.T., Winslow, L.A., 2007. Small lakes dominate a random sample of regional lake characteristics. *Freshw. Biol.* 52, 814–822. <https://doi.org/10.1111/j.1365-2427.2007.01730.x>
- Harriman, R., Curtis, C., Edwards, A.C., 1998. An Empirical Approach for Assessing the Relationship between Nitrogen Deposition and Nitrate Leaching from Upland Catchments in the United Kingdom Using Runoff Chemistry, in: Wieder, R.K., Novák, M., Černý, J. (Eds.), *Biogeochemical Investigations at Watershed, Landscape, and Regional Scales: Refereed Papers from BIOGEMON, The Third International Symposium on Ecosystem Behavior; Co-Sponsored by Villanova University and the Czech Geological Survey; Held at Villanova University, Villanova Pennsylvania, USA, June 21--25, 1997.* Springer Netherlands, Dordrecht, pp. 193–203. https://doi.org/10.1007/978-94-017-0906-4_19
- Harrison, J.A., Deemer, B.R., Birchfield, M.K., O'Malley, M.T., 2017. Reservoir Water-Level Drawdowns Accelerate and Amplify Methane Emission. *Environ. Sci. Technol.* 51, 1267–1277. <https://doi.org/10.1021/acs.est.6b03185>
- Harrison, J.A., Maranger, R.J., Alexander, R.B., Giblin, A.E., Jacinthe, P.-A., Mayorga, E., Seitzinger, S.P., Sobota, D.J., Wollheim, W.M., 2009. The regional and global significance of nitrogen removal in lakes and reservoirs. *Biogeochemistry* 93, 143–157. <https://doi.org/10.1007/s10533-008-9272-x>
- Hasan, M.R., Soto, S., 2017. Improving feed conversion ration and its impact on reducing greenhouse gas emissions in aquaculture. Rome.
- Hatton-Ellis, T., 2015. Evidence Review of Lake Eutrophication in Wales.
- Hayes, N.M., Deemer, B.R., Corman, J.R., Razavi, N.R., Strock, K.E., 2017. Key differences between lakes and reservoirs modify climate signals: A case for a new conceptual model. *Limnol. Oceanogr. Lett.* 2, 47–62. <https://doi.org/doi:10.1002/lol2.10036>
- Henderson-Sellers, B., 1979. *Reservoirs. The History of Water Supply.* The Macmillian Press.
- Henderson, R., Chips, M., Cornwell, N., Hitchins, P., Holden, B., Hurley, S., Parsons, S.A., Wetherill, A., Jefferson, B., 2008. Experiences of algae in UK waters: a treatment perspective. *Water Environ. J.* 22, 184–192. <https://doi.org/10.1111/j.1747-6593.2007.00100.x>
- Hensen, A., Skiba, U., Famulari, D., 2013. Low cost and state of the art methods to measure nitrous oxide emissions. *Environ. Res. Lett.* 8.
- Hertwich, E.G., 2013. Addressing Biogenic Greenhouse Gas Emissions from Hydropower in LCA. *Environ. Sci. Technol.* 47, 9604–9611. <https://doi.org/10.1021/es401820p>
- Hirsch, P.E., Eloranta, A.P., Amundsen, P.-A., Brabrand, Å., Charmasson, J., Helland, I.P., Power, M., Sánchez-Hernández, J., Sandlund, O.T., Sauterleute, J.F., Skoglund, S., Ugedal, O., Yang, H., 2017. Effects of water level regulation in alpine hydropower reservoirs: an ecosystem perspective with a special emphasis on fish. *Hydrobiologia* 794, 287–301. <https://doi.org/10.1007/s10750-017-3105-7> LB - Hirsch2017
- Hofmann, M., Schellnhuber, H.J., 2010. Ocean acidification: a millennial challenge. *Energy Environ. Sci.* 3, 1883–1896. <https://doi.org/10.1039/C000820F>

- Holgerson, M.A., Raymond, P.A., 2016. Large contribution to inland water CO₂ and CH₄ emissions from very small ponds. *Nat. Geosci.* 9, 222.
- Holliday, V.J., Warburton, J., Higgitt, D.L., 2008. Historic and contemporary sediment transfer in an upland Pennine catchment, UK. *Earth Surf. Process. Landforms* 33, 2139–2155. <https://doi.org/doi:10.1002/esp.1660>
- Hope, D., Billett, M.F., Cresser, M.S., 1994. A review of the export of carbon in river water: Fluxes and processes. *Environ. Pollut.* 84, 301–324. [https://doi.org/https://doi.org/10.1016/0269-7491\(94\)90142-2](https://doi.org/https://doi.org/10.1016/0269-7491(94)90142-2)
- Hope, D., Billett, M.F., Milne, R., Brown, T.A., 1997. Exports of organic carbon in British rivers. *Hydrol. Process.* 11, 325–344. [https://doi.org/doi:10.1002/\(SICI\)1099-1085\(19970315\)11:3<325::AID-HYP476>3.0.CO;2-I](https://doi.org/doi:10.1002/(SICI)1099-1085(19970315)11:3<325::AID-HYP476>3.0.CO;2-I)
- Hope, D., Dawson, J.J.C., Cresser, M.S., Billett, M.F., 1995. A method for measuring free CO₂ in upland streamwater using headspace analysis. *J. Hydrol.* 166, 1–14. [https://doi.org/https://doi.org/10.1016/0022-1694\(94\)02628-O](https://doi.org/https://doi.org/10.1016/0022-1694(94)02628-O)
- Hope, D., Palmer, S.M., Billett, M.F., Dawson, J.J.C., 2004. Variations in dissolved CO₂ and CH₄ in a first-order stream and catchment: an investigation of soil–stream linkages. *Hydrol. Process.* 18, 3255–3275. <https://doi.org/10.1002/hyp.5657>
- Hope, D., Palmer, S.M., Billett, M.F., Dawson, J.J.C., 2001. Carbon dioxide and methane evasion from a temperate peatland stream. *Limnol. Oceanogr.* 46, 847–857. <https://doi.org/10.4319/lo.2001.46.4.0847>
- Houser, J.N., Bade, D.L., Cole, J.J., Pace, M.L., 2003. The dual influences of dissolved organic carbon on hypolimnetic metabolism: organic substrate and photosynthetic reduction. *Biogeochemistry* 64, 247–269. <https://doi.org/10.1023/A:1024933931691>
- Hu, M., Chen, D., Dahlgren, R.A., 2016. Modeling nitrous oxide emission from rivers: a global assessment. *Glob. Chang. Biol.* 22, 3566–3582. <https://doi.org/doi:10.1111/gcb.13351>
- Hu, Z., Lee, J.W., Chandran, K., Kim, S., Sharma, K., Brotto, A.C., Khanal, S.K., 2013. Nitrogen transformations in intensive aquaculture system and its implication to climate change through nitrous oxide emission. *Bioresour. Technol.* 130, 314–320. <https://doi.org/https://doi.org/10.1016/j.biortech.2012.12.033>
- Hughes, D.D., Holliman, P.J., Jones, T., Freeman, C., 2013. Temporal variations in dissolved organic carbon concentrations in upland and lowland lakes in North Wales. *Water Environ. J.* 27, 275–283. <https://doi.org/10.1111/wej.12025>
- Humborg, C., MÖRTH, C.-M., SUNDBOM, M., BORG, H., BLENCKNER, T., GIESLER, R., ITTEKOT, V., 2010. CO₂ supersaturation along the aquatic conduit in Swedish watersheds as constrained by terrestrial respiration, aquatic respiration and weathering. *Glob. Chang. Biol.* 16, 1966–1978. <https://doi.org/10.1111/j.1365-2486.2009.02092.x>
- Hunting, E.R., White, C.M., van Gemert, M., Mes, D., Stam, E., van, H.G., Geest, der, Kraak, M.H.S., Admiraal, W., 2013. UV radiation and organic matter composition shape bacterial functional diversity in sediments. *Front. Microbiol.* 4, 317. <https://doi.org/10.3389/fmicb.2013.00317>
- Huttunen, J.T., Alm, J., Liikanen, A., Juutinen, S., Larmola, T., Hammar, T., Silvola, J., Martikainen, P.J., 2003a. Fluxes of methane, carbon dioxide and nitrous oxide in boreal lakes and potential anthropogenic effects on the aquatic greenhouse gas emissions. *Chemosphere* 52, 609–621. <https://doi.org/https://doi.org/10.1016/S0045->

- Huttunen, J.T., Juutinen, S., Alm, J., Larmola, T., Hammar, T., Silvola, J., Martikainen, P.J., 2003b. Nitrous oxide flux to the atmosphere from the littoral zone of a boreal lake. *J. Geophys. Res. Atmos.* 108. <https://doi.org/10.1029/2002JD002989>
- Huttunen, J.T., Väisänen, T.S., Heikkinen, M., Hellsten, S., Nykänen, H., Nenonen, O., Martikainen, P.J., 2002. Exchange of CO₂, CH₄ and N₂O between the atmosphere and two northern boreal ponds with catchments dominated by peatlands or forests. *Plant Soil* 242, 137–146. <https://doi.org/10.1023/A:1019606410655>
- Huttunen, J.T., Väisänen, T.S., Hellsten, S.K., Heikkinen, M., Nykänen, H., Jungner, H., Niskanen, A., Virtanen, M.O., Lindqvist, O. V, Nenonen, O.S., Martikainen, P.J., 2002. Fluxes of CH₄, CO₂, and N₂O in hydroelectric reservoirs Lokka and Porttipahta in the northern boreal zone in Finland. *Global Biogeochem. Cycles* 16, 3–17. <https://doi.org/doi:10.1029/2000GB001316>
- Hyojin, J., Tae Kyung, Y., Seung-Hoon, L., Hojeong, K., Jungho, I., Ji-Hyung, P., 2016. Enhanced greenhouse gas emission from exposed sediments along a hydroelectric reservoir during an extreme drought event. *Environ. Res. Lett.* 11, 124003.
- Hyvönen, R., Olsson, B.A., Lundkvist, H., Staaf, H., 2000. Decomposition and nutrient release from *Picea abies* (L.) Karst. and *Pinus sylvestris* L. logging residues. *For. Ecol. Manage.* 126, 97–112. [https://doi.org/https://doi.org/10.1016/S0378-1127\(99\)00092-4](https://doi.org/https://doi.org/10.1016/S0378-1127(99)00092-4)
- IPCC., 2014. Anthropogenic and Natural Radiative Forcing, in: Intergovernmental Panel on Climate, C. (Ed.), *Climate Change 2013 – The Physical Science Basis: Working Group I Contribution to the Fifth Assessment Report of the Intergovernmental Panel on Climate Change*. Cambridge University Press, Cambridge, pp. 659–740. <https://doi.org/Doi:10.1017/cbo9781107415324.018>
- IPCC, 2014. *Climate Change 2014: Synthesis Report. Contribution of Working Groups I, II and III to the Fifth Assessment Report of the Intergovernmental Panel on Climate Change*. Geneva, Switzerland.
- Jähne, B., Münnich, K.O., Bössinger, R., Dutzi, A., Huber, W., Libner, P., 1987. On the parameters influencing air-water gas exchange. *J. Geophys. Res. Ocean.* 92, 1937–1949. <https://doi.org/10.1029/JC092iC02p01937>
- Jarvie, H.P., King, S.M., Neal, C., 2017. Inorganic carbon dominates total dissolved carbon concentrations and fluxes in British rivers: Application of the THINCARB model – Thermodynamic modelling of inorganic carbon in freshwaters. *Sci. Total Environ.* 575, 496–512. <https://doi.org/https://doi.org/10.1016/j.scitotenv.2016.08.201>
- Johnson, M.S., Billett, M.F., Dinsmore, K.J., Wallin, M., Dyson, K.E., Jassal, R.S., 2010. Direct and continuous measurement of dissolved carbon dioxide in freshwater aquatic systems—method and applications. *Ecohydrology* 3, 68–78. <https://doi.org/10.1002/eco.95>
- Johnson, M.S., Weiler, M., Couto, E.G., Riha, S.J., Lehmann, J., 2007. Storm pulses of dissolved CO₂ in a forested headwater Amazonian stream explored using hydrograph separation. *Water Resour. Res.* 43. <https://doi.org/10.1029/2007WR006359>
- Johnson, P.C.D., 2014. Extension of Nakagawa & Schielzeth's R²GLMM to random slopes models. *Methods Ecol. Evol.* 5, 944–946. <https://doi.org/10.1111/2041-210X.12225>
- Jones, D.L., Willett, V.B., 2006. Experimental evaluation of methods to quantify dissolved

- organic nitrogen (DON) and dissolved organic carbon (DOC) in soil. *Soil Biol. Biochem.* 38, 991–999. <https://doi.org/https://doi.org/10.1016/j.soilbio.2005.08.012>
- Jones, J.B., Mulholland, P.J., 1998. Methane input and evasion in a hardwood forest stream: Effects of subsurface flow from shallow and deep pathway. *Limnol. Oceanogr.* 43, 1243–1250. <https://doi.org/10.4319/lo.1998.43.6.1243>
- Jones, T.G., 2006. Climate change and dissolved organic carbon: impacts on drinking water supplies. University of Bangor.
- Jonsson, A., Karlsson, J., Jansson, M., 2003. Sources of Carbon Dioxide Supersaturation in Clearwater and Humic Lakes in Northern Sweden. *Ecosystems* 6, 224–235. <https://doi.org/10.1007/s10021-002-0200-y>
- Kahn, J.R., Freitas, C.E., Petre, M., 2014. False Shades of Green: The Case of Brazilian Amazonian Hydropower. *Energies* 7, 6063–6082.
- Kankaala, P., Huotari, J., Peltomaa, E., Saloranta, T., Ojala, A., 2006. Methanotrophic activity in relation to methane efflux and total heterotrophic bacterial production in a stratified, humic, boreal lake. *Limnol. Oceanogr.* 51, 1195–1204. <https://doi.org/10.4319/lo.2006.51.2.1195>
- Kaplan, L.A., Newbold, J.D., 2003. 4 - The Role of Monomers in Stream Ecosystem Metabolism, in: Findlay, S.E.G., Sinsabaugh, R.L.B.T.-A.E. (Eds.), *Aquatic Ecology*. Academic Press, Burlington, pp. 97–119. <https://doi.org/https://doi.org/10.1016/B978-012256371-3/50005-6>
- Karlsson, J., Jansson, M., Jonsson, A., 2007. Respiration of allochthonous organic carbon in unproductive forest lakes determined by the Keeling plot method. *Limnol. Oceanogr.* 52, 603–608. <https://doi.org/10.4319/lo.2007.52.2.0603>
- Keller, M., Stallard, R.F., 1994. Methane emission by bubbling from Gatun Lake, Panama. *J. Geophys. Res. Atmos.* 99, 8307–8319. <https://doi.org/doi:10.1029/92JD02170>
- Kelly, C.A., Rudd, J.W.M., Bodaly, R.A., Roulet, N.P., St.Louis, V.L., Heyes, A., Moore, T.R., Schiff, S., Aravena, R., Scott, K.J., Dyck, B., Harris, R., Warner, B., Edwards, G., 1997. Increases in Fluxes of Greenhouse Gases and Methyl Mercury following Flooding of an Experimental Reservoir. *Environ. Sci. Technol.* 31, 1334–1344. <https://doi.org/10.1021/es9604931>
- Kelly, V.J., 2001. Influence of reservoirs on solute transport: A regional-scale approach. *Hydro. Process.* 15, 1227–1249. <https://doi.org/10.1002/hyp.211>
- Kiene, R.P., 1991. Production and consumption of methane in aquatic systems, in: Rogers, J.E., Whitman, W.B. (Eds.), *Microbial Production and Consumption of Greenhouse Gases: Methane, Nitrogen Oxides and Halomethanes*. American Society for Microbiology, Washington DC, pp. 111–146.
- Kling, G.W., Kipphut, G.W., Miller, M.C., 1991. Arctic Lakes and Streams as Gas Conduits to the Atmosphere: Implications for Tundra Carbon Budgets. *Science* (80-). 251, 298–301. <https://doi.org/10.1126/science.251.4991.298>
- Knowles, R., 1982. Denitrification. *Microbiol. Rev.* 46, 43–70.
- Koehler, A.-K., Murphy, K., Kiely, G., Sottocornola, M., 2009. Seasonal variation of DOC concentration and annual loss of DOC from an Atlantic blanket bog in South Western Ireland 95, 231–242. <https://doi.org/10.1007/s10533-009-9333-9>

- Kokic, J., Wallin, M.B., Chmiel, H.E., Denfeld, B.A., Sobek, S., 2015. Carbon dioxide evasion from headwater systems strongly contributes to the total export of carbon from a small boreal lake catchment. *J. Geophys. Res. Biogeosciences* 120, 13–28. <https://doi.org/10.1002/2014jg002706>
- Kokic, J., Wallin, M.B., Chmiel, H.E., Denfeld, B.A., Sobek, S., 2015. Carbon dioxide evasion from headwater systems strongly contributes to the total export of carbon from a small boreal lake catchment. *J. Geophys. Res. Biogeosciences* 120, 13–28. <https://doi.org/10.1002/2014jg002706>
- Kortelainen, P., Ortelainene, P., Rantakari, M., Huttunen, J.T., Mattsson, T., Alm, J., Juutinen, S., Larmola, T., Silvola, J., Martikainen, P.J., 2006. Sediment respiration and lake trophic state are important predictors of large CO₂ evasion from small boreal lakes. *Glob. Chang. Biol.* 12, 1554–1567. <https://doi.org/10.1111/j.1365-2486.2006.01167.x>
- Koschorreck, M., 2000. Methane turnover in exposed sediments of an Amazon floodplain lake. *Biogeochemistry* 50, 195–206. <https://doi.org/10.1023/a:1006326018597> LB - Koschorreck2000
- Koschorreck, M., Darwich, A., 2003. Nitrogen dynamics in seasonally flooded soils in the Amazon floodplain. *Wetl. Ecol. Manag.* 11, 317–330. <https://doi.org/10.1023/b:wetl.0000005536.39074.72> LB - Koschorreck2003
- Krinner, G., 2003. Impact of lakes and wetlands on boreal climate. *J. Geophys. Res. Atmos.* 108. <https://doi.org/10.1029/2002JD002597>
- Kroeze, C., Dumont, E., Seitzinger, S., 2010. Future trends in emissions of N₂O from rivers and estuaries. *J. Integr. Environ. Sci.* 7, 71–78. <https://doi.org/10.1080/1943815x.2010.496789>
- Kumar, A., Schei, T., Ahenkorah, A., Rodriguez, R. C. Devernay, J.M., Freitas, M., Hall, D., Killingtveit, Å., Liu, Z., 2011. Hydropower. In: IPCC Special Report on Renewable Energy Sources and Climate Change Mitigation. Cambridge University Press, United Kingdom and New York, NY, USA.
- Leach, J.. A., Larsson, A., Wallin, B.M., Nilsson, M.B., Laudon, H., 2016. Twelve year interannual and seasonal variability of stream carbon export from a boreal peatland catchment. *J. Geophys. Res. Biogeosciences* 121, 1851–1866. <https://doi.org/doi:10.1002/2016JG003357>
- Lee, K.E., Lorenz, D.L., Petersen, J.C., Greene, J.B., 2012. Seasonal patterns in nutrients, carbon, and algal responses in wadeable streams within three geographically distinct areas of the United States, 2007-08, Scientific Investigations Report. Reston, VA. <https://doi.org/10.3133/sir20125086>
- Levy, P.E., Burden, A., Cooper, M.D.A., Dinsmore, K.J., Drewer, J., Evans, C., Fowler, D., Gaiawyn, J., Gray, A., Jones, S.K., Jones, T., McNamara, N.P., Mills, R., Ostle, N., Sheppard, L.J., Skiba, U., Sowerby, A., Ward, S.E., Zieliński, P., 2012. Methane emissions from soils: synthesis and analysis of a large UK data set. *Glob. Chang. Biol.* 18, 1657–1669. <https://doi.org/doi:10.1111/j.1365-2486.2011.02616.x>
- Levy, P.E., Cowan, N., van Oijen, M., Famulari, D., Drewer, J., Skiba, U., 2017. Estimation of cumulative fluxes of nitrous oxide: uncertainty in temporal upscaling and emission factors. *Eur. J. Soil Sci.* 68, 400–411. <https://doi.org/10.1111/ejss.12432>
- Levy, P.E., Gray, A., Leeson, S.R., Gaiawyn, J., Kelly, M.P.C., Cooper, M.D.A., Dinsmore, K.J.,

- Jones, S.K., Sheppard, L.J., 2011. Quantification of uncertainty in trace gas fluxes measured by the static chamber method. *Eur. J. Soil Sci.* 62, 811–821. <https://doi.org/doi:10.1111/j.1365-2389.2011.01403.x>
- Li, Q., Zhang, S., 2014. Carbon emission from global hydroelectric reservoirs revisited. *Environ. Sci. Pollut. Res.* 21, 13636–13641. <https://doi.org/10.1007/s11356-014-3165-4>
- Li, S., Zhang, Q., Bush, R.T., Sullivan, L.A., 2015. Methane and CO₂ emissions from China's hydroelectric reservoirs: a new quantitative synthesis. *Environ. Sci. Pollut. Res.* 22, 5325–5339. <https://doi.org/10.1007/s11356-015-4083-9>
- Li, Z., Zhang, Z., Lin, C., Chen, Y., Wen, A., Fang, F., 2016a. Soil–air greenhouse gas fluxes influenced by farming practices in reservoir drawdown area: A case at the Three Gorges Reservoir in China. *J. Environ. Manage.* 181, 64–73. <https://doi.org/http://dx.doi.org/10.1016/j.jenvman.2016.05.080>
- Li, Z., Zhang, Z., Lin, C., Chen, Y., Wen, A., Fang, F., 2016b. Soil–air greenhouse gas fluxes influenced by farming practices in reservoir drawdown area: A case at the Three Gorges Reservoir in China. *J. Environ. Manage.* 181, 64–73. <https://doi.org/https://doi.org/10.1016/j.jenvman.2016.05.080>
- Li, Z., Zhang, Z., Xiao, Y., Guo, J., Wu, S., Liu, J., 2014. Spatio-temporal variations of carbon dioxide and its gross emission regulated by artificial operation in a typical hydropower reservoir in China. *Environ. Monit. Assess.* 186, 3023–3039. <https://doi.org/10.1007/s10661-013-3598-0>
- Li, Z., Zhang, Z., Xiao, Y., Guo, J., Wu, S., Liu, J., 2014. Spatio-temporal variations of carbon dioxide and its gross emission regulated by artificial operation in a typical hydropower reservoir in China. *Environ. Monit. Assess.* 186, 3023–3039.
- Lima, I.B.T., 2005. Biogeochemical distinction of methane releases from two Amazon hydroreservoirs. *Chemosphere* 59, 1697–1702. <https://doi.org/https://doi.org/10.1016/j.chemosphere.2004.12.011>
- Liu, X.-L., Liu, C.-Q., Li, S.-L., Wang, F.-S., Wang, B.-L., Wang, Z.-L., 2011. Spatiotemporal variations of nitrous oxide (N₂O) emissions from two reservoirs in SW China. *Atmos. Environ.* 45, 5458–5468. <https://doi.org/https://doi.org/10.1016/j.atmosenv.2011.06.074>
- Livingston, G.P., Hutchinson, G.L., 1995. Enclosure-Based Measurements of Trace Gas Exchange: Applications and Sources of Error., in: *Biogenic Trace Gases: Measuring Emissions from Soil and Water*. Blackwell Science Ltd, Oxford, UK, pp. 15–51.
- Long, H., Vihermaa, L., Waldron, S., Hoey, T., Quemin, S., Newton, J., 2015. Hydraulics are a first-order control on CO₂ efflux from fluvial systems. *J. Geophys. Res. Biogeosciences* 120, 1912–1922. <https://doi.org/10.1002/2015jg002955>
- Lundin, E.J., Giesler, R., Persson, A., Thompson, M.S., Karlsson, J., 2013. Integrating carbon emissions from lakes and streams in a subarctic catchment. *J. Geophys. Res. Biogeosciences* 118, 1200–1207. <https://doi.org/10.1002/jgrg.20092>
- MacIntyre, S., Wanninkhof, R., Chanton, J.P., 1995. Trace gas exchange in freshwater and coastal marine systems, in: *Matson, P., Harriss, R. (Eds.), Methods in Ecology: Trace Gases*. pp. 52–97.
- Maeck, A., DelSontro, T., McGinnis, D.F., Fischer, H., Flury, S., Schmidt, M., Fietzek, P., Lorke, A., 2013. Sediment Trapping by Dams Creates Methane Emission Hot Spots. *Environ. Sci.*

- Technol. 47, 8130–8137. <https://doi.org/10.1021/es4003907>
- Magin, K., Somlai-Haase, C., Schäfer, R.B., Lorke, A., 2017. Regional-scale lateral carbon transport and CO₂ evasion in temperate stream catchments. *Biogeosciences* 14, 5003–5014. <https://doi.org/10.5194/bg-14-5003-2017>
- Marescaux, A., Thieu, V., Garnier, J., 2018. Carbon dioxide, methane and nitrous oxide emissions from the human-impacted Seine watershed in France. *Sci. Total Environ.* 643, 247–259. <https://doi.org/https://doi.org/10.1016/j.scitotenv.2018.06.151>
- Matson, P.A., Billow, C., Hall, S., Zachariassen, J., 1996. Fertilization practices and soil variations control nitrogen oxide emissions from tropical sugar cane. *J. Geophys. Res. Atmos.* 101, 18533–18545. <https://doi.org/10.1029/96JD01536>
- Matthews, C.J.D., Joyce, E.M., Louis, V.L. St., Schiff, S.L., Venkiteswaran, J.J., Hall, B.D., Bodaly, R.A. (Drew), Beaty, K.G., 2005. Carbon Dioxide and Methane Production in Small Reservoirs Flooding Upland Boreal Forest. *Ecosystems* 8, 267–285. <https://doi.org/10.1007/s10021-005-0005-x>
- Mayer, L., Thornton, K.H., Schick, L., 2011. Bioavailability of organic matter photodissolved from coastal sediments. *Aquat. Microb. Ecol.* 64, 275–284.
- Mcdowell, R.W., Larned, S.T., Houlbrooke, D.J., 2009. Nitrogen and phosphorus in New Zealand streams and rivers: Control and impact of eutrophication and the influence of land management. *New Zeal. J. Mar. Freshw. Res.* 43, 985–995. <https://doi.org/10.1080/00288330909510055>
- McGinnis, D.F., Bilsley, N., Schmidt, M., Fietzek, P., Bodmer, P., Premke, K., Lorke, A., Flury, S., 2016. Deconstructing Methane Emissions from a Small Northern European River: Hydrodynamics and Temperature as Key Drivers. *Environ. Sci. Technol.* 50, 11680–11687. <https://doi.org/10.1021/acs.est.6b03268>
- Megonigal, J.P., Hines, M.E., Visscher, P.T., 2004. Anaerobic metabolism: linkages to trace gases and aerobic processes., in: Schlesinger, W.H. (Ed.), *Biogeochemistry*. Elsevier-Pergamon., Oxford, UK, pp. 317–424.
- Mendonça, R., Roland, F., Pacheco, F., Vidal, L.O., Barros, N., Kosten, S., 2012. Greenhouse Gas Emissions from Hydroelectric Reservoirs: What Knowledge Do We Have and What is Lacking? INTECH Open Access Publisher.
- Mengis, M., Gächter, R., Wehrli, B., 1997. Sources and sinks of nitrous oxide (N₂O) in deep lakes. *Biogeochemistry* 38, 281–301. <https://doi.org/10.1023/a:1005814020322>
- Met Office, 2018. UK climate - Historic station data [WWW Document]. URL <https://www.metoffice.gov.uk/public/weather/climate-historic/#?tab=climateHistoric>
- Met Office, 2016. Regional values - Annual 2016 [WWW Document]. Met Off. URL <http://www.metoffice.gov.uk/climate/uk/summaries/2016/annual/regional-values>
- Met Office, 2015. 2015 weather summaries [WWW Document]. Met Off. URL <http://www.metoffice.gov.uk/climate/uk/summaries/2015>
- Mikha, M.M., Rice, C.W., Milliken, G.A., 2005. Carbon and nitrogen mineralization as affected by drying and wetting cycles. *Soil Biol. Biochem.* 37, 339–347. <https://doi.org/https://doi.org/10.1016/j.soilbio.2004.08.003>
- Molot, L., Dillon, P., 1996. Storage of terrestrial carbon in boreal lake sediments and evasion to the atmosphere. *Global Biogeochem. Cycles* 10, 483–492.

<https://doi.org/doi:10.1029/96GB01666>

- Moore, T.R., Knowles, R., 1989. THE INFLUENCE OF WATER TABLE LEVELS ON METHANE AND CARBON DIOXIDE EMISSIONS FROM PEATLAND SOILS. *Can. J. Soil Sci.* 69, 33–38. <https://doi.org/10.4141/cjss89-004>
- Moran, M.A., Zepp, R.G., 1997. Role of photoreactions in the formation of biologically labile compounds from dissolved organic matter. *Limnol. Oceanogr.* 42, 1307–1316. <https://doi.org/10.4319/lo.1997.42.6.1307>
- Mosher, J., Fortner, A., Phillips, J., Bevelhimer, M., Stewart, A., Troia, M., 2015. Spatial and Temporal Correlates of Greenhouse Gas Diffusion from a Hydropower Reservoir in the Southern United States. *Water* 7, 5910.
- Munro, L.A., Wallace, I.S., 2016. Scottish Fish Farm Production Survey 2016.
- Nakagawa, S., Johnson, P.C.D., Schielzeth, H., 2017. The coefficient of determination R² and intra-class correlation coefficient from generalized linear mixed-effects models revisited and expanded. *J. R. Soc. Interface* 14, 20170213. <https://doi.org/10.1098/rsif.2017.0213>
- Nakagawa, S., Schielzeth, H., 2013. A general and simple method for obtaining R² from generalized linear mixed-effects models. *Methods Ecol. Evol.* 4, 133–142. <https://doi.org/10.1111/j.2041-210x.2012.00261.x>
- Natchimuthu, S., Wallin, M.B., Klemetsson, L., Bastviken, D., 2017. Spatio-temporal patterns of stream methane and carbon dioxide emissions in a hemiboreal catchment in Southwest Sweden. *Sci. Rep.* 7, 39729. <https://doi.org/10.1038/srep39729> <https://www.nature.com/articles/srep39729#supplementary-information>
- Neal, C., Robson, A.J., 2000. A summary of river water quality data collected within the Land–Ocean Interaction Study: core data for eastern UK rivers draining to the North Sea. *Sci. Total Environ.* 251–252, 585–665. [https://doi.org/https://doi.org/10.1016/S0048-9697\(00\)00397-1](https://doi.org/https://doi.org/10.1016/S0048-9697(00)00397-1)
- Nilsson, M., Sagerfors, J., Buffam, I., Laudon, H., Eriksson, T., Grelle, A., Klemetsson, L., Weslien, P., Lindroth, A., 2008. Contemporary carbon accumulation in a boreal oligotrophic minerogenic mire – a significant sink after accounting for all C-fluxes. *Glob. Chang. Biol.* 14, 2317–2332. <https://doi.org/10.1111/j.1365-2486.2008.01654.x>
- Niquette, P., Servais, P., Savoie, R., 2001. Bacterial Dynamics in the drinking water distribution system of Brussels. *Water Res.* 35, 675–682. [https://doi.org/https://doi.org/10.1016/S0043-1354\(00\)00303-1](https://doi.org/https://doi.org/10.1016/S0043-1354(00)00303-1)
- Nirmal Rajkumar, A., Barnes, J., Ramesh, R., Purvaja, R., Upstill-Goddard, R.C., 2008. Methane and nitrous oxide fluxes in the polluted Adyar River and estuary, SE India. *Mar. Pollut. Bull.* 56, 2043–2051. <https://doi.org/https://doi.org/10.1016/j.marpolbul.2008.08.005>
- Nutt, N., Perfect, C., 2011. Allan Water Natural Flood Management Techniques Scoping Study. Centre for River EcoSystems Science.
- Obrador, B., von Schiller, D., Marcé, R., Gómez-Gener, L., Koschorreck, M., Borrego, C., Catalán, N., 2018. Dry habitats sustain high CO₂ emissions from temporary ponds across seasons. *Sci. Rep.* 8, 3015. <https://doi.org/10.1038/s41598-018-20969-y>
- Oelbermann, M., Schiff, S.L., 2010. Inundating contrasting boreal forest soils: CO₂ and CH₄ production rates. *Écoscience* 17, 216–224. <https://doi.org/10.2980/17-2-3245>
- Ostrovsky, I., McGinnis, D.F., Lapidus, L., Eckert, W., 2008. Quantifying gas ebullition with

- echosounder: the role of methane transport by bubbles in a medium-sized lake. *Limnol. Oceanogr. Methods* 6, 105–118. <https://doi.org/10.4319/lom.2008.6.105>
- Pace, M., Prairie, Y.T., 2005. Respiration in Lakes, in: PJB, W. (Ed.), *Respiration in Aquatic Ecosystem*. Oxford University Press, USA.
- Pace, M.L., Cole, J.J., Carpenter, S.R., Kitchell, J.F., Hodgson, J.R., Van de Bogert, M.C., Bade, D.L., Kritzberg, E.S., Bastviken, D., 2004. Whole-lake carbon-13 additions reveal terrestrial support of aquatic food webs. *Nature* 427, 240–243. <https://doi.org/10.1038/nature02227>
- Paranaíba, J.R., Barros, N., Mendonça, R., Linkhorst, A., Isidorova, A., Roland, F., Almeida, R.M., Sobek, S., 2018. Spatially Resolved Measurements of CO₂ and CH₄ Concentration and Gas-Exchange Velocity Highly Influence Carbon-Emission Estimates of Reservoirs. *Environ. Sci. Technol.* 52, 607–615. <https://doi.org/10.1021/acs.est.7b05138>
- Pawson, R.R., Evans, M.G., Allott, T.E.H.A., 2012. Fluvial carbon flux from headwater peatland streams: significance of particulate carbon flux. *Earth Surf. Process. Landforms* 37, 1203–1212. <https://doi.org/10.1002/esp.3257>
- Peters, V., Conrad, R., 1996. Sequential reduction processes and initiation of CH₄ production upon flooding of oxic upland soils. *Soil Biol. Biochem.* 28, 371–382. [https://doi.org/https://doi.org/10.1016/0038-0717\(95\)00146-8](https://doi.org/https://doi.org/10.1016/0038-0717(95)00146-8)
- Pickard, A.E., Heal, K. V, McLeod, A.R., Dinsmore, K.J., 2017. Temporal changes in photoreactivity of dissolved organic carbon and implications for aquatic carbon fluxes from peatlands. *Biogeosciences* 14, 1793–1809. <https://doi.org/10.5194/bg-14-1793-2017>
- Pighini, S., Ventura, M., Miglietta, F., Wohlfahrt, G., 2018. Dissolved greenhouse gas concentrations in 40 lakes in the Alpine area. *Aquat. Sci.* 80, 32. <https://doi.org/10.1007/s00027-018-0583-2>
- Pinheiro, J., Bates, D., DebRoy, S., Sarkar, D., 2015. *nlme: Linear and Nonlinear Mixed Effects Models*.
- Porter, K.D.H., Reaney, S.M., Quilliam, R.S., Burgess, C., Oliver, D.M., 2017. Predicting diffuse microbial pollution risk across catchments: The performance of SCIMAP and recommendations for future development. *Sci. Total Environ.* 609, 456–465. <https://doi.org/https://doi.org/10.1016/j.scitotenv.2017.07.186>
- Prairie, Y.T., Alm, J., Beaulieu, J., Barros, N., Battin, T., Cole, J., del Giorgio, P., DelSontro, T., Guérin, F., Harby, A., Harrison, J., Mercier-Blais, S., Serça, D., Sobek, S., Vachon, D., 2017. Greenhouse Gas Emissions from Freshwater Reservoirs: What Does the Atmosphere See? *Ecosystems*. <https://doi.org/10.1007/s10021-017-0198-9> LB - Prairie2017
- Prairie, Y.T., Alm, J., Beaulieu, J., Barros, N., Battin, T., Cole, J., Del Giorgio, P., DelSontro, T., Guérin, F., Harby, A., Harrison, J., Mercier-Blais, S., Serça, D., Sobek, S., Vachon, D., 2018. Greenhouse Gas Emissions from Freshwater Reservoirs: What Does the Atmosphere See? *Ecosystems* 21, 1058–1071. <https://doi.org/10.1007/s10021-017-0198-9>
- Prairie, Y.T., Bird, D.F., Cole, J.J., 2002. The summer metabolic balance in the epilimnion of southeastern Quebec lakes. *Limnol. Oceanogr.* 47, 316–321. <https://doi.org/10.4319/lo.2002.47.1.0316>
- Premke, K., Attermeyer, K., Augustin, J., Cabezas, A., Casper, P., Deumlich, D., Gelbrecht, J., Gerke, H.H., Gessler, A., Grossart, H.-P., Hilt, S., Hupfer, M., Kalettka, T., Kayler, Z.,

- Lischeid, G., Sommer, M., Zak, D., 2016. The importance of landscape diversity for carbon fluxes at the landscape level: small-scale heterogeneity matters. *Wiley Interdiscip. Rev. Water* 3, 601–617. <https://doi.org/10.1002/wat2.1147>
- R Core Team, 2018. R: A language and environment for statistical computing.
- Ramchunder, S.J., Brown, L.E., Holden, J., 2013. Rotational vegetation burning effects on peatland stream ecosystems. *J. Appl. Ecol.* 50, 636–648. <https://doi.org/doi:10.1111/1365-2664.12082>
- Rantakari, M., Kortelainen, P., 2008. Controls of organic and inorganic carbon in randomly selected Boreal lakes in varied catchments. *Biogeochemistry* 91, 151–162. <https://doi.org/10.1007/s10533-008-9266-8>
- Rantakari, M., Kortelainen, P., 2005. Interannual variation and climatic regulation of the CO₂ emission from large boreal lakes. *Glob. Chang. Biol.* 11, 1368–1380. <https://doi.org/10.1111/j.1365-2486.2005.00982.x>
- Rasilo, T., Prairie, Y.T., del Giorgio, P.A., 2015. Large-scale patterns in summer diffusive CH₄ fluxes across boreal lakes, and contribution to diffusive C emissions. *Glob. Chang. Biol.* 21, 1124–1139. <https://doi.org/10.1111/gcb.12741>
- Rawlins, B.G., Palumbo-Roe, B., Goody, D.C., Worrall, F., Smith, H., 2014. A model of potential carbon dioxide efflux from surface water across England and Wales using headwater stream survey data and landscape predictors. *Biogeosciences* 11, 1911–1925. <https://doi.org/10.5194/bg-11-1911-2014>
- Raymond, P.A., Hartmann, J., Lauerwald, R., Sobek, S., McDonald, C., Hoover, M., Butman, D., Striegl, R., Mayorga, E., Humborg, C., Kortelainen, P., Dürr, H., Meybeck, M., Ciais, P., Guth, P., 2013. Global carbon dioxide emissions from inland waters. *Nature* 503, 355. <https://doi.org/10.1038/nature12760>
<https://www.nature.com/articles/nature12760#supplementary-information>
- Raymond, P.A., Zappa, C.J., Butman, D., Bott, T.L., Potter, J., Mulholland, P., Laursen, A.E., McDowell, W.H., Newbold, D., 2012. Scaling the gas transfer velocity and hydraulic geometry in streams and small rivers. *Limnol. Oceanogr. Fluids Environ.* 2, 41–53. <https://doi.org/10.1215/21573689-1597669>
- Reichstein, M., Bahn, M., Ciais, P., Frank, D., Mahecha, M.D., Seneviratne, S.I., Zscheischler, J., Beer, C., Buchmann, N., Frank, D.C., Papale, D., Rammig, A., Smith, P., Thonicke, K., van der Velde, M., Vicca, S., Walz, A., Wattenbach, M., 2013. Climate extremes and the carbon cycle. *Nature* 500, 287. <https://doi.org/10.1038/nature12350>
- Reverey, F., Grossart, H.-P., Premke, K., Lischeid, G., 2016. Carbon and nutrient cycling in kettle hole sediments depending on hydrological dynamics: a review. *Hydrobiologia* 775, 1–20. <https://doi.org/10.1007/s10750-016-2715-9> LB - Reverey2016
- Reynolds, B., Edwards, A., 1995. Factors influencing dissolved nitrogen concentrations and loadings in upland streams of the UK. *Agric. Water Manag.* 27, 181–202. [https://doi.org/https://doi.org/10.1016/0378-3774\(95\)01146-A](https://doi.org/https://doi.org/10.1016/0378-3774(95)01146-A)
- Rich, P.H., Wetzel, R.G., 1978. Detritus in the Lake Ecosystem. *Am. Nat.* 112, 57–71. <https://doi.org/10.1086/283252>
- Rinke, K., Kuehn, B., Bocaniov, S., Wendt-Potthoff, K., Büttner, O., Tittel, J., Schultze, M., Herzsprung, P., Rönicke, H., Rink, K., Dietze, M., Matthes, M., Paul, L., Friese, K., 2013. Reservoirs as sentinels of catchments: The Rappbode Reservoir Observatory (Harz

- Mountains, Germany). *Environ. Earth Sci.* 69, 523–536. <https://doi.org/10.1007/s12665-013-2464-2>
- Rocher-Ros, G., Giesler, R., Lundin, E., Salimi, S., Jonsson, A., Karlsson, J., 2017. Large Lakes Dominate CO₂ Evasion From Lakes in an Arctic Catchment. *Geophys. Res. Lett.* 44, 12,212-254,261. <https://doi.org/10.1002/2017GL076146>
- Rodhe, W., 1964. Effects of impoundment on water chemistry and plankton in Lake Ransaren (Swedish Lappland). *SIL Proceedings, 1922-2010* 15, 437–443. <https://doi.org/10.1080/03680770.1962.11895558>
- Roehm, C., Tremblay, A., 2006. Role of turbines in the carbon dioxide emissions from two boreal reservoirs, Québec, Canada. *J. Geophys. Res. Atmos.* 111. <https://doi.org/10.1029/2006JD007292>
- Roehm, C.L., Prairie, Y.T., del Giorgio, P.A., 2009. The pCO₂ dynamics in lakes in the boreal region of northern Québec, Canada. *Global Biogeochem. Cycles* 23. <https://doi.org/10.1029/2008GB003297>
- Roland, F., Vidal, L., Pacheco, F., Barros, N., Assireu, A., Ometto, J.H.B., Cimleris, A.P., Cole, J., 2010. Variability of carbon dioxide flux from tropical (Cerrado) hydroelectric reservoirs. *Aquat. Sci.* 72, 283–293. <https://doi.org/10.1007/s00027-010-0140-0>
- Rosa, L., dos Santos, M., Matvienko, B., dos Santos, E., Sikar, E., 2004. Greenhouse Gas Emissions from Hydroelectric Reservoirs in Tropical Regions. *Clim. Change* 66, 9–21. <https://doi.org/10.1023/B:CLIM.0000043158.52222.ee>
- Rosamond, M.S., Thuss, S.J., Schiff, S.L., 2012. Dependence of riverine nitrous oxide emissions on dissolved oxygen levels. *Nat. Geosci.* 5, 715–718. <https://doi.org/10.1038/ngeo1556>
- Rowell, D.L., 1994. *Soil science: Methods & Applications*. Longman Scientific & Technical, Harlow, Essex, UK . <https://doi.org/doi:10.1002/jsfa.2740660423>
- Rudd, J.W.M., Hecky, R.E., Harris, R., Kelly, C.A., 1993. Are hydroelectric reservoirs significant sources of greenhouse gases. *Ambio* 22, 246–248.
- Sand-Jensen, K.A.J., Pedersen, N.L., SØndergaard, M., 2007. Bacterial metabolism in small temperate streams under contemporary and future climates. *Freshw. Biol.* 52, 2340–2353. <https://doi.org/10.1111/j.1365-2427.2007.01852.x>
- Santana, V.M., Alday, J.G., Lee, H., Allen, K.A., Marrs, R.H., 2015. Prescribed-burning vs. wildfire: management implications for annual carbon emissions along a latitudinal gradient of *Calluna vulgaris*-dominated vegetation. *Biogeosciences Discuss.* 2015, 17817–17849. <https://doi.org/10.5194/bgd-12-17817-2015>
- Sawakuchi, H.O., Bastviken, D., Sawakuchi, A.O., Krusche, A. V., Ballester, M.V.R., Richey, J.E., 2014. Methane emissions from Amazonian Rivers and their contribution to the global methane budget. *Glob. Chang. Biol.* 20, 2829–2840. <https://doi.org/doi:10.1111/gcb.12646>
- Schade, J.D., Bailio, J., McDowell, W.H., 2016. Greenhouse gas flux from headwater streams in New Hampshire, USA: Patterns and drivers. *Limnol. Oceanogr.* 61, S165–S174. <https://doi.org/doi:10.1002/lno.10337>
- Schiller, D. von, Marcé, R., Obrador, B., Gómez-Gener, L., Casas-Ruiz, J.P., Acuña, V., Koschorreck, M., 2014. Carbon dioxide emissions from dry watercourses. *Int. Waters* 4, 377–382. <https://doi.org/10.5268/iw-4.4.746>

- Schimel, D., 2007. Carbon cycle conundrums. *Proc. Natl. Acad. Sci.* 104, 18353–18354.
<https://doi.org/10.1073/pnas.0709331104>
- Scholz, C., Jones, T.G., West, M., Ehbair, A.M.S., Dunn, C., Freeman, C., 2016. Constructed wetlands may lower inorganic nutrient inputs but enhance DOC loadings into a drinking water reservoir in North Wales. *Environ. Sci. Pollut. Res.* 23, 18192–18199.
<https://doi.org/10.1007/s11356-016-6991-8>
- Schubert, C.J., Diem, T., Eugster, W., 2012. Methane Emissions from a Small Wind Shielded Lake Determined by Eddy Covariance, Flux Chambers, Anchored Funnels, and Boundary Model Calculations: A Comparison. *Environ. Sci. Technol.* 46, 4515–4522.
<https://doi.org/10.1021/es203465x>
- Schulz, M., Faber, E., Hollerbach, A., Schröder, H.G., Güde, H., 2001. The methane cycle in the epilimnion of Lake Constance. *Arch. für Hydrobiol.* 151, 157–176.
<https://doi.org/10.1127/archiv-hydrobiol/151/2001/157>
- Seitzinger, S.P., Kroeze, C., 1998. Global distribution of nitrous oxide production and N inputs in freshwater and coastal marine ecosystems. *Global Biogeochem. Cycles* 12, 93–113.
<https://doi.org/10.1029/97GB03657>
- Serça, D., Deshmukh, C., Pighini, S., Oudone, P., Vongkhamsoo, A., Guédant, P., Rode, W., Godon, A., Chanudet, V., Descloux, S., Guérin, F., 2016. Nam Theun 2 Reservoir four years after commissioning: significance of drawdown methane emissions and other pathways. *Hydroécol. Appl.* 19, 119–146.
- Skiba, U., Jones, S.K., Drewer, J., Helfter, C., Anderson, M., Dinsmore, K., McKenzie, R., Nemitz, E., Sutton, M.A., 2013. Comparison of soil greenhouse gas fluxes from extensive and intensive grazing in a temperate maritime climate. *Biogeosciences* 10, 1231.
- Skinner, J.A., Lewis, K.A., Bardon, K.S., Tucker, P., Catt, J.A., Chambers, B.J., 1997. An Overview of the Environmental Impact of Agriculture in the U.K. *J. Environ. Manage.* 50, 111–128.
<https://doi.org/https://doi.org/10.1006/jema.1996.0103>
- Sobek, S., Algesten, G., Bergström, A.-K., Jansson, M., Tra, L.J., 2003. The catchment and climate regulation of pCO₂ in boreal lakes. *Glob. Chang. Biol.* 9, 630–641.
<https://doi.org/10.1046/j.1365-2486.2003.00619.x>
- Sobek, S., DelSontro, T., Wongfun, N., Wehrli, B., 2012. Extreme organic carbon burial fuels intense methane bubbling in a temperate reservoir. *Geophys. Res. Lett.* 39, L01401.
<https://doi.org/10.1029/2011gl050144>
- Sobek, S., Durisch-Kaiser, E., Zurbrügg, R., Wongfun, N., Wessels, M., Pasche, N., Wehrli, B., 2009. Organic carbon burial efficiency in lake sediments controlled by oxygen exposure time and sediment source. *Limnol. Oceanogr.* 54, 2243–2254.
<https://doi.org/10.4319/lo.2009.54.6.2243>
- Sobek, S., Tranvik, L.J., Cole, J.J., 2005. Temperature independence of carbon dioxide supersaturation in global lakes. *Global Biogeochem. Cycles* 19.
<https://doi.org/10.1029/2004GB002264>
- Sobek, S., Tranvik, L.J., Prairie, Y.T., Kortelainen, P., Cole, J.J., 2007. Patterns and regulation of dissolved organic carbon: An analysis of 7,500 widely distributed lakes. *Limnol. Oceanogr.* 52, 1208–1219. <https://doi.org/10.4319/lo.2007.52.3.1208>
- Sollberger, S., Wehrli, B., Schubert, C.J., DelSontro, T., Eugster, W., 2017. Minor methane emissions from an Alpine hydropower reservoir based on monitoring of diel and seasonal

- variability. *Environ. Sci. Process. Impacts* 19, 1278–1291.
<https://doi.org/10.1039/C7EM00232G>
- Soued, C., del Giorgio, P.A., Maranger, R., 2015. Nitrous oxide sinks and emissions in boreal aquatic networks in Québec. *Nat. Geosci.* 9, 116.
- Soumis, N., Duchemin, É., Canuel, R., Lucotte, M., 2004. Greenhouse gas emissions from reservoirs of the western United States. *Global Biogeochem. Cycles* 18, GB3022.
<https://doi.org/10.1029/2003gb002197>
- Spiller, M., McIntosh, B.S., Seaton, R.A.F., Jeffrey, P., 2013. Implementing Pollution Source Control—Learning from the Innovation Process in English and Welsh Water Companies. *Water Resour. Manag.* 27, 75–94. <https://doi.org/10.1007/s11269-012-0161-7>
- St. Louis, V.L., Kelly, C.A., Duchemin, É., Rudd, J.W.M., Rosenberg, D.M., 2000. Reservoir Surfaces as Sources of Greenhouse Gases to the Atmosphere: A Global Estimate: Reservoirs are sources of greenhouse gases to the atmosphere, and their surface areas have increased to the point where they should be included in global inventories o. *Bioscience* 50, 766–775. [https://doi.org/10.1641/0006-3568\(2000\)050\[0766:rsasog\]2.0.co;2](https://doi.org/10.1641/0006-3568(2000)050[0766:rsasog]2.0.co;2)
- Stanley, E., Powers, S., Lottig, N., Buffam, I., Crawford, J.T., 2012. Contemporary changes in dissolved organic carbon (DOC) in human-dominated rivers: is there a role for DOC management? *Freshw. Biol.* 57, 26–42. <https://doi.org/10.1111/j.1365-2427.2011.02613.x>
- Stanley, E.H., Casson, N.J., Christel, S.T., Crawford, J.T., Loken, L.C., Oliver, S.K., 2016. The ecology of methane in streams and rivers: patterns, controls, and global significance. *Ecol. Monogr.* 86, 146–171. <https://doi.org/doi:10.1890/15-1027>
- Stevens, P.A., Norris, D.A., Williams, T.G., Hughes, S., Durrant, D.W.H., Anderson, M.A., Weatherley, N.S., Hornung, M., Woods, C., 1995. Nutrient losses after clearfelling in Beddgelert Forest: a comparison of the effects of conventional and whole-tree harvest on soil water chemistry. *For. An Int. J. For. Res.* 68, 115–131.
<https://doi.org/10.1093/forestry/68.2.115>
- Stimson, A., Allott, T.E.H., Boulton, S., Evans, M.G., 2017. Fluvial organic carbon composition and concentration variability within a peatland catchment—Implications for carbon cycling and water treatment. *Hydrol. Process.* 31, 4183–4194.
<https://doi.org/10.1002/hyp.11352>
- Stimson, A.G., Allott, T.E.H., Boulton, S., Evans, M.G., 2017. Reservoirs as hotspots of fluvial carbon cycling in peatland catchments. *Sci. Total Environ.* 580, 398–411.
<https://doi.org/https://doi.org/10.1016/j.scitotenv.2016.11.193>
- Stocker, T.F., Qin, D., Plattner, G.-K., Alexander, L.V., Allen, S.K., Bindoff, N.L., F.-M., Bréon, J.A., Church, U., Cubasch, S., Emori, P., Forster, P., Friedlingstein, N., Gillett, J.M., Gregory, D.L., Hartmann, E., Jansen, B., Kirtman, R., Knutti, K., Krishna Kumar, P., Vaughan, D.G., Xie, S.-P., 2013. Technical Summary. In: *Climate Change 2013: The Physical Science Basis. Contribution of Working Group I to the Fifth Assessment Report of the Intergovernmental Panel on Climate Change*. Cambridge University Press, Cambridge, UK and New York, USA.
- Straskraba, M., Tundisi, J.G., Duncan, A., 1993. *Comparative Reservoir Limnology and Water Quality Management*, 1st ed, Developments in Hydrobiology. Springer, Netherlands.
<https://doi.org/10.1007/978-94-017-1096-1>

- Strauss, E.A., Richardson, W.B., Bartsch, L.A., Cavanaugh, J.C., Bruesewitz, D.A., Imker, H., Heinz, J.A., Soballe, D.M., 2004. Nitrification in the Upper Mississippi River: patterns, controls, and contribution to the NO₃- budget. *J. North Am. Benthol. Soc.* 23, 1–14. [https://doi.org/10.1899/0887-3593\(2004\)023<0001:nitumr>2.0.co;2](https://doi.org/10.1899/0887-3593(2004)023<0001:nitumr>2.0.co;2)
- Striegl, R.G., Kortelainen, P., Chanton, J.P., Wickland, K.P., Bugna, G.C., Rantakari, M., 2001. Carbon dioxide partial pressure and ¹³C content of north temperate and boreal lakes at spring ice melt. *Limnol. Oceanogr.* 46, 941–945. <https://doi.org/10.4319/lo.2001.46.4.0941>
- Striegl, R.G., Michmerhuizen, C.M., 1998. Hydrologic influence on methane and carbon dioxide dynamics at two north-central Minnesota lakes. *Limnol. Oceanogr.* 43, 1519–1529. <https://doi.org/10.4319/lo.1998.43.7.1519>
- Sturm, K., Yuan, Z., Gibbes, B., Werner, U., Grinham, A., 2014. Methane and nitrous oxide sources and emissions in a subtropical freshwater reservoir, South East Queensland, Australia. *Biogeosciences* 11, 5245–5258. <https://doi.org/10.5194/bg-11-5245-2014>
- Sun, P., Zhuge, Y., Zhang, J., Cai, Z., 2012. Soil pH was the main controlling factor of the denitrification rates and N₂/N₂O emission ratios in forest and grassland soils along the Northeast China Transect (NECT). *Soil Sci. Plant Nutr.* 58, 517–525. <https://doi.org/10.1080/00380768.2012.703609>
- Talbot, C., Hole, R., 1994. Fish diets and the control of eutrophication resulting from aquaculture. *J. Appl. Ichthyol.* 10, 258–270. <https://doi.org/10.1111/j.1439-0426.1994.tb00165.x>
- Tang, K.W., McGinnis, D.F., Frindte, K., Brüchert, V., Grossart, H.-P., 2014. Paradox reconsidered: Methane oversaturation in well-oxygenated lake waters. *Limnol. Oceanogr.* 59, 275–284. <https://doi.org/10.4319/lo.2014.59.1.0275>
- Teodoru, C.R., Bastien, J., Bonneville, M.-C., del Giorgio, P.A., Demarty, M., Garneau, M., Hélie, J.-F., Pelletier, L., Prairie, Y.T., Roulet, N.T., Strachan, I.B., Tremblay, A., 2012. The net carbon footprint of a newly created boreal hydroelectric reservoir. *Global Biogeochem. Cycles* 26. <https://doi.org/10.1029/2011GB004187>
- Teodoru, C.R., Nyoni, F.C., Borges, A. V, Darchambeau, F., Nyambe, I., Bouillon, S., 2015. Dynamics of greenhouse gases (CO₂, CH₄, N₂O) along the Zambezi River and major tributaries, and their importance in the riverine carbon budget. *Biogeosciences* 12, 2431–2453. <https://doi.org/10.5194/bg-12-2431-2015>
- Teodoru, C.R., Prairie, Y.T., del Giorgio, P.A., 2011. Spatial Heterogeneity of Surface CO₂ Fluxes in a Newly Created Eastmain-1 Reservoir in Northern Quebec, Canada. *Ecosystems* 14, 28–46. <https://doi.org/10.1007/s10021-010-9393-7>
- The Public Water Supplies (Scotland) Regulations 2014, 2014.
- Thuss, S.J., Venkiteswaran, J.J., Schiff, S.L., 2014. Proper Interpretation of Dissolved Nitrous Oxide Isotopes, Production Pathways, and Emissions Requires a Modelling Approach. *PLoS One* 9, e90641. <https://doi.org/10.1371/journal.pone.0090641>
- Tönno, I., Ott, K., Nöges, T., 2005. Nitrogen Dynamics in the Steeply Stratified, Temperate Lake Verevi, Estonia. *Hydrobiologia* 547, 63–71. <https://doi.org/10.1007/s10750-005-4145-y> LB - Tönno2005
- Tranvik, L.J., Downing, J.A., Cotner, J.B., Loiselle, S.A., Striegl, R.G., Ballatore, T.J., Dillon, P., Finlay, K., Fortino, K., Knoll, L.B., Kortelainen, P.L., Kutser, T., Larsen, S., Laurion, I., Leech,

- D.M., McCallister, S.L., McKnight, D.M., Melack, J.M., Overholt, E., Porter, J.A., Prairie, Y., Renwick, W.H., Roland, F., Sherman, B.S., Schindler, D.W., Sobek, S., Tremblay, A., Vanni, M.J., Verschoor, A.M., von Wachenfeldt, E., Weyhenmeyer, G.A., 2009. Lakes and reservoirs as regulators of carbon cycling and climate. *Limnol. Oceanogr.* 54, 2298–2314. https://doi.org/10.4319/lo.2009.54.6_part_2.2298
- Tremblay, A., Lambert, M., Demers, C., 2005. Greenhouse Gas Emissions — Fluxes and Processes. Springer, Berlin, Heidelberg. https://doi.org/https://doi.org/10.1007/978-3-540-26643-3_2
- Turnipseed, D.P., Sauer, V.B., 2010. Techniques and Methods, in: Discharge Measurements at Gaging Stations. U.S. Geological Survey, Reston, VA, p. 106.
- USEPA, 1993. AQ2 - USEPA Approved Methods [WWW Document]. AQ2 Environ. Methods List Rev 5. URL <https://www.seal-analytical.com/Methods/DiscreteMethods/AQ2EPAMethods/tabid/76/language/en-US/Default.aspx>
- Vachon, D., Prairie, Y.T., Guillemette, F., del Giorgio, P.A., 2017. Modeling Allochthonous Dissolved Organic Carbon Mineralization Under Variable Hydrologic Regimes in Boreal Lakes. *Ecosystems* 20, 781–795. <https://doi.org/10.1007/s10021-016-0057-0> LB - Vachon2017
- Van Geest, G.J., Roozen, F.C.J.M., Coops, H., Roijackers, R.M.M., Buijse, A.D., Peeters, E.T.H.M., Scheffer, M., 2003. Vegetation abundance in lowland flood plain lakes determined by surface area, age and connectivity. *Freshw. Biol.* 48, 440–454. <https://doi.org/10.1046/j.1365-2427.2003.01022.x>
- Venkateswaran, J.J., Rosamond, M.S., Schiff, S.L., 2014. Nonlinear Response of Riverine N₂O Fluxes to Oxygen and Temperature. *Environ. Sci. Technol.* 48, 1566–1573. <https://doi.org/10.1021/es500069j>
- Verpoorter, C., Kutser, T., Seekell, D.A., Tranvik, L.J., 2014. A global inventory of lakes based on high-resolution satellite imagery. *Geophys. Res. Lett.* 41, 6396–6402. <https://doi.org/10.1002/2014GL060641>
- Verrill, D.D., Berry, C.R., 1995. Effectiveness of an Electrical Barrier and Lake Drawdown for Reducing Common Carp and Bigmouth Buffalo Abundances. *North Am. J. Fish. Manag.* 15, 137–141. [https://doi.org/doi:10.1577/1548-8675\(1995\)015<0137:EOAEB>2.3.CO;2](https://doi.org/doi:10.1577/1548-8675(1995)015<0137:EOAEB>2.3.CO;2)
- von Fischer, J.C., Hedin, L.O., 2007. Controls on soil methane fluxes: Tests of biophysical mechanisms using stable isotope tracers. *Global Biogeochem. Cycles* 21. <https://doi.org/doi:10.1029/2006GB002687>
- Vonk, J.E., Gustafsson, Ö., 2013. Permafrost-carbon complexities. *Nat. Geosci.* 6, 675.
- Waldron, S., Flowers, H., Arlaud, C., Bryant, C., McFarlane, S., 2009. The significance of organic carbon and nutrient export from peatland-dominated landscapes subject to disturbance, a stoichiometric perspective. *Biogeosciences* 6, 363–374. <https://doi.org/10.5194/bg-6-363-2009>
- Wallage, Z.E., Holden, J., McDonald, A.T., 2006. Drain blocking: An effective treatment for reducing dissolved organic carbon loss and water discolouration in a drained peatland. *Sci. Total Environ.* 367, 811–821. <https://doi.org/https://doi.org/10.1016/j.scitotenv.2006.02.010>
- Wallin, M.B., Campeau, A., Audet, J., Bastviken, D., Bishop, K., Kokic, J., Laudon, H., Lundin, E.,

- Löfgren, S., Natchimuthu, S., Sobek, S., Teutschbein, C., Weyhenmeyer, G.A., Grabs, T., 2018. Carbon dioxide and methane emissions of Swedish low-order streams—a national estimate and lessons learnt from more than a decade of observations. *Limnol. Oceanogr. Lett.* 3, 156–167. <https://doi.org/10.1002/lol2.10061>
- Wallin, M.B., Grabs, T., Buffam, I., Laudon, H., Ågren, A., Öquist, M.G., Bishop, K., 2013. Evasion of CO₂ from streams – The dominant component of the carbon export through the aquatic conduit in a boreal landscape. *Glob. Chang. Biol.* 19, 785–797. <https://doi.org/10.1111/gcb.12083>
- Wallin, M.B., Löfgren, S., Erlandsson, M., Bishop, K., 2014. Representative regional sampling of carbon dioxide and methane concentrations in hemiboreal headwater streams reveal underestimates in less systematic approaches. *Global Biogeochem. Cycles* 28, 465–479. <https://doi.org/10.1002/2013GB004715>
- Wallin, M.B., Öquist, M.G., Buffam, I., Billett, M.F., Nisell, J., Bishop, K.H., 2011. Spatiotemporal variability of the gas transfer coefficient (KCO₂) in boreal streams: Implications for large scale estimates of CO₂ evasion. *Global Biogeochem. Cycles* 25. <https://doi.org/10.1029/2010GB003975>
- Wallin, M.B., Weyhenmeyer, G.A., Bastviken, D., Chmiel, H.E., Peter, S., Sobek, S., Klemedtsson, L., 2015. Temporal control on concentration, character, and export of dissolved organic carbon in two hemiboreal headwater streams draining contrasting catchments. *J. Geophys. Res. Biogeosciences* 120, 832–846. <https://doi.org/10.1002/2014JG002814>
- Walling, D.E., Webb, B.W., 1985. Estimating the discharge of contaminants to coastal waters by rivers: Some cautionary comments. *Mar. Pollut. Bull.* 16, 488–492. [https://doi.org/https://doi.org/10.1016/0025-326X\(85\)90382-0](https://doi.org/https://doi.org/10.1016/0025-326X(85)90382-0)
- Wang, H., Wang, W., Yin, C., Wang, Y., Lu, J., 2006. Littoral zones as the “hotspots” of nitrous oxide (N₂O) emission in a hyper-eutrophic lake in China. *Atmos. Environ.* 40, 5522–5527. <https://doi.org/https://doi.org/10.1016/j.atmosenv.2006.05.032>
- Wang, Q., Dore, J.E., McDermott, T.R., 2017. Methylphosphonate metabolism by *Pseudomonas* sp. populations contributes to the methane oversaturation paradox in an oxic freshwater lake. *Environ. Microbiol.* 19, 2366–2378. <https://doi.org/10.1111/1462-2920.13747>
- Wanninkhof, R., 1992. Relationship between wind speed and gas exchange over the ocean. *J. Geophys. Res. Ocean.* 97, 7373–7382. <https://doi.org/doi:10.1029/92JC00188>
- Ward, J., 1963. Hierarchical Grouping to Optimize an Objective Function. *J. Am. Stat. Assoc.* 58, 236–244. <https://doi.org/10.1080/01621459.1963.10500845>
- Webb, N.R., 1998. The traditional management of European heathlands. *J. Appl. Ecol.* 35, 987–990. <https://doi.org/doi:10.1111/j.1365-2664.1998.tb00020.x>
- Weise, L., Ulrich, A., Moreano, M., Gessler, A., E. Kayler, Z., Steger, K., Zeller, B., Rudolph, K., Knezevic-Jaric, J., Premke, K., 2016. Water level changes affect carbon turnover and microbial community composition in lake sediments. *FEMS Microbiol. Ecol.* 92, fiw035-fiw035. <https://doi.org/10.1093/femsec/fiw035>
- Weiss, R.F., 1974. Carbon dioxide in water and seawater: the solubility of a non-ideal gas. *Mar. Chem.* 2, 203–215. [https://doi.org/https://doi.org/10.1016/0304-4203\(74\)90015-2](https://doi.org/https://doi.org/10.1016/0304-4203(74)90015-2)
- Weiss, R.F., Price, B.A., 1980. Nitrous oxide solubility in water and seawater. *Mar. Chem.* 8,

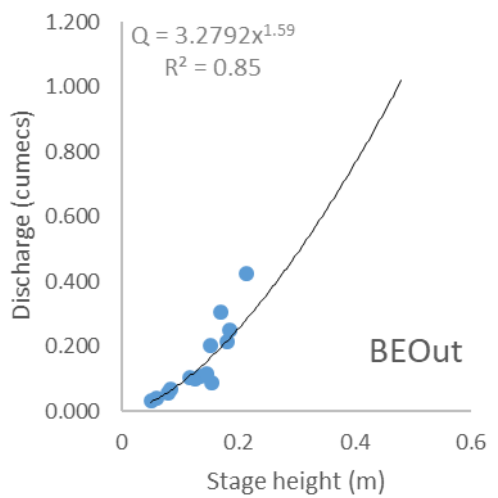
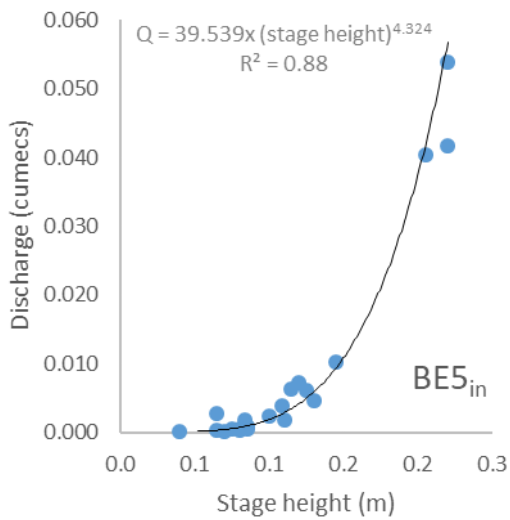
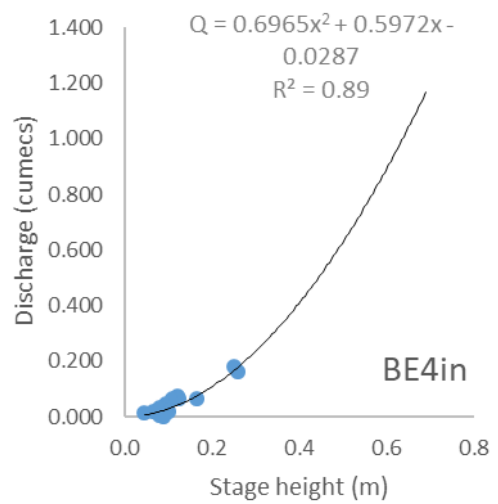
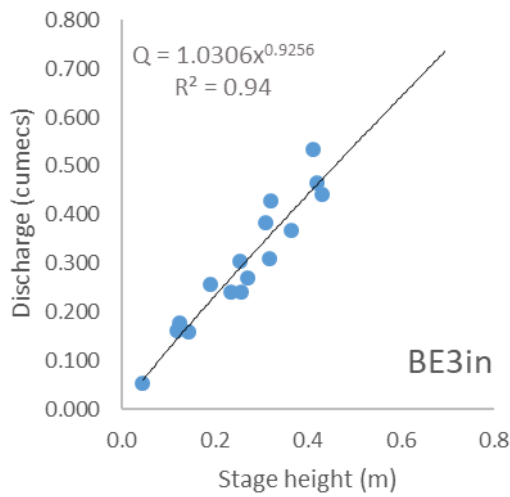
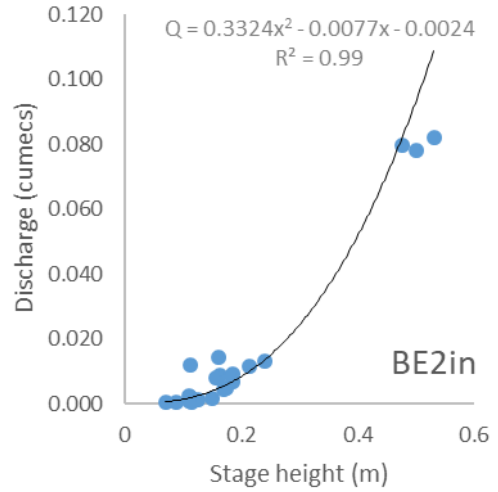
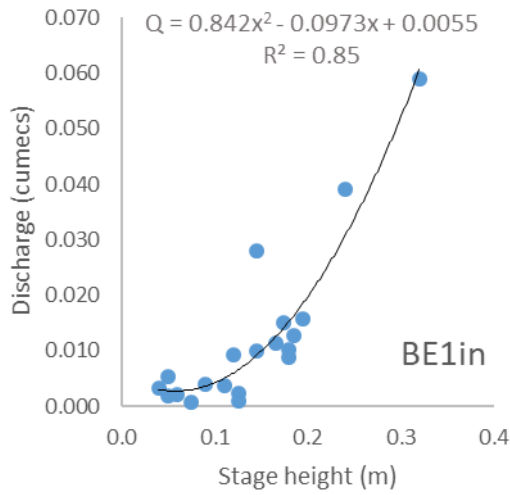
347–359. [https://doi.org/10.1016/0304-4203\(80\)90024-9](https://doi.org/10.1016/0304-4203(80)90024-9)

- West, M., Fenner, N., Gough, R., Freeman, C., 2017. Evaluation of algal bloom mitigation and nutrient removal in floating constructed wetlands with different macrophyte species. *Ecol. Eng.* 108, 581–588. <https://doi.org/https://doi.org/10.1016/j.ecoleng.2017.07.033>
- Whitfield, C., Aherne, J., Baulch, H., 2011. Controls on greenhouse gas concentrations in polymictic headwater lakes in Ireland. *Sci. Total Environ.* 410–411, 217–225. <https://doi.org/https://doi.org/10.1016/j.scitotenv.2011.09.045>
- Whitfield, C.J., Aherne, J., Gibson, J.J., Seabert, T.A., Watmough, S.A., 2010. The controls on boreal peatland surface water chemistry in Northern Alberta, Canada. *Hydrol. Process.* 24, 2143–2155. <https://doi.org/doi:10.1002/hyp.7637>
- Whitfield, S., Reed, M., Thomson, K., Christie, M., Stringer, L.C., Quinn, C.H., Anderson, R., Moxey, A., Hubacek, K., 2011. Managing Peatland Ecosystem Services: Current UK Policy and Future Challenges in a Changing World. *Scottish Geogr. J.* 127, 209–230. <https://doi.org/10.1080/14702541.2011.616864>
- Wiesenburg, D.A., Guinasso, N.L., 1979. Equilibrium solubilities of methane, carbon monoxide, and hydrogen in water and sea water. *J. Chem. Eng. Data* 24, 356–360. <https://doi.org/10.1021/je60083a006>
- Xiang, W., Wan, X., Yan, S., Wu, Y., Bao, Z., 2013. Inhibitory effects of drought induced acidification on phenol oxidase activities in Sphagnum-dominated peatland. *Biogeochemistry* 116, 293–301. <https://doi.org/10.1007/s10533-013-9859-8>
- Xiong, Z.-Q., Xing, G.-X., Zhu, Z.-L., 2007. Nitrous Oxide and Methane Emissions as Affected by Water, Soil and Nitrogen1 1Project supported by the National Natural Science Foundation of China (Nos. 30390080 and 30390081). *Pedosphere* 17, 146–155. [https://doi.org/https://doi.org/10.1016/S1002-0160\(07\)60020-4](https://doi.org/https://doi.org/10.1016/S1002-0160(07)60020-4)
- Xu, J., Morris, P.J., Liu, J., Holden, J., 2018. Hotspots of peatland-derived potable water use identified by global analysis. *Nat. Sustain.* 1, 246–253. <https://doi.org/10.1038/s41893-018-0064-6>
- Yamamoto, S., Alcauskas, J.B., Crozier, T.E., 1976. Solubility of methane in distilled water and seawater. *J. Chem. Eng. Data* 21, 78–80. <https://doi.org/10.1021/je60068a029>
- Yang, H., Xing, Y., Xie, P., Ni, L., Rong, K., 2008. Carbon source/sink function of a subtropical, eutrophic lake determined from an overall mass balance and a gas exchange and carbon burial balance. *Environ. Pollut.* 151, 559–568. <https://doi.org/https://doi.org/10.1016/j.envpol.2007.04.006>
- Yang, L., Lu, F., Wang, X., Duan, X., Song, W., Sun, B., Chen, S., Zhang, Q., Hou, P., Zheng, F., Zhang, Y., Zhou, X., Zhou, Y., Ouyang, Z., 2012. Surface methane emissions from different land use types during various water levels in three major drawdown areas of the Three Gorges Reservoir. *J. Geophys. Res. Atmos.* 117. <https://doi.org/doi:10.1029/2011JD017362>
- Yang, M., Geng, X., Grace, J., Lu, C., Zhu, Y., Zhou, Y., Lei, G., 2014. Spatial and Seasonal CH₄ Flux in the Littoral Zone of Miyun Reservoir near Beijing: The Effects of Water Level and Its Fluctuation. *PLoS One* 9, e94275. <https://doi.org/10.1371/journal.pone.0094275>
- Yang, M., Geng, X.M., Grace, J., Jia, Y.F., Liu, Y.Z., Jiao, S.W., Shi, L.L., Lu, C., Zhou, Y., Lei, G.C., 2015. Responses of N₂O flux to water level fluctuation and other environmental factors at littoral zone of Miyun Reservoir: a comparison with CH₄ fluxes. *Biogeosciences*

- Discuss. 12, 5333–5363. <https://doi.org/10.5194/bgd-12-5333-2015>
- Zanchettin, D., Traverso, P., Tomasino, M., 2008. Po River discharges: a preliminary analysis of a 200-year time series. *Clim. Change* 89, 411–433. <https://doi.org/10.1007/s10584-008-9395-z> LB - Zanchettin2008
- Zevenbergen, L.W., Thorne, C.R., 1987. Quantitative analysis of land surface topography. *Earth Surf. Process. Landforms* 12, 47–56. <https://doi.org/10.1002/esp.3290120107>
- Zhang, J., Jiang, Y., Gao, Y., Wu, Y., Luo, W., Zhou, Z., Wang, F., 2013. CO₂ emission from Dianshan Lake in summer, East China. *Chinese J. Geochemistry* 32, 430–435. <https://doi.org/10.1007/s11631-013-0652-0>
- Zhao, Y., Wu, B.F., Zeng, Y., 2013. Spatial and temporal patterns of greenhouse gas emissions from Three Gorges Reservoir of China. *Biogeosciences* 10, 1219–1230. <https://doi.org/10.5194/bg-10-1219-2013>
- Zhen-Gang, J., 2008. Introduction. *Hydrodyn. Water Qual.*, Wiley Online Books. <https://doi.org/doi:10.1002/9780470241066.ch1>
- Zheng, H., Zhao, X., Zhao, T., Chen, F., Xu, W., Duan, X., Wang, X., Ouyang, Z., 2011. Spatial–temporal variations of methane emissions from the Ertan hydroelectric reservoir in southwest China. *Hydrol. Process.* 25, 1391–1396. <https://doi.org/10.1002/hyp.7903>
- Zohary, T., Ostrovsky, I., 2011. Ecological impacts of excessive water level fluctuations in stratified freshwater lakes. *Int. Waters* 1, 47–59. <https://doi.org/10.5268/iw-1.1.406>

Appendix I – Flow rating curves

Black Esk reservoir catchment



Baddingsill reservoir catchment

